The Regulation of TDP-43 Ubiquitinylation

by UBE2E Ubiquitin-conjugating Enzymes

and Ubiquitin Isopeptidase Y

Dissertation

zur Erlangung des Grades eines
Doktors der Naturwissenschaften

der Mathematisch-Naturwissenschaftlichen Fakultät
und
der Medizinischen Fakultät
der Eberhard-Karls-Universität Tübingen

vorgelegt
von

Friederike Hans
aus Neuruppin, Deutschland

August - 2014

Tag der mündlichen Prüfung: 10. November 2014

Dekan der Math.-Nat. Fakultät: Prof. Dr. W. Rosenstiel

Dekan der Medizinischen Fakultät: Prof. Dr. I. B. Autenrieth

1. Berichterstatter: Prof. Dr. Philipp J. Kahle

2. Berichterstatter: Prof. Dr. Ralf-Peter Jansen

Prüfungskommission: Prof. Dr. Philipp J. Kahle

                                  Prof. Dr. Ralf-Peter Jansen

                                  Prof. Dr. Elisa Izaurralde

                                  Prof. Dr. Manuela Neumann

Ich erkläre, dass ich die zur Promotion eingereichte Arbeit mit dem Titel: *„The regulation of TDP-43 ubiquitinylation by UBE2E ubiquitin-conjugating enzymes and ubiquitin isopeptidase Y"* selbstständig verfasst, nur die angegebenen Quellen und Hilfsmittel benutzt und wörtlich oder inhaltlich übernommene Stellen als solche gekennzeichnet habe. Ich versichere an Eides statt, dass diese Angaben wahr sind und dass ich nichts verschwiegen habe. Mir ist bekannt, dass die falsche Abgabe einer Versicherung an Eides statt mit Freiheitsstrafe bis zu drei Jahren oder mit Geldstrafe bestraft wird.

Tübingen, den _____ _____

                    Datum   Unterschrift

"Let us keep looking, in spite of everything. Let us keep searching. It is indeed the best method of finding, and perhaps, thanks to our efforts, the verdict we will give to such a patient tomorrow will not be the same that we must give this patient today"

Jean-Martin Charcot, 28th February 1888

Content

List of Figures

List of Tables

Abbreviations

Generally accepted abbreviations and units are not listed. Abbreviations in Table 2.1 are listed in the table legend.

Ø	control
3-AT	3-amino-1,2,4-triazole
3-MA	3-methyladenine
aa	amino acid
AbA	aureobasidin A
ALS (f/sALS)	Amyotrophic lateral sclerosis (familial/sporadic ALS)
APS	ammonium persulfate
Baf	bafilomycin A1
BCA	bicinchoninic acid
BSA	bovine serum albumin
C	carboxy
CB	coiled body
CDK	cyclin-dependent kinase
cDNA	coding DNA
C. elegans	*Caenorhabditis elegans*
CFTR	cystic fibrosis transmembrane conductance regulator
CHMP	charged multivesicular protein
CTF	C-terminal fragment
CUE	coupling of ubiquitin conjugation to endoplasmic reticulum degradation
Δ	deletion
DENN	differentially expressed in normal and neoplastic cells
DEPC	diethylpyrocarbonate
DMEM	Dulbecco's modified eagle medium
DMSO	dimethyl sulfoxide
DTT	dithiothreitol
DUB	deubiquitinating enzyme
ECL	enhanced chemiluminescence
E. coli	*Escherichia coli*
EDTA	ethylenediaminetetraacetic acid
EEA1	early endosome antigen 1
EGFP	enhanced green fluorescent protein
EGFR	epidermal growth factor receptor
EGTA	ethylene glycol tetraacetic acid
eIF	eukaryotic initiation factor
ERK	extracellular signal regulated kinases
ESCRT	endosomal sorting complexes required for transport
EWSR	Ewing sarcoma break region 1
EXOSC10	exosome component 10, PM/Scl-100 (polymyositis/scleroderma autoantigen 2, 100kDa)
FCS	fetal calv serum
FET	FUS, EWSR1 and TAF15 gene family
FIG4	gene encoding for FIG4 homolog SAC1 lipid phosphatise domain containing protein
FL	full length
FTD	Frontotemporal dementia
FTLD (f/sFTLD)	Frontotemporal lobar degeneration (familial/sporadic FTLD)
FUS	fused in sarcoma
Gal4-AD/-BD	Gal4 activation domain/ binding domain
GAPDH	Glyceraldehyde 3-phosphate dehydrogenase
GEM	Gemini of coiled body
GFP	green fluorescent protein
GRD	glycine-rich domain

GRN	gene encoding progranulin
HA	hemagglutinin
HDAC6	histone deacetylase 6
HECT	homologous to E6-AP carboxy-terminus
HEK	human embryonic kidney
HEPES	4-(2-hydroxyethyl)-1-piperazineethanesulfonic acid
His	histidine
HIV	human immunodeficiency virus
hnRNP	heterogenous nuclear ribonucleoprotein
hPBGD	human porphobilinogen deaminase
HRP	horseradish peroxidise
Hrs	hepatocyte growth factor-regulated tyrosine kinase substrate
IBMPFD	inclusion body myopathy with Paget's disease of bone and frontotemporal dementia
IF	immunofluorescence
ISG15	Interferon-induced 17 kDa protein
IP	immunoprecipitation
iPS	inducible pluripotent stem cell
KPNA4	karyopherin alpha 4 (importin subunit alpha-4)
LAMP-1	lysosomal-associated membrane protein 1
LB	Luria Bertani
LC3	microtubule-associated protein 1A/1B-light chain 3
LSM6	U6 snRNA-associated Sm-like protein LSm6
MAPK	mitogen-activated protein kinases
MAPT	gene encoding the microtubule associated protein tau
MED6	Mediator of RNA polymerase II transcription subunit 6
miRNA	micro RNA
MIT	microtubule interacting and transport
MND	motor neuron disease
mRNA	messenger RNA
MVB	multivesicular body
N	amino
NES	nuclear export signal
NFL	low molecular weight neurofilament
NLS	nuclear localization sequence
NLSmut	NLS (1/2) mutated
Ni-NTA	nickel-nitrilotriacetic acid
NP-40	Nonident P-40
NZF	nuclear protein localization 4 zinc finger
OPTN	gene encoding for optineurin
ORF	open reading frame
pA	poly-adenylation site
PAGE	polyacrylamide gel electrophoresis
P-body	processing body
PBS	phosphate buffered saline
PCR	polymerase chain reaction
PDL	poly-D-lysine
PEG	polyethylene glycol
PFA	paraformaldehyde
PML-NB	promyelotic leukaemia nuclear bodies
pre-mRNA	precursor mRNA
PTPIP51	protein tyrosine phosphatase-interacting protein-51
PVDF	polyvinylidene fluoride
Q/N	glutamine/asparagine
RACK1	receptor for activated C kinase 1
RAN	repeat associated non-ATG initiated
RBM45	RNA-binding protein 45
REP	rough eye phenotype
RING	Really Interesting New Gene
RIPA	radio immunoprecipitation assay

RNAi	RNA interference
RRM	RNA recognition motif
SAP	shrimp alkaline phosphatise
S. cerevisiae	*Saccharomyces cerevisiae*
scr	scrambled
SDS	sodium dodecyl sulphate
SH3	src homology 3
shRNA	small hairpin RNA
siRNA	small interfering RNA
SKAR	ribosomal S6 kinase 1 (S6K1) Aly/REF-like target
SMN	survival motor neuron
snRNP	small nuclear ribonucleoprotein
SOD1	superoxide dismutase 1
sqRT-PCR	semi-quantitative reverse transcription PCR
SQSTM1	gene encoding for p62/sequestosome-1
STAM	signal transducing adaptor molecule
SUMO	small ubiquitin-like modifier
TAF15	TATA box binding protein associated factor
T-Ag	SV-40 large T antigen
TAR	transactive response
TARDBP	gene encoding human TDP-43
TBE	Tris borate buffer
TBPH	*Drosophila* ortholog of TDP-43
TBS	Tris buffered saline
TDP-43	TAR DNA-binding protein of 43kDa
TEMED	N,N,N',N'-tetramethylethylendiamine
Ub	ubiquitin
UBC	ubiquitin-conjugating
UBPY	ubiquitin isopeptidase Y
UBQLN2	gene encoding for ubiquilin-2
UIM	ubiquitininteracting motif
UPS	ubiquitin proteasome system
USP	ubiquitin-specific proteases
UTR	untranslated region
VAPB	VAMP-associated protein B
VCP	valosin-containing protein
VHS	Vps27/Hrs/STAM
v/v	volume per volume
w/v	weight per volume
wt	wild type
XαGal	5-bromo-4-chloro-3-indolyl-α-D-galactopyranoside
Y2H	yeast two-hybrid

1   Summary

The TAR DNA binding protein of 43kDa (TDP-43) is the major component of insoluble protein aggregates in amyotrophic lateral sclerosis (ALS) and a subgroup of fronto-temporal lobar degeneration (FTLD-TDP). Within these pathological aggregates TDP-43 is phosphorylated, ubiquitinylated and fragmented. The nucleic acid binding protein TDP-43 participates in mRNA splicing, stability, and transport as well as miRNA biogenesis. Therefore, this protein is part of distinct complexes whose functions are not fully understood.

This study aimed to identify novel TDP-43 protein interactors, which may allow to get further insights into the functions of this protein. To this end, a yeast two-hybrid screen was performed utilizing as bait a C-terminal fragment (CTF) that is comprised of the RNA recognition motif 2 (RRM2) and the protein binding glycine-rich domain, and a human adult brain cDNA library. Ten positive clones with partial cDNAs were found, of which seven full length cDNAs could be cloned. Their interactions with full-length TDP-43 and CTF were confirmed with coimmunoprecipitation and colocalization in human embryonic kidney (HEK293E) cells.

TDP-43 is ubiquitinylated in pathological inclusions. Therefore, the roles of the class III E2 ubiquitin-conjugating enzyme UBE2E3 and the ubiquitin isopeptidase UBPY in ubiquitinylation of TDP-43 were further investigated. The inhibition of the proteasome in HEK293E cells resulted in the ubiquitinylation and a shift of TDP-43 into insoluble fractions. The three class III E2 enzymes UBE2E1, UBE2E2 and UBE2E3 can enhance the ubiquitinylation of TDP-43 upon overexpression, whereas the catalytically inactive UBE2E3 C145S failed to promote TDP-43 ubiquitinylation. Conversely, silencing of UBE2E3 reduced the amount of ubiquitinylated TDP-43. Additionally, the overexpression of UBPY reduced the ubiquitinylation of CTF and a nuclear import impaired TDP-43 mutant. This was dependent on the peptidase activity of UBPY, since two catalytically inactive mutants failed to reduce the ubiquitinylation of TDP-43. In this study the ubiquitinylation pattern of 15 out of 48 known pathogenic TDP-43 mutants was investigated. Only the TDP-43 K263E mutant was excessively ubiquitinylated. The ubiquitinylation of TDP-43 K263E was further enhanced upon proteasomal inhibition as well as UBE2E3 expression, but it was decreased by UBPY overexpression or UBE2E3 silencing. In *Drosophila melanogaster*, UBPY silencing in the eye enhanced a neurodegenerative TDP-43 phenotype and levels of insoluble higher molecular weight TDP-43 and ubiquitin were increased.

In summary, UBE2E3 and UBPY regulate TDP-43 ubiquitinylation, solubility and possibly neurodegenerative effects. As such, UBPY might participate in decreasing pathological levels of aggregation-prone ubiquitinylated TDP-43.

Zusammenfassung

Das TAR DNA bindende Protein 43 (TDP-43) ist die Hauptkomponente unlöslicher Proteineinschlüsse in amyotropher Lateralsklerose (ALS) und einem Teil der frontotemporalen Lobärdegeneration (FTLD-TDP). Innerhalb dieser pathologischen Einschlüsse ist TDP-43 phosphoryliert, ubiquitinyliert und fragmentiert. Das Nukleinsäure-bindende Protein TDP-43 ist an verschiedenen Schritten des RNA-Metabolismus beteiligt, indem es mit unterschiedlichen Proteinkomplexen interagiert. Die Aufgaben, die TDP-43 innerhalb dieser Komplexe erfüllt, sind noch immer unklar.

Das Ziel dieser Arbeit war die Identifizierung neuer Protein-Interaktoren von TDP-43, um dessen Funktionen besser zu verstehen. Zu diesem Zweck wurde ein Hefe-2-Hybrid Screen durchgeführt. Hierfür wurden ein C-terminales Fragment (CTF) von TDP-43, welches die Protein-bindende Domäne enthält, sowie eine cDNA Bibliothek verwendet, welche aus Gehirnmaterial eines erwachsenen Menschen gewonnen wurde. Zehn positive Treffer wurden entdeckt, die partielle cDNAs enthielten. Die vollständigen cDNAs von sieben Treffern wurden kloniert und deren Interaktionen mit TDP-43 und CTF mit Hilfe von Immunopräzipitation und Kolokalisation in humanen embryonalen Nierenzellen (HEK293E) bestätigt.

TDP-43 liegt in pathologischen Einschlüssen ubiquitinyliert vor. Deshalb wurde die Beteiligung des Klasse III E2 Ubiquitin-konjugierenden Enzyms UBE2E3 und der Ubiquitin-Isopeptidase UBPY an der Ubiquitinylierung von TDP-43 genauer untersucht. Die Hemmung des Proteasoms führte zur Anreicherung von unlöslichem, ubiquitinyliertem und auch fragmentiertem TDP-43. Die Überexpression der drei bekannten Klasse III UBE2E Enzyme UBE2E21, UBE2E2 und UBE2E3 verstärkte die Ubiquitinylierung von TDP-43, wohingegen die katalytisch inaktive UBE2E3 Mutante C145S dies nicht vermochte. Umgekehrt verminderte die Herunterregulierung von UBE2E3 mittels RNA-Interferenz die Ubiquitinylierung von TDP-43. Weiterhin wurde die Ubiquitinylierung von 15 pathogenen TDP-43 Mutanten untersucht, die sich jedoch größtenteils wie wild-typisches TDP-43 verhielten. Auffallend war die TDP-43 K263E Mutante, welche stark ubiquitinyliert war. Dies wurde durch die Inhibierung des Proteasoms und die Überexpression von UBE2E3 weiter verstärkt. Umgekehrt verminderte sowohl RNA-Interferenz von UBE2E3 als auch die Überexpression von UBPY die Ubiquitinylierung der K263E Mutante. Weiterhin konnte gezeigt werden, dass UBPY die Ubiquitinylierung von K263E, CTF und einer zytoplasmatischen TDP-43 Mutante reduziert. Dies erfolgte jedoch nicht durch zwei katalytisch inaktive UBPY Mutanten. Schließlich wurde der neurodegenerative Phänotyp von humanem TDP-43

im Auge eines *Drosophila melanogaster* Toxizitätsmodels durch die Herunterregulierung von UBPY verstärkt. Weiterhin führte die UBPY RNA-Interferenz im Fliegenauge zu einer Anreicherung von unlöslichem und höher molekularem TDP-43.

Diese Arbeit zeigt, dass UBE2E3 und UBPY an der Regulierung der Ubiquitinylierung, Löslichkeit und möglicherweise an neurodegenerativen Effekten von TDP-43 beteiligt sind. Somit könnte UBPY an der Verminderung der pathologischen Menge von zur Aggregation neigendem TDP-43 beteiligt sein.

2 Introduction

2.1 TDP-43 proteinopathies

Many neurodegenerative diseases share the presence of insoluble protein aggregates, which are - if localized intracellularly - often ubiquitinylated and abnormally phosphorylated. The two seemingly distinct neurodegenerative diseases amyotrophic lateral sclerosis (ALS) and a subgroup of frontotemporal lobar degeneration (FTLD-TDP) exhibit inclusions positive for the TAR DNA-binding protein of 43kDa (TDP-43) (Arai et al., 2006; Neumann et al., 2006). In the last decade it became apparent that both distinct diseases represent the ends of a disease spectrum with overlapping symptoms, which are now summarized as TDP-43 proteinopathies. Noteworthy, TDP-43 pathology is also observed in 20-60% of Alzheimer's disease and Lewy body disorders, in Guamanian ALS-parkinsonism-dementia complex, in some cases of hippocampal sclerosis, in Huntington's disease and in the rare Perry syndrome (summarized in Baloh, 2011; Geser et al., 2010; Mackenzie et al., 2010b). However, in these diseases the amount and distribution of TDP-43 pathology is limited and different when compared to ALS and FTLD-TDP cases. Therefore, only ALS and FTLD will be introduced here.

2.1.1 ALS - clinical characteristics and pathology

ALS, also known as Lou Gehrig's disease, is the most common adult onset motor neuron disease (MND). It was first described by Jean-Martin Charcot in the 1870s and is characterized by progressive muscle wasting (atrophy) due to degeneration of lower motor neurons in the spinal cord and their axons, and of upper motor neurons in the motor cortex (lateral sclerosis). Further symptoms are muscle spasticity, and difficulties in speaking, swallowing and breathing (dysarthria, dysphagia, dyspnea). Within 3-5 years after disease onset patients typically die due to respiratory failure. The prevalence for ALS among Caucasians ranges from 1.2-4.0 per 100000 person/year, with males affected slightly more often than females (Gordon, 2013). To date, ALS cannot be cured and the only live-prolonging treatment is with the anti-glutamatergic agent Riluzole that might reduce exitotoxicity in ALS (Bensimon et al., 1994). Other therapies aim to reduce symptoms and improve the quality of life of the patients.

The pathology of ALS includes Bunina bodies and skein-like or Lewy-body-like ubiquitin-positive inclusions (Okamoto et al., 2008), mainly in lower motor neurons and less frequently in upper motor neurons (Cairns et al., 2007). Other cellular abnormali-

ties are mitochondrial vacuolization, fragmentation of the Golgi apparatus and abnormalities at the neuromuscular junction (Blokhuis et al., 2013). Interestingly, TDP-43 and ubiquitin positive inclusions are found in about 97% of all ALS cases, and thus TDP-43 is the major ubiquitinylated protein in such inclusions (Ling et al., 2013). Inclusions in the remaining 3% of ALS cases are either positive for superoxide dismutase 1 (SOD1) or Fused in Sarcoma (FUS).

2.1.2 FTLD - clinical characteristics and pathology

FTLD is one of the most common causes of early-onset dementia (Rossor et al., 2010). The term FTLD summarizes a clinically, pathologically and genetically heterogeneous group of disorders which are characterized by progressive decline in behaviour or language and associated with atrophy in the frontal and temporal lobe of the brain. Frontotemporal dementia (FTD) is the clinical syndrome of FTLD. Depending on the early and predominant symptoms, three types of FTD can be classified: the behavioural variant (bvFTD), and the two language variants semantic dementia (SD) and progressive nonfluent aphasia (PNFA) (Rabinovici and Miller, 2010). The median survival is rated to 6-11 years from onset of symptoms and 3-4 years from diagnosis, though time of survival varies among the three clinical subtypes (Rabinovici and Miller, 2010). As for ALS, there is no cure for FTLD, thus therapies focus on symptomatic treatment. The strongest biological rationale for treatment is the modification of serotonin uptake with selective inhibitors, as patients show deficits in the serotonin system (Huey et al., 2006).

Three major proteins characterize the pathology of FTLD. In about 45% of the FTLD patients the pathological depositions are positive for the microtubule associated protein tau, while another 45% show TDP-43 inclusions and 9% exhibit abnormal accumulations of FUS (Ling et al., 2013). Thus, FTLD is classified into FTLD-Tau, FTLD-TDP and FTLD-FUS (Figure 2.1). A rare fourth subgroup with inclusions that show
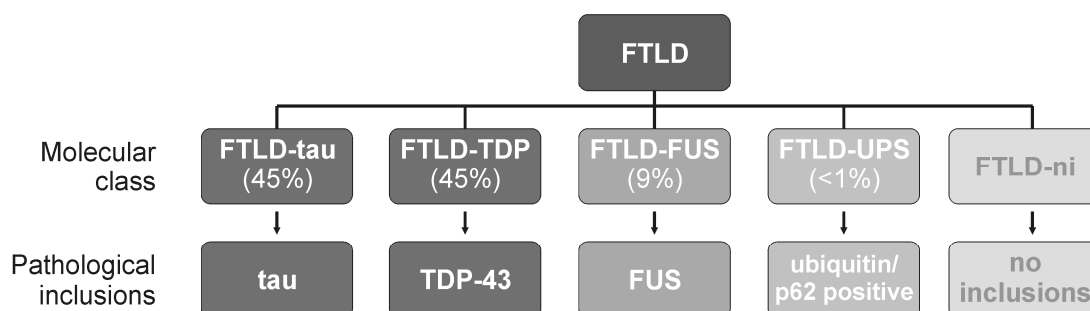
Figure 2.1 Molecular and neuropathological classification of FTLD. Based on the molecular pathology of the major inclusion proteins, three distinct subgroups of FTLD were identified: FTLD-Tau, FTLD-TDP and FTLD-FUS. The inclusions of FTLD-TDP and -FUS are also immunoreactive for ubiquitin. The molecular pathology FTLD-UPS is still not determined, but contains proteins of the ubiquitin-proteasome system. FTLD-ni cases exhibit no inclusions (ni). Adapted from (Mackenzie et al., 2010a).

immunoreactivity for components of the ubiquitin-proteasome system (FTLD-UPS) is still pathologically unidentified (Halliday et al., 2012). Additionally, rare cases without inclusions are designated FTLD-ni (no inclusions).

2.1.3 FTLD-MND

ALS and FTLD are not two distinct conditions but the ends of a disease spectrum with overlapping clinical, pathological and genetic features (Figure 2.2). In ALS, cognitive and behavioural impairment is observed in half of the patients and about 15% meet criteria for FTLD (Ringholz et al., 2005; Wheaton et al., 2007). Also, 10-15% of FTLD cases are accompanied by MND, mostly in patients with bvFTD (Hodges et al., 2003), thus manifesting an overlap of ALS with FTLD. FTLD-MND patients can first show symptoms of either FTLD or ALS and additional symptoms develop upon disease progression, usually within 6-12 months (Bak and Hodges, 2001). Generally, the survival time of FTLD-MND is shorter than of pure ALS or FTLD (Hodges et al., 2003).

2.2 Genetic causes of ALS and FTLD

ALS and FTLD are not only linked clinically and pathologically. Common genetic mutations confirm the connection of both diseases. The majority of ALS cases are sporadic (sALS), while only 5-10% have a familial background (Leblond et al., 2014; Ling et al., 2013). The mutations in *C9ORF72, SOD1, TARDBP* and *FUS* account for over 50% of familial ALS (fALS), and they are rarely detected in sALS. About 50% of the FTLD cases are genetically linked. Mutations in *MAPT* and *GRN* contribute to approximately 20% of FTLD cases. However, mutations in *TARDBP* and *FUS* are rarely observed in FTLD. Further mutated genes have also been reported for rare cases of ALS, but the causes of the remaining cases of fALS and the majority of sALS and FTLD are still unknown. In Figure 2.2 the major mutated genes are plotted according to the ratio of known mutations that give rise to ALS and FTLD. All known mutated genes involved in ALS, FTLD and FTLD-MND are summarized in Table 2.1.
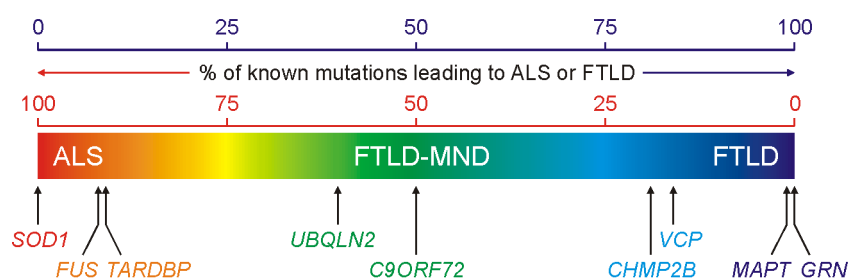
Figure 2.2 Clinical and genetical overlap of ALS and FTLD. ALS and FTLD represent the outer ends of a spectrum of neurodegenerative disorders with overlapping symptoms. The major genetic causes for both diseases are plotted according to the ratio of known mutations that lead to ALS or FTLD. Modified from Ling et al. (2013).

Table 2.1 Genetics and pathology of ALS and FTLD modified from Ling et al. (2013).

	Diseases	Locus	Mutated gene (protein)	Protein function	Heredity	fALS	sALS	FTLD	Patholog. inclusions	References
Typical ALS	ALS1	21q22.1	*SOD1* (superoxide dismutase 1)	Detoxification enzyme	AD	10-20%	2%	-	SOD1	Rosen et al. (1993)
	ALS6, FTLD	16-11.2	*FUS* (Fused in sarcoma)	RNA processing	AD, AR	5%	<1%	<1%	FUS	Kwiatkowski et al. (2009); Vance et al. (2009)
	ALS10, FTLD	1p36.22	*TARDBP* (TAR DNA-binding protein of 43kDa)	RNA processing	AD	3%	1.5%	<1%	TDP-43	Kabashi et al. (2008); Sreedharan et al. (2008); Van Deerlin et al. (2008)
	ALS9, PD	14q11.2	*ANG* (Angiogenin)	Angiogenic activity	AD				TDP-43	Greenway et al. (2006)
	ALS11, CMT4J	6q21	*FIG4* (phosphoinositide 5-phosphatase)	Lipid metabolism	AD					Chow et al. (2009)
	ALS12, POAG, PDB	10p15-p14	*OPTN* (Optineurin)	Multifunction	AD, AR	4%	<1%	-	TDP-43	Maruyama et al. (2010)
	ALS14, FTLD, IBMPFD	9p13.3	*VCP* (Valosin-containing protein)	Protein quality control	AD	1%	1%	1%	TDP-43	Johnson et al. (2010); Watts et al. (2004)
		12q24	*DAO* (D-amino acid oxidase)	Amino acid metabolism	AD					Mitchell et al. (2010)
		17p13.2	*PFN1* (Profilin)	Cytoskeleton	AD					Wu et al. (2012)
	ALS13, SCA2	12q24.12	*ATXN2* (ataxin-2)	RNA processing	Risk factor				TDP-43	Elden et al. (2010)
	MSP	5q13.2	*HNRNPA1* (hnRNPA1)	RNA processing	AD					Kim et al. (2013)
	MSP	12q22.11	*HNRPA2B1* (hnRNPA2/B1)	RNA processing	AD					Kim et al. (2013)
	PDB	5q35.3	*SQSTM1* (p62/sequestosome-1)	Protein degradation	AD					Fecto et al. (2011); Teyssou et al. (2013)
		21q12.2	*EWSR1* (Ewing sarcoma break region 1)	RNA processing	AD					Couthouis et al. (2012)
		17q12	*TAF15* (TATA box binding protein associated factor)	RNA processing	AD					Couthouis et al. (2011)
	ALS3	18q21	unknown	unknown	AD					Hand et al. (2002)
	ALS7	20p13	unknown	unknown	AD					Sapp et al. (2003)

	Diseases	Locus	Mutated gene (protein)	Protein function	Heredity	fALS	sALS	FTLD	Patholog. inclusions	References
Atypical ALS	ALS2, infantile-onset HSP	2q33.1	*ALS2* (Alsin)	Vesicle trafficking	AR					Hadano et al. (2001)
	ALS5, HSP	15q15-21	*SPG11* (Spatacsin)	Axonal transport	AR					Daoud et al. (2012)
	ALS4, AOA2	9q13.3	*SETX* (Senataxin)	RNA processing	AD					Chen et al. (2004)
	ALS8, late-onset SMA	20q13.3	*VAPB* (VAMP-associated protein)	Vesicle trafficking	AD					Nishimura et al. (2004)
FTLD-MND	FTLD-MND	9q21-22	*C9ORF72* (C9ORF72)	Unknown	AD	12-25%	6-7%	10-50% (fFTLD), 5-7% (sFTLD)	TDP-43	DeJesus-Hernandez et al. (2011); Renton et al. (2011)
	FTLD-MND	9p13.3	*SIGMAR1* (Non-opioid receptor 1)	Signal transduction	AD, AR					Luty et al. (2010)
	FTLD-MND-X	Xp11.21	*UBQLN2* (Ubiquilin-2)	Protein degradation	XD	<1%		>1%	TDP-43, FUS	Deng et al. (2011b)
FTLD	FTLD-Tau	17Q21	*MAPT* (Microtuble-associated protein tau)	Cytoskeleton	AD			10%	Tau	Hutton et al. (1998)
	FTLD-TDP	17q21.31	*GRN* (Progranulin)	Inflammation	AD			10%	TDP-43	Baker et al. (2006); Cruts et al. (2006)
	FTLD-UPS	3p11.2	*CHMP2B* (Charged multivesicular protein 2B)	Vesicle trafficking	AD	<1%		<1%	p62	Parkinson et al. (2006); Skibinski et al. (2005)
	FTLD-TDP	7p21.3	*TMEM106B* (Transmembrane protein 106B)	Lysosome function	Risk factor					Van Deerlin et al. (2010)

Abbreviations: AD - autosomal dominant; **AR** - autosomal recessive; **XD** - X-linked dominant; **AOA2** - ataxia-ocular apraxia-2; **CMT4J** - Charcot-Marie-Tooth disease type 4J; **HSP** - hereditary spastic paraplegia; **IBMPFD** - inclusion body myopathy with Paget's disease of the bone; **MSP** - multisystem proteinopathy; **PD** - Parkinson's disease; **PDB** - Paget's disease of the bone; **POAG** - primary open angle glaucoma; **SCA2** - spinocerebellar ataxia type 2; **SMA** - spinal muscular atrophy

2.2.1 Genetic implications for altered RNA metabolism in ALS and FTLD

Many of the disease-causing mutations were identified in genes encoding proteins with functions in RNA metabolism, among them TDP-43, the three FET proteins Fused in sarcoma (FUS), Ewing sarcoma break region 1 (EWSR) and TATA box binding protein associated factor (TAF15), angiogenin, senataxin, ataxin-2, and the heteronuclear ribonucleoproteins hnRNPA1 and hnRNPA2/B1. Moreover, a hexanucleotide repeat expansion in the *C9ORF72* gene supports RNA mediated toxicity. Thus, aberrant RNA processing might play an important role in the pathogenesis of ALS and FTLD. Next, a short overview of ALS, FTLD and FTLD-MND genetically associated proteins partitioning in RNA metabolism is given. The contributions of TDP-43, FUS and C9ORF72 are of high interest.

TARDBP/ TDP-43

Mutations in *TARDBP*, which encodes for the DNA/RNA binding protein TDP-43, account for 3% of fALS cases, and are rarely observed in sALS and FTLD (Lattante et al., 2013). 48 mutations are known to date, of which 47 lead to the change of a single amino acid (Lattante et al., 2013). Most mutations are located in the C-terminus of TDP-43 that is important for protein-protein interactions (see below). TDP-43 will be introduced in detail in chapter 2.3.

FUS/ Fused in sarcoma

The DNA/RNA binding protein FUS is predominantly localized in the nucleus and has functions in transcriptional regulation, splicing and transport of RNAs to the cytoplasm (Lagier-Tourenne et al., 2010; Ling et al., 2013). FUS is also recruited to stress granules and is detected in dendritic RNA granules and spines in neurons (Bentmann et al., 2012). Thus, FUS shares functional homology with TDP-43 (see below). The so far 58 known mutations are clustered in the RNA binding domain at the C-terminus of FUS or in the central glycine-rich domain (GRD), and were identified in 5% of fALS, in less than 1% of sALS and in rare cases of FTLD (Kwiatkowski et al., 2009; Lattante et al., 2013; Vance et al., 2009). Several ALS-linked mutations lead to a redistribution of FUS to the cytoplasm, pointing towards loss of nuclear function of the protein. FUS positive inclusions are rarely detected in ALS, but in most cases of FTLD patients with ubiquitin-positive and TDP-43 negative inclusions (Figure 2.1). It is noteworthy that ALS-linked mutations were identified in the genes encoding EWSR and TAF15 (Couthouis et al., 2012; Couthouis et al., 2011). Together with FUS, these proteins comprise the FET proteins that are similar in function and structure (Tan and Manley, 2009). Moreover, EWSR and TAF15 are also detected in FTLD-FUS inclusions

(Mackenzie and Neumann, 2012). However, the mutations in *EWSR* and *TAF15* remain to be proven causative for ALS.

C9ORF72/ C9ORF72

Recently, a GGGGCC hexanucleotide repeat expansion in the first intron between the first and second non-coding exon of the *C9ORF72* gene on chromosome 9 was identified in sporadic and familial ALS and FTLD (DeJesus-Hernandez et al., 2011; Gijselinck et al., 2012; Renton et al., 2011). This mutation is the most common genetic cause for familial ALS and FTLD (12-25% and 10-50%, respectively), and is also found in many patients of these diseases with no familial background (6-7% in sALS and 5-7% in sFTLD) (Heutink et al., 2014). Hexanucleotide repeat expansions were also detected in rare cases of Alzheimer's disease and in corticobasal and ataxic syndromes (Harms et al., 2013; Kohli et al., 2013; Lindquist et al., 2013), though the identification in some Alzheimer's disease patients could also point towards a false diagnosis. Indeed, some of the Alzheimer's disease cases were *post mortem* diagnosed with FTLD (Kohli et al., 2013)

C9ORF72 is translated into two proteins of 222aa and 481aa that share the same N-terminus, but the longer protein exhibits an expanded C-terminus. The function of the C9ORF72 transcript is unknown. A <u>d</u>ifferentially <u>e</u>xpressed in <u>n</u>ormal and <u>n</u>eoplastic cells (DENN) domain was identified in the N-terminus of both C9ORF72 proteins. This domain is also present in GDP-GTP exchange factors that activate Rab GTPases, suggesting a role of the C9ORF72 transcript in Rab GTPase-dependent membrane trafficking (Levine et al., 2013; Zhang et al., 2012). The subcellular localization of the protein is not well studied, since only few specific antibodies are available. One report showed that the overexpressed C9ORF72 protein is located in the nucleus and cytoplasm and, additionally, is secreted (Farg et al., 2014).

Three hypothesises are considered about the pathogenic mechanism of the hexanucleotide repeat expansion (reviewed in Heutink et al., 2014). First, a reduced expression of the C9ORF72 transcript due to the repeat expansion suggests a loss-of-function. This finds support from the analysis of C9ORF72 mRNA and protein level in patient derived induced pluripotent stem (iPS) cell lines and lymphoblasts as well as in *post mortem* brain tissue (Belzil et al., 2013; Ciura et al., 2013; DeJesus-Hernandez et al., 2011; Donnelly et al., 2013; Gijselinck et al., 2012; Waite et al., 2014). Second, the RNA transcripts of the repeat could form toxic nuclear RNA foci. These repeat-containing RNA aggregates were detected in brains from patients and in iPS cell lines, and were shown to disrupt the RNA metabolism through the sequestration of RNA binding proteins and other RNAs (DeJesus-Hernandez et al., 2011; Donnelly et al., 2013; Lagier-Tourenne et al., 2013; Mizielinska et al., 2013; Sareen et al., 2013).

Third, it was suggested that r̲epeat a̲ssociated n̲on-ATG initiated (RAN) translation takes place within the repeat expansion. This is followed by the aggregation of the toxic dipeptide repeat proteins. In support of this hypothesis, dipeptide repeat proteins were detected with specific antibodies in *post mortem* brains, that are consistently characterized by TDP-43 pathology, and patient derived iPS cells (Ash et al., 2013; Donnelly et al., 2013; Mori et al., 2013). However, the dipeptide repeat proteins were found in brain regions not affected by TDP-43 inclusions and poorly correlate with the clinical phenotypes (Mackenzie et al., 2014). Interestingly, RAN-translated proteins from another non-coding repeat expansions disease, fragile X-associated tremor ataxia syndrome, are also associated with cellular toxicity (Todd et al., 2013).

All three hypothesises are plausible, but none of them is conclusively established yet. It is also conceivable that two or a combination of all three mechanisms are involved in the disease pathogenesis, though this is unclear at the moment.

HNRNPA1 and *HNRNPA2B1*/ hnRNPA1 and hnRNPA2B1

Recently, missense mutations in the prion-like domains of the two hnRNPA1 and hnRNPA2B1 were identified in families of multisystem proteinopathy (MSP) and in one case of fALS (Kim et al., 2013). Usually, the prion-like domains in hnRNPs are important for their assembly in RNA granules (Kato et al., 2012). The identified mutations enhance the fibrillization of hnRNPA1 and hnRNPA2B1and promote their incorporation into stress granules (Kim et al., 2013). Thus, it is possible that mutations in other RNA-binding proteins with prion-like domains will be identified, that might also contribute to neurodegenerative proteinopathies. Indeed, TDP-43, FUS, EWSR1 and TAF15 also harbour prion-like domains (King et al., 2012; Neumann et al., 2011).

2.2.2 Further genetically associated proteins

MAPT/ tau

Under physiological conditions, alternative splicing of the *MAPT* gene generates several tau proteins that stabilize microtubules and are most abundant in neurons. Tau-positive, but ubiquitin and TDP-43 negative inclusions of great variability are detected in 45% of FTLD patients, and 44 different mutations in *MAPT* also genetically link tau to FTLD (http://www.molgen.ua.ac.be/). However, tau depositions are detected in several other neurodegenerative diseases, such as Alzheimer's disease or progressive supranuclear palsy that are summarized as tauopathies.

GRN/ progranulin

Progranulin is a glycoprotein that contains 7.5 repeats of the highly conserved 12 cysteine granulin motif (Bateman and Bennett, 2009). After secretion and the removal of the signal peptide, the mature granulin can be cleaved into active 6kDa granulin peptides (granulin A-G) by many extracellular proteases (Kessenbrock et al., 2008; Suh et al., 2012). The multifunctional progranulin was implicated in the regulation of cell division, migration, tissue repair, inflammation as well as in cancer (Bateman and Bennett, 2009; He and Bateman, 2003; He et al., 2002). 63 mutations in *GRN* are known, which account for approximately 20% of fFTLD and 1-5% of fFTLD (Gijselinck et al., 2008). The pathogenicity of some mutants is unknown, but for most mutations a loss-of-function was described. They introduce premature terminations of the mRNA, which is subsequently degraded via nonsense-mediated RNA decay, or lead to the loss of mRNA by nuclear degradation due to mutations within the Kozak sequence (Baker et al., 2006; Cruts et al., 2006). Additionally, one mutation in the N-terminal signal peptide inhibits the secretion of progranulin (Mukherjee et al., 2006). How mutated progranulin and TDP-43 are related in FTLD-TDP remains to be established.

SOD1/ superoxide dismutase 1

The superoxide dismutase (SOD1) dissipates free superoxide radicals in the cell. Over 170 mutations in the SOD1 gene are the most frequent cause of fALS, accounting for approximately 20% of fALS cases (Abel et al., 2012). SOD1 positive inclusions in ALS are negative for TDP-43 (Tan et al., 2007), thus a different pathogenesis is likely. However, it is not well understood how *SOD1* mutations contribute to ALS pathogenesis. A toxic-gain-of-function was suggested, because many mutants still exhibit their enzymatic activity. Moreover, misfolded wild-type (wt) SOD1 was recently suggested to contribute to sALS pathogenesis (Rotunno and Bosco, 2013).

2.2.3 Genetic implications for altered protein homeostasis in ALS and FTLD

Furthermore, mutations in genes which encode for proteins involved in the protein degradation or the maintenance of protein homeostasis contribute to ALS, FTLD and FTLD-MND. These proteins are ubiquilin-2 (*UBQLN2*), valosin-containing protein (*VCP*), vesicle-associated membrane protein-associated protein B/C (*VAPB*), p62/sequestosome-1 (*SQMST1*), optineurin (*OPTN*), FIG4 homolog SAC1 lipid phosphatise domain containing protein (*FIG4*) and charged multivesicular body protein 2b (*CHMP2B*). Ubiquilin-2, p62, optineurin and VCP are directly associated with the degradation of proteins, while CHMP2B and FIG4 participate in the maturation of autophagosomes.

UBQLN2/ ubiquilin-2

Ubiquilin-2 binds polyubiquitinylated proteins and guides them to the proteasome for degradation (Ko et al., 2004). Ubiquilins are also associated with autophagy (Rothenberg et al., 2010). Rare mutations in *UBQLN2* cause a small subset of ALS and FTLD-MND, whereas ubiquilin-2 positive depositions, that also co-localize with TDP-43, FUS and p62, are a common pathological feature among many cases of ALS, FTLD-MND and FTLD (Deng et al., 2011b). Interestingly, the expression of ubiquilin-2 with ALS-linked mutations was shown to impair the overall protein degradation in cells (Deng et al., 2011b).

SQSTM1/ p62

The ubiquitin and LC3 binding protein p62/ sequestosome-1 targets also polyubiquitinylated proteins for degradation either by the proteasome or by autophagy. p62 is detected in pathological depositions in many neurodegenerative diseases, among them fALS, sALS and FTLD. Partial coimmunoreactivity with TDP-43 or ubiquilin-2 was also reported (Brettschneider et al., 2012; Teyssou et al., 2013). Missense and deletion mutations in *SQSTM1* were identified in about 1% of ALS and FTLD (Fecto et al., 2011; Kwok et al., 2014; Le Ber et al., 2013; Rubino et al., 2012; Teyssou et al., 2013).

VCP/ valosin-containing protein

VCP is a highly expressed member of the type II <u>A</u>TPase <u>a</u>ssociated with diverse cellular <u>a</u>ctivities (AAA) superfamily. VCP was shown to bind polyubiquitinylated proteins, and subjected them to multiple protein degradation pathways like autophagic and proteasomal clearance, or recycling pathways like endosomal sorting (Meyer et al., 2012). Mutations in *VCP* account for about 1% of fALS and sALS cases (Johnson et al., 2010; Koppers et al., 2012), though they were first identified as a cause for the rare inclusion body myopathy with Paget's dieseas of bone and frontotemporal dementia (IBMPFD) (Watts et al., 2004). A reduction of cellular ATP production was mediated by VCP mutants via mitochondrial uncoupling, which enhances the vulnerability of cells to cytotoxicity (Bartolome et al., 2013).

OPTN/ optineurin

The multifunctional protein optineurin binds polyubiquitinylated proteins and serves in analogy to p62 as an autophagy adapter protein (Wild et al., 2011). However, one study suggested that optineurin has a function in autophagic clearance of protein aggregates in an ubiquitin independent manner (Korac et al., 2013). Deletion, nonsense and missense mutations in *OPTN* are associated with ALS, but not FTD (Del Bo et al.,

2011; Maruyama et al., 2010). Optineurin-positive depositions were described for many neurodegenerative diseases (Osawa et al., 2011). However, optineurin pathology in ALS is controversial. In one study optineurin depositions were detected in all SOD1-negative subjects (Deng et al., 2011a). In another report optineurin was detected in inclusions immunoreactive for TDP-43 or SOD1 and in a case with mutated optineurin (Maruyama et al., 2010), but a third study did not detect optineurin pathology in cases with *OPTN* mutations (Ito et al., 2011).

VAPB/ vesicle-associated membrane protein-associated protein B/C

VAPB is an integral membrane protein of the endoplasmatic reticulum (ER) and interacts with the outer mitochondrial membrane protein tyrosine phosphatase-interacting protein-51 (PTPIP51) (De Vos et al., 2012), thus regulating ER-mitochondria associations (Stoica et al., 2014). Moreover, unfolded protein response is activated upon elevation of VAPB level (Chen et al., 2010; Kanekura et al., 2006). The expression of neither wt nor mutant VAPB in the nervous system of mice induces a neurodegenerative phenotype, but cytoplasmic accumulations immunoreactive for ubiquitin, p62 and TDP-43 develop in motor neurons of the spinal cord in 18-month old mice (Qiu et al., 2013; Tudor et al., 2010). Mutations in *VAPB* are rare and were initially identified in a Brazilian family with atypical ALS (Nishimura et al., 2004). However, the deletion variant S160 was also detected in healthy controls at low frequency (Landers et al., 2008). Moreover, a recent study detected *VAPB* mutations in Swedish, Portuguese and Icelandic patients with fALS or sALS, but also in healthy adult relatives (Ingre et al., 2013). Thus, it is questionable whether mutations in *VAPB* contribute to the pathogenesis of ALS.

FIG4/ phosphoinositide 5-phosphatase

FIG4 is translated into a phosphoinositide 5-phosphatase that plays an indirect role in autophagy and in retrograde membrane trafficking from the lysosome and late endosome to the Golgi apparatus (Rutherford et al., 2006; Suzuki and Ohsumi, 2007; Zhang et al., 2007a). Mutations in *FIG4* were first detected as a cause for Charcot-Marie-Tooth disease type 4J, an autosomal ressessive motor and sensory neuropathy (Chow et al., 2007). Later, one study identified several *FIG4* missense and truncation mutations in 2% of ALS and in primary lateral sclerosis cases from a cohort of European ancestry, with truncation mutations leading to a loss of phosphatase activity (Chow et al., 2009). Interestingly, brains from *FIG4* knockout mice exhibit disruption of autophagy in neurons and glial cells (Ferguson et al., 2009). However, further studies are not available to prove the importance of *FIG4* mutations in ALS.

CHMP2B/ charged multivesicular body protein 2B

CHMP2B is a component of the endosomal sorting complex (ESCRT)-III that is impor-
tant for the formation of the multivesicular bodies (MVBs). It is involved in protein
sorting and turnover. Rare mutations in *CHMP2B* were first identified in a large Dan-
ish family with autosomal dominant FTLD (Skibinski et al., 2005), and later confirmed
in some ALS cases (Cox et al., 2010; Parkinson et al., 2006). *CHMP2B* mutations are
the only cause of the rare FTLD-UPS with pathological inclusions positive for p62 and
ubiquitin (Mackenzie et al., 2010a), and lead to C-terminal truncation of the protein.
Interestingly, one study showed that the gene knockout or the overexpression of
CHMP2B wt in mice has no phenotype, whereas expression of a C-terminally trun-
cated mutant CHMP2B causes progressive neurological decline, axonal pathology and
early death of the animals (Ghazi-Noori et al., 2012). This indicates a toxic gain-of-
function. Moreover, the expression of CHMP2B mutants led to the inhibition of auto-
phagic clearance and an increase of ubiquitin-positive inclusions (Filimonenko et al.,
2007).

Summary and conclusion

In conclusion, mutations in *UBQLN2*, *VCP*, *SQSTM1*, *OPTN* and *CHMP2B* may point to-
wards an altered protein homeostasis with a deficiency in the clearance of proteins as
an important factor of the pathogenesis of ALS, FTLD and FTLD-MND. Additionally,
many of the proteins encoded by these genes are often detected in aggregates of non-
mutation carriers and patients suffering from other neurodegenerative diseases like
Alzheimer's or Parkinson's disease. This supports a more general role of aberrant
protein clearance or protein homeostasis in neuronal degeneration. On the other
hand, the genetic evidence of *VAPB* and *FIG4* as genes involved in ALS is not fully con-
vincing. Only one or a few reports of single pedigrees or cases were published, and
VAPB mutations were also detected in healthy controls, suggesting minor roles of
these proteins.

However, the molecular mechanisms how all these proteins contribute to the patho-
genesis of neurodegenerative diseases - regardless whether their functions point to-
wards failure of proper protein degradation or altered RNA metabolism - remain
poorly understood and require further investigations. Of great interest is TDP-43,
since it is detected in pathological depositions in 45% of FTLD patients and almost all
cases of ALS that are FUS and SOD1 negative. Moreover, there is a strong genetic link-
age of TDP-43 and ALS. Thus, unravelling the role of TDP-43 in these diseases likely
contributes to the understanding the pathogenesis of ALS and FTLD.

2.3   Characterization of TDP-43

The TDP-43 encoding gene *TARDBP* is located on locus 1p36.22 and exhibits 6 exons and 5 introns. *TARDBP* is conserved in human, mouse, *Drosophila*, and *C. elegans* (Wang et al., 2004b). The 414aa long protein is ubiquitously expressed in most tissues and exhibits many functions in the RNA metabolism and some in transcriptional regulation. Moreover, in TDP-43 proteinopathies the protein is mislocalized, aggregated, truncated into C-terminal fragments, phosphorylated and ubiquitinylated. The structure and localization as well as the many functions and the pathological alterations of TDP-43 are introduced in the following sections.

2.3.1   The structure of TDP-43

TDP-43 is a member of the heterogeneous nuclear ribonucleoprotein (hnRNP) family, a group of RNA binding proteins (Buratti and Baralle, 2008). As such, TDP-43 exhibits two N-terminal RNA recognition motifs (RRM1 and RRM2), a bipartite nuclear localization sequence (NLS), a leucine-rich nuclear export signal (NES) and a C-terminal glycine-rich domain (GRD, see Figure 2.3).

The two RRMs preferentially bind UG-rich repeats and fold into highly conserved three-dimensional conformations, and bind RNA primarily with RRM1 (Ayala et al., 2005; Buratti and Baralle, 2001; Kuo et al., 2009; Mackness et al., 2014; Ou et al., 1995). In detail, it was shown that RRM2 has a low binding affinity to RNA, whereas the affinity of RRM1 to bind RNA is much higher. The tethering of RRM2 to RRM1 further enhances the RNA affinity and stability of RRM1 (Mackness et al., 2014). Furthermore, the determination of the NMR structure of RRM1 and RRM2 in complex
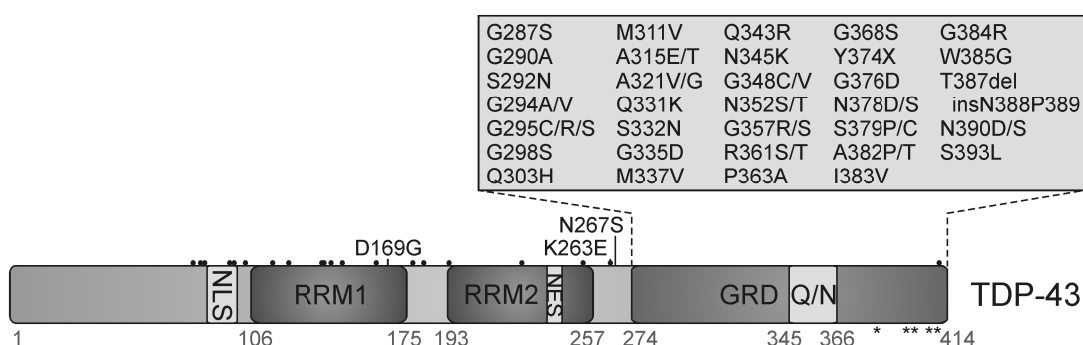
Figure 2.3 Schematic overview of the domain structure of TDP-43 with the RNA recognition motif (RRM) 1 and 2, the C-terminal glycine-rich domain (GRD) including a glutamate/ asparagine (Q/N)-rich prion-like region, the bipartite nuclear localization site (NLS, aa 82-98) and the nuclear export signal (NES, aa 239-250). Known pathogenic mutations are indicated (Lattante et al., 2013) and known phosphorylation sites (S379, S403/404, S409/410) are labelled with asterisks (*) (Hasegawa et al., 2008). The 20 lysine residues (possible ubiquitinylation sites) are indicated with dots (•). Modified from Lee et al. (2012) and Janssens and Van Broeckhoven (2013).

with a UG-rich RNA oligonucleotide of 12 bases revealed that both RRMs bind ten nucleotides, of which six are recognized sequence specifically (Lukavsky et al., 2013). A central guanine residue in the oligonucleotide was shown to be crucial for the binding of RNA through the stabilization of both RRMs. A classical RRM domain is comprised of four β-strands (β2-β3-β1-β5), but RRM2 contains an additional β4-strand next to β5 that is involved in protein-protein interactions, especially in the dimerization of TDP-43 (Kuo et al., 2009). RRM1 also plays an important role in the binding of TG-rich DNA sequences, which is supported by RRM2 (Kuo et al., 2014).

The bipartite NLS and a NES in RRM2 allow TDP-43 to shuttle between the nucleus and the cytoplasm, though the protein is predominantly localized in the nucleus (Ayala et al., 2008b; Winton et al., 2008a). The deletion of NLS or NES induces cytoplasmic or nuclear TDP-43 aggregation, respectively (Ayala et al., 2008b; Winton et al., 2008a; Zhang et al., 2013), which seems to be an important aspect of disease pathogenesis (see chapter 2.3.4). The import of TDP-43 into the nucleus is mediated by the classical karyopherin-dependent nuclear import pathway (Nishimura et al., 2010).

The C-terminal GRD of TDP-43 is less conserved among species. The whole C-terminal domain is involved in protein-protein-interactions, RNA processing, transcriptional regulation, and influences solubility and cellular localization of TDP-43 (Abhyankar et al., 2007; Ayala et al., 2008b). TDP-43 interacts with other hnRNPs via its C-terminus (see below). The identification of an RNA-binding arginine-arginine-glycine (RGG) sequence in the GRD suggests that the C-terminus participates also in protein-RNA interactions (Ou et al., 1995). Interestingly, the C-terminus of TDP-43 exhibits a glutamine/asparagine (Q/N)-rich region with prion-like properties (aa345-366) (Fuentealba et al., 2010; King et al., 2012; Wang et al., 2004b).

TDP-43 forms physiologically active homodimers via the N-terminus, RRM2 and the Q/N-rich C-terminal region (Kuo et al., 2014; Kuo et al., 2009; Shiina et al., 2010; Wang et al., 2013; Zhang et al., 2013). The first ten amino acid residues are necessary for proper homodimerization (Zhang et al., 2013). Furthermore, homodimerization happens independently of DNA or RNA binding of TDP-43 (Zhang et al., 2013). Under oxidative stress, TDP-43 can be cross-linked via cysteine oxidation and disulphide bond formation (Cohen et al., 2012). This leads to decreased solubility, and a possibly non-active TDP-43 dimer.

2.3.2 Subnuclear localization of TDP-43

Nuclear TDP-43 is concentrated in euchromatin regions of the nucleoplasm, including perichromatin fibrils, which are sites of transcription and cotranscriptional splicing. However, TDP-43 is absent in the nucleolus, where rRNA transcription takes place, and in transcriptionally silent heterochromatin (Casafont et al., 2009). An overexpressed short mouse TDP-43 variant was detected in a novel type of nuclear bodies that were termed T-bodies. These T-bodies overlapped with Cajal bodies (CBs), promyelotic leukaemia nuclear bodies (PML-NBs), Gemini of coiled bodies (GEMs) and SC35 speckles, but TDP-43 is not a component of these nuclear bodies (Wang et al., 2002). The overlap of GEMs with T-bodies was proposed to be mediated by the interaction of TDP-43 and the survival of motor neuron (SMN) protein (see also below). However, another study that investigated the localization of endogenous TDP-43 in rat neurons did not observe a localization of TDP-43 in CBs (Casafont et al., 2009). It was suggested that T-bodies link different nuclear bodies, forming a network for the processes of transcription and splicing (Wang et al., 2002).

The nucleus contains several nuclear bodies with distinct functions in transcription and splicing. CBs contain proteins important for mRNA biogenesis and, thus, exhibit several functions in the RNA metabolism. These are assembly and recycling of small nuclear ribonucleic particles (snRNPs), pre-mRNA splicing, histone mRNA processing and maintenance of telomerases (Handwerger and Gall, 2006). The signature protein of CBs is coilin. CBs associate with GEMs through the interaction of coilin with the GEM protein SMN protein and they function together in assembly and recycling of snRNPS, though they do not contain snRNPs (Cioce and Lamond, 2005). PML-NBs contain the PML protein and are associated with several cellular functions, as they transiently store and release proteins, among them transcription factors and transcriptional regulators. It is not established how transcription is regulated by PML-NBs (Bernardi and Pandolfi, 2007). SC35 speckles are rather indirectly involved in transcription and splicing, as they store and modify factors of the pre-mRNA processing machinery and are located in proximity to active transcription sites (Lamond and Spector, 2003).

The localization of TDP-43 within multiple discrete subnuclear structures that are involved in the regulation of transcription and splicing is consistent with the role of TDP-43 in transcription and splicing (see below).

2.3.3 Cellular functions of TDP-43

Transcriptional regulation

TDP-43 was first characterized for its role in DNA binding and transcriptional regula-
tion of human immunodeficiency virus 1 (HIV) (Ou et al., 1995). TDP-43 as a DNA
binding protein functions in the transcriptional repression of the spermatid-specific
mouse gene *SP-10* in somatic tissues (Abhyankar et al., 2007). The role of TDP-43 in
transcriptional regulation is further supported by its interaction with proteins in-
volved in transcription, such as methyl CpG-binding protein 2 (MeCP2) (Freibaum et
al., 2010; Sephton et al., 2011).

RNA binding properties of TDP-43

The regulatory functions of TDP-43 in RNA metabolism are much better investigated.
TDP-43 preferentially binds UG-rich repeats, for which RRM1 is important (Ayala et
al., 2011b; Ayala et al., 2005; Buratti and Baralle, 2001). However, TDP-43 also binds
to poly(A)$_n$, GC-rich or poly-pyrimidine rich sequences, and a $(UG)_nUA(UG)_m$ sequence
(Narayanan et al., 2013; Sephton et al., 2011; Xiao et al., 2011). Several high through-
put studies were conducted to identify RNAs that are bound and regulated by TDP-43
in mouse and human brain as well as in neuronal cell lines (Colombrita et al., 2012;
Narayanan et al., 2013; Polymenidou et al., 2011; Sephton et al., 2011; Tollervey et al.,
2011; Xiao et al., 2011). It was shown that TDP-43 binds over 6000 RNA species in
mouse brain, representing 30% of the total mouse transcriptome and highlighting
that TDP-43 is involved in the regulation of multiple cellular processes. The preferen-
tial binding sites of TDP-43 were in long introns (>100kb), in 3' untranslated regions
(UTRs) of mRNAs, near exon-intron junctions, but also in intronic regions far away
(>2kb) from exons, and in long non-coding RNAs (ncRNAs). These studies also em-
phasise the role of TDP-43 for the regulation of splicing in the brain. They show that
TDP-43 probably mediates alternative splicing of many transcripts encoding proteins
that regulate neuronal development, synaptic function and RNA metabolism or have
been implicated in neurological diseases (Polymenidou et al., 2011; Tollervey et al.,
2011). Thus, alterations of TDP-43 level in disease likely affect the transcription, sta-
bility and splicing of many RNAs.

mRNA splicing and regulation of mRNA stability

TDP-43 preferentially binds sequences with at least 6 UG-repeats in proximity of 5'
and 3' splice sites of pre-mRNAs, which promotes inclusion or skipping of exons
(Buratti and Baralle, 2012). More specifically, TDP-43 mediates skipping of the hu-
man cystic fibrosis transmembrane conductance regulator (CFTR) exon 9, the apoli-
poprotein A2 (ApoA2) exon 3, the eukaryotic translation termination factor 1 (ETF1),

the retinoid X receptor gamma (RXRG), and a breast cancer 1 (BRCA1)- mutated substrate (Ayala et al., 2006; Buratti et al., 2001; Mercado et al., 2005; Passoni et al., 2012). On the other hand, TDP-43 is involved in the inclusion of the SMN2 exon 7 and of the exon junction complex component ribosomal S6 kinase 1 (S6K1) Aly/REF-like target (SKAR) exon 3 (Bose et al., 2008; Fiesel et al., 2012; Shiga et al., 2012). It is noteworthy that aberrant splicing of CFTR exon 9 produces a non-functional CFTR protein, which is observed in cystic fibrosis patients. TDP-43 binds a $(UG)_m(U)_n$ regulatory repeat in the 3'splice site of CFTR intron 8 (Buratti et al., 2001), and mutations in this repeat are associated with cystic fibrosis.

Besides its modulation of splicing, TDP-43 also regulates the turnover and stability of mRNAs. TDP-43 binding stabilises the mRNAs of histone deacetylase 6 (HDAC6), human low molecular weight neurofilament (NFL), autophagy-related protein 7 (ATG7) and Futsch, which is the *Drosophila* homologue of microtubule-associated protein 1B (MAP1B) (Bose et al., 2011; Fiesel et al., 2010; Godena et al., 2011; Strong et al., 2007; Volkening et al., 2009). The knockdown of TDP-43 leads to an destabilization of HDAC6 mRNA, which impairs neurite outgrowth of differentiated human neuroblastoma cells (Fiesel et al., 2011). In line, TDP-43 inhibits an unproductive splicing of the serine/arginine-rich splicing factor 2 (SC35) mRNA, thus indirectly stabilizing the SC35 mRNA (Dreumont et al., 2010). Contrary, the mRNAs of cyclin-dependent kinase 6 (CDK6), progranulin and vascular endothelial growth factor A (VEGF-A) are destabilized in the presence of TDP-43 (Ayala et al., 2008a; Colombrita et al., 2012; Fiesel et al., 2010).

TDP-43 autoregulation

Importantly, TDP-43 autoregulates its own mRNA levels via a negative feedback loop, and thus controls its protein expression (Avendano-Vazquez et al., 2012; Ayala et al., 2011b; Polymenidou et al., 2011; Tollervey et al., 2011). Therefore, TDP-43 binds to an extended binding region in its own 3' UTR, which contains several non-UG sequences. When nuclear levels of TDP-43 are low the most efficient polyadenylation site pA1 of the TDP-43 mRNA is used, whereas high nuclear TDP-43 level result in the use of the suboptimal splice sites pA2, pA3 and pA4 (Avendano-Vazquez et al., 2012). This leads to a fast degradation of the TDP-43 mRNA, resulting in constant TDP-43 levels within cells. Consistently this autoregulation was also shown in TDP-43 transgenic mice (Igaz et al., 2011; Xu et al., 2011). Since TDP-43 can form aggregates in disease (see chapter 2.3.4) this autoregulation may be important. Aggregate formation could lead to reduced level of free nuclear TDP-43, which then may stimulate an increased TDP-43 production. This could further enhance the formation of aggregates, which might lead to cell stress or even cell death. The reduced level of free nu-

clear TDP-43 could also have serious consequences on processing and stability of many RNAs (Budini and Buratti, 2011).

TDP-43 and microRNA biogenesis

Beside its role in mRNA pathways and transcription regulation, an interaction of TDP-43 with components of the microRNA (miRNA) processing complexes Drosha and Dicer was reported (Fukuda et al., 2007; Gregory et al., 2004; Kawahara and Mieda-Sato, 2012; Ling et al., 2010). Additionally, TDP-43 localizes to the perichromatin fibres in which miRNA biogenesis is thought to occur (Casafont et al., 2009). A functional role of TDP-43 in miRNA biogenesis was demonstrated, as TDP-43 knockdown alters the level of distinct miRNAs, such as let-7b, miR-663, miR-132 and mir-143 (Buratti et al., 2010; Kawahara and Mieda-Sato, 2012). These small non-coding RNA molecules regulate the transcriptional and posttranscriptional expression of genes.

Cytoplasmic localization of TDP-43: Stress granules and other RNA granules

Although TDP-43 is predominantly nuclear, it can shuttle to the cytoplasm, where it colocalizes with other RNA binding proteins in RNA granules. These can be RNA transport granules in axons, stress granules and processing bodies (P-bodies), which contain the RNA decay machinery (Alami et al., 2014; Dewey et al., 2011; Dewey et al., 2012; Fallini et al., 2012; Moisse et al., 2009; Volkening et al., 2009; Wang et al., 2008). In the cytoplasm of primary motor neurons TDP-43 associates with SMN in axonal RNA transport granules, together with further axonal mRNA-binding proteins such as fragile X mental retardation protein (FMRP), IMP1, Hu-antigen D (HuD) and Staufen (STAU1) (Fallini et al., 2012; Wang et al., 2008). A direct interaction with IMP1 and HuD was also reported. This suggests a function for TDP-43 in axonal transport of RNAs and regulation of axonal growth.

Under conditions of oxidative and osmotic stress, TDP-43 redistributes from the nucleus to the cytoplasm into reversible stress granules. These RNA-protein complexes transiently store non-translating mRNAs, translation initiation components, and many additional proteins that affect the function of mRNAs. Thus, stress granule formation allows the selective translation of stress-response proteins, such as heat-shock proteins (Buchan and Parker, 2009). Specifically, direct interactions of TDP-43 with the stress granule markers T cells restricted intracellular antigen-1 (TIA-1), eIF3, and with polyadenylate-binding protein 1 (PABPC1) were shown (Freibaum et al., 2010; Liu-Yesucevitz et al., 2010). The incorporation of TDP-43 into stress granules is dependent on its ability to bind RNAs with RRM1 (Freibaum et al., 2010).

In stress granules, TDP-43 is probably involved in the trafficking or the stabilization of mRNAs (Colombrita et al., 2009; Dewey et al., 2011; Freibaum et al., 2010; Liu-

Yesucevitz et al., 2010; McDonald et al., 2011). Interestingly, TDP-43 was shown to directly interact with FUS, another RNA-binding protein that is implicated in ALS and FTLD (Freibaum et al., 2010; Kim et al., 2010; Ling et al., 2010). FUS is also recruited into stress granules and other RNA granules (Bentmann et al., 2012). Thus, it is possible that FUS and TDP-43 function in a similar pathway.

The protein interactome of TDP-43

TDP-43 usually functions as a part of multiple complexes. This became most apparent in a global proteomic screen which detected 261 TDP-43 interacting proteins that either cluster a nuclear network that regulates RNA splicing and other aspects of nuclear RNA metabolism, or in the cytoplasm, which regulate mRNA translation, stability and transport (Freibaum et al., 2010). They showed that TDP-43 interaction with some proteins is dependent on TDP-43 interaction with RNA, whereas other interactions are RNA-independent. A list of approximately 30 until now validated TDP-43 protein interactors can be found in Budini et al. (2014). Some of the interactions might be relevant in the development of ALS or FTLD. Thus, for a better understanding of its functional roles, it is important to study protein interactions of TDP-43.

The first published interactor of TDP-43 was the murine SMN protein that co-localizes with TDP-43 in nuclear GEMs (Tsuiji et al., 2013; Wang et al., 2002). Thus, TDP-43 may act as a scaffold for nuclear bodies through the interaction with SMN (Wang et al., 2002). As an hnRNP family member, the GRD of TDP-43 mediates interaction with several other hnRNP proteins, specifically hnRNPs A1, A2/B1, C1/C2, and A3, (Buratti et al., 2005; D'Ambrogio et al., 2009). Further interactors of this protein family were identified in proteomic screens (Freibaum et al., 2010; Jeronimo et al., 2007; Ling et al., 2010), confirming a role of TDP-43 in hnRNP complexes which regulate mRNA splicing and other steps of gene expression (Buratti and Baralle, 2010).

Furthermore, TDP-43 interacts RNA-dependently with ataxin-2, a polyglutamine protein that is mutated in spinocerebellar ataxia type 2, and also a risk factor for ALS (Elden et al., 2010). It was reported, that ataxin-2 enhances TDP-43 toxicity in yeast and *Drosophila* (Elden et al., 2010). Moreover, enhanced levels of ataxin-2 impair the assembly of TDP-43 and also of FUS, into RNA granules (Nihei et al., 2012). This leads to an aberrant cytoplasmic distribution of both proteins, which might impair the RNA quality control. The interaction of TDP-43 with ubiquilin-2, another transcript of an ALS-linked gene (see chapter 2.2), suggests that ubiquilin-2 is involved in the clearance of TDP-43 (Cassel and Reitz, 2013). It was proposed that aberrant clearance of TDP-43 and its C-terminal fragments might play a role in neurotoxicity mediated by TDP-43.

2.3.4 Pathology of TDP-43 in FTLD-TDP and ALS

The presence of abnormal protein aggregates in the cytoplasm of neurons is characteristic for many neurodegenerative diseases. In 2006, TDP-43 was identified as the hallmark protein in pathological inclusions of most ALS and half of FTLD patients (Arai et al., 2006; Neumann et al., 2006). In neurons and glia cells of these patients, TDP-43 is ubiquitinylated, hyperphosphorylated, mislocalized, aggregated and cleaved into C-terminal fragments (CTFs) (see Figure 2.4).

Moreover, the identification of mutations in *TARDBP* mainly in ALS patients, but also in some rare FTLD cases, further emphasizes the role of TDP-43 in the pathogenesis of these neurodegenerative diseases. The underlying mechanistic pathogenicity of these modifications remains poorly understood. The next section gives an overview of known pathological modifications of this protein.

Mislocalization and nuclear clearance of TDP-43

In ALS and FTLD-TDP, TDP-43 mislocalizes to the cytoplasm in form of aggregates, accompanied by nuclear clearance of TDP-43 in surviving neuronal cells (Neumann et al., 2006). Some nuclear mislocalization was also described in form of aggregates with lenticular morphology (see Figure 2.4F) (Davidson et al., 2007; Mackenzie et al., 2011). Nuclear clearance is an early event, as it is observed in cells with pre-inclusions. These cells do not contain inclusions but exhibit diffuse cytoplasmic and ubiquitin negative TDP-43 staining (Brandmeir et al., 2008; Geser et al., 2008; Giordana et al., 2010). The clearance of nuclear TDP-43 is thought to disrupt the normal nuclear function of TDP-43 as knockdown in human cell lines induces morphological nuclear defects, altered neurite outgrowth, dysregulation of the cell cycle and an increased cell death (Ayala et al., 2008a; Iguchi et al., 2009).

The localization of TDP-43 can be influenced by several factors. The redistribution of TDP-43 into stress granules can be induced by stressors, like oxidative and osmotic stress and axotomy, which increases cytoplasmic TDP-43 reversible in a time-dependent manner (Moisse et al., 2009; Sato et al., 2009). Further, it was demonstrated in a human neuroblastoma cell line and in *Drosophila* that disease associated VCP mutations cause a redistribution of TDP-43 into the cytoplasm (Gitcho et al., 2009; Ritson et al., 2010). Cytoplasmic inclusion bodies of TDP-43 was also observed in myofibrils and frontal cortex of a VCP knock-in mouse (Badadani et al., 2010). Also, a polymorphism, which lies between the bipartite NLS of TDP-43 (A90V), results in an increased cytoplasmic localization (Winton et al., 2008b). The downregulation of endogenous TDP-43 homologues was observed in a few mice, *Drosophila* and *C. elegans* transgenic animal models that overexpressed human TDP-43 variants (see the overview of all current TDP-43 animal models in Liu et al., 2013). However, it is not
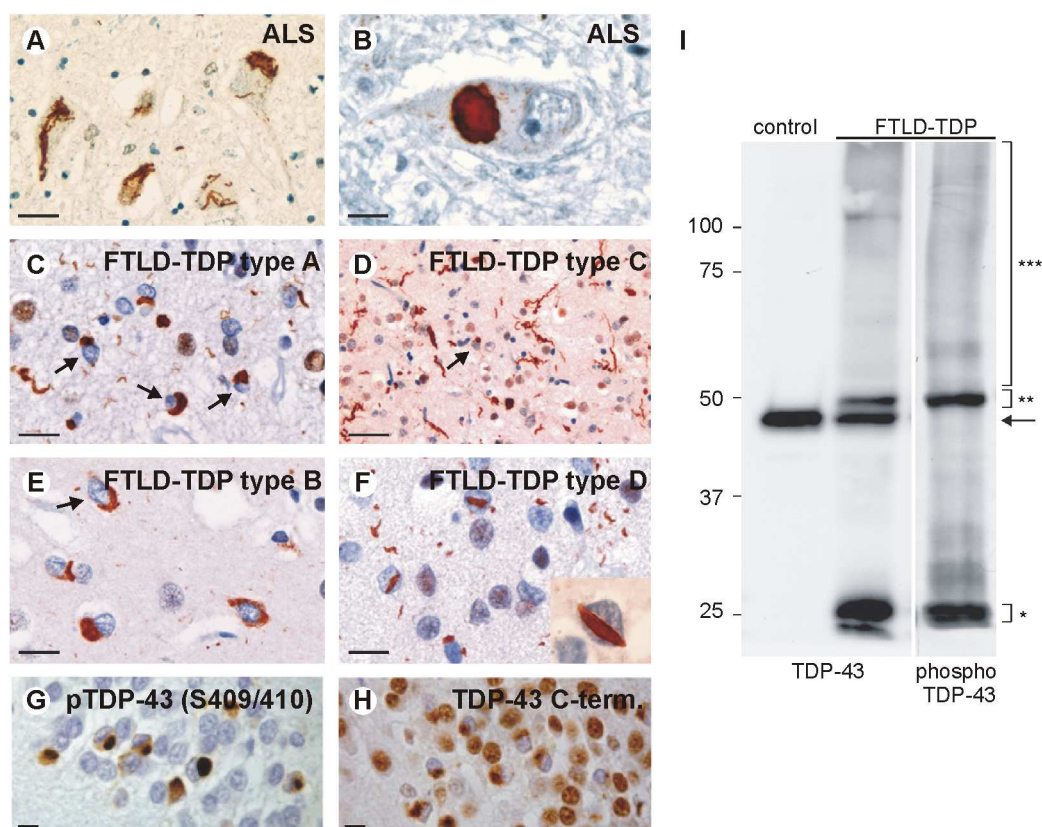
Figure 2.4 Pathological features of TDP-43 in ALS and FTLD-TDP. A+B Immunohistochemistry of TDP-43 in ALS motor neuron tissue shows skein-like (A) and round (B) inclusions. **C-F** The four distinct morphological subtypes of FTLD-TDP pathology adapted to the new classification system (Mackenzie et al., 2011): type A with compact neuronal cytoplasmic inclusions and short dystrophic neurites that are characteristic for GRN mutations (C); type C with long dystrophic neurites and few neuronal cytoplasmic inclusions (D); type B with compact and granular neuronal cytoplasmic inclusions (E); and type D with numerous lentiform neuronal intra-nuclear inclusions (see insert) is characteristic for FTLD-TDP with VCP mutations (F). **G+H** Staining of hippocampus from FTLD-TDP brain tissue with an anti-phospho S409/410 TDP-43 antibody shows pathologic inclusions (G), whereas an antibody raised against the C-terminus of TDP-43 shows numerous cytoplasmic inclusions and nuclear staining of non-inclusion bearing cells (H). Scale bars: 40µm (D), 20µm (A, C), 15µm (E, F), and 10µm (B, G, H). Nuclear depletion of TDP-43 in cells with cytoplasmic inclusions is indicated with arrows. **I** Biochemical analysis of urea fractions from control or FTLD-TDP brain tissues show pathological bands of 25kDa (*) and 45kDa (**, probably phospho-TDP-43), and a high molecular-weight smear (***, probably ubiquitinylated TDP-43) in FTLD-TDP brain but not in control tissue. The arrow indicates unmodified TDP-43 wt. Phosphorylated TDP-43 is detected with anti-phospho TDP-43 (S409/410) specific antibody. Modified from Mackenzie et al. (2010b) (A-F, I) and Neumann et al. (2009) (G+H).

known if autoregulation of TDP-43 level contributes to nuclear clearance in diseased human brain.

TDP-43 insolubility and aggregation

Insoluble protein aggregates are observed in most neurodegenerative diseases. However, in most cases it is unknown whether these inclusions are either harmful, protective or both. The localization of sarkosyl-insoluble TDP-43 positive aggregates differs in ALS and FTLD-TDP. In ALS, TDP pathology is detected in neurons and glia cells of the primary cortex, brainstem motor nuclei, spinal cord and the associated white mat-

ter tracts (Mackenzie et al., 2007; Neumann et al., 2006). The morphology of inclusions is variable and includes small round granules, compact Lewy body-like inclusions, ubiquitinylated and non-ubiquitinylated skeins and diffuse cytoplasmic inclusions (see Figure 2.4A+B) (Mackenzie et al., 2010b; Neumann et al., 2006; Strong et al., 2007). The accumulations of TDP-43 in FTLD-TDP are widespread in the brain. They are found in the frontotemporal neocortex and in dentate granule cells of the hippocampus. In FTLD-MND inclusions were additionally observed in the brainstem and the spinal cord (Arai et al., 2006; Davidson et al., 2007; Neumann et al., 2006). Four neuropathological subtypes of FTLD-TDP (type A-D) are described and present a variety of cytoplasmic, neuritic and intranuclear inclusions (see Figure 2.4C-F) (Mackenzie et al., 2011).

In vitro, purified recombinant TDP-43 exhibits rapid self-aggregation-properties in suspension, which look like depositions in degenerating neurons of ALS and FTLD-TDP (Johnson et al., 2009). The aggregation of TDP-43 *in vitro* and *in vivo* is increased by some pathogenic mutations and relies on RRM2 and the C-terminus, in which a potential prion-like domain was identified (Cushman et al., 2010; Guo et al., 2011; Johnson et al., 2008; Johnson et al., 2009). The prion-like character is supported by a study which showed that *in vitro* preformed recombinant TDP-43 fibrils can be taken up by TDP-43 overexpressing HEK293T cells and triggers formation of intracellular aggregates (Furukawa et al., 2011). Furthermore, the C-terminus shows protease K resistance, which is a marker for prions (Guo et al., 2011). However, the pathogenic TDP-43 deposits in ALS and FTLD do not exhibit amyloid character like aggregated proteins in most other neurodegenerative diseases, since they are not stained with amyloid-specific dyes, such as thioflavin T and Congo red (Kwong et al., 2008).

TDP-43 aggregation is very complex and can be modified by many internal and external factors. Overexpression of human TDP-43 induces rare aggregate formation in many animal models, such as rodents (reviewed in Cohen et al., 2011; Wegorzewska and Baloh, 2011) and fly (reviewed in Romano et al., 2012). However, a correlation was not observed between the number of inclusions and neurodegeneration (Igaz et al., 2011). Furthermore, aggregates are seldom seen upon overexpression of TDP-43 full-length (FL) in cell culture, but TDP-43 with mutated NLS or CTFs form many cytoplasmic inclusions, which are often phosphorylated and ubiquitinylated (Arai et al., 2010; Igaz et al., 2009; Nonaka et al., 2009a; Voigt et al., 2010; Winton et al., 2008a; Yang et al., 2010; Zhang et al., 2009). This cytoplasmic aggregation of TDP-43 is increased upon knockdown of the nuclear transport protein karyopherin-β1 or cellular apoptosis susceptibility proteins (Nishimura et al., 2010).

Several external factors might also enhance aggregation propensity of TDP-43. Among them are interaction with polyglutamine protein ataxin-2, overexpression of

ubiquilin-1, mutations within ubiquilin-2 or inhibition of extracellular signal-regulated kinase (ERK)1/2 (Ayala et al., 2011a; Deng et al., 2011b; Elden et al., 2010; Kim et al., 2009). Furthermore, heat shock response seems to play a role in aggregate formation, as upregulation of molecular chaperones increases solubility and reduces toxicity of TDP-43, especially of CTFs (Crippa et al., 2010; Gregory et al., 2012). A key role in TDP-43 aggregation seems to be played by the proteasomal as well as the autophagic machinery, since aggregate formation is reduced by p62/ sequestosome-1 overexpression or inhibition of the deubiquitinylation enzyme USP14 (Brady et al., 2011; Lee et al., 2010). Consistently, the inhibition of the proteasome in cell culture systems increases levels of endogenous TDP-43 and phospho-TDP-43 positive aggregates, while it blocks degradation of overexpressed CTFs, and enhances toxicity (Nonaka et al., 2009a; van Eersel et al., 2011; Winton et al., 2008a; Zhang et al., 2010).

The possible toxicity of TDP-43 aggregation is controversially discussed. On the one hand, overexpression of TDP-43 in yeast is only toxic upon aggregation (Johnson et al., 2008). Toxicity also depends on RNA binding properties of TDP-43 (Elden et al., 2010; Ihara et al., 2013; Johnson et al., 2008; Voigt et al., 2010). On the other hand, overexpression of TDP-43 was shown to be toxic without the formation of aggregates (Arnold et al., 2013; Wegorzewska et al., 2009), indicating that *in vivo* aggregation is possibly not an absolute requirement for TDP-43 mediated neurodegeneration.

Recently, the hypothesis was introduced that aggregates of TDP-43 or other neuropathological proteins, arise from stress granules (Dewey et al., 2012; Dormann et al., 2010; Li et al., 2013; Wolozin, 2012). These are normally reversible, but the disrupted RNA granule formation in disease or prolonged stress might result in insoluble aggregates (Parker et al., 2012). Thus, stress granules might be the initial core for further aggregation. However, the exact process of TDP-43 aggregation and their function remains poorly understood.

C-terminal fragments of TDP-43

Different CTFs of TDP-43 are found in inclusions in diseased brain and they show distinct patterns in ALS and FTLD-TDP (Hasegawa et al., 2008; Tsuji et al., 2012). The predominant species of truncated TDP-43 is of 25kDa (Hasegawa et al., 2008; Igaz et al., 2008; Inukai et al., 2008; Neumann et al., 2006). However, a 35kDa fragment was found in lymphoblastoid cell lines, which were derived from TDP-43 mutation carriers (Kabashi et al., 2008; Rutherford et al., 2008). This fragment is also variably present in human brain lysates from ALS and FTLD-TDP, but does not correlate with disease status (Lee et al., 2012). Interestingly, CTFs are found in FTLD-TDP (see Figure 1.4H+I) and ALS brain, while inclusions in spinal cord exhibit predominantly full-length TDP-43 (Igaz et al., 2008; Neumann et al., 2009). This argues for a distinct

TDP-43 species composition in brain versus spinal cord cells and may indicate that TDP-43 truncation might not be necessary for TDP-43 mediated neurodegeneration. CTFs were also found in TDP-43 overexpressing rodent animal models. It was consistently shown that the amount of CTFs increases during disease progression (Stallings et al., 2010; Tsai et al., 2010; Wils et al., 2010; Xu et al., 2010).

CTFs of TDP-43 are probably generated by proteolytic cleavage of TDP-43 FL. It is also possible that they originate from alternative splice variants or cryptic transcription start sites (Nishimoto et al., 2010). A potential TDP-43 processing protease is caspase 3, which generates 25kDa and 35kDa fragments of TDP-43 *in vitro* and in cell culture (Dormann et al., 2009; Nishimoto et al., 2010; Zhang et al., 2007b). In addition, the Ca^{2+}-dependent cysteine protease calpain is also able to cleave TDP-43 in its C-terminal region, thus generating 33, 34 and 36kDa N-terminal fragments (Yamashita et al., 2012). The exact amino acid sequence of all CTFs is still unknown. N-terminal sequencing of truncated TDP-43 from FTLD-TDP brain lysates identified arginine 208 as one specific cleavage site (Igaz et al., 2009), whereas Nonaka and colleagues identified D219 and D247 as possible cleavage sites (Nonaka et al., 2009b). Interestingly, these and other CTFs expressed in various cell lines behave in the same manner as pathological CTFs as they form ubiquitinylated and phosphorylated aggregates (Igaz et al., 2009).

The toxicity of truncated TDP-43 is not well understood. CTFs were shown to be aggregation prone and toxic when overexpressed in various cell lines (Fallini et al., 2012; Igaz et al., 2009; Nonaka et al., 2009b; Zhang et al., 2009), and impair neurite outgrowth during differentiation of cultured rodent neurons (Yang et al., 2010). Contrary, one study showed that the *de novo* intranuclear cleavage of TDP-43 FL does not generate aggregating CTFs (Pesiridis et al., 2011). Instead they are translocated and rapidly degraded, and aggregation only takes place when a "second hit" was present, such as misfolded CTFs. Moreover, in *Drosophila* models of TDP-43 overexpression, a toxic-gain-of function of TDP-43 FL rather than of CTFs was demonstrated, probably due to the RNA binding properties of TDP-43 FL (Li et al., 2010; Voigt et al., 2010).

A few studies showed that nuclear TDP-43 is depleted and mislocalized into cytoplasmic inclusion upon overexpression of CTFs (Caccamo et al., 2009; Igaz et al., 2009; Nonaka et al., 2009b; Yang et al., 2010), though this observation is not consistent in the literature. The mislocalization of TDP-43 also caused the downregulation of NFL mRNA, indicating that CTFs are sufficient to impair TDP-43 mediated NFL stabilization (Caccamo et al., 2009). Additionally, truncated TDP-43 also impairs splicing activity of TDP-43, illustrated by decreased skipping of CFTR exon 9 (Igaz et al., 2009; Nishimoto et al., 2010; Nonaka et al., 2009b; Zhang et al., 2009). Thus, the roles of

CTFs in TDP-43 proteinopathies are not entirely clear. Open questions regarding their procession, modification and of their possibly mediated toxicity remain.

Phosphorylation and ubiquitinylation of TDP-43

In contrast to normal conditions, TDP-43 is phosphorylated and ubiquitinylated in diseased tissue (see Figure 2.4G+I). It is still uncertain whether these modifications cause neurodegeneration or are secondary to the formation of aggregates.

The phosphorylation of TDP-43 likely occurs before ubiquitinylation in disease, as TDP-43 ubiquitin-negative but phospho-positive pre-inclusions were described (Hasegawa et al., 2008; Neumann et al., 2009). This modification is found at serine residues 379, 403/404 and 409/410 (see Figure 2.3) of pathological but not normal nuclear TDP-43 in FTLD-TDP and ALS (Hasegawa et al., 2008; Inukai et al., 2008). Up to date, phosphorylation in particular at serine 409/410 is the best pathological marker of abnormal TDP-43 inclusion in FTLD-TDP (Figure 2.4I) and ALS (Hasegawa et al., 2008; Inukai et al., 2008; Neumann et al., 2009). CTFs are more phosphorylated than TDP-43 FL in diseased brain, whereas phosphorylated TDP-43 FL is found primarily in spinal cord of ALS patients (Hasegawa et al., 2008; Neumann et al., 2009). TDP-43 is possibly phosphorylated by the casein kinase-1 (CK1) and CK2, and the cell division cycle kinase 7 (CDC7) (Hasegawa et al., 2008; Inukai et al., 2008; Liachko et al., 2013). The phosphorylation seems to promote oligomerization or fibril formation of TDP-43, at least *in vitro*. In line, the *Drosophila* homolog of CK1ε, doubletime, mediates the *in vivo* formation of TDP-43 oligomers that results in cellular toxicity (Choksi et al., 2014).

While data suggest that phosphorylation modulates solubility, aggregation and toxicity of TDP-43 in disease (Braak et al., 2010; Igaz et al., 2009; Liachko et al., 2010; Zhang et al., 2010), other results demonstrate that mutation of phosphorylation sites does not affect aggregation, toxicity, cell survival and cleavage of TDP-43 (Dormann et al., 2009; Nishimoto et al., 2010; Zhang et al., 2009). Interestingly, studies in *C. elegans* indicate that blocking of TDP-43 phosphorylation improves neurodegeneration of ALS-associated mutants, though TDP-43 wt neurotoxicity is not attenuated (Liachko et al., 2010). However, in *Drosophila* hyperphosphorylation of human CTFs reduces aggregation and toxicity and is proposed as a compensatory defence mechanism to prevent the aggregation of pathogenic TDP-43 (Li et al., 2011).

The ubiquitinylation of TDP-43 might take place after phosphorylation, but before the formation of insoluble inclusions (Giordana et al., 2010; Urushitani et al., 2010). In diseased brain and spinal cord of TDP-43 proteinopathies both cytoplasmic and nuclear TDP-43 inclusions are often positive for ubiquitin (Arai et al., 2006; Neumann et al., 2006). However, ubiquitin-negative pathologies are observed in some cases of

cytoplasmic inclusions in glia cells, in neurons with pre-inclusions and in neurons in the CA1 region (Brandmeir et al., 2008; Hatanpaa et al., 2008; Neumann et al., 2007).

The causation for aggregation of abnormally modified TDP-43 remains unknown. It is suggested that a failure in depletion of TDP-43 occurs in TDP-43 proteinopathies. The pathogenic inclusions of TDP-43 are positive for ubiquilin-2 and p62/ sequestosome-1, which target other proteins for degradation (Arai et al., 2003; Deng et al., 2011b). Furthermore, mutations in *UBQLN2*, *SQSTM1* and *VCP* are associated with ALS and FTLD-TDP (see also chapter 2.2) (Deng et al., 2011b; Fecto et al., 2011; Johnson et al., 2010; Watts et al., 2004). In addition, pathogenic TDP-43 mutants were also shown to be more stable than TDP-43 wt (Ling et al., 2010). Thus, it is likely that impairment of the UPS and reduced degradation of TDP-43 contribute to the disease.

Usually, ubiquitinylation targets proteins towards either degradation by the proteasome or by autophagy (see chapter 2.4). Therefore, the ubiquitinylated form of TDP-43 in ALS and FTLD-TDP cannot distinguish which pathway is involved in disease pathogenesis. Controversially, some reports indicate that TDP-43 is degraded by the proteasome (Kabashi et al., 2008; Rutherford et al., 2008; Tashiro et al., 2012; van Eersel et al., 2011; Winton et al., 2008a; Zhang et al., 2010), while others point towards autophagic clearance (Caccamo et al., 2009; Filimonenko et al., 2007; Wang et al., 2012) or the involvement of both pathways (Brady et al., 2011; Scotter et al., 2014; Urushitani et al., 2010; Wang et al., 2010).

TDP-43 has 20 lysine residues, which are possible targets for ubiquitinylation. Most of them are located in the N-terminal region and only five in RRM2 and the C-terminus, of which most CTFs consist (see Figure 2.3). Four potential ubiquitinylation sites were identified in RRM1 (K102, K114, K145 and K161) in a 33.5kDa N-terminal splicing variant of TDP-43, comprised of amino acids 1-277 (Dammer et al., 2012). Thus, these lysine residues cannot be the ubiquitinylation sites of the highly ubiquitinylated 25kDa CTFs found in ALS and FTLD-TDP inclusions. Moreover, inactivation of these four lysine residues by mutation in TDP-43 wt also did not alter the amount and solubility of ubiquitinylated TDP-43, emphasizing that other lysine residues of TDP-43 wt or CTFs are conjugated with ubiquitin (Dammer et al., 2012). TDP-43 can be polyubiquitinylated via K48- and K63-linked ubiquitin-chains, pointing to proteasomal or autophagosomal degradation (Hebron et al., 2013; Urushitani et al., 2010). Up to date, it remains unknown which enzymes participate in ubiquitinylation of TDP-43. It was suggested that the contributing E3 ubiquitin ligase(s) are located in the cytoplasm (Urushitani et al., 2010). One likely candidate ubiquitin ligase is parkin, since it ubiquitinylates TDP-43 *in vitro* (Hebron et al., 2013). To understand these posttranslational modifications of TDP-43, it is important to identify other enzymes that are involved in the ubiquitinylation and/or phosphorylation of TDP-43 FL or CTFs.

Pathogenic mutations of TDP-43 in ALS and FTLD

The identification of 48 missense mutations and of one nonsense mutation in TDP-43 in patients provides additional evidence for a role of TDP-43 in ALS, FTLD-TDP and FTLD-MND (summarized in Lattante et al., 2013). Interestingly, most of the pathogenic TDP-43 mutations are clustered in exon 6, which encodes for RRM2 and the aggregation-prone C-terminus (see Figure 2.3). This might imply altered protein-binding properties of the mutants. Moreover, the mutations were predominantly detected in patients with classical ALS in terms of age and site of disease onset and without cognitive decline (Kabashi et al., 2008). Only rare cases of mutant TDP-43 were described in FTLD, ALS patients with dementia or Parkinsonism (Lattante et al., 2013). The current prevalence for TDP-43 mutations is ~3% in fALS and ~1.5% in sALS patients (Lattante et al., 2013). However, the TDP-43 pathology from sALS cases with mutations is indistinguishable from the pathology of most sALS cases (Pamphlett et al., 2009; Van Deerlin et al., 2008).

Up to date, many studies did not provide evidence for altered functions of TDP-43 mutants, such as splicing activity, mRNA binding and processing and protein binding (D'Ambrogio et al., 2009; Fiesel et al., 2010; Freibaum et al., 2010; Watanabe et al., 2013). Only one study found slightly enhanced splicing activity of mutant TDP-43 Q331K for some RNA targets, but a loss-of-function against other RNA targets (Arnold et al., 2013). On the other hand, the overexpression of some ALS associated mutants increased the truncation and formation of insoluble aggregates and enhanced toxicity (Arai et al., 2010; Barmada et al., 2010; Guo et al., 2011; Johnson et al., 2009; Kabashi et al., 2010; Nonaka et al., 2009b; Sreedharan et al., 2008). Motor neurons generated from iPS cells that were derived from M337V mutation carriers exhibit increased level of soluble but also detergent-resistant TDP-43, decreased survival and enhanced vulnerability (Bilican et al., 2012).

Moreover, some TDP-43 mutants further accumulate upon proteasomal inhibition (Kabashi et al., 2008; Rutherford et al., 2008). Controversial, two studies showed that pathogenic mutants of TDP-43 exhibit enhanced half-lives which correlate with an acceleration of disease onset (Ling et al., 2010; Watanabe et al., 2013), yet another study recently reported that two of the mutants, which were analysed in the previously mentioned studies, are less stable than TDP-43 wt (Araki et al., 2014). Thus it still needs to be shown whether pathogenic mutants enhance or decrease the stability of TDP-43. The disease associated mutants might also facilitate stress granule formation (Dewey et al., 2011; Liu-Yesucevitz et al., 2010), though a disruption of stress granule assembly the by the R361S mutation was observed (McDonald et al., 2011).

The available data from transgenic animals overexpressing human TDP-43 with pathogenic mutations are controversial. While some reports demonstrate increased neurodegeneration and toxicity of TDP-43 pathogenic mutants compared to TDP-43 wt in rodents (Arnold et al., 2013; Swarup et al., 2011; Zhou et al., 2010), others did not observe this effect in mice (Stallings et al., 2010; Xu et al., 2011). Thus, it was suggested that TDP-43 toxicity is rather depending on the level of overexpression than on distinct properties of mutant and wt TDP-43 (Li et al., 2010; Stallings et al., 2010; Wils et al., 2010; Xu et al., 2013). A severe phenotype was observed in a rat model overexpressing the M337V mutation, which developed progressive weakness, early death and widespread neurodegeneration most severe in the spinal cord (Zhou et al., 2010). However, in the cortex of these animals a diffuse TDP-43 localization and only some aggregates were detected. The progressive motor abnormalities and widespread neurodegeneration were also observed in A315T transgenic mice, in which ubiquitin immunoreactive neuronal aggregates were negative for TDP-43 (Wegorzewska et al., 2009). This possibly points to altered DNA/RNA-binding properties of TDP-43 mutants instead of a toxic-gain-of-function of aggregated TDP-43 as disease promoting feature. One functional alteration of pathogenic mutant TDP-43 was seen in axonal trafficking of TDP-43 granules in motor neurons derived from ALS patients with TDP-43 mutations and in *Drosophila* motor neurons (Alami et al., 2014).

In summary, most pathogenic mutants are indistinguishable to TDP-43 wt in terms of localization and function, but some exhibit altered properties in the formation of CTFs and aggregates, and in toxicity.

Concluding remarks on the pathogenesis of TDP-43

Many studies have been conducted to identify the molecular and cellular mechanisms by which TDP-43 contributes to the pathogenesis of ALS and FTLD. However, the impact of the cleavage, phosphorylation, ubiquitinylation and aggregation of TDP-43 as well as the nuclear depletion on the disease pathogenesis remain poorly understood. These alterations are the subject of many studies and discussions, of which two main hypotheses are emerging.

It is conceivable that nuclear loss-of-functional TDP-43 causes alterations in RNA pathways, since TDP-43 seems to be a global player in the regulation of RNAs and interacts with many different RNAs. A general dysfunction of RNA homeostasis in ALS and FTLD is supported by the identifications of mutations in further proteins that possess distinct function in the regulation of RNAs - transcription, mRNA splicing, translation, RNA transport, and formation of ribonucleoprotein particles. Among them are FUS, ataxin-2, sentaxin and hnRNPs. The large number of TDP-43 RNA targets makes it difficult to identify distinct RNAs that might contribute to the patho-

genesis of ALS or FTLD, especially when TDP-43 is nuclear depleted or aggregated. TDP-43 is probably of great importance in disease development, because its levels are tightly regulated through autoregulation, and knockout of TDP-43 in mouse or fly is lethal. Furthermore, the identification of the molecular mechanisms by which hexanucleotide repeat expansions in C9ORF72 are involved in ALS and FTLD might provide important information for the understanding of the disease pathogenesis.

On the other hand, the insoluble aggregates or the aberrant modifications might confer a toxic gain-of-function. Though some pathogenic mutants of TDP-43 exhibit enhanced aggregation propensities, it is TDP-43 wt that is deposited in the majority of TDP-43 proteinopathies, implicating that other unknown factors account for its mislocalization and aggregation. A rather general failure of protein degradation in ALS and FTLD is supported by mutations in genes encoding proteins with distinct functions in protein homeostasis, among them ubiquilin-2, p62, VCP, optineurin, CHMP2B, VABP, and FIG4. However, it is also possible that the aggregates are not toxic, as several animal models exhibit neurodegenerative phenotypes but not neuronal aggregates. Furthermore, the nuclear depletion of TDP-43 is also observed in cells with a diffuse cytoplasmic TDP-43 staining, the pre-inclusions. This might indicates that the toxic forms are soluble or oligomeric, and the formation of aggregates is rather an attempt of the cell to protect itself from the toxic oligomers.

The mechanisms that underlie the aberrant cleavage, phosphorylation and ubiquitinylation of TDP-43 are not well understood. Therefore, it is important to understand how and by which TDP-43 interactors these modifications are regulated. It is possible that both - a loss-of-function with implications for altered RNA regulations as well as a toxic gain-of-function of TDP-43 that is promoted by dysfunctions in the protein degradation pathways - contribute to disease initiation and progression.

2.4 The cellular ubiquitin system

The posttranslational modification of cellular proteins with the highly conserved 76 amino acid protein ubiquitin is involved in the regulation of many processes in the cell. This so called ubiquitinylation is a dynamic process and modulates protein activity and stability, ubiquitin-dependent signalling pathways, gene transcription, protein localization, and degradation of proteins.

The ubiquitinylation of proteins occurs in three steps mediated by three enzymes: the ubiquitin-activating enzyme (E1), a ubiquitin-conjugating enzyme (E2) and a ubiquitin ligase (E3) (Figure 2.5A). First, ubiquitin is activated at its C-terminus by the E1 enzyme in an ATP dependent manner, forming a thioester bond with the E1. This activated ubiquitin is transferred in a second step to the active site cysteine of an E2
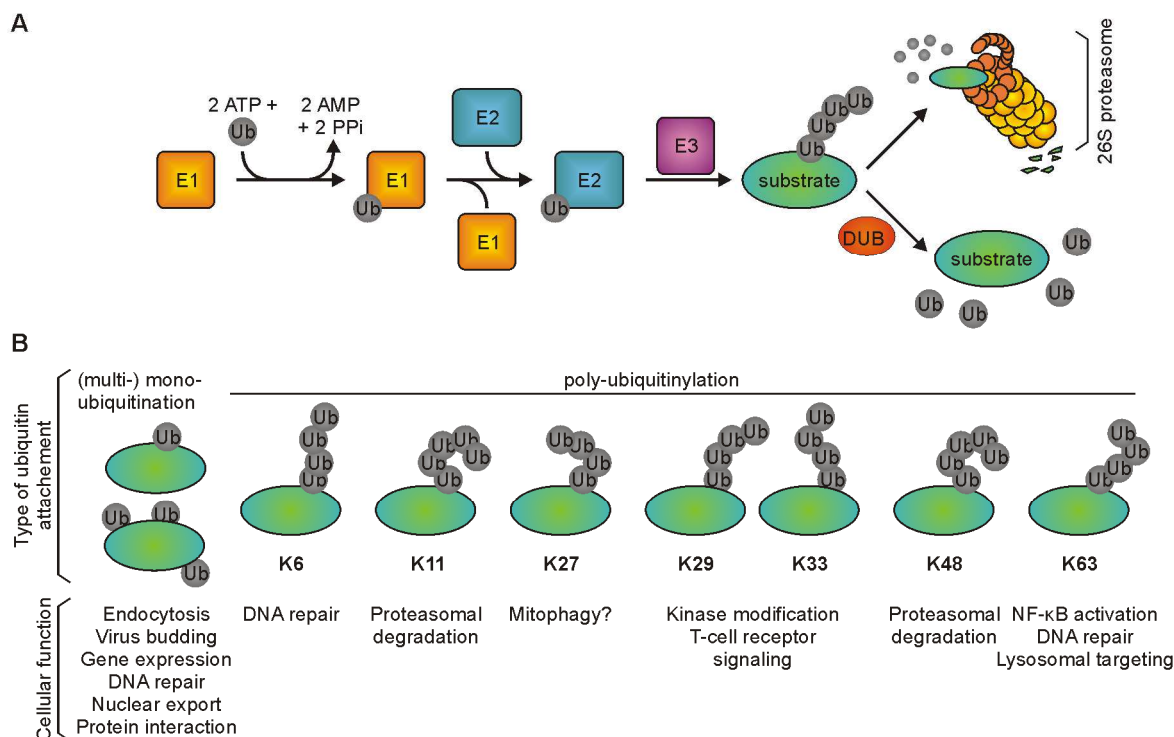
Figure 2.5 The (de-)ubiquitinylation reaction and types of ubiquitin linkage. A The ubiquitinylation occurs through the sequential action of three classes of enzymes. The E1 ubiquitin-activating enzyme transfers an activated ubiquitin to an E2 ubiquitin-conjugating enzyme. An E3 ubiquitin ligase mediates the ubiquitinylation of the target substrate or the elongation of a polyubiquitin chain. The enzymatic removal of ubiquitin is performed by deubiquitinating enzymes (DUBs). **B** The different types of ubiquitinylation and their supposed cellular functions.

enzyme, of which 31 functional enzymes are known in human (van Wijk and Timmers, 2010). In a third step an E3 ligase mediates the formation of an isopeptide-bond between the activated ubiquitin and, usually, the ε-amino group of a lysine residue of the substrate protein. Rather unusual ubiquitinylations of the N-terminus of proteins and of other nucleophilic amino acids like threonine, serine and cysteine have also been described (Cadwell and Coscoy, 2005; Ciechanover and Ben-Saadon, 2004; Ishikura et al., 2010; Shimizu et al., 2010; Tait et al., 2007).

There are more than 600 E3s in mammalian cells that provide as distinct E2-E3 pairs specificity of the ubiquitinylation (Metzger et al., 2012). Most E3 ligases belong either to the homologous to E6-AP carboxy-terminus (HECT) domain or the really interesting new gene (RING) finger domain family. Further RING-related E3s express U-box domains (UBD), plant homeodomains (PHDs) or leukemia associated protein (LAP) finger (Deshaies and Joazeiro, 2009). The HECT E3 ubiquitin ligases actively take up E2-bound ubiquitin via thioester linkages and then transfer the ubiquitin to the substrate, whereas RING E3s mediate ubiquitin transfer from E2s directly to the substrate without forming a thioester bond with ubiquitin (Metzger et al., 2012).

After the initial ubiquitinylation, further ubiquitin molecules can be conjugated to one of the seven lysine residues, but also to the C-terminal carboxyl group, of the ubiquitin molecule which is already attached to the substrate (Komander and Rape, 2012). Thus, different types of polyubiquitin chains are formed, which are associated with different cellular and developmental processes and protein functions (Figure 2.5B).

The K48 polyubiquitinylation targets proteins to degradation by the proteasome (Pickart, 1997). The K63-polyubiquitinylation of proteins is usually associated with autophagic clearance of the conjugated protein or organelle, whereas functions of the other mono- and polyubiquitinylations are less well understood. Monoubiquitinylation does not usually lead to proteolytic degradation, but regulates cellular localization, trafficking and transcriptional activity of a protein (Komander and Rape, 2012).

A proteolytic breakdown is essential for maintenance of proper protein folding, protein turnover, cell cycle, development, regulation of gene expression, signal transduction, antigen processing and further processes in cells. There are two major degradation pathways for misfolded or no longer required proteins and organelles in eukaryotic cells: the UPS and the autophagy-lysosomal pathway (Clague and Urbe, 2010). In macroautophagy - usually referred to as autophagy - cytoplasmic organelles or components are enclosed by a double membrane to form an autophagosome, which then fuses with the lysosome. In another form of autophagy called microautophagy cytoplasmic material is directly endocytosed by the lysosome.

The majority of misfolded and short-lived proteins are degraded by proteasomes, for which they are usually tagged with ubiquitin. The mammalian 26S proteasome is a multi-protein complex located in the cytoplasm and as well in the nucleus (von Mikecz, 2006). It is comprised of a barrel shaped 20S core protein and two flanking 19S regulatory caps. The 19S regulatory caps recognize polyubiquitinylated proteins as substrates for the 20S proteasome. The recognition requires at least a chain of four K48-linked ubiquitin molecules attached to the substrate is sufficient, though the proteasome has the capacity to degrade certain unfolded or damaged proteins which are non-ubiquitinylated (Goldberg, 2003). The ubiquitin chain is removed from the protein by a deubiquitinating enzyme (DUB) before it enters the 20S proteasome for digestion into peptides. These are further degraded to amino acids by peptidases in the cytoplasm.

Ubiquitinylations are dynamic posttranslational modifications. For the maintenance of ubiquitin homeostasis, ubiquitin has to be recycled once the ubiquitinylated substrate reaches its destinations for breakdown or fulfils its physiological function. Importantly, monomeric ubiquitin is generated from linear polymers of ubiquitin as

they emerge from ribosomes. DUBs ensure selectivity of these processes. About 90 DUBs are encoded in the human genome, of which 79 are predicted to be active (Clague et al., 2012). They are grouped into two classes, containing a total of five families. The first class of papain-like cysteine proteases comprise four distinct DUB families: ubiquitin-specific proteases (USPs), ubiquitin-C-terminal hydrolases (UCHs), ovarian tumor domain proteases (OTUs) and members of the Josephin domain (MJD) family. The second class and the fifth family are the JAB1/MPN/MOV34 Zn^{2+} dependent metalloproteases (JAMM) (Komander et al., 2009). The substrate specificity of the distinct DUBs is dependent on the subcellular localization, the specific binding interactions and the linkage preference of the catalytic domain. DUBs recognize ubiquitin via low affinity interactions by various ubiquitin-binding domains, including UIM, CUE, NZF as well as certain VHS and SH3 domains (Dikic et al., 2009). Thus, DUBs control membrane trafficking and protein quality control, signalling pathways, transcriptional activity and DNA repair (reviewed in Clague et al., 2012).

2.5 The class III UBE2E ubiquitin-conjugating enzymes

2.5.1 Characterization of the class III UBE2E enzymes

The E2 ubiquitin conjugating enzymes can be divided into four classes (Figure 2.6B). E2 enzymes are comprised either solely of a highly conserved ubiquitin-conjugating (UBC) domain of about 150 amino acids (class I), the UBC domain with a C-terminal or an N-terminal extension (class II and class III) or both extensions (class IV) (van Wijk and Timmers, 2010). Additionally to the catalytic cysteine, the UBC domain also contains conserved features which are required for the interaction with both E1 and E3 enzymes (Wenzel et al., 2011b).

The three human class III UBE2E ubiquitin-conjugating enzymes are called UBE1E1 (UbcH6), UBE2E2 (UbcH8) and UBE2E3 (UbcH9) (Figure 2.6A). They are 100% identical to their mouse orthologs UbcM3, Ube2e2 and UbcM2, and are highly conserved in animals (Ito et al., 1999; Matuschewski et al., 1996). The three enzymes share a conserved UBC fold with over 93% identity. Including their N-terminal extensions, the overall homology between the UBE2E enzymes is 78-85% (Figure 3.15), suggesting a functional overlap of these E2 enzymes (Mirza et al., 2010).

UBE2E3 is highly expressed in murine brain and retinal cells (Mirza et al., 2010) and in human skeletal muscle (Ito et al., 1999), though low levels were detected in many other tissues (Ito et al., 1999; Mirza et al., 2010). The three UBE2E enzymes are nuclear localized and their importin-II mediated nuclear import is triggered by charging of the E2s at their catalytic cysteine residue with ubiquitin (Plafker et al., 2004). Con-
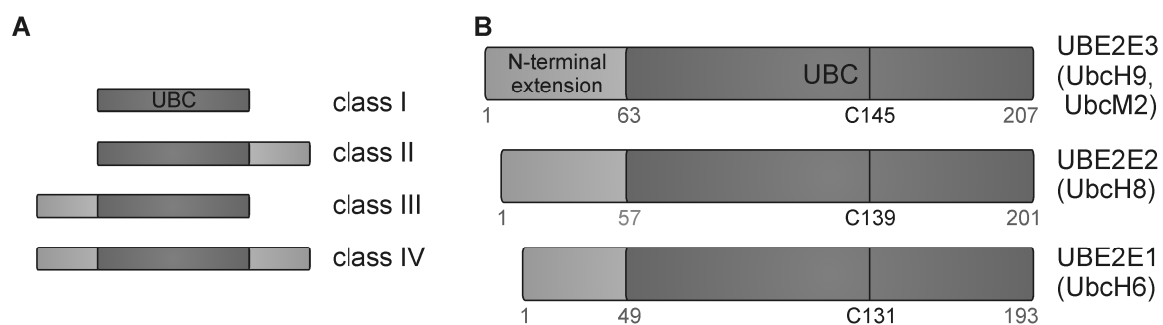
Figure 2.6 Domain structures of UBE2E enzymes and classes of E2 enzymes. A Schematically depicted are the four classes of E2 enzymes and their overall domain structure with a central ~150aa UBC domain and N- or/and C-terminal extensions of variable length. **B** The domain structures of UBE2E3, UBE2E2 and UBE2E1 with their UBC domains (Mirza et al., 2010; Schumacher et al., 2013), N-terminal extensions, and catalytic cysteines (Debonneville and Staub, 2004; Ito et al., 1999). The catalytic cysteine residues of UBE2E2 and UBE2E1 were identified by similarity to UBE2E3.

sistently, mutating the active site cysteine impaired the binding to the nuclear transport receptor and, thus, they are not shuttled into the nucleus. UBE2E3 is a functional E2 ubiquitin-conjugating enzyme, forming thioester-bonds with ubiquitin in an E1 dependent manner (Ito et al., 1999). All three UBE2Es exhibit autoactivation activity, as they can either ubiquitinylate lysine (UBE2E2 and UBE2E3) or the catalytic cysteine residue (UBE2E1) in their own peptide (David et al., 2010; Sheng et al., 2012). Moreover, they can perform polyubiquitinylation conjugations in the absence of E3 ligases and substrates, catalyzing K48- (all UBE2Es), K11- and likely K63-directed (UBE2E2 and UBE2E3) polyubiquitinylation reactions *it vitro* (David et al., 2010). It was demonstrated that the UBC domain alone of all three UBE2Es is capable of mediating polyubiquitinylation of substrates, while the N-terminal extensions inhibits this, leading to monoubiquitinylation (Schumacher et al., 2013).

2.5.2 Cellular functions of class III UBE2E enzymes

Several studies identified possible E3 ubiquitin ligases for the class III UBE2E ubiquitin conjugating enzymes. Interestingly, a large number of RING E3 ligases interacted in a yeast two-hybrid based interaction study with the three UBE2Es, disclosing them as hub E2 enzymes (van Wijk and Timmers, 2010). Another yeast two-hybrid screen identified the specific interactions of UBE2E2 and UBE2E3 with ARA54 and RNF8 (Ito et al., 2001). Additionally, all UBE2Es bound the RING-domain of the heterodimer E3 BRCA1-BARD1, resulting in monoautoubiquitinylation of BRCA1 (Christensen et al., 2007). Furthermore, Debonneville and Staub (2004) demonstrated that UBE2E3 and the HECT E3 ligase Nedd4-2 regulate the activity of the epithelial sodium chanel (ENac) in *Xenopus laevis* oocytes, also showing that a distinct phenylalanine residue (F122) is essential for the interaction of UBE2E3 with Nedd4-2. Since UBE2E3 is able to bind activated Cul3-ligases and their putative substrate adaptor RCBTB1, but also

further cullins, it was suggested that the E2 can regulate the activity of cullin-based E3 ligase complexes (Plafker et al., 2009).

UBE2E enzymes are functional in different events. UBE2E1 is involved in the ubiquitinylation of the *SCA1* gene product ataxin-1 even in absence of an E3 ligase (Hong et al., 2008). It was also shown that UBE2E1 regulates the transcriptional repression activity of ataxin-1 (Lee et al., 2008). Surprisingly, UBE2E2 can catalyze the conjugation of the ubiquitin like protein ISG15 to the influenza A NS1 protein (Zhao et al., 2004; Zhao et al., 2010). UBE2E3 is involved in human immunodeficiency virus type 1 (HIV-1) replication (Dziuba et al., 2012). Moreover, UBE2E3 has a role in development, as the E2 is required for proliferation of retinal pigment epithelial (RPE) cells, regulating the balance between RPE cell proliferation and differentiation (Plafker et al., 2008). Notably, UBE2E3 enhances the stability and transcriptional activity of the transcription factor nuclear factor E2-related factor 2 (Nrf2), by forming a complex upon alkylation of the non-catalytic cysteine 136 in UBE2E3 (Plafker et al., 2010). Thus, the constitutively degraded Nrf2 is stabilized, can shuttle to the nucleus and activates the transcription of detoxifying genes. Moreover, the functional homologues of UBE2E3, Ubc4 and Ubc5, mediate the degradation of misfolded and oxidatively damaged proteins (Matuschewski et al., 1996; Medicherla and Goldberg, 2008; Seufert and Jentsch, 1990).

2.6   The ubiquitin isopeptidase Y

2.6.1   Structure and localization of UBPY

The ubiquitin isopeptidase Y (UBPY) is a cysteine protease of the USP family, also known as USP8. UBPY is comprised of a conserved cysteine box and a histidine box in its C-terminal region (Figure 2.7) (Gnesutta et al., 2001). UBPY exhibits an N-terminal microtubule interacting and transport (MIT) domain and a Rhodanese-like domain (Gnesutta et al., 2001; Row et al., 2007). The MIT domain is essential for the binding to the MVB proteins CHMP1B, CHMP1B, CHMP7 and CHMP4C (Row et al., 2007). Additionally, the E3 ligase Nrdp1 interacts with UBPY via the Rhodanese-like domain (De Ceuninck et al., 2013; Wu et al., 2004). The DUB also contains two non-classical Src homology 3 (SH3) domain binding motifs in the central region (Kato et al., 2000). These are important for the binding to other proteins, among them the signal transducing adaptor molecule 2 (STAM2) (Gnesutta et al., 2001; Harkiolaki et al., 2003; Kaneko et al., 2003; Kato et al., 2000).

UPBY is conserved in eukaryotes. The cytoplasmic DUB is expressed weakly in most mouse tissues, but highly expressed in mouse testis and brain neurons (Bruzzone et
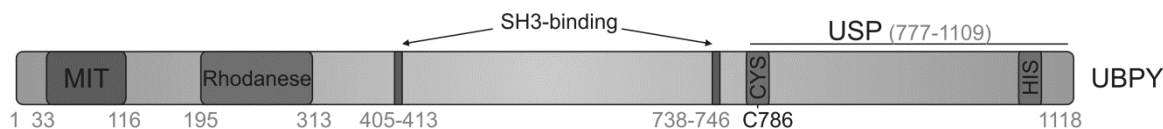
Figure 2.7 Domain structure of UBPY. Depicted is a schematic view of the human UBPY with the microtubule interacting and transport (MIT) domain, Rhodanese-like domain, two Src homology 3 (SH3) binding domains, the catalytic cystein C786, and the cysteine box (CYS, amino acids 778-796) and histidine box (HIS, amino acids 1061-1070) in the C-terminal ubiquitin-specific protease (USP) domain.

al., 2008; Gnesutta et al., 2001). UBPY was detected in gray and white matter of mouse spinal cord, more precisely, in the cell body, axonal microtubules and synaptic terminals of neurons, but not in glia cells (Paiardi et al., 2014). Thus, UBPY might exhibit special functions in neuronal tissue.

2.6.2   Regulation of UBPY activity

UBPY is a growth regulated protein, which accumulates upon growth stimulation in human fibroblasts, but decreases when cells undergo growth arrest by contact inhibition (Naviglio et al., 1998). This suggested a possible role in the control of mammalian cell proliferation. Furthermore, phosphorylation of S680 in a predicted 14-3-3 binding motif induces 14-3-3ε binding, which maintains UBPY in the cytosol and reduces DUB activity, whereas dephosphorylation during M-phase enhances DUB activity in dividing cells (Ballif et al., 2006; Mizuno et al., 2007). The mutation of serine 680 to alanine resulted in a constitutively active UBPY (Mukai et al., 2010). An Akt-dependent phosphorylation at threonine 907 stabilizes the activity of UBPY (Cai et al., 2010; Cao et al., 2007), suggesting that Akt-mediated growth and survival signals might use UBPY as a downstream effector. A reciprocal regulation of UBPY and the E3 ligase Nrdp1 was demonstrated, where UBPY stabilizes Nrdp1 by deubiquitinylation and UBPY is destabilized by Nrdp1 mediated ubiquitinylation (De Ceuninck et al., 2013). Thus, UBPY expression and activity is tightly regulated.

2.6.3   Cellular functions of UBPY

UBPY is a functionally active DUB, which hydrolases K48- and K63-linked ubiquitin-chains as well as (multi-)monoubiquitinylations of receptor tyrosine kinases *in vitro* (Row et al., 2006). The best studied function of UBPY is the regulation of post-internalisation trafficking of several plasma membrane receptors in a substrate specific way, thus indirectly affecting downstream signalling. Therefore, UBPY interacts with the ESCRT-0 complex, comprised of hepatocyte growth factor-regulated tyrosine kinase substrate (Hrs) and STAM, and with several CHMP proteins of the ESCRT-III complex (Berlin et al., 2010a; Berlin et al., 2010b; Mizuno et al., 2005; Row et al.,

2007). Hrs is deubiquitinylated and hence stabilized by UBPY, protecting the ESCRT-0 complex from degradation (Kato et al., 2000; Niendorf et al., 2007; Row et al., 2006; Zhang et al., 2014). The depletion of UBPY results in increased overall ubiquitinylation and endocytic swelling accompanied by the accumulation of ubiquitinylated species on endosomes (Naviglio et al., 1998), emphasizing the important role of the protein in endosomal sorting.

UBPY directly mediates stabilization, recycling or degradation of cell surface receptors. For example, the DUB directly deubiquitinylates the two G-protein coupled receptors protease-activated receptor 2 (PAR2) and δ-opioid-receptor (DOR), targeting these proteins for lysosomal trafficking and degradation (Hasdemir et al., 2009; Hislop et al., 2009). Contrary, deubiquitinylation of the wingless/Wnt pathway receptor frizzled and the hedgehog pathway component smoothened protects these receptors from lysosomal turnover, thus prolonging signalling of the morphogens wingless/Wnt and hedgehog, respectively (Li et al., 2012; Mukai et al., 2010; Xia et al., 2012). Conflicting results have been observed for the role of UBPY in lysosomal targeting of the epithelial growth factor receptor (EGFR). Some reports showed that EGFR deubiquitinylation by UBPY stimulates lysosomal turnover of the receptor (Alwan and van Leeuwen, 2007; Bowers et al., 2006; Row et al., 2006). More convincingly, UBPY protects EGFR from degradation by direct deubiquitinylation, thus promoting recycling of the receptor (Berlin et al., 2010b; Cai et al., 2010; Mizuno et al., 2005; Niendorf et al., 2007). Thus, UBPY functions are closely related to the ESCRT dependent trafficking of various receptors.

UBPY knockout mice and flies are embryonic lethal, probably due to decreased cell proliferation (Mukai et al., 2010; Niendorf et al., 2007). Thus the *in vivo* functions of UBPY are barely known. The conditional inactivation of UBPY in adult mice causes a severe liver failure with progressive loss of growth receptors and enlarged endosomes (Niendorf et al., 2007). The UBPY deficiency in flies also showed an accumulation of membrane proteins in enlarged endosomes (Zhang et al., 2014). In addition, the knockdown of UBPY in zebrafish embryos resulted in abnormal CNS development (Tse et al., 2009). Remarkably, the Wobbler mouse, a model for a motor neuron degeneration disorder, exhibited in oligodendrocytes an unusually heavy immunoreactivity for UBPY, and neurons displayed aggregates of UBPY and Vsp54, a member of the Golgi-associated retrograde tethering complex (Paiardi et al., 2014). Thus, an influence of UBPY on the neuron-oligodendrocytes interaction in neurodegenerative disorders was proposed. Since UBPY knockdown in mice and flies is embryonic lethal, cellular models of UBPY overexpression or silencing have to be used to learn more of the functions and regulation of UBPY.

2.7   Objectives

The RNA/DNA binding protein TDP-43 is found in pathological, ubiquitin-positive inclusions in a wide spectrum of neurodegenerative diseases, including ALS and FTLD-TDP. How TDP-43 contributes to the pathogenesis of these TDP-43 proteinopathies remains unknown. There are two hypothesises that are widely discussed:

A toxic-gain-of-function might be caused by the predominantly cytoplasmic inclusions that are comprised of insoluble, ubiquitinylated and hyperphosphorylated TDP-43 as well as C-terminal fragments. This accumulation also suggests that the processing, modification and degradation of TDP-43 is impaired or misregulated. A possible loss-of-function due to the nuclear depletion and mislocalization of TDP-43 in cells with inclusions was suggested. Since the main functions of TDP-43 are in the regulation of transcription, mRNA splicing, RNA transport, translation and miRNA biogenesis, this loss-of-nuclear-function possibly affects the TDP-43 dependent RNA metabolism.

TDP-43 is supposed to execute its functions as part of protein complexes. At the beginning of this study only a few interacting proteins of TDP-43 were known. The identification of novel protein interactors of TDP-43 allows the better understanding of the physiological roles of TDP-43, and therefore also of the pathogenicity of this protein. To this end, a yeast two-hybrid screen was performed with an adult human cDNA library as prey and a C-terminal fragment of TDP-43 as bait. Ten novel interactors were identified. Some of them are proteins associated with several steps of the RNA metabolism, while another group of target proteins regulates cellular ubiquitinylation reactions.

Here the focus was set on the investigation of the regulation of TDP-43 ubiquitinylation by the class III E2 ubiquitin-conjugating enzyme UBE2E3 and the ubiquitin isopeptidase UBPY. Five specific questions were investigated in this study.

1) Is the ubiquitinylation of TDP-43 regulated by UBE2E3 and UBPY?
2) Is the ubiquitinylation of TDP-43 a signal for proteolytic breakdown by the proteasome or autophagy?
3) Does the ubiquitinylation of TDP-43 alter its stability and turnover, solubility and aggregation, and functional activity? Can this be regulated by UBE2E3 and UBPY?
4) Are pathogenic mutants of TDP-43 differentially ubiquitinylated compared to TDP-43 wt?
5) Does silencing of the *Drosophila* orthologs of UBPY or UBE2E3 - dUBPY and UbcD2 - alter a neurotoxic phenotype in TDP-43 transgenic flies?

3   Results

3.1   Yeast Two-hybrid screen for novel TDP-43 interactors

At the beginning of this study, only a few protein interactors of TDP-43 were known. Questions regarding the interaction of TDP-43 with other proteins and their implications on TDP-43 function, toxicity or pathogenesis remain. Therefore, we performed Y2H screens to identify novel protein interactors of TDP-43 and tried to ascertain the functional role of these interactions more specifically. The Y2H screens were conducted with TDP-43 wt as well as a TDP-43 C-terminal fragment (CTF$_{193-414}$, see Figure 3.1). Further experiments in this study were performed with CTF$_{172-414}$, a construct lacking the glycine-rich domain (ΔGRD), 15 pathogenic mutants, and TDP-43 with a mutated NLS.

3.1.1   TDP-43 autoactivation, toxicity and dimerization in yeast

Two important issues, which have to be addressed in a Y2H screen, are the exclusion of autoactivation and toxicity of the bait-protein in yeast. First, the autoactivation of TDP-43 FL and a 25kDa C-terminal fragment (CTF$_{193-414}$) was investigated. Therefore, the yeast strain Y2HGold expressing the bait-proteins fused to the binding domain
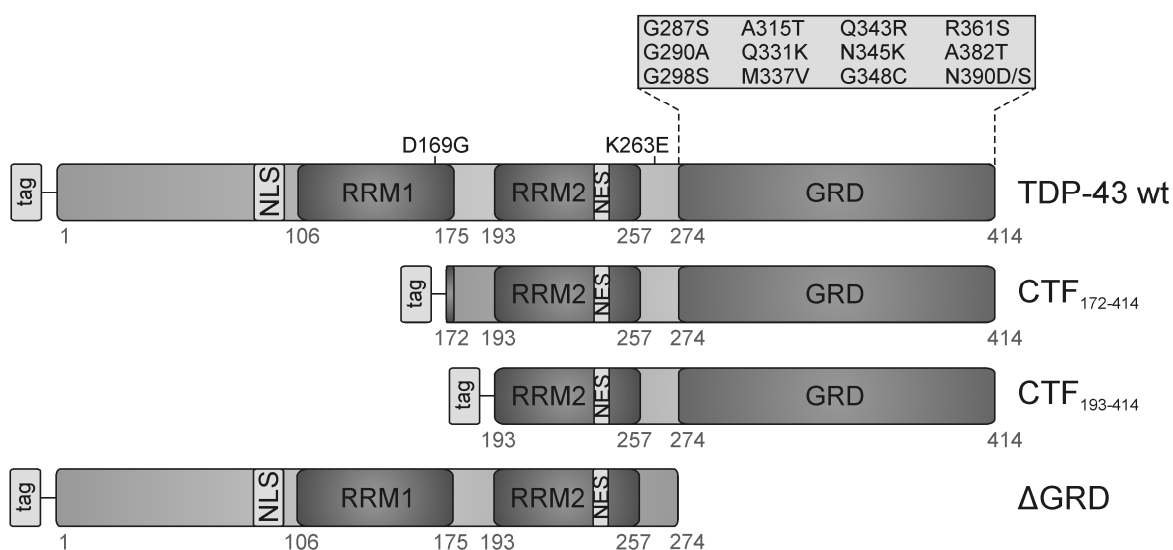
Figure 3.1 TDP-43 constructs used in this study. In this study TDP-43 wt, a 25kDa and a 22kDa C-terminal fragment (CTF172-414 and CTF193-414, respectively) and TDP-43 lacking the glycine rich domain (ΔGRD) were used. Depicted are also pathogenic mutants used in this study. The constructs were N-terminally tagged with Gal4 transcription factor activation (AD) and binding domain (BD) for expression in yeast or with Flag, 6xHis or the fluorescent proteins mCherry or EGFP for mammalian expression.

(BD) or the activation domain (AD) of the Gal4 transcription factor were cultivated on selective medium plates lacking leucine and tryptophane (-LT), on -LT supplemented with X-alpha-Gal (XαGal) or the yeast antibiotic Aureobasidin A (AbA, Figure 3.2A). After three days, we found that both BD-TDP-43 FL and CTF$_{193-414}$ grew on -LT plates, but not on -LT+Aba. Furthermore, yeast colonies did not turn blue on -LT+XαGal plates, showing that BD-FL and - CTF$_{193-414}$ did not autoactivate the Gal4-reporter system.

The expression of TDP-43 in yeast was shown to be toxic (Johnson et al., 2008), but the Y2H system was used in other studies that successfully identified novel TDP-43 protein interactors (Kim et al., 2009; Lehner and Sanderson, 2004; Stelzl et al., 2005). To exclude TDP-43 toxicity in our Y2H system, it was analyzed whether AD- or BD-fused TDP-43 FL and CTF$_{193-414}$ expression decrease growth of yeast in liquid selective medium (Figure 3.2B+C). Yeast cells expressing any of the four fusion proteins did not grow considerably slower than control yeast (Figure 3.2B+C, AD- and BD-Ø). The observed growth differences were rather due to slightly varying starting OD$_{600}$. Another toxicity assay was performed, in which the size and number of yeast colonies expressing the BD- or AD-fused bait proteins were compared to control yeast. Yeast colonies expressing TDP-43 or control vectors did not differ in size and number, supporting the non-toxicity of TDP-43 in Y2HGold (data not shown). Thus, both TDP-43 FL and CTF$_{193-414}$ are suitable to be used as bait proteins in a Y2H system, at least concerning autoactivation and toxicity.
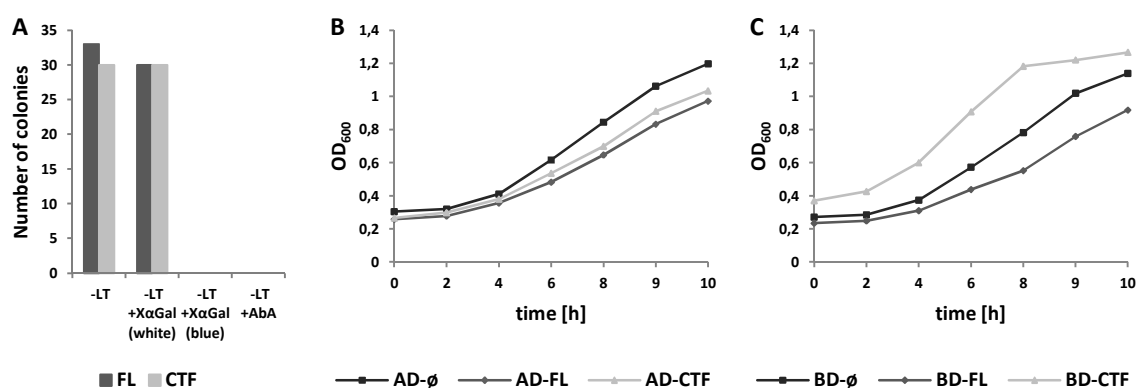
Figure 3.2 Autoactivation and toxicity of TDP-43 FL and CTF$_{193-414}$ in Y2HGold. A No autoactivation of TDP-43 FL and CTF193-414 in Y2HGold. BD-TDP-43 FL or CTF193-414 was co-transformed with AD-Ø in Y2HGold. A 1/100 dilution of transformed yeast was plated onto selective medium plates: -LT (selecting for co-transformed yeast), -LT + X-α-Gal (blue color indicating autoactivation) and -LT + 80ng/ml Aureobasidin A (-LT + AbA, growth indicating autoactivation). The yeast colonies were counted after 3d at 30°C. **B+C** No toxicity of TDP-43 FL and CTF193-414 in yeast. Y2HGold transformed with TDP-43 FL or CTF193-414 fused to either AD or BD of Gal4 transcription factor were cultivated in liquid yeast medium lacking leucine (B) or tryptophane (C) for 10h. Growth of yeast cells was tracked via measurement of optical density at 600nm (OD600) every second hour until stationary growth phase was reached. A-C Each experiment was performed once.

Identifying novel protein interactors of TDP-43 in a Y2H screen requires a positive control of TDP-43 protein interaction and shows that TDP-43 can interact with a known partner in the yeast enviroment. Therefore, we wanted to confirm the known interactions of TDP-43 FL, as well as two C-terminal fragments ($CTF_{172-414}$ and $CTF_{193-414}$) with SMN1 (Wang et al., 2002) and hnRNPA2 (Buratti et al., 2005) in our Y2H system (Fig. 3.3). Additionally, the reported dimerization of TDP-43 was examined (Kuo et al., 2009). Only yeast grown on selective medium plates lacking leucine, tryptophane and adenine (-LTA) were definied as minimal stringency for an adequate interaction, because too much background yeast growth on -LTH plates was observed.

The interactions of TDP-43 FL and CTF with SMN1 or hnRNPA2 in yeast were not appropriate to serve as positive controls. BD-SMN1 showed a weak interaction with $CTF_{172-414}$ on -LTA selective medium plates, and none with TDP-43 FL or $CTF_{193-414}$, as either very few or no colonies grew. Few colonies of BD-hnRNPA2 and AD-TDP-43 FL expressing yeast on -LTA selective medium plates were found. Thus, the interaction of the two considered positive control proteins with TDP-43 was weak (Figure 3.3). The inverse interaction of AD-hnRNPA2 with BD-TDP-43 was not detected at all. However, the dimerization of TDP-43 FL as well as the dimerization among CTFs was strong even on the highest stringency plates (-LT+AbA). The strongest interaction observed was the binding of the AD-SV40 large T antigen with BD-p53 that served as a positive control for a working Y2H system (Figure 3.3). Additionally, the expression of AD- and BD-TDP-43 (FL, $CTF_{172-414}$ and $CTF_{193-414}$), SMN1 and hnRNPA2 in Y2HGold was verified with western blot analysis (Figure 3.4). All proteins were expressed at
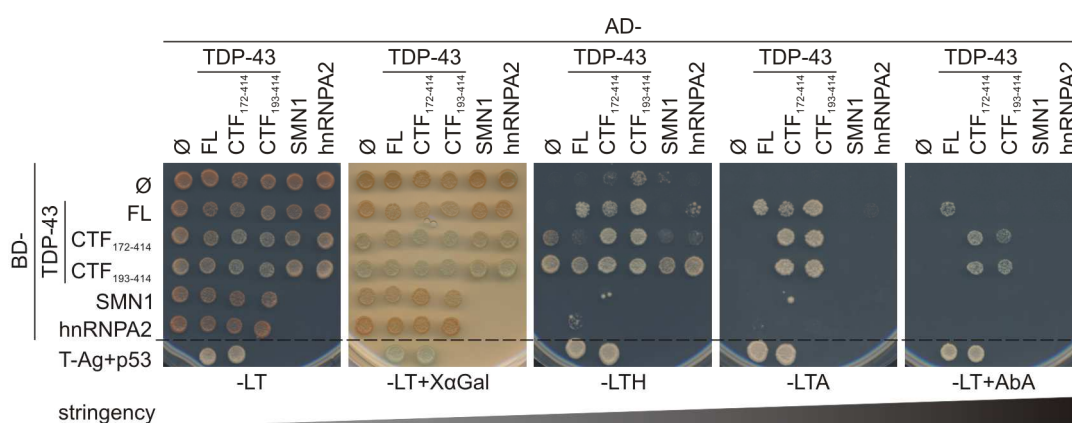
Figure 3.3 TDP-43 dimerization is a suitable positive control for TDP-43 protein interaction in yeast. To identify interactors of TDP-43 suitable as positive controls in yeast, 6x104 cells of the yeast strain Y2HGold, expressing AD- and BD-TDP-43 FL, CTF172-414, CTF193-414, SMN1, hnRNPA2 or control (Ø) constructs in different combinations, as indicated, were spotted onto the following selective medium plates and incubated for 4d at 30°C: -LT (selecting for co-transformed yeast), -LT + X-alpha-Gal (-LT + XαGal), - leucinge/ - tryptophane/ - histidine (-LTH), - leucine/ - tryptophane/ - adenine (-LTA), and -LT + AbA (80ng/ml). The interaction of AD-SV40 large T antigen and BD-p53 (Ø T-Ag + p53) served as a control of a working Y2H. The experiment was performed twice.
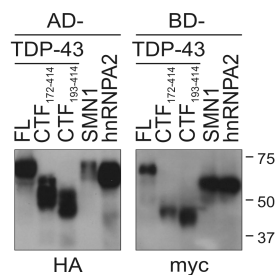
Figure 3.4 Confirmation of AD- and BD-TDP-43, SMN1 and hnRNPA2 expression in Y2HGold. Extracts of Y2HGold cells expressing TDP-43 FL, CTF172-414, CTF193-414, SMN1 or hnRNPA2 either fused to AD- or BD-domain of Gal4 transcription factor were analyzed with western blot for the expression level of the proteins. The AD-fused proteins were detected with anti-HA antibody, while the BD-fused proteins were detected with anti-myc-antibody. This experiment was performed one time.

sufficient levels, ruling out that some interactions could not be detected because of low protein expression. Therefore, dimerizations of TDP-43 FL and of $CTF_{193-414}$, were considered as positive TDP-43 interactions and confirm interactions in yeast.

3.1.2   The Y2H screens

All Y2H screens of this study were performed using the Matchmaker™ Gold Yeast Two-Hybrid system and were performed with a human adult brain cDNA library (Mate & PlateTM library, both Clontech) containing partial cDNAs. In the first screen TDP-43 FL was used as bait. High stringency selective medium plates (-LT+AbA) were chosen for the first screen, according to the manufactures recommendations. The TDP-43 dimerization that served as a positive control was detectable with this stringency (see Figure 3.3). The mating efficiency was 3.25% (efficiency from 2-5% should be readily achieved, according to the user manual) and approximately 3.12×10^6 cDNA clones were screened, almost covering the library with 3.2×10^6 clones. 60 primary positive clones were found after 7d. These were further analyzed to distinguish genuine positive from false positive interactions by retransformation of the isolated library cDNA constructs with BD-TDP-43 FL or -Ø into yeast, followed by spotting on several selective medium plates (for a detailed description of analysis see chapter 5.2.5). Under very high stringency almost all hits were either false positive (growth of BD-TDP-43 FL and BD-Ø co-expressing yeast) or showed no interaction with BD-TDP-43 FL at all. The only prey showing interaction with TDP-43 was identified by sequencing: a C-terminal part of exosome component 10 (EXOSC10). The interaction of this protein with TDP-43 was already found in a global Y2H screen (Lehner and Sanderson, 2004). We confirmed the interaction of full-length AD-EXOSC10 with BD-$CTF_{172-414}$ and $CTF_{192-414}$ in yeast, but not with TDP-43 FL (Figure 3.5). However, we did not identify any novel TDP-43 interactors with this first Y2H screen. Assuming that the stringency in this first Y2H screen was too high, we repeated the screen, this time on -LTH selective medium plates supplemented with the competitive inhibitor of
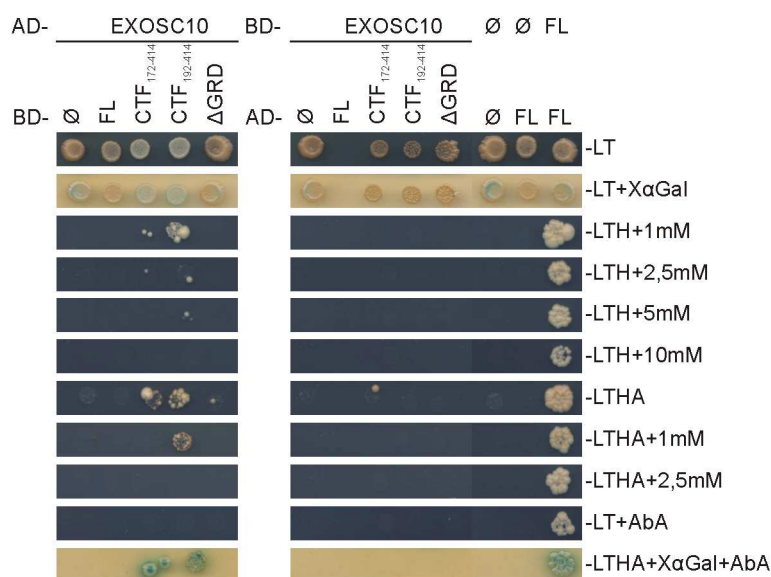
Figure 3.5 Interaction of TDP-43 with EXOSC10 in yeast. The spotting of 6x104 Y2HGold cells co-expressing full-length EXOSC10 and TDP-43 FL, CTF172-414, CTF192-414 or TDP-43 lacking the gly-cine-rich domain (aa1-273, ΔGRD) was performed in dublicates on selective medium plates: -LT (selecting for co-transformed yeast), -LTH, -LTH + 3-AT in increasing concentrations, -LTHA, -LTHA + 3-AT in increasing concentrations, -LT+AbA (80ng/ml) and -LTHA+X+AbA. Yeast was cultivated at 30°C for 11d. Depicted is one spot of two for each condition. This experiment was performed once.

the product of the *HIS3* gene, 2,5mM 3-Amino-1,2,4-triazole (3-AT). This prevents background growth of yeast in which transcription of the HIS3 reporter gene is not activated, as this reporter can be leaky.

The second Y2H screen with TDP-43 FL yielded 35 primary positive clones. The mating efficiency was 1.25% and 1.75×10^6 cDNA library clones were screened. Thus, only half of the library clones were covered, though a number of 1×10^6 screened independent clones is considered as sufficient, according to the manufacturer. As in the first screen, only one hit could be confirmed upon retransformation. The already published interaction of karyopherin alpha 4 (KPNA4) was not further validated (Nishimura et al., 2010). Sequencing of the cDNA library plasmids of all primary positive hits revealed that almost all contained 3'UTRs instead of protein-coding sequences, implying that protein sequences were expressed in the Y2H screen which are probably not encoded in the human genome.

Since the initial attempts to identify novel interactors of TDP-43 FL did not yield any novel results, another screen was performed using CTF$_{192-414}$ as bait. This construct contains RRM2 and the protein binding domain GRD, and is from now on referred to as CTF. The subset of interactors binding to N-terminally TDP-43 could not be covered. For this screen -LTHA + 2.5mM 3-AT selective medium plates were chosen. This was a higher stringency than compared to the second screen, trying to reduce the number of false positive hits. The mating efficiency of 5% was high and approximately 5.76×10^6 cDNA clones were screened, representing 1.8-fold coverage of the

brain cDNA library. 75 primary positive clones were found after 7d growth at 30°C and additional ~500 after 11d, of which a total number of ~230 were further analyzed (for a detailed description of analysis see chapter 5.2.5). Out of these 230 ten novel primary clones were found and the whole sequences were identified (Table 3.1). Some of them were represented repeatedly among all positive hits in this screen. Since the indentified cDNA FLJ57086 shares 98% homology with the Mediator of RNA polymerase II transcription sub-unit 6 (MED6), this protein was assumed as positive interactor. Also in this third screen most of the identified primary positive TDP-43 interactors were either translated 3'UTRs that were often very short (<20aa), or very short translated genomic sequences.

In summary the two Y2H screens with TDP-43 FL yielded the known interactors EXOSC10 and KPNA4, while in the Y2H screen using CTF ten novel binding partners of TDP-43 were found (Table 3.1).

3.1.3 Confirmation of TDP-43 FL and CTF interactions with the novel targets in yeast

The interactions of BD-CTF with the primary positive hits were confirmed upon re-transformation in yeast (Figure 3.6), with all targets growing at least at intermediate stringency -LTHA + 5mM 3-AT. UBPY was the only target showing weak interaction with TDP-43 FL. It is also noteworthy that UBPY is the only confirmed interactor from among the 7d primary positive clones, and all other hits were identified from yeast colonies which grew after 11d post-mating.

The full-length cDNAs of seven of the ten hits could be cloned. The growth of yeast retransformed with full-length LSM6, MED6 or RACK1 confirmed the interaction with CTF, but not TDP-43 FL (Figure 3.7). An interaction of RBM45 was detected both with CTF and FL. On the other hand, yeast expressing AD-full-length-UBPY or -UBE2E3 and BD-TDP-43 FL or CTF did not grow on any stringency beside selection for cotransformation (-LT). In case of UBPY the C-terminal part (aa876-1118) identified form the cDNA library is much smaller than the full-length protein, assuming that folding of full-length UBPY hides the interaction site of TDP-43 FL and CTF. Interestingly, RACK1 occurred as an interactor of TDP-43 FL in a global proteomic approach (Freibaum et al., 2010) and interaction of the TDP-43 fly ortholog TBPH with RACK1 was found in a protein interaction map of *Drosophila melanogaster* (Giot et al., 2003). Furthermore, RBM45 colocalized with TDP-43 in pathological inclusions of ALS and FTLD-TDP-43 patients (Collins et al., 2012). Thus, our Y2H screen was suitable to identify known interactors as well as new binding partners of TDP-43.

Table 3.1 Overview of positive Y2H hits. The UniProt accession number, similarity of cDNA library with homologous sequence, size of proteins, and strength of interaction with TDP-43 FL and CTF upon retransformation of the positive hits are shown. MED6 was assumed as a positive interactor, because its first 121 amino acids share 98% homology with cDNA FLJ57086. Strength of interaction: + weak, ++ moderate, +++ strong. aa - amino acids; [a] Partial cDNA sequences from Y2H hits were not sequenced till stop codon; [b] cDNA sequence ends with stop codon, though reference sequence has later stop codon; n.d. - not determined

Symbol	Name	Accession Number (translated amino acids in Y2H)	Identities	Protein size [aa]	Homologous hit	Strength of interaction in Y2H with TDP-43	
						FL	CTF
BEX2	Brain-expressed X-linked protein 2	Q9BXY8 (aa1-128)	118/128 (92%)	128		-	+++
CTAGE5	Cutaneous T-cell lymphoma-associated antigen 5	O15320 (aa442-615)[b]	132/174 (75%)	804		-	+++
GPR137B	Integral membrane protein GPR137B	O60478 (aa292-399)	108/108 (100%)	399		+	+++
LSM6	U6 snRNA-associated Sm-like protein LSm6	P62312 (aa62-80)	19/19 (100%)	80		-	++
cDNA FLJ57086	cDNA FLJ57086, highly similar to RNA polymerase transcriptional regulation mediator, subunit 6 homolog	B4DTY4 (aa1-128)	128/128 (100%)	128	MED6	-	+++
MED6	Mediator of RNA polymerase II transcription subunit 6	O75586 (aa1-121)	119/121 (98%)	246			
RACK1 (GNB2L1)	Receptor for Activated C Kinase 1	P63244 (aa78-290)[a]	213/213 (100%)	317		-	+++
RBM45	RNA-binding protein 45	Q8IUH3 (aa59-284)[a]	214/226 (94%)	476		n.d.	+++
RNF2	E3 ubiquitin-protein ligase RING2	Q99496 (aa276-336)	61/61 (100%)	336		-	++
UBE2E3	Ubiquitin-conjugating enzyme E2 E3	Q969T4 (aa126-207)	82/82 (100%)	207	UBE2E1, UBE2E2	-	++
UBPY (USP8)	Ubiquitin isopeptidase Y	P40818 (aa877-1088)*	212/212 (100%)	1118		+	+++
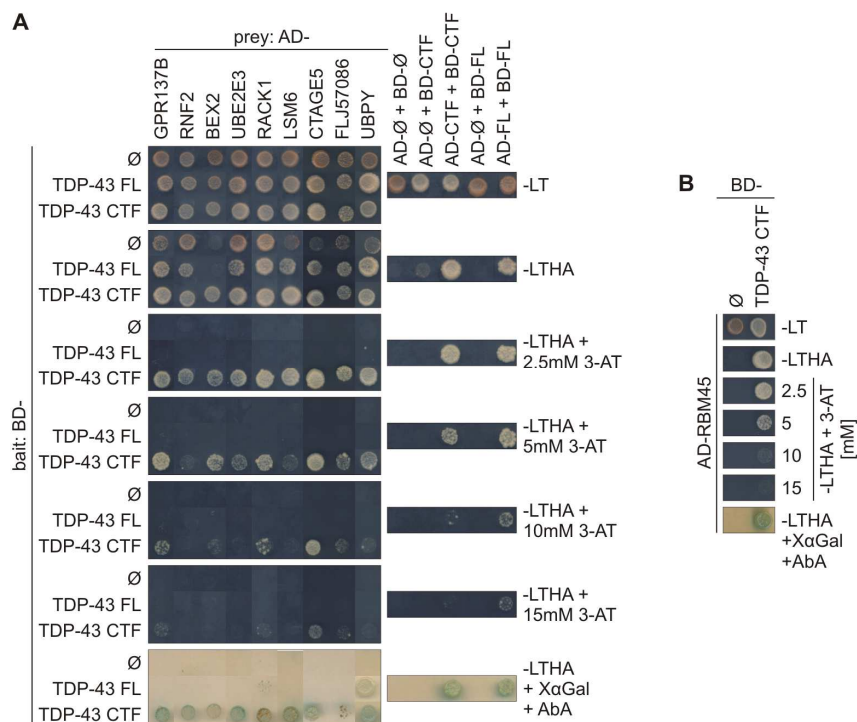
Figure 3.6 Confirmation of TDP-43 interactions with the primary positive Y2H clones. A+B AD-library plasmids that were isolated from primary positive clones and contained partial cDNAs, were retransformed into Y2HGold together with BD-TDP-43 FL, CTF or control (Ø) plasmids. To confirm the interactions of the candidate-AD-prey with BD-TDP-43 FL and CTF, $6x10^4$ yeast cells were spotted in duplicates onto the following selective medium plates and incubated for 7d at 30°C: -LT (selecting for co-transformed yeast), -LTHA, -LTHA + 3-AT in increasing concentrations, as indicated, and -LTHA + X + AbA (80ng/ml). The dimerization of TDP-43 FL or CTF was used as a positive control. One yeast spot for each transformation is shown. The experiments were performed once.
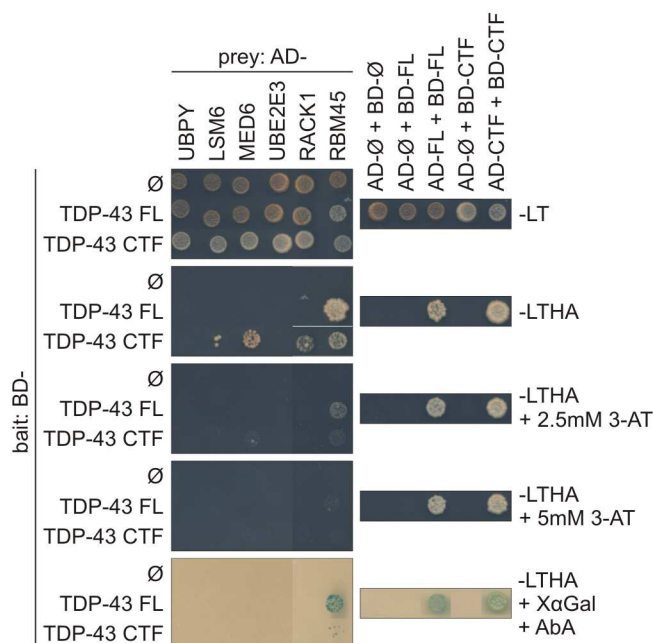
Figure 3.7 Confirmation of Y2H interaction of TDP-43 FL or CTF with full-length interactors. AD-UBPY, -LSM6, - MED6, -UBE2E3, -RACK1 or -RBM45 were co-transformed with BD-TDP-43 FL or CTF or control vector (Ø) into Y2HGold cells. $6x10^4$ co-transformed yeast cells were spotted in duplicates onto the indicated selective medium plates and cultivated for 7d at 30°C. This experiment was performed twice and one of two spots per condition is shown. When this experiment was done, RNF cDNA was not cloned, yet.

3.1.4   Interaction and colocalization of TDP-43 with the new targets in HEK293E cells

Further verifications of the interaction of TDP-43 with the targets identified in the Y2H screen were carried out in human embryonic kidney (HEK293E) cells. Coimmunoprecipitation experiments were performed using mCherry-tagged TDP-43 FL and CTF, and tagged LSM6, MED6, UBE2E3, UBPY, RACK1, RNF2 and RBM45 (Figure 3.8A-E). The binding of LSM6, MED6, UBPY, RNF2 and RBM45 with CTF was stronger than with TDP-43 FL, which reflects the findings in yeast (compare Figure 3.8A, B, D and E with Figure 3.6). On the other hand, mCherry-TDP-43 FL and CTF bound to RACK1 with the same intensity (Figure 3.8C). Coimmunoprecipitation of CTF with UBE2E3 was just slightly above background, and could not be detected for mCherry-TDP-43 FL at all. Interestingly, overexpressed myc-UBE2E3 was able to bind to immunoprecipitated Flag-tagged TDP-43 FL (Figure 3.8F). The interaction of overexpressed UBPY and TDP-43 was also confirmed in this setup (Figure 3.8G). This might indicate that the N-terminal mCherry-tag interferes with the binding of UBE2E3 to TDP-43. Nevertheless, the weak interaction of TDP-43 with UBE2E3 could still be functionally relevant, as binding of E2 enzymes with their targets is transient.

The Y2H interactions could be verified in a mammalian overexpression system. Next we analyzed the sub-cellular localization of the targets and their colocalization with endogenous (Figure 3.9A) or overexpressed (Figure 3.9B) Flag-TDP-43 with dual-labelled immunofluorescence staining. Therefore, myc-tagged targets were overexpressed in HEK293E. TDP-43, either endogenous or Flag-tagged, was mainly localized in the nucleus, but some cytoplasmic staining was also observed upon longer exposure (not shown). MED6, RBM45 and RNF2 were exclusively detected in the nucleus, showing overlap with nuclear TDP-43. LSM6 showed a nuclear as well as a cytoplasmic distribution. UBE2E3 was found in both the nucleus and the cytoplasm, mainly depending on the strength of overexpression. Cells with weak or moderate level showed nuclear staining for myc-UBE2E3, whereas strongly expressed UBE2E3 was found in comparable levels in both compartments. Overexpressed RACK1 and UBPY were localized in the cytoplasm. All nuclear localized targets showed signal-overlap with endogenous and exogenous TDP-43 in the nucleus. The cytoplasmic colocalization of TDP-43 and UBPY could only be detected upon longer exposure of cytoplasmic TDP-43 staining (see Figure 3.24A).
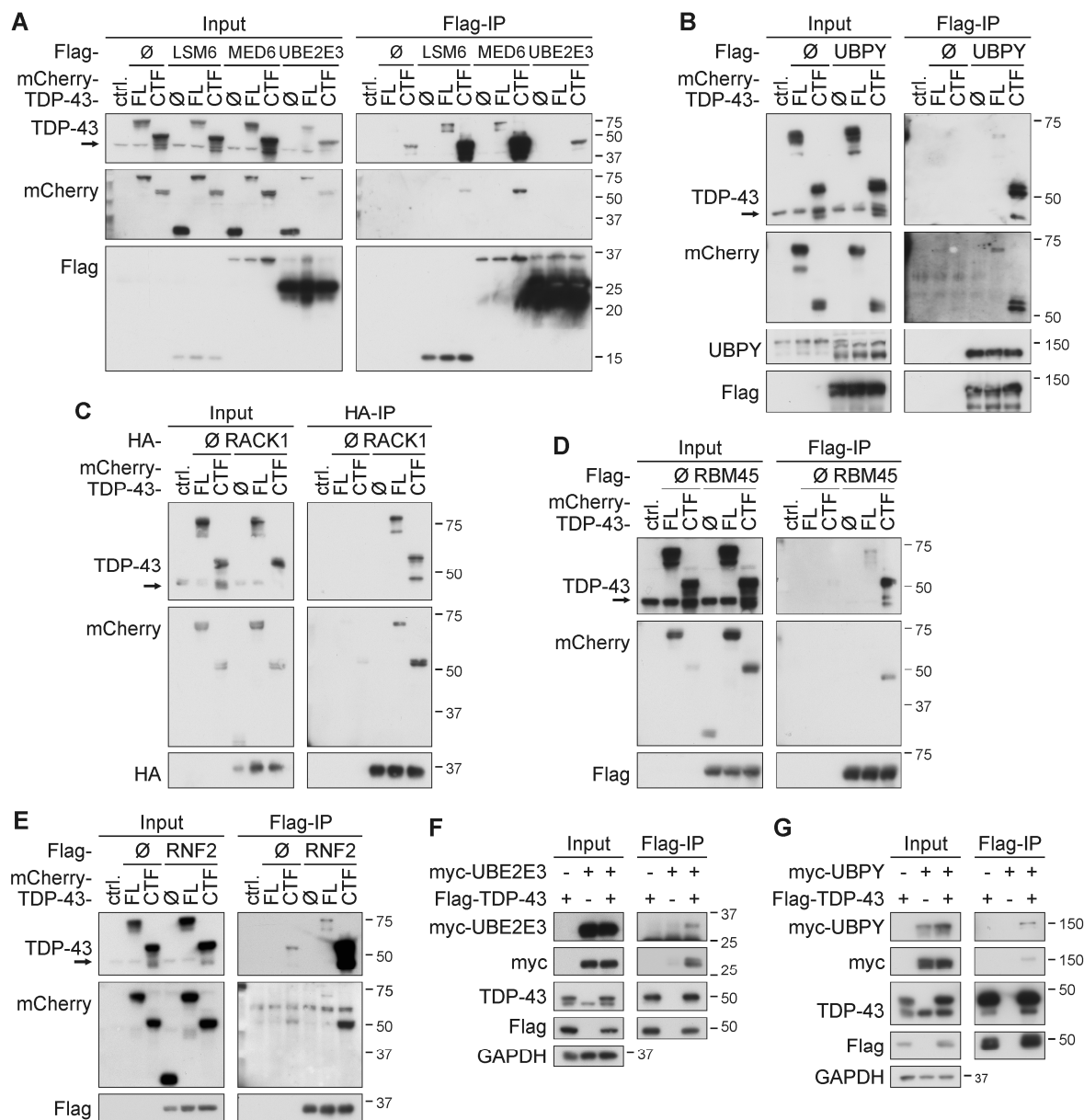
Figure 3.8 Coimmunoprecipitation of TDP-43 with the Y2H interactors. A-E HEK293E cells were co-transfected with mCherry-TDP-43 FL, CTF or control vector (ctrl) along with control vectors (Ø), Flag-tagged LSM6, MED6, UBE2E3 (A), UBPY (B), RBM45 (D), RNF2 (E), or HA-tagged RACK1 (C). This was followed by lysis and immunopreciptiation with anti-Flag (A,B,D,E) or anti-HA coupled sepharose beads (C). Western blotting of total cell lysates (Input) and immunoprecipitates (Flag-IP or HA-IP) was performed. The proteins were detected with antibodies against TDP-43, dsRed (mCherry), Flag or HA, and UBPY, as indicated. The endogenous TDP-43 bands (arrows) confirm even input loading. F+G Flag-TDP-43 and myc-UBE2E3 (F) or -UBPY (G) were co-expressed in HEK293E cells. TDP-43 was immunoprecipitated from cell lysates with anti-Flag affinity gel. Total protein (Input) and (co-) immunoprecipitated proteins (Flag-IP) were analyzed by western blot. The following proteins were stained: UBE2E3 (F), UBPY (G), myc, TDP-43, Flag and GAPDH, as indicated.
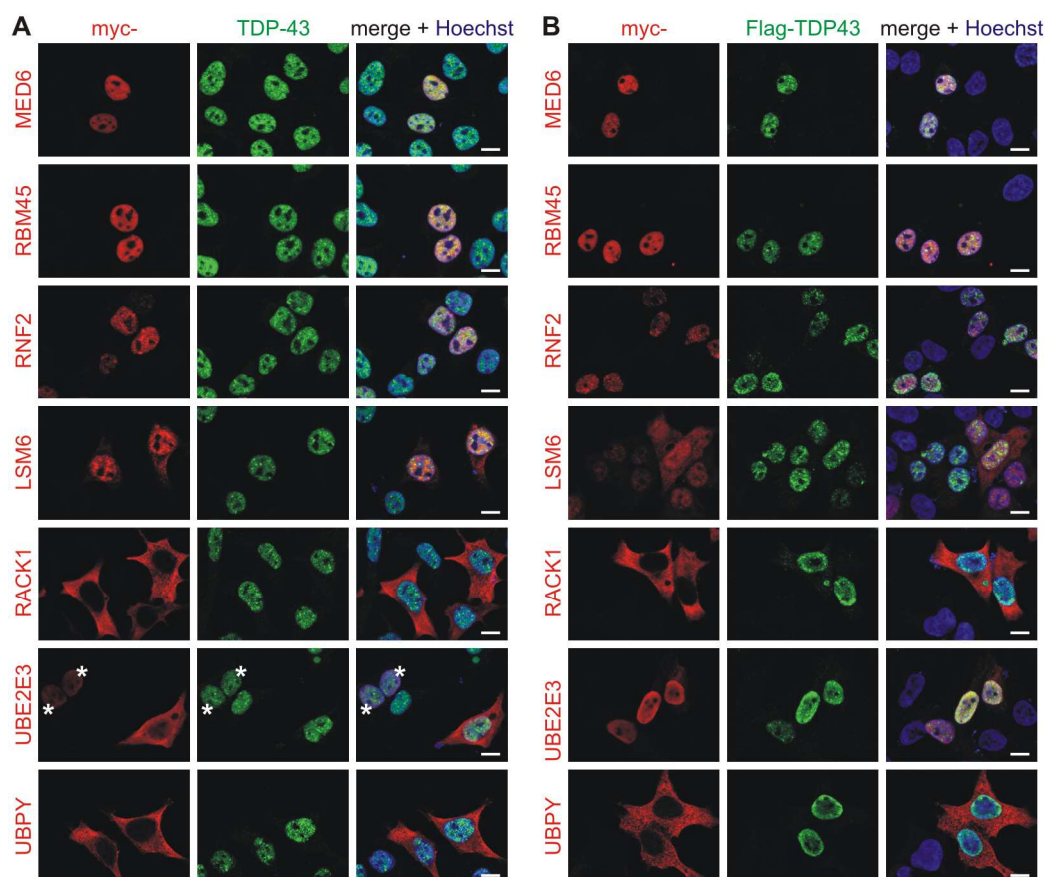
Figure 3.9 Colocalization of endogenous or Flag-TDP-43 wt with Y2H targets. A HEK293E cells were transfected with myc-MED6, -RBM45, -RNF2, -LSM6, -RACK1, -UBE2E3 or -UBPY. After 96h cells were fixed, permeabilized and stained for endogenous TDP-43 (rabbit-anti-TDP-43, green) and the indicated myc-tagged interactors (mouse-anti-myc, red). The cells expressing moderate levels of myc-UBEE3 are indicated with asterisks (*). **B** The same myc-tagged interactors as in (A) were co-expressed with Flag-TDP-43 wt in HEK293E cells and dual-labeled for overexpressed TDP-43 (rabbit-anti-Flag, green) and myc-interactors (mouse-anti-myc, red). Merged images include nuclear counter-staining with Hoechst 33342 (blue). Scale bars correspond to 10µm.

Most interactions of the targets with TDP-43 were stronger with the mainly cyto-plasmic CTF than with the predominantly nuclear TDP-43 FL, both in yeast and in co-immunoprecipitation. Thus the colocalization of the targets with EGFP-tagged TDP-43 FL and CTF were investigated. Since CTF is rapidly turned over, the introduction of an EGFP- or mCherry-tag stabilizes this construct. EGFP-TDP-43 FL was nuclear local-ized, as seen for endogenous and Flag-tagged TDP-43, while EGFP-CTF was also found to a great extend in the cytoplasm. We asked if a colocalization of the targets could be seen with CTF by overexpressing EGFP-tagged CTF and whether this co-expression may cause changes in the subcellular localization of the interactors (Figure 3.10). The cytoplasmically distributed Y2H targets colocalized only with EGFP-CTF, while nu-clear targeted proteins colocalized with EGFP-TDP-43 FL and the nuclear portion of CTF. However, the cellular localization of all targets was unaffected upon co-expression with EGFP-CTF (Figure 3.10).
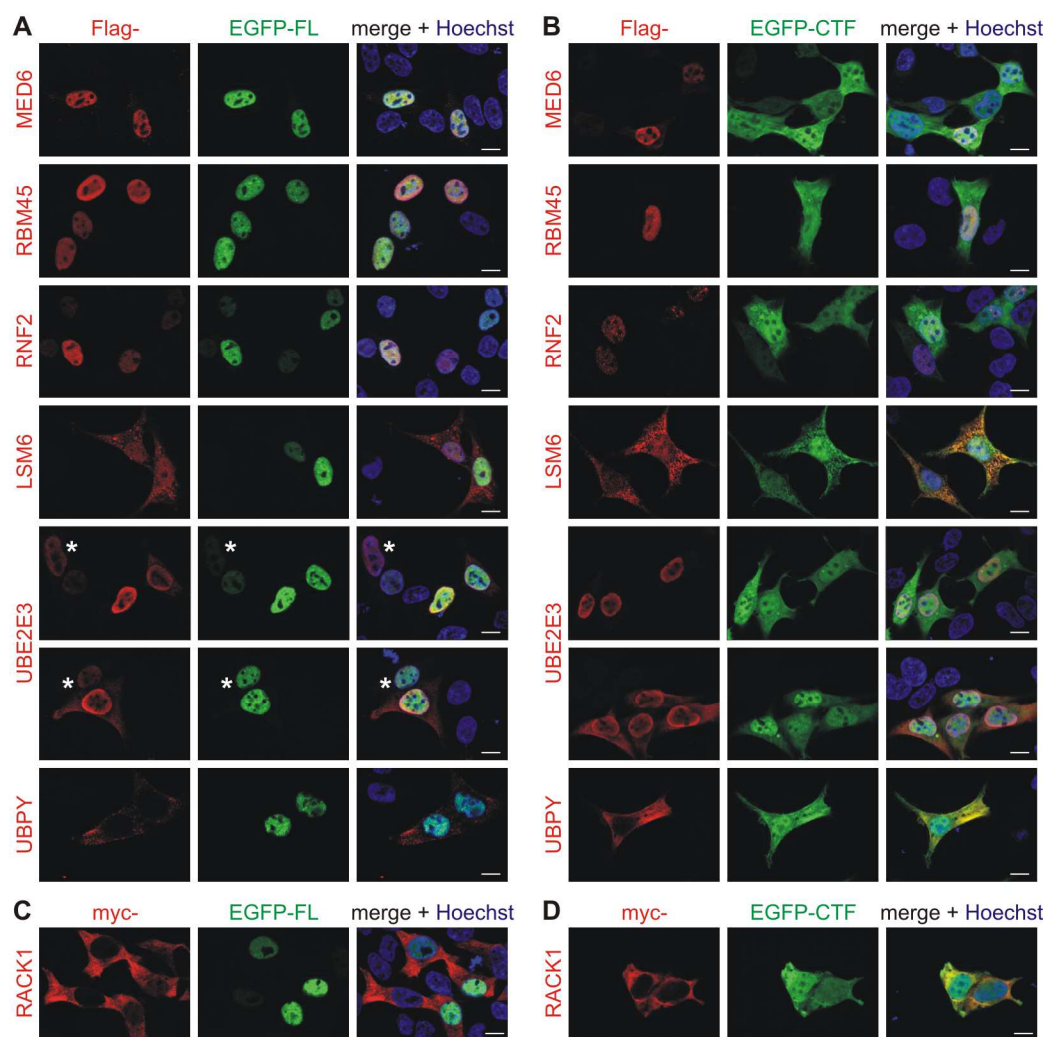
Figure 3.10 Colocalization of EGFP-TDP-43 FL or CTF with Y2H interactors. A+B Flag-tagged MED6, RBM45, RN2, LSM6, UBE2E3 or UBPY were co-expressed either with EGFP-TDP-43 FL (A) or CTF (B) in HEK293E cells. Interactors were stained with mouse-anti-Flag (red). **C+D** HEK293E cells transfected with EGFP-TDP-43 FL (C) or CTF (D) and myc-RACK1 were labeled with mouse-anti-myc (red). **A-D** Merged images include nuclear counterstaining with Hoechst 33342 (blue). Scale bars correspond to 10μm. Cells that express moderate levels of myc-UBEE3 are indicated with asterisk (*).

Since LSM6, RACK1 and UBPY are localized partly or exclusively in the cytoplasm, we asked whether a nuclear import impaired TDP-43 NLS mutant (NLSmut) was able to colocalized with or bind stronger to these Y2H targets. Therefore, the colocalization and coimmunoprecipitation of LSM6, RACK1 and UBPY with a nuclear import impaired TDP-43 NLSmut was examined (Figure 3.11). In an immunofluorescence approach, TDP-43 NLSmut was localized mostly in the cytoplasm (Figure 3.11A). The targets exhibited signal overlap with NLSmut in the cytoplasm, as all overexpressed proteins were evenly distributed over the whole cytoplasm. In the coimmunoprecipitation experiments, Flag-TDP-43 NLSmut bound much stronger than wt to cytoplasmic UBPY (Figure 3.11B). An interaction of LSM6 was only detectable with NLSmut but not with TDP-43 wt (Figure 3.11C), indicating that the interactions of UBPY and LSM6 are possibly taking place in the cytoplasm. Unexpectedly, RACK1 immunoprecipitated equal amounts of TDP-43 wt and NLSmut.
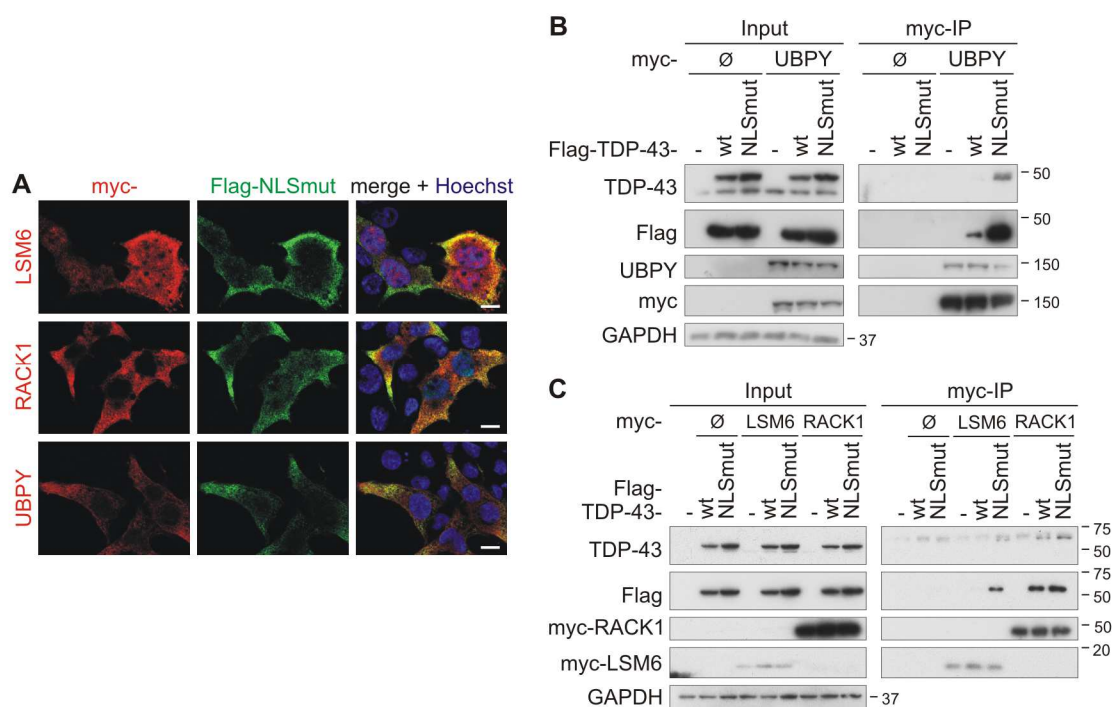
Figure 3.11 Colocalization and coimmunoprecipitation of wt and nuclear impaired TDP-43 with UBPY, LSM6 and RACK1. A Cytoplasmically localized myc-LSM6, -RACK and -UBPY were co-expressed with nuclear import impaired Flag-TDP-43 (NLSmut). Targets were stained with mouse-anti-myc (red) and NLSmut with rabbit-anti-Flag (green). Merged images including nuclear counterstaining with Hoechst 33342 (blue) are to the right. Scale bars, 10μm. **B+C** HEK293E cells were transfected with Flag-TDP-43 wt, nuclear impaired NLSmut and myc-UBPY (A), -LSM6, -RACK1 (both B) or empty vectors (Ø). The cells were lysed and myc-immunoprecipitation was performed. Total protein (Input) and eluates (myc-IP) were analyzed with western blot for TDP-43, Flag, UBPY (only A), myc and GAPDH.

In summary, the interaction of all identified targets was confirmed in HEK293E cells at least with CTF, but for most also with TDP-43 FL. Moreover, a nuclear overlap for all targets localized in this compartment was observed, whereas the cytoplasmic interactors colocalized with EGFP-CTF and a nuclear import impaired NLS mutant. LSM6, RACK1 and UBPY also bound these cytoplasmic TDP-43 variants.

3.2 Characterization of TDP-43 ubiquitinylation

TDP-43 positive inclusions in the brain and spinal cord of FTLD and ALS patients also contain ubiquitin (Arai et al., 2006; Neumann et al., 2006). Furthermore, accumulations of TDP-43 and ALS-linked mutations in proteins that participate within degradation pathways implicate failure of clearance of TDP-43 as a primary disease mechanism. Three of the identified and confirmed interactors are involved in ubiquitinylation events within the cell: the class III E2 ubiquitin-conjugating enzyme UBE2E3, the E3 ubiquitin ligase RNF2 and the ubiquitin-isopeptidase UBPY. The ubiquitinylation and degradation of TDP-43 is not well understood and might play an important role in inclusion formation. Therefore, the contributions of these three enzymes to the TDP-43 ubiquitinylation were investigated more thoroughly in this

study. The ubiquitinylation and degradation of TDP-43 is controversial. Some reports indicate that TDP-43 is degraded by the proteasome (Kabashi et al., 2008; Rutherford et al., 2008; van Eersel et al., 2011; Winton et al., 2008a; Zhang et al., 2010), while others point to an autophagic clearance (Caccamo et al., 2009; Filimonenko et al., 2007; Wang et al., 2012) or involvement of both pathways (Brady et al., 2011; Scotter et al., 2014; Urushitani et al., 2010; Wang et al., 2010).

First, the potential degradation of TDP-43 via the UPS or the autophagy-lysosomal system was investigated (Figure 3.12). Therefore, the proteasomal inhibitor MG-132, the inhibitor of the lysosomal ATPase bafilomycin A1 (Baf), and the autophagy inhibitor 3-methyladenine (3-MA) was used. The inhibition of the proteasomal or lysosomal function or both did not alter steady-state level of TDP-43 in sequentially extracted HEK293E cells within 24h (Figure 3.12A). This points towards a long lifespan and slow turnover of TDP-43. Interestingly, upon MG-132 treatment for 6h and 24h TDP-43 positive, higher molecular weight smears as well as 35kDa and 25kDa TDP-43 fragments were observed in the insoluble urea fractions. These could be sta-
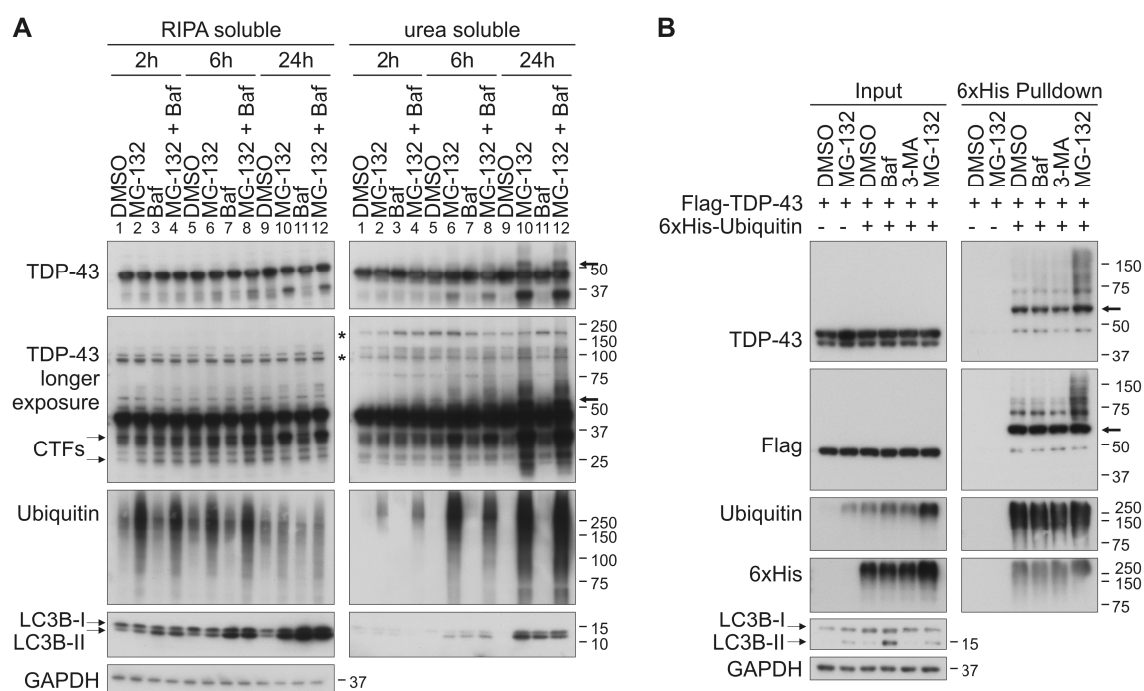
Figure 3.12 TDP-43 is ubiquitinylated upon proteasomal inhibition. A HEK293E cells were treated with the lysosomal inhibitor bafilomycin A1 (Baf, 20nM), the proteasomal inhibitor MG-132 (10µM), both or DMSO for 2h, 6h or 24h, as depicted. The cells were subjected to sequential extraction with RIPA buffer and urea buffer. The lysates were subjected to western blot analysis and probed with antibodies against TDP-43, ubiquitin, and LC3. GAPDH served as loading control. Asterisks label unspecific bands. **B** TDP-43, HEK293E cells overexpressing Flag-TDP-43 and 6xHis-tagged ubiquitin or vector control (-) were treated for 3h with MG-132, bafilomycin A1, the autophagy inhibitor 3-MA (5mM) or DMSO. Ni-NTA-purification for 6xHis-tagged ubiquitin modified species was performed with urea soluble protein lysates. Western blots of total protein lysates (Input) and purified Ni-NTA agarose eluates (6xHis-Pulldown) were probed with antibodies against TDP-43, Flag, ubiquitin, LC3 and GAPDH, as indicated. Arrows (bold) point towards monoubiquitinylated TDP-43 (see Figure 3.19).

bilized CTFs or N-terminal fragments of TDP-43. Bafilomycin A1 alone had no effect on TDP-43 higher molecular weight smear formation and fragment appearance. Furthermore, the combinational inhibition of lysosomal and proteasomal function did not increase the MG-132 induced effects on TDP-43.

Next, it was confirmed that the higher molecular weight smear is ubiquitinylated TDP-43. Therefore, Flag-TDP-43 and 6xHis-ubiquitin were overexpressed in HEK293E cells, lysed with 8M urea buffer and a pulldown of 6xHis-ubiquitin-conjugated proteins was performed with Ni-NTA agarose (Figure 3.12B). TDP-43 was slightly ubiquitinylated under basal conditions which was dramatically increased after MG-132 treatment, while blocking of lysosomal function had no effect. Thus, proteasomal inhibition increased ubiquitinylated TDP-43 and was used as a model for further studies of TDP-43 ubiquitinylation.

Next, it was asked if MG-132 or bafilomycin A1 had an influence on the localization of endogenous and Flag-tagged TDP-43. (Figure 3.13A+B). The treatment of HEK293E cells with MG-132 for up to 18h did not alter nuclear TDP-43 localization. Within this timeframe no TDP-43 accumulation or aggregates were observed. The cells started to detach from the coverslips after 20h proteasomal inhibition with 10μM MG-132 and treatment longer than 24h was toxic. Thus, TDP-43 localization could not be monitored much longer than in this immunofluorescence experiment. In summary, no prominent relocalization of TDP-43 was observed upon proteasomal inhibition.
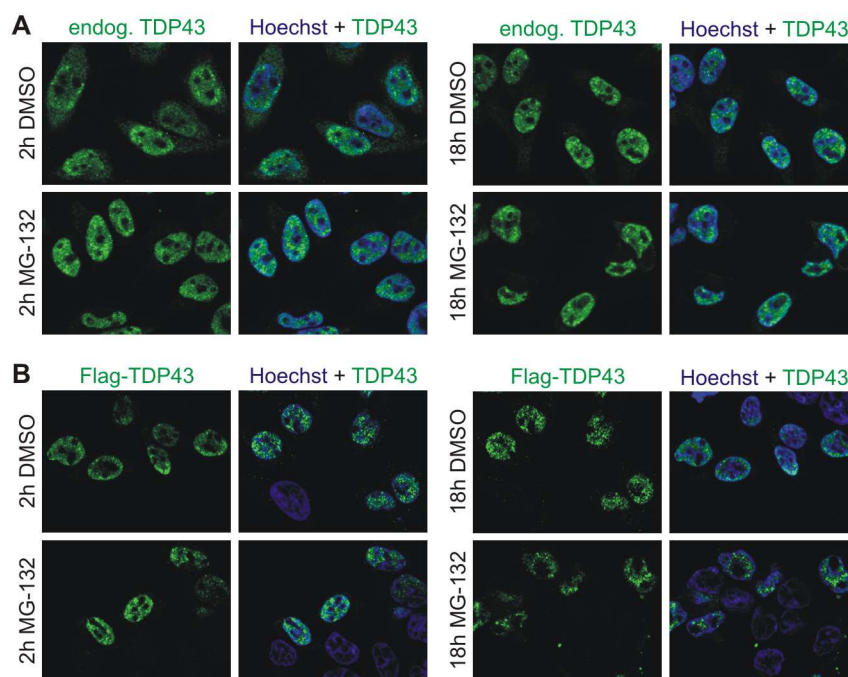
Figure 3.13 Effect of proteasomal inhibition on the localization of endogenous and exogenous TDP-43. A+B Non-transfected (A) or Flag-TDP-43 overexpressing (B) HEK293E cells were treated with 10μM MG-132 or DMSO control for 2 and 18h, respectively. The cells were labeled with rabbit-anti-TDP-43 antibody (A, green) or mouse-anti-Flag (B, green) and nuclei were counterstained with Hoechst 33342 (blue). Scale bars accord to 10μm.

As shown in coimmunoprecipitations above (Figure 3.8A+B) UBE2E3 and UBPY interact stronger with CTF than TDP-43 FL. Due to the fact that proteasomal inhibition stabilized endogenous fragments of TDP-43, it was asked whether UBE2E3 and UBPY were able to bind these fragments. Therefore, Flag-UBE2E3 or -UBPY were overexpressed in HEK293E cells and proteasomal degradation was inhibited for 6h or 20h with MG-132, followed by Flag-immunoprecipitation and western blot analysis (Figure 3.14). Binding of UBE2E3 to endogenous TDP-43 FL was not observed, but some 35kDa TDP-43 fragments were coimmunoprecipitated upon MG-132 treatment. Interestingly, Flag-UBPY bound both endogenous full-length TDP-43 and 35kDa fragment, regardless of the proteasomal status. Thus, overexpressed UBPY interacted with endogenous TDP-43, while the UBE2E3 interaction with TDP-43 FL might be not stable enough. Also, the low amounts of the 35kDa TDP-43 fragment were too low for detection with coimmunoprecipitation.
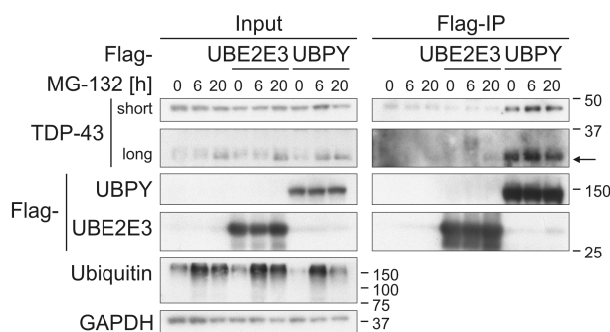
Figure 3.14 Coimmunoprecipitation of endogenous full-length and lower molecular weight TDP-43 species with UBE2E3 and UBPY. HEK293E cells transiently overexpressing Flag-UBE2E3 or -UBPY were treated with MG-132 (10μM) for 6h or 20h to increase 35kDa fragments of TDP-43. The cellular lysates were immunoprecipitated for Flag-tagged proteins. The total cell lysates (Input) and (co-) immunoprecipitated proteins (Flag-IP) were subjected to western blotting and probed with antibodies against TDP-43, Flag, and ubiquitin. GAPDH served as loading control. The arrow indicates the 35kDa TDP-43 fragment.

3.3 Regulation of TDP-43 ubiquitinylation by UBE2E ubiquitin-conjugating enzymes

3.3.1 The localization of UBE2E1, UBE2E2 and UBE2E3 in HEK293E

UBE2E3 has a high similarity with its two class III E2 enzyme family members UBE2E1 and UBE2E2. The C-terminal fragment of UBE2E3, which was translated from the partial cDNA found in the Y2H screen, shares 97% homology to the C-termini of UBE2E1 and UBE2E2 (Figure 3.15). Therefore, it is possible that all three E2s can (functionally) interact with TDP-43.

The subcellular localization of endogenous and overexpressed UBE2E1, UBE2E2 and UBE2E3 was investigated in immunofluorescence staining of HEK293E cells (Figure 3.16). Both endogenous UBE2E1 and UBE2E3 were nuclear, whereas all three exogenous myc-tagged E2 enzymes were additionally detected in the cytoplasm, depending on the extent of overexpression. The localization of endogenous UBE2E2 could not be investigated as the antibody did not recognize endogenous UBE2E2 in immunofluorescence. Furthermore, all E2 enzymes showed nuclear overlap with endogenous TDP-43, and the overexpression of the E2s did not alter the localization of TDP-43.

```
UBE2E3   MSSDRQRSDDESPSTSSGSSDADQRDPAAPEPEEQEERKPSATQQKKNTKLS-SKTTAKLSTSAKRIQKELAEIT 74
UBE2E2   MSTEAQRVDD-SPSTSGGSSDGDQRESVQQEPE-REQVQP----KKKEGKIS-SKTAAKLSTSAKRIQKELAEIT 68
UBE2E1   MSDDDSRAST---SSSSSSSSNQQTEKETNTPK-----------KKESKVSMSKNSKLLSTSAKRIQKELADIT 60
         ** : .* .    *:*..**. :* :    *:          **: *:* **.:  **************:**
                                                                ↑

Y2H cDNA                                                  KVTFRTRIYHCNINSQGVICLDIL

UBE2E3   LDPPPNCSAGPKGDNIYEWRSTILGPPGSVYEGGVFFLDITFSSDYPFKPPKVTFRTRIYHCNINSQGVICLDIL 149
UBE2E2   LDPPPNCSAGPKGDNIYEWRSTILGPPGSVYEGGVFFLDITFSPDYPFKPPKVTFRTRIYHCNINSQGVICLDIL 143
UBE2E1   LDPPPNCSAGPKGDNIYEWRSTILGPPGSVYEGGVFFLDITFTPEYPFKPPKVTFRTRIYHCNINSQGVICLDIL 135
         *********************************************:.:****************************

Y2H cDNA KDNWSPALTISKVLLSICSLLTDCNPADPLVGSIATQYVTNRAEHDRLARQWTKRYAT

UBE2E3   KDNWSPALTISKVLLSICSLLTDCNPADPLVGSIATQYVTNRAEHDRLARQWTKRYAT 207
UBE2E2   KDNWSPALTISKVLLSICSLLTDCNPADPLVGSIATQYVTNRAEHDRMARQWTKRYAT 201
UBE2E1   KDNWSPALTISKVLLSICSLLTDCNPADPLVGSIATQYMTNRAEHDRMARQWTKRYAT 193
         *************************************:*******:*********
```

Figure 3.15 Alignment of the amino acid sequence of the class III E2 ubiquitin-conjugating enzymes and the translated cDNA found in the Y2H screen. The sequences sharing homology with the Y2H prey protein are in black, the residual N-terminal sequences are in grey, while not-conserved amino acids in the prey protein homologous sequence are in red. The red arrow indicates the start of the core UBC domain with high homology. The homologies between the E2s are 83% for E1:E2, 78% for E1:E3 and 85% for E2:E3. The alignment was performed with ClustalW2 (Larkin et al., 2007).

Figure 3.16 Different sub-cellular localization of endo- and exogenous UBE2E ubiquitin conjugating enzymes. HEK293E cells, either overexpressing myc-UBE2E1, -UBE2E2 or -UBE2E3 or non-transfected, were immuno-labled for endo- and exogenous UBE2E enzymes with rabbit-anti-UBE2E1 or rabbit-anti-UBE2E2 and mouse-anti-TDP-43, or mouse-anti-UBE2E3 (clone 7E8) and rabbit-anti-TDP-43, as indicated. Rabbit-anti-UBE2E2 did not detect endogenous UBE2E2 in this application. Nuclei were stained with Hoechst 33342 (blue). Merged images are to the right, scale bars apply to all images and accord to 10µm. Asterisks label nuclear localized myc-UBE2E cells.

Additionally, the specificity of the antibodies against the E2 enzymes was analyzed to rule out cross reactivity with other UBE2E enzymes (Figure 3.17). Therefore, UBE2E1 and UBE2E3 were knocked down with three or four different siRNAs, respectively, and immunofluorescence staining of both E2s was performed with the cells (Figure 3.17A+B). The rabbit-anti-UBE2E1 and the mouse-anti-UBE2E3 (clone 7E8) antibodies specifically recognised their target. UBE2E1 silenced cells exhibited almost no staining with the rabbit-anti-UBE2E1 antibody, whereas UBE2E3 silenced cells were equally stained (Figure 3.17). Likewise, a UBE2E3 signal was almost not detectable in cells silenced for UBE2E3, but it was found in cells silenced for UBE2E1. Since the UBE2E2 antibody did not recognize endogenous E2 in the immunofluorescence approach, its specificity in immunofluorescence could not be verified. The TDP-43 levels were not altered in cells silenced for these E2 enzymes. Furthermore, specificity of the antibodies was verified in western blot analysis (Figure 3.17C). Three out of the four tested antibodies - rabbit-anti-UBE2E1, mouse-anti-UBE2E3 (MABS17) and mouse-anti-UBE2E3 (clone 7E8) - recognized their cognate endogenous E2 as well as their myc-tagged protein, but not the other E2 enzymes. Only the rabbit-anti-UBE2E2 antibody stained besides the myc-UBE2E2 protein also very weakly the overexpressed UBE2E1 and UBE2E3, but not the endogenous UBE2E1 and UBE2E3. Therefore, the UBE2E2 antibody worked well in western blot, but not in immunofluorescence. The higher molecular weight smears of myc-tagged E2 enzymes probably represent the ubiquitin-bound E2 proteins. Thus, the used antibodies detected specifically their cognate UBE2E enzyme and showed minimal or no cross reactivity.
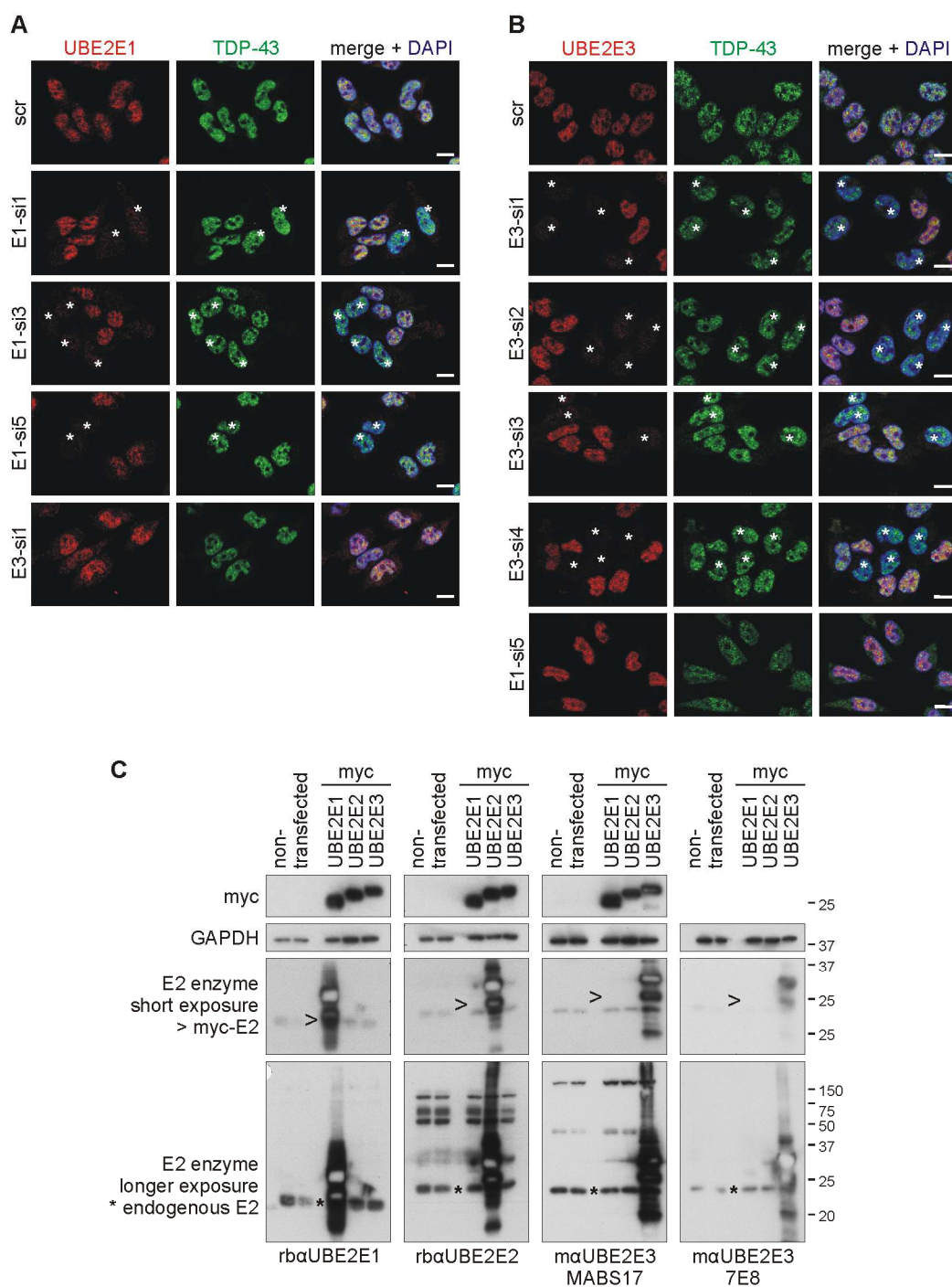
Figure 3.17 Specificity of the UBE2E enzyme antibodies. A+B UBE2E1 and UBE2E3 antibody specificity in an immunofluorescence approach. The expression of endogenous UBE2E1 (A) and UBE2E3 (B) in HEK293E cells was downregulated with three and four different siRNAs, respectively. The cells were double-stained for rabbit-anti-UBE2E1 and mouse-anti-TDP-43 (A) or mouse-anti-UBE2E3 (7E8) and rabbit-anti-TDP-43 (B). Merged images including nuclear counterstaining with Hoechst 33342 (blue) are to the right. Asterisks mark E2 silenced cells. Scale bars accord to 10μm. **C** Specificity of antibodies against UBE2E enzymes in western blot analysis. RIPA-lysates of HEK293E cells overexpressing myc-UBE2E1, -UBE2E2 or -UBE2E3 and non-transfected control cells were analyzed with western blot. The membranes were stained with anti-myc-HRP, mouse-anti-GAPDH and either rabbit-anti-UBE2E1, rabbit-anti-UBE2E2, mouse-anti-UBE2E3 (MABS17) or mouse-anti-UBE2E3 (clone 7E8). The arrowheads (>) label myc-tagged E2 enzymes. Because MABS17 detected endogenous UBE2E3 in western blot analysis better than clone 7E8, this antibody was chosen for further western blot analysis. MABS17 did not work in immunofluorescence approaches. Therefore, 7E8 was used in immunofluorescence. Asterisks label endogenous E2 enzymes. These experiments were performed once.

3.3.2 UBE2E ubiquitin-conjugating enzymes enhance TDP-43 ubiquitinylation

Next, it was investigated if the above shown nuclear signal overlap of UBE2E3 with TDP-43 as well as the limited binding of both proteins has a functional consequence. It was asked whether this E2 enzyme is involved in ubiquitinylation of TDP-43 (Figure 3.18). In addition, we examined if other closely (UBE2E1, UBE2E2) or more distantly (UBE2N, UBE2C) related E2 enzymes are able to ubiquitinylate TDP-43. Therefore, the E2 enzymes were co-expressed with Flag-TDP-43 and 6xHis-ubiquitin in HEK293E cells. The proteasome was inhibited for 2h to increase TDP-43 ubiquitinylation and ubiquitinylated proteins were isolated with Ni-NTA agarose pulldown. The overexpression of the E2 enzymes for 48h did not alter the steady state level of endogenous or Flag-TDP-43. Upon overexpression of UBE2E3, TDP-43 was strongly ubiquitinylated (Figure 3.18A, pulldown lane 5+6), whereas co-expression of the catalytically impaired UBE2E3 C145S failed to increase ubiquitinylation of TDP-43 (lane 7+8). UBE2E1 and UBE2E2 overexpression also increased TDP-43 ubiquitinylation (lane 9+10 and 13+14, respectively). The more distantly related UBE2N and UBE2C only slightly increased the level of ubiquitinylated TDP-43 (lane 11+12 and 15+16, respectively), though they were expressed at comparable levels like the other E2 enzymes. Interestingly, the inhibition of the proteasome did not further stabilize the ubiquitinylation of TDP-43 by UBE2Es. Only weak increase of ubiquitinylated TDP-43 upon UBE2N or UBE2C overexpression was observed (compare even with uneven lane numbers).

Since a decrease of mCherry-TDP-43 FL and CTF upon UBE2E3 overexpression was observed in HEK293E cells, the influence of the ubiquitinylation by UBE2E3 on the solubility of TDP-43 was investigated. Therefore, HEK293E cells were separated into NP-40 soluble and insoluble urea fractions. UBE2E3 overexpression had no effect on TDP-43 steady-state level in the NP-40 fraction, but induced a strong increase of TDP-43 in the insoluble urea fraction (Figure 3.18B). Ubiquitinylated TDP-43 species were exclusively detected in the insoluble urea fraction. Interestingly, UBE2E3 C145S co-expression also led to an accumulation of non-conjugated TDP-43 in the urea fraction, indicating that the UBE2E3/TDP-43 complex might be less soluble and therefore difficult to detect with coimmunoprecipitation.

Post mortem brain with TDP-43 positive inclusions also showed phosphorylation of this protein. Therefore, the phosphorylation status of ubiquitinylated TDP-43 was estimated. Pulldown samples from insoluble urea fractions of HEK293E cells co-expressing Flag-TDP-43 and myc-UBE2E3 were analyzed, because these contained a high amount of ubiquitinylated TDP-43, that might also be phosphorylated. However, only a weak phosphorylation of ubiquitinylated TDP-43 at S409/410 was detected (Figure 3.18C).

Figure 3.18 UBE2E enzymes enhance TDP-43 ubiquitinylation and insolubility. A UBE2E enzymes enhanced ubiquitinylation of TDP-43. HEK293E cells were triple-transfected for 48h with Flag-TDP-43, 6xHis-vector control (-) or 6xHis-ubiquitin (+) and myc-tagged E2 enzymes UBE2E3, catalyti-

cally inactive UBE2E3 C145S, UBE2E2, UBE2N, UBE2E1 or UBE2C or myc-vector control (-). The cells were treated with MG-132 (10µM) or DMSO for 2h prior to the lysis with urea buffer. The 6xHis-ubiquitin-conjugated proteins were pulled down from the cell lysates. The total protein lysates (Input) and Ni-NTA agarose eluates (6xHis Pulldown) were subjected to western blotting using antibodies agains TDP-43, Flag, ubiquitin, 6xHis, myc-tagged E2 enzymes and GAPDH. **B** Flag-TDP-43 was overexpressed with 6xHis-vector control (-) or 6xHis-ubiquitin (+) and myc-vector control (-) or myc-UBE2E3 wt or C145S in HEK293E cells. The proteasome was inhibited with MG-132 for 2h and a sequential extraction of NP-40 soluble and urea soluble proteins was performed. The 6xHis-ubiquitin conjugated proteins were isolated from both fractions and western blots of total cell lysates and pulldown eluates were stained for TPD-43, Flag, ubiquitin, 6xHis, myc and GAPDH. The amount of analyzed insoluble protein corresponded to approximately one twentieth (5%) of soluble protein concentration. **C** Analysis of phosphorylation of ubiquitinylated TDP-43. HEK293E cells were transfected and lysed as in B (without UBE2E3 C145S overexpression). The pulldown of ubiquitinylated proteins was subjected to western blot analysis and stained for total TDP-43, phosphorylated TDP-43 (S409/410), myc and GAPDH. The arrows indicate monoubiquitinylated TDP-43 (see Figure 3.1).

The overexpression of UBE2E3 as well as long proteasomal inhibition, was usually accompanied by the appearance of an approximately 55kDa TDP-43 band, both in western blot analysis of total protein lysates and 6xHis pulldown eluates. Upon longer exposure this band was also detectable without MG-132 treatment or E2 overexpression (see Figure 3.12B). To prove that this band represents a monoubiquitinylated TDP-43 form, 6xHis-tagged TDP-43 was isolated from HEK293E cells in the presence of endogenous ubiquitin (Figure 3.19). The pulldown of 6xHis-tagged TDP-43 ensured the enrichment of ubiquitinylated protein. Only after overexpression of UBE2E3, the 55kDa band was detected with two different antibodies (MAB1510 and UO508). These antibodies detect mono- and polyubiquitin moieties. On the other hand an antibody which specifically detects only polyubiquitinylated proteins (clone FK1) failed to detect the 55kDa band. Thus, TDP-43 was found to be mono- and polyubiquitinylated after overexpressing UBE2E3. It remains to be shown whether TDP-43 can also be multi-monoubiquitinylated.

The results of this section show that UBE2E enzymes participate in the ubiquitinylation of TDP-43 and that ubiquitinylated TDP-43 is insoluble. Furthermore, TDP-43 is shifted into insoluble urea fractions upon UBE2E3 expression. Additionally, the TDP-43 monoubiquitinylation is increased by UBE2E3 overexpression.
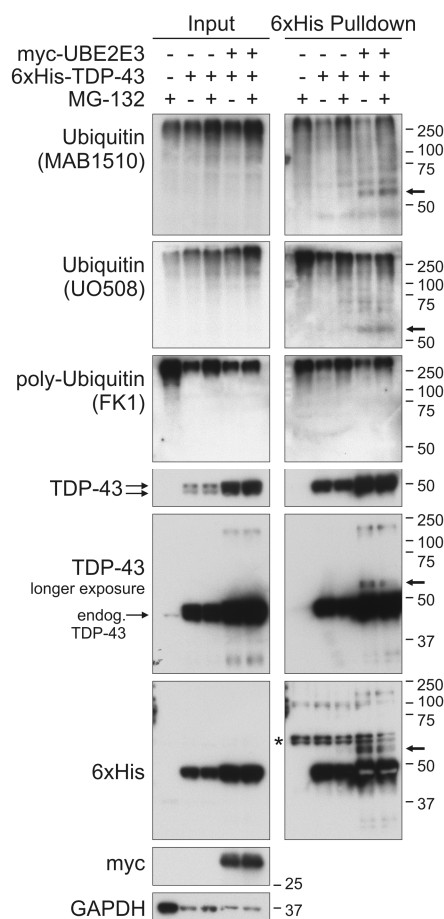
Figure 3.19 TDP-43 is monoubiquitinylated. 6xHis-TDP-43 (+) was co-expressed in HEK293E cells with myc-UBE2E3 (+) or vector controls (-) in the presence of endogenous ubiquitin. After proteasomal inhibition with MG-132 (10µM) for 2h, the cells were lysed in 8M urea buffer and Ni-NTA purification of 6xHis-TDP-43-conjugated proteins was performed. The total cell lysates (Input) and the pulldown eluates (6xHis Pulldown) were subjected to western blot analysis and probed for TDP-43, 6xHis, myc, and GAPDH. Mono- and polyubiquitinylated moieties were detected with mouse-anti-ubiquitin (MAB1510 and UO508) and polyubiquitinylated proteins with mouse-anti-ubiquitin (clone FK1). The experiment was performed twice.

3.3.3 The influence of UBE2E3 on the formation of TDP-43 fragments

Next, it was investigated how UBE2E3 overexpression alters the formation and stability of the endogenous TDP-43 35kDa fragment. HEK293E cells transfected with myc-UBE2E3 wt or C145S were treated with MG-132 for 6h or 20h, followed by sequential extraction into a RIPA soluble and an insoluble urea fraction (Figure 3.20). A reduction of the TDP-43 steady-state levels was observed upon proteasomal inhibition for 20h, but total protein was also decreased as compared with the loading control GAPDH. The TDP-43 35kDa fragments of the soluble and insoluble fractions were stabilized after 20h of MG-132 treatment. Surprisingly, UBE2E3 overexpression did not further increase the amount of this TDP-43 fragment. Unfortunately, TDP-43 ubiquitinylation was not detected in the urea fraction, as seen before (Figure 3.18C), probably due to a new rabbit-anti-TDP-43 antibody batch, that was used in this experiment.
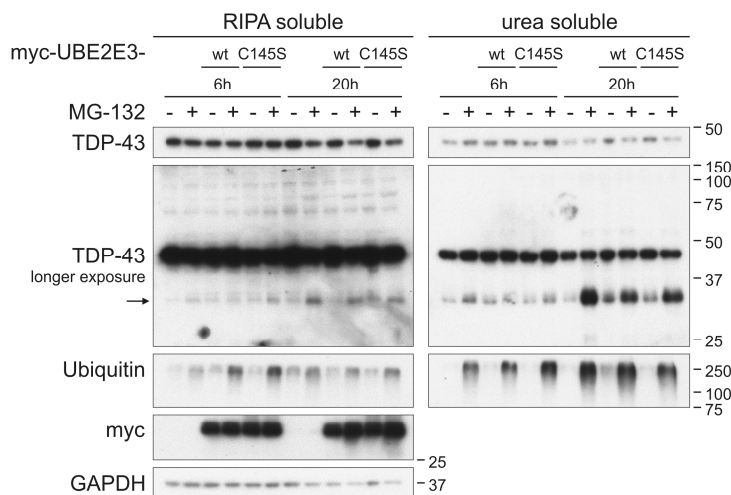
Figure 3.20 Effect of UBE2E3 on TDP-43 fragment formation and stability. HEK293E cells were transfected with myc-UBE2E3 wt or catalytically inactive C145S and proteasome was inhibited with MG-132 (10μM) for 6 or 20h. The cells were sequentially extracted and equal amounts of RIPA and urea fractions were analyzed with western blot. TDP-43, ubiquitin, myc and GAPDH were detected.

Thus, we could not conclude whether UBE2E3 increased ubiquitinylation of the 35kDa fragments.

3.3.4   Decrease of TDP-43 ubiquitinylation by UBE2E3 silencing can be rescued

In this study, so far an overexpression model was used that did not reflect physiological events. Therefore, modelling a loss-of-function is also important when studying protein function. This can be achieved by protein inactivation with specific inhibitors, silencing on mRNA level with siRNA or shRNA or gene knock out in animal models.

Thus, in an inverse approach the influence of the knockdown of UBE2E3 on the ubiquitinylation of TDP-43 was investigated. Therefore, HEK293E cells were transientliy silenced with four siRNAs targeting UBE2E3 (Figure 3.21). Silencing of UBE2E3 with si1 followed by Flag-TDP-43 overexpression and proteasomal inhibition, strongly decreased ubiquitinylation of TDP-43 (Figure 3.21A). However, transfection of the three other siRNAs (si2-4) had no effect on ubiquitinylated TDP-43. The class III E2 enzymes are very similar, both in their nucleotide and amino acid sequence. Thus, it was analyzed if the downregulation of UBE2E3 using si1 had side effects on the mRNA levels of UBE2E1 and UBE2E2. Moreover, it is possible that all three UBE2Es could compensate for the loss of the other E2 enzyme function.

Therefore, UBE2E3 was silenced with si1-4 and the mRNA level of all three E2 enzymes were analyzed with sqRT-PCR (Figure 3.21B+C). Indeed, the UBE2E3 downregulation was accompanied by increased mRNA level of UBE2E2 and, especially, UBE2E1 when silenced with si2-4, whereas silencing with si1 did not increase mRNA level of these E2 enzymes to the same degree.
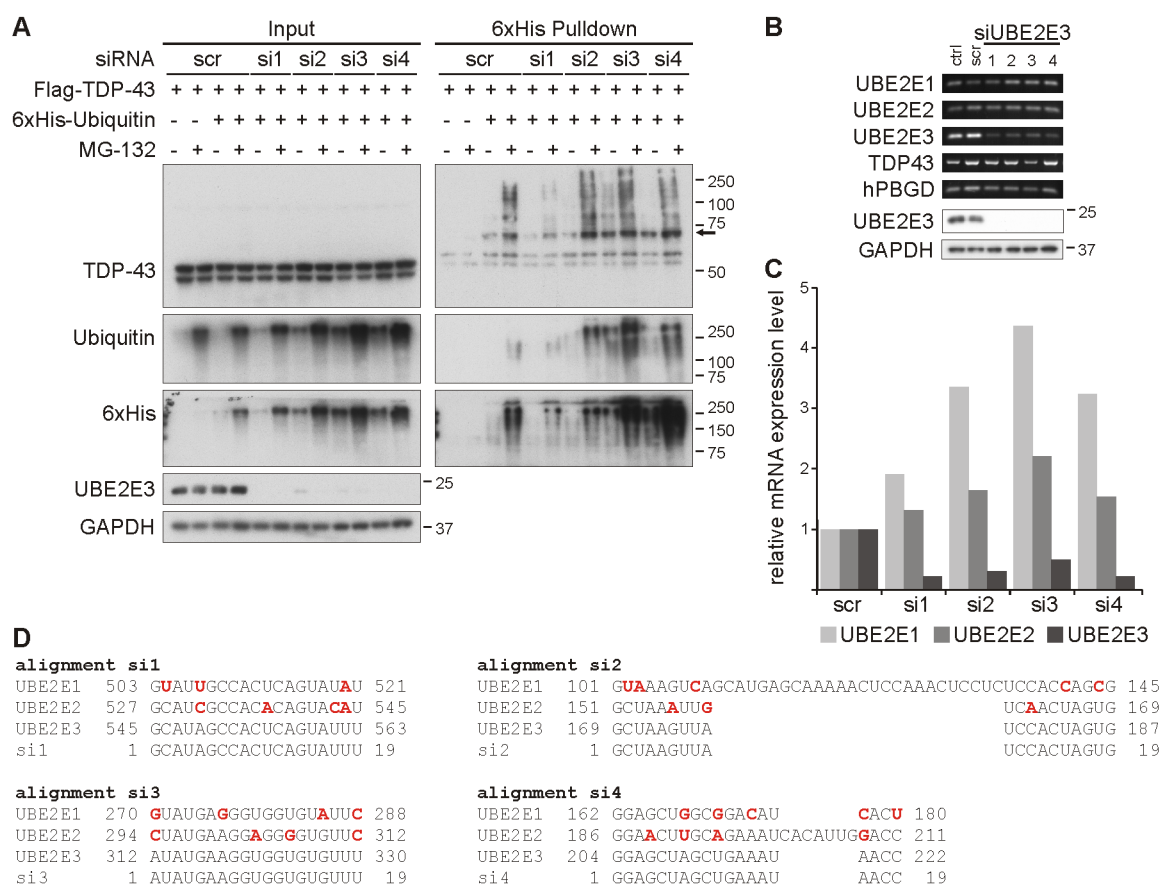
Figure 3.21 One out of four UBE2E3 siRNAs decreases level of ubiquitinylated TDP-43. A Silencing of UBE2E3 with si1 reduces ubiquitinylated TDP-43 level. HEK293E cells were silenced three times with scrambled (scr) or one out of four UBE2E3-directed siRNAs (si1-4) over 72h. 4h after the last silencing, the cells were transfected with Flag-TDP-43 and 6xHis-ubiquitin or vector control (-). After additional 24h protein overexpression, the proteasome was inhibited with MG-132 (10μM) for 2h and the urea soluble cell lysates were prepared. The pulldown of 6xHis-ubiquitin-conjugated proteins was performed and the total cell lysates (Input) and the pulldown eluates (6xHis Pulldown) were subjected to western blotting and stained with antibodies against TDP-43, ubiquitin, 6xHis, UBE2E3 and GAPDH, as indicated. The arrow labels monoubiquitinylated TDP-43. **B** HEK293E cells were transfected with scrambled siRNA or si1-4 UBE2E3 and the RNA was isolated. The levels of UBE2E3, UBE2E2, UBE2E1 mRNA and of the housekeeping gene hPBGD were analyzed by sqRT-PCR. **C** Relative E2 enzyme mRNA levels (from B) were normalized to hPBGD. This experiment was done 3 times with the same trend. **D** Alignment of si1-4 with UBE2E E2 enzyme sequences. Alignments with full length sequences of the E2 enzymes were performed with ClustalW2 (Larkin et al., 2007). Sequences complementary to siRNAs are depicted. Non-siRNA-complementary bases are marked in red.

An alignment of the siRNA target sequences with mRNA of the E2 enzymes revealed, that the si1 target sequence is more similar to UBE2E1 and UBE2E2 mRNA than the si2-4 target sequences (Figure 3.21D). Therefore, it is likely that si1 could also affect the levels of UBE2E1 and UBE2E2 mRNA or at least inhibit the compensatory upregulation of UBE2E1 and UBE2E2.

Next, we confirmed the specificity of the decreased TDP-43 ubiquitinylation upon UBE2E3 downregulation by reintroduction of myc-tagged UBE2E3 wt or the catalytically inactive mutant. Therefore, UBE2E3 was silenced three times with si1 in HEK293E cells, followed by overexpression of Flag-TDP-43, 6xHis-ubiquitin and myc-

UBE2E3 wt or C145S for 24h and proteasomal inhibition with MG-132 for 2h (Figure 3.22A). Indeed, pulldown showed that UBE2E3 wt overexpression rescued the reduced ubiquitinylation level of TDP-43 (compare 6xHis pulldown lane 7+8 with 9+10), whereas the catalytically inactive C145S UBE2E3 mutant failed (compare 6xHis pulldown lane 7+8 with 13+14). UBE2E3 could not fully rescue TDP-43 ubiquitinylation (compare 6xHis pulldown lane 5+6 with 9+10). A reason for that could be that overexpressed myc-UBE2E3 is also downregulated by UBE2E3 siRNA (Figure 3.22A input).

Thus, a si1 resistant UBE2E3 was cloned by changing seven nucleotides in the siRNA binding site without altering the amino acid sequence. While non mutated myc-UBE2E3 wt was silenced by UBE2E3 si1 to 80%, the overexpression of the si1 resistant myc-UBE2E3 si1mut resulted only in a downregulation of 40% (Figure 3.22B). In one out of three repetitions, UBE2E3 si1mut could rescue TDP-43 ubiquitinylation upon UBE2E3 silencing with si1 completely (Figure 3.22C), whereas in the two other experiments, ubiquitinylated TDP-43 level were comparable with the ones observed with UBE2E3 wt (Figure 3.22A).

Possibly, not all of the exogenous UBE2E3 wt or si1mut is catalytically active. Levels of overexpressed UBE2E3 are much higher than endogenous UBE2E3. Therefore, it is conceivable that exogenous UBE2E3 accumulated, decreasing the amount of catalytically active E2 enzyme.
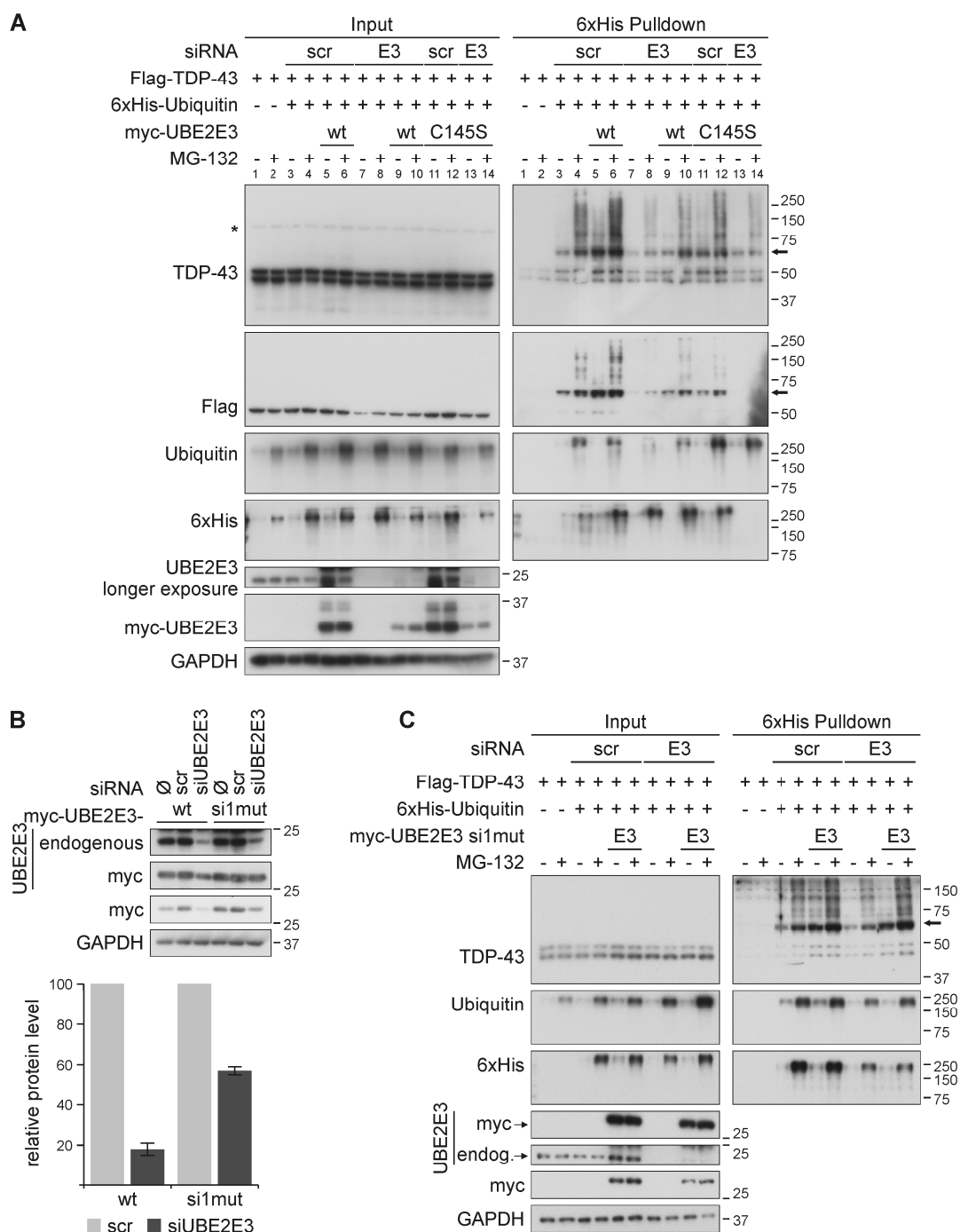
Figure 3.22 Decrease of ubiquitinylated TDP-43 upon UBE2E3 silencing can be rescued with UBE2E3 overexpression. A Rescue of UBE2E3 silencing with UBE2E3 wt overexpression. HEK293E cells were silenced three times with scrambled (scr) or UBE2E3-directed (E3) siRNA over 72h. The cells were triple-transfected with Flag-TDP-43, 6xHis-ubiquitin or vector control (-) and myc-tagged UBE2E3 wt or catalytically inactive C145S mutant 4h after the third silencing. The proteins were overexpressed for 24h, followed by 2h proteasome inhibition with MG-132 (10μM). The urea soluble cell lysates were prepared, the pulldown of 6xHis-ubiquitin-conjugated proteins was performed and the total cell lysates (Input) and pulldown eluates (6xHis Pulldown) were subjected to western blotting using antibodies against TDP-43, ubiquitin, 6xHis, UBE2E3, myc and GAPDH, as indicated. **B** Silencing resistance of UBE2E3 si1mut against UBE2E3 silencing with si1. Silencing of UBE2E3 with si1, followed by overexpression of myc-UBE2E3 wt or si1mut, showed an 80% reduction of UBE2E3 wt, but only 40% reduction of si1mut. **C** UBE2E3 si1mut can rescue TDP-43 ubiquitinylation upon silencing of UBE2E3 with si1. Silencing and rescue of UBE2E3 was performed as in (A) without UBE2E3 C145S. The arrows point to monoubiquitinylated TDP-43. B+C These experiments were performed twice.

3.3.5   Regulation of the ubiquitinylation of CTFs by UBE2E3

The interaction of UBE2E3 with TDP-43 was identified in a Y2H screen using CTF. However, the regulation of TDP-43 ubiquitinylation was investigated so far with TDP-43 FL, though very weak interactions of UBE2E3 and endogenous CTF or mCherry-CTF were detected. Therefore the ubiquitinylation of two differentially tagged CTFs and the regulation of UBE2E3 on the ubiquitinylation was investigated (Figure 3.23A+B).

First, we asked whether UBE2E3 can ubiquitinylate the 25kDa Flag-CTF and if this might stabilize this fragment from degradation (Figure 3.23A). The Flag-CTF construct exhibits typically fast turnover and is therefore detected in very small amounts. Thus, proteasomal inhibition with MG-132 was applied for up to 6h to increase the stability of this fragment. This time was sufficient to stabilize endogenous 35kDa fragments of TDP-43 in a previous experiment (Figure 3.12A). However, the Flag-CTF signal was very weak upon proteasomal inhibition or UBE2E3 expression. Thus, it was not stabilized, and ubiquitinylated CTF was below the detection level. Flag-TDP-43 FL ubiquitinylation was observed upon MG-132 treatment for 2h and was even further enhanced when the proteasome was inhibited for 6h. As was already shown above in Figure 3.18, the UBE2E3 overexpression also increased the amount of ubiquitinylated Flag-TDP-43 FL.

Next, the ubiquitinylation of mCherry-tagged TDP-43 FL and CTF was analysed in HEK293E cells with a pulldown experiment. We found that UBE2E3 enhances the ubiquitinylation of mCherry-TDP-43 FL (Figure 3.23B), which is in agreement with our previous results. Additionally, proteasomal inhibition with MG-132 slightly enhanced the ubiquitinylation of mCherry-TDP-43 FL. Surprisingly, mCherry-CTF was strongly ubiquitinylated and co-expression of the E2 decreased the amount of the ubiquitinylated CTF (Figure 3.23B), though steady-state levels were not affected. The inhibition of the UPS did not alter the amount of ubiquitinylated CTF, likely because of the already saturated ubiquitinylation of CTF (see the strong ubiquitinylation level of mCherry-CTF in Figure 3.23B). The co-expression of the strongly ubiquitinylated mCherry-CTF and the ubiquitin-conjugating enzyme UBE2E3 might have induced an upregulation of DUBs, which subsequently deubiquitinylated the CTF.

In this section it was demonstrated that TDP-43 colocalized with endogenous UBE2E enzyme. TDP-43 is ubiquitinylated upon overexpression of these proteins, whereas silencing of the UBE2E3 enzyme with one out of four siRNAs reduced ubiquitinylated TDP-43. This was rescued by UBE2E3 overexpression. Furthermore, co-expression with UBE2E3 led to a solubility shift of TDP-43. Thus, UBE2E ubiquitin-conjugating enzymes participate in the ubiquitinylation of TDP-43.
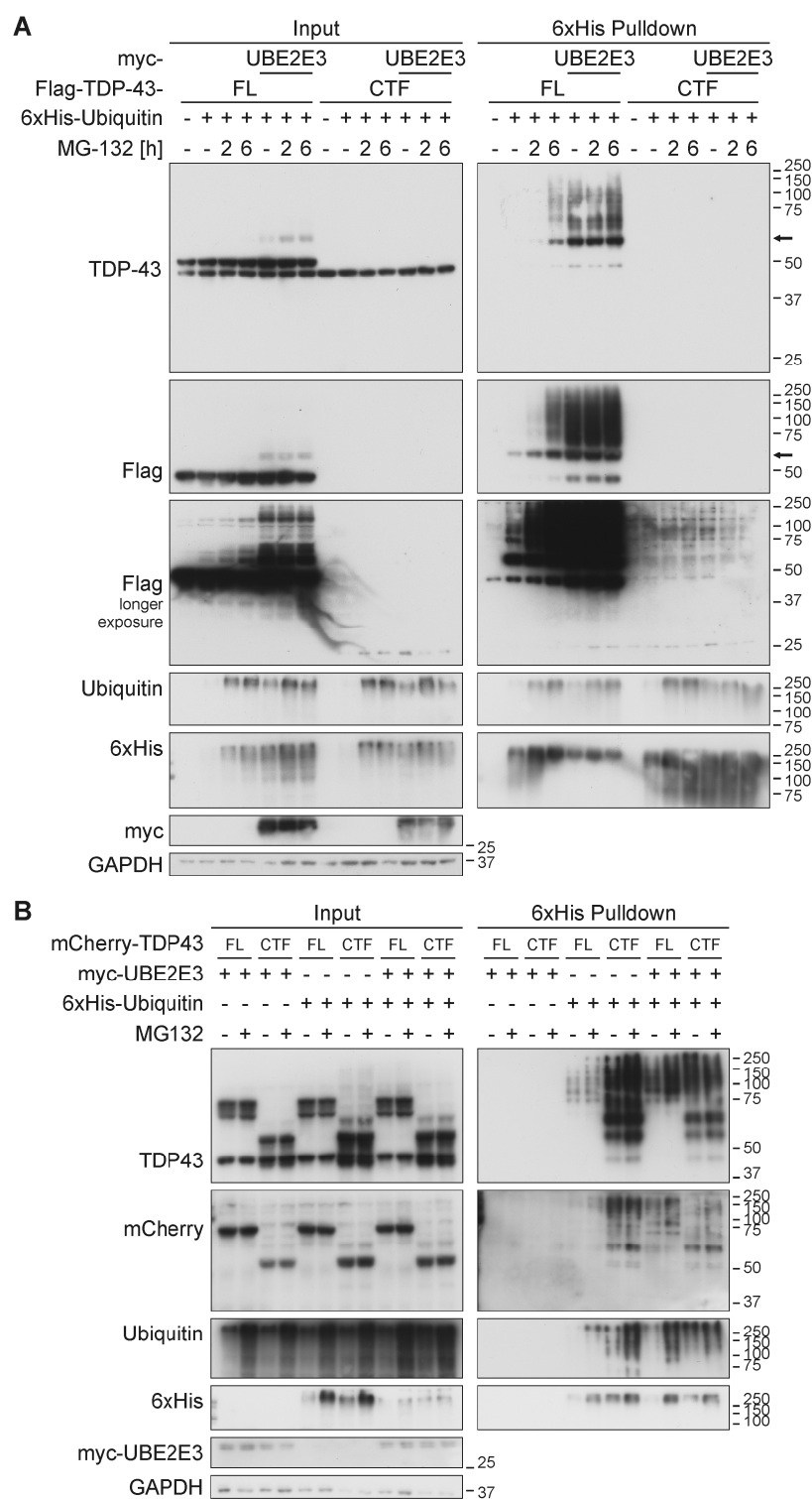
Figure 3.23 Effect of UBE2E3 overexpression on ubiquitinylation of Flag/mCherry-TDP-43 FL and CTF. A UBE2E3 co-expression does not lead to a detectable stabilization or ubiquitinylation of Flag-CTF. HEK293E cells were triple-transfected with Flag-TDP-43 FL or CTF, myc-UBE2E3 and 6xHis-ubiquitin (+) or vector control (-). The proteasome was inhibited with MG-132 (10μM) for 2 or 6h to stabilize Flag-CTF. 6xHis-ubiquitin-conjugated proteins were pulled down from urea lysates. Western blots of total protein (Input) and pulldown eluates (6xHis Pulldown) were stained with antibodies against TDP-43, Flag, ubiquitin, 6xHis and myc. GAPDH served as loading control. Arrow points to monoubiquitinylated TDP-43. **B** UBE2E3 increases ubiquitinylation of mCherry-TDP-43 FL, but decreases ubiquitinylated mCherry-CTF. mCherry-tagged TDP-43 FL or CTF were overexpressed with

myc-UBE2E3 (+) and 6xHis-ubiquitin or vector controls (-). The cells were treated with MG-132 (10μM) for 2h, followed by harsh lysis with urea buffer. 6xHis-ubiquitin-conjugated proteins were isolated with Ni-NTA agarose. Western blots of total protein (Input) and eluates (6xHis Pulldown) were probed with anti-TDP-43, -living colors dsRed (mCherry), -ubiquitin, -6xHis, -myc and -GAPDH. The experiments were repeated twice.

3.4   The regulation of TDP-43 ubiquitinylation by UBPY

In the Y2H screen we also identified a deubiquitinylation enzyme, UBPY. Thus, ubiquitinylation of TDP-43 may possibly be regulated in both directions: attachment and proteolytic cleavage of ubiquitin-chains. The next part investigated the influence of UBPY on the ubiquitinylation status of TDP-43.

3.4.1   The ubiquitin isopeptidase Y

UBPY is known as an ESCRT-0 complex associated DUB that regulates the endosomal transport, sorting, and degradation of several plasma membrane receptors (see chapter 2.6). In this study, UBPY was identified as a TDP-43 binding protein. The subcellular localization of UBPY and colocalization with TDP-43 was studied in HEK293E cells (Figure 3.24). Endogenous UBPY was distributed in vesicle-like structures in the whole cytoplasm, which did not colocalize with the early endosomal marker EEA1 or the lysosomal marker LAMP-1 (Figure 3.24B+C). Interestingly, the more dense localization of UBPY in proximity of the nucleus was also positive for the cis-Golgi marker GM130 (Figure 3.24D). Some of the UBPY-positive punctae also colocalized with endogenous, cytoplasmic TDP-43 upon longer exposure (Figure 3.24A). After cellular stress, TDP-43 can be incorporated into stress granules in the cytoplasm (see chapter 2.3.3). Therefore, it was investigated whether UBPY also colocalizes with stress granules, since these might be a cytoplasmic interaction site of TDP-43 and UBPY. After the induction of stress granule formation with arsenite treatment for 30min, no colocalization of UBPY with the stress granule marker eIF3 was detected (Figure 3.24E), while TDP-43 positive stress granules were clearly observed (Figure 3.24F).

3.4.2   Effect of UBPY overexpression on TDP-43 ubiquitinylation

UBPY is localized in the cytoplasm, but TDP-43 is mostly found in the nucleus. To study the impact of UBPY on TDP-43 ubiquitinylation two cytoplasmic localized TDP-43 constructs were used: mCherry-CTF, which is distributed in the whole cell and very strongly ubiquitinylated (see Figure 3.10B for EGFP-CTF, and Figure 3.23B), and the nuclear import impaired TDP-43 NLSmut (Figure 3.25). UBPY bound stronger to the more cytosolic NLSmut than to nuclear TDP-43 wt as was shown above (Figure 3.11B), possibly indicating that the interaction is taking place in the cytoplasm. As
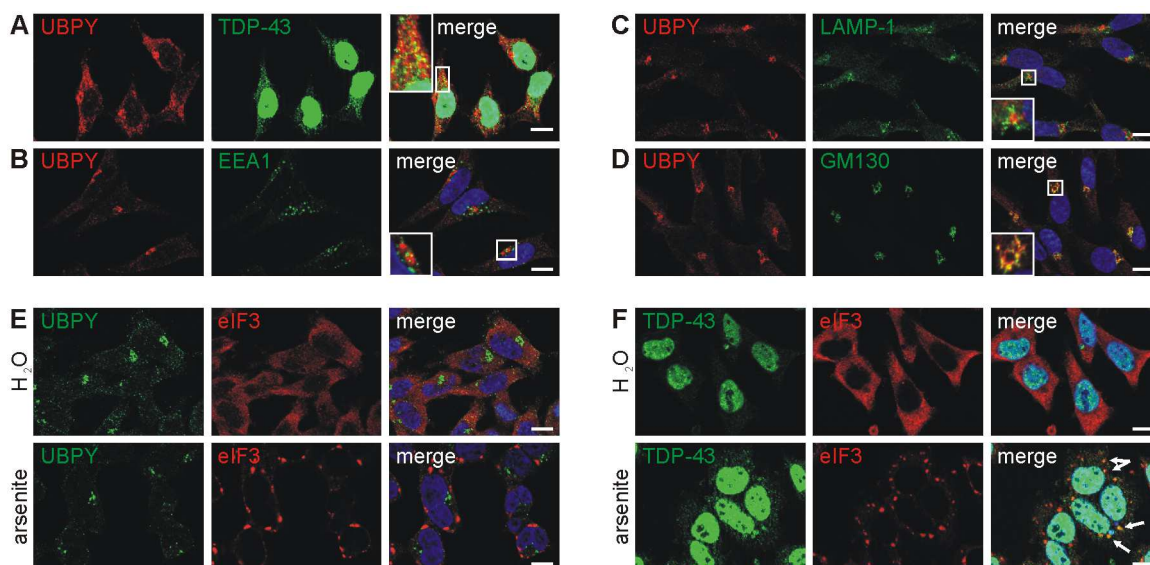
Figure 3.24 Characterization of UBPY subcellular localization in HEK293E cells. A Colocalization of endogenous UBPY and TDP-43. The cells were stained with rabbit-anti-UBPY (red) and mouse-anti-TDP-43 antibodies (green). **B-D** Cytoplasmic localization of endogenous UBPY. The cells were dual-labeled with antibodies against UBPY (red) and the early endosomal marker EEA1 (A, green), the lysosomal marker LAMP-1 (B, green) or the cis-golgi marker GM130 (C, green). **E+F** No colocalization of UBPY with stress granules. Stress granule formation was induced with 500µM arsenide treatment for 30min. Endogenous UBPY was stained with a rabbit-anti-UBPY antibody (E, green), endogenous TDP-43 with a mouse-anti-TDP-43 antibody (F, green, longer exposure) and stress granules were labeled with a goat-anti-eIF3 antibody (red). A-F, merged images including nuclear counterstaining with Hoechst 33342 (blue) are to the right. The arrows point towards TDP-43 positive stress granules. Scale bars correspond to 10µm.

UBPY is a deubiquitinylating enzyme, a decrease of ubiquitinylated TDP-43 was expected upon overexpression of the DUB.

The overexpression of UBPY wt resulted in a strong decrease of ubiquitinylated mCherry-CTF, regardless of the proteasomal activity (Figure 3.25A). The ubiquitinylation of Flag-TDP-43 NLSmut was reduced likewise in cells transfected with UBPY wt (Figure 3.25B, compare pulldown lane 7+8 with 9+10). In addition, reduced ubiquitinylation of Flag-TDP-43 wt was also observed after MG-132 treatment in this experiment (compare lane 3 with 5). The catalytically inactive UBPY mutant C786S and an UBPY variant that lacks the C-terminus where the active site cysteine is located (ΔC), did not decrease the ubiquitinylation of mCherry-CTF and Flag-TDP-43 NLSmut. This indicates that only catalytically active UBPY is able to deubiquitinylate CTF variants of TDP-43. The steady-state levels of the TDP-43 proteins were also not altered.

Furthermore, the solubility of ubiquitinylated mCherry-CTF upon UBPY overexpression was analyzed (Figure 3.25C). HEK293E cells that overexpressed mCherry-CTF and UBPY were separated into a NP-40 soluble and an insoluble urea fraction. The ubiquitinylated mCherry-CTF was mainly detected in the insoluble urea fraction. These levels were reduced when UBPY wt was overexpressed, but co-expression of UBPY C786S and ΔC even increased amount of ubiquitinylated TDP-43, suggesting a
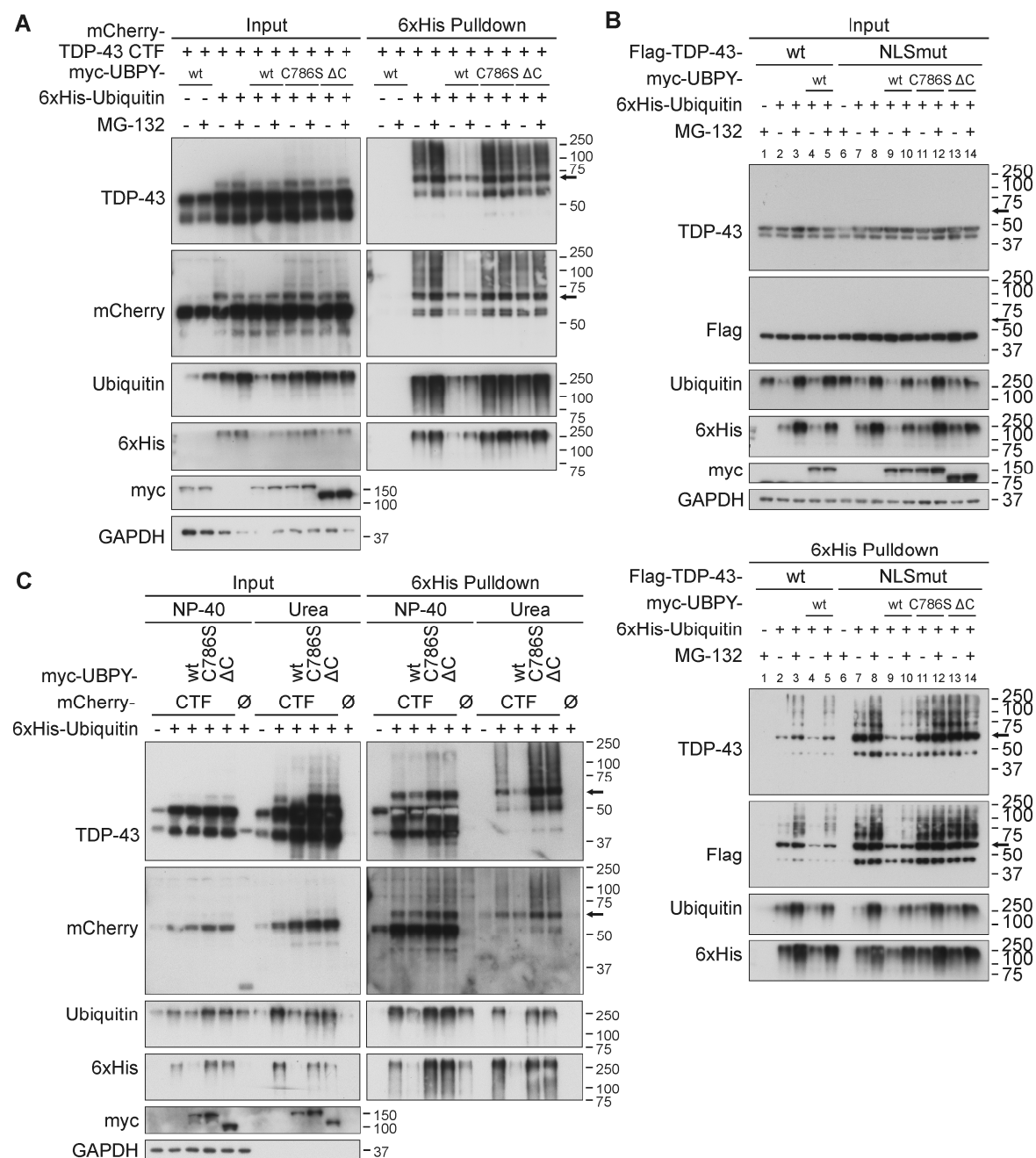
Figure 3.25 Exogenous UBPY deubiquitinylates TDP-43 CTF and NLSmut. A UBPY deubiquitinylates mCherry-TDP-43 CTF independently of proteasomal activity. mCherry-tagged TDP-43 CTF was overexpressed with 6xHis-ubiquitin (+) and myc-UBPY wt, the catalytically inactive mutant C786S or UPBY lacking the ubiquitin C-terminal hydrolase domain (ΔC), or vector controls (-) in HEK293E cells for 48h. After proteasomal inhibition with MG-132 (10μM) for 2h, cells were lysed and Ni-NTA purification of 6xHis-ubiquitin-conjugated proteins was performed. The total cell lysates (Input) and the pulldown eluates (6xHis Pulldown) were western blotted and stained with antibodies against TDP-43, mCherry, ubiquitin, 6xHis, myc and GAPDH. **B** UBPY deubiquitinylates cytosolically localized TDP-43 NLSmut. The experiment was performed as in (A), but Flag-TDP-43 wt or NLSmut were overexpressed. Western blots were probed with antibodies for TDP-43, Flag, ubiquitin, 6xHis, myc and GAPDH. **C** Pulldown of ubiquitinylated mCherry-CTF from soluble and insoluble fractions. HEK293E cells were transfected with 6x-His-ubiquitin (+), mCherry-TDP43 CTF or mCherry-control vector (Ø), and myc-UBPY wt, C786S or ΔC. After 48h protein expression, the cells were subjected to sequential extraction, yielding a NP-40- and urea-soluble fraction. 6xHis-ubiquitin-conjugated proteins were isolated with Ni-NTA purification. Total protein (Input) and pulldown eluates (6xHis Pulldown) were analyzed by western blotting. The membranes were stained for TDP-43, mCherry, ubiquitin, 6xHis, myc and GAPDH. The arrows mark monoubiquitinylated TDP-43.

dominant-negative effect of the two catalytically inactive DUB mutants. UPBY wt co-expression did not alter the portion of mCherry-CTF level in the soluble and insoluble fraction, like UBE2E3 co-expression did for Flag-TDP-43 wt (see Figure 3.18). The mCherry-tag alone was not ubiquitinylated in the insoluble fraction. Thus, the ubiquitinylation of the mCherry-CTF construct reflects the ubiquitin formation on the CTF. Of note, the overexpression of UBPY decreased the total levels of ubiquitinylated and 6xHis-ubiquitin conjugated proteins. It is likely that UBPY is capable to deubiquitinylate many substrates.

Thus, exogenous UBPY can decrease the ubiquitinylation of TDP-43. In particular, cytoplasmic Flag-TDP-43 NLSmut and mCherry-CTF were deubiquitinylated to a greater extent than TDP-43 FL. It remains to be shown whether UBPY deubiquitinylates soluble TDP-43 FL or if the DUB can also remove ubiquitin-chains from already insoluble TDP-43 FL.

3.4.3 Silencing of UBPY

Since overexpression of the DUB strongly reduced the ubiquitinylation of TDP-43, we next asked whether a reduction of UBPY protein level by siRNA treatment increases the TDP-43 ubiquitinylation. Therefore, HEK293E cells were silenced with specific siRNAs against UBPY. Unfortunately, siRNAs from Qiagen as well as from Ambion failed to reduce UBPY protein levels to a sufficient amount. In addition, some toxic effects were observed in HEK293E cells (Figure 3.26A+B).

Next, five lentiviral transduced shRNAs were used to stably silence UBPY in HEK293E cells (Figure 3.26C). Most of them efficiently silenced UBPY, but when these stably silenced cells were used for subsequent pulldown experiments, in which Flag-TDP-43 and 6xHis-ubiquitin were overexpressed, the silencing efficiency vanished and therefore, a possible reduction of TDP-43 ubiquitinylation was not observed (Figure 3.26D). Finally, we obtained the mamma carcinoma cell line MCF-7 from C. Carraway (Cao et al., 2007), which was stably silenced for UBPY (Figure 3.26E-G). Silencing of UBPY was moderate in western blot and sqRT-PCR analysis (Figure 3.26E+F), but obvious in immunofluorescence (Figure 3.26G). Nonetheless, these cells were not used for further investigations of UBPY knockdown on TDP-43 ubiquitinylation, because of an odd TDP-43 staining: all cells which displayed a nuclear TDP-43 signal also exhibited a strong cytoplasmic staining, whereas other cells seemed to be depleted of TDP-43 completely. This was not an effect of UBPY silencing as the odd TDP-43 staining pattern was also observed in control MCF-7 cells. Due to this difficulties it could not be investigate how silencing of UBPY affects TDP-43 ubiquitinylation in cell lines. However, we were able to knockdown UBPY in *Drosophila melanogaster* (see chapter 3.8, below).
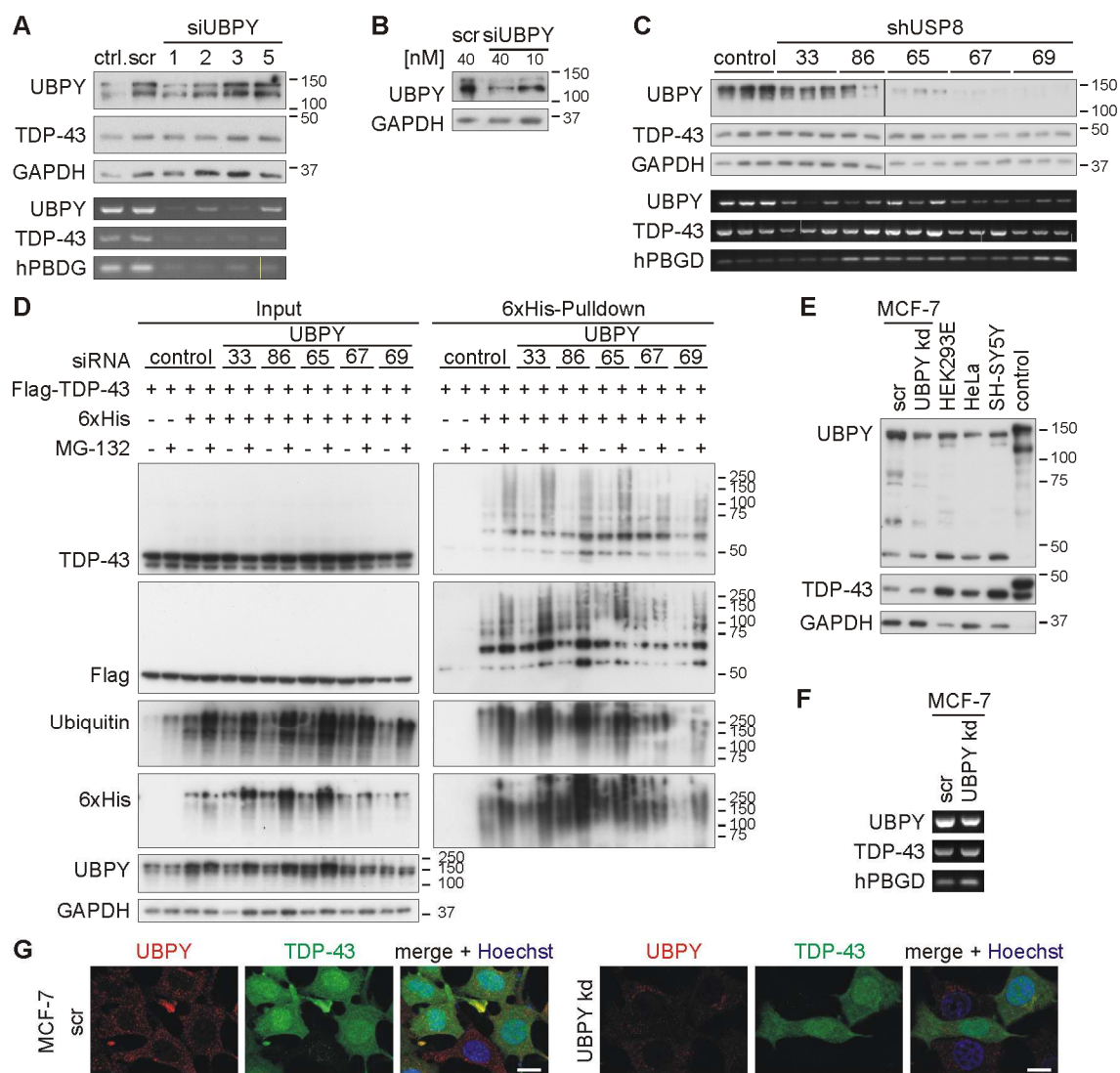
Figure 3.26 Different approaches to silence UBPY. A HEK293E cells were silenced three times within 72h for UBPY with four different siRNAs (si1, 2, 3 and 5, 10nM each, Qiagen) or with scrambled control (scr). 24h after the third siRNA transfection protein and RNA were isolated. Equal amounts of protein were analyzed by western blot for levels of UBPY, TDP-43 and GAPDH. The cDNA was reverse transcribed from mRNA and a sqRT-PCR was performed for UBPY, TDP-43 and hPBDG. **B** The knockdown of UBPY in HEK293E cells was done with an siRNA from Ambion. The cells were transfected twice in 48h intervals with 10 or 40nM UBPY or scrambled siRNAs. RIPA lysates were prepared, subjected to western blot and stained for UBPY and GAPDH. **C** UBPY was stably silenced in HEK293E with five different lentivirally transduced shRNAs. A non-mammalian shRNA served as control. Two weeks after viral transduction efficiency of UBPY knockdown was assessed on protein level with western blot and on mRNA level with sqRT-PCR. Western blots were stained for UBPY, TDP-43 and GAPDH, and PCR products were analyzed for levels UBPY, TDP-43 and hPBDG, as indicated. **D** Stably silenced HEK293E cells from (C), once frozen at -170°C and were thawed and double-transfected with Flag-TDP-43 and either 6xHis-ubiquitin or control (-). The urea cell lysates were used for pulldown of 6xHis-ubiquitin-conjugated proteins with Ni-NTA agarose. Western blotting was performed with total protein lysates (Input) and pulldown eluates (6xHis Pulldown). Membranes were stained for TDP-43, Flag, ubiquitin, 6xHis, UBPY and GAPDH. **E-G** Characterization of UBPY expression levels in stable UBPY knockdown MCF-7 cells. **E** Protein lysates of MCF-7 control (scr) or UBPY knockdown (UBPY kd) cells were subjected to western blot analysis together with lysates from HEK293E, HeLa and SH-SY5Y cells. HEK293E cells overexpressing myc-UBPY (and Flag-TDP-43) served as control. Western Blots were stained for UBPY, TDP-43 and GAPDH. **F** UBPY knockdown efficiency in MCF-7 cells was determined by sqRT-PCR. **G** Immunofluorescence staining of endogenous UBPY (red) and endogenous TDP-43 (green) in MCF-7 control (scr, left) or UBPY knockdown (UBPY kd, right). Nuclei were stained with Hoechst 33342 (blue). Scale bars correspond to 10μm.

3.4.4 Effect of UBPY on CTF accumulation

In *post mortem* brain of ALS and FTLD-TDP patients, ubiquitinylated TDP-43 is detected in pathological inclusions. Therefore, it was investigated whether the UBPY co-expression alters the accumulation of the aggregation-prone mCherry-CTF in HEK293E cells (Figure 3.27). The proteasomal activity was inhibited with MG-132 up to 14h to induce accumulation of mCherry-CTF. In transfected cells few mCherry-CTF positive accumulations were observed after 0h, 2h and 6h MG-132 treatment (Figure 3.27). After proteasomal inhibition for 14h, about 85% of the transfected cells contained accumulated mCherry-CTF. This was not affected by UBPY co-expression (Figure 3.27A,C+D). The control mCherry-protein alone hardly accumulated upon MG-132 treatment up to 6h, whereas accumulations were found in 60% of transfected cells after 14h proteasomal inhibition. However, these accumulations were much smaller than mCherry-CTF (compare Figure 3.27A+C with B, 14h).
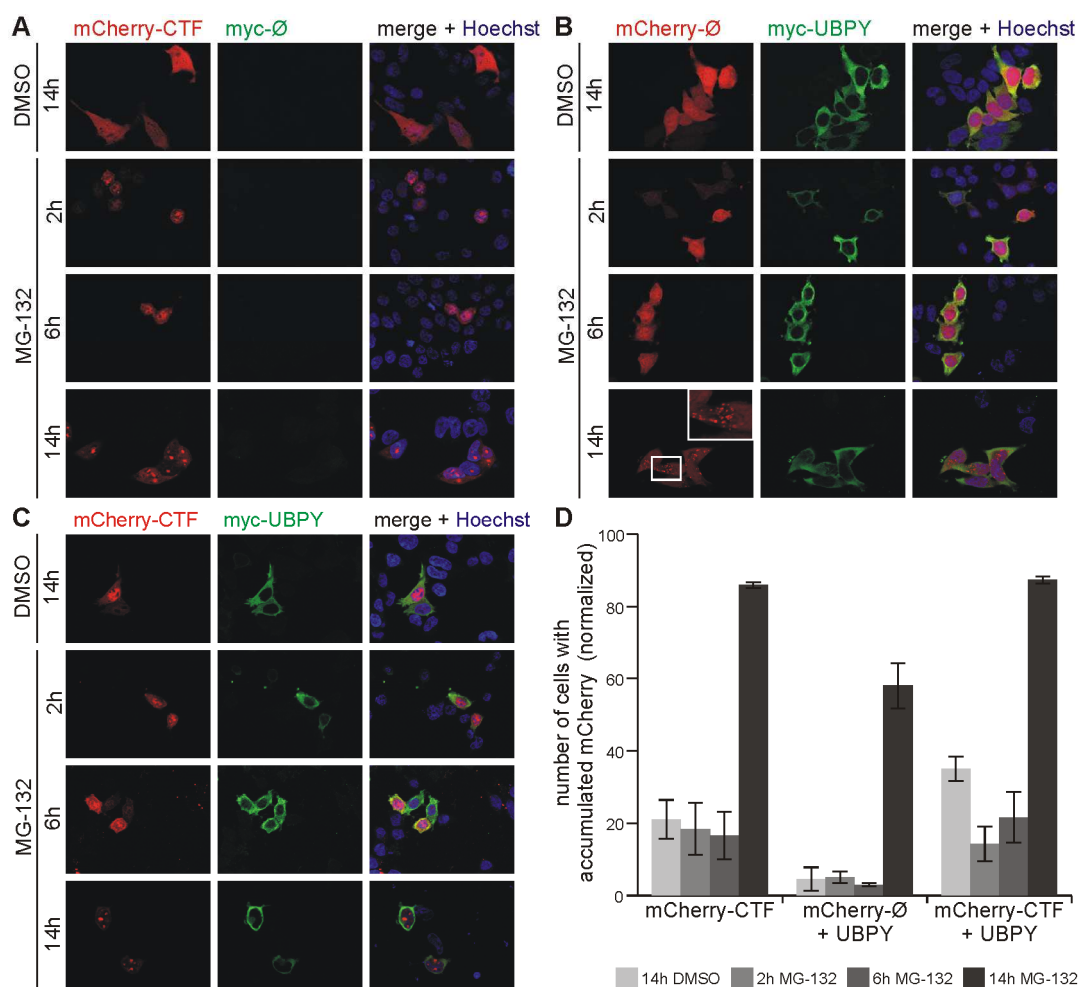
Figure 3.27 UBPY overexpression does not alter mCherry-CTF accumulation upon proteasomal inhibition. A-C Myc-UBPY and mCherry-CTF (red) or vector controls (Ø) were overexpressed in HEK293E cells for 72h. MG-132 (10µm) was applied for up to 14h, as indicated, to inhibit proteasomal function. Overexpressed UBPY was stained with mouse-anti-myc (green) and nuclei were counterstained with Hoechst 33342 (blue). **D** Quantification of mCherry accumulation upon UBPY overexpression. At least 100 (double-) transfected cells per condition were analyzed for mCherry-positive accumulations. Two independent experiments were quantified. Error bars represent standard deviation.

3.5   Regulation of TDP-43 ubiquitinylation by the E3 ligase RNF2

Beside the two new TDP-43 interaction partners UBE2E3 and UBPY, the E3 ligase RNF2 was found as a positive hit in the Y2H screen. As shown above RNF2 is able to coimmunoprecipitate with TDP-43 FL and CTF, and colocalizes with TDP-43 in the nucleus. Therefore, we examined whether RNF2 is involved in the ubiquitinylation of TDP-43. HEK293E cells were co-transfected with Flag-TDP-43 and myc-RNF2 together with 6xHis-ubiquitin constructs (Figure 3.28). The pulldown of 6xHis-ubiquitin-conjugated proteins showed, that ubiquitinylation of Flag-TDP-43 is not altered after RNF2 overexpression and proteasomal inhibition.

It was reported that RNF2 mediates monoubiquitinylation of histone H2A, thus playing a central role in histone code and gene regulation. Moreover, as a member of the polycomb-group genes RNF2 modifies epigenetic silencing of target genes (Sparmann and van Lohuizen, 2006; Wang et al., 2004a). Thus, the interaction of TDP-43 and RNF2 must not necessarily alter ubiquitinylation of TDP-43, but might alter gene expression. It is also possible, that the interaction is non-functional or that the cognate E2 enzyme is not expressed in HEK293E cells. In addition, an internal control of RNF2 reactivity was missing in this system. Therefore, the functional interaction of TDP-43 with RNF2 was not further investigated in this study and remains to be further elucidated.
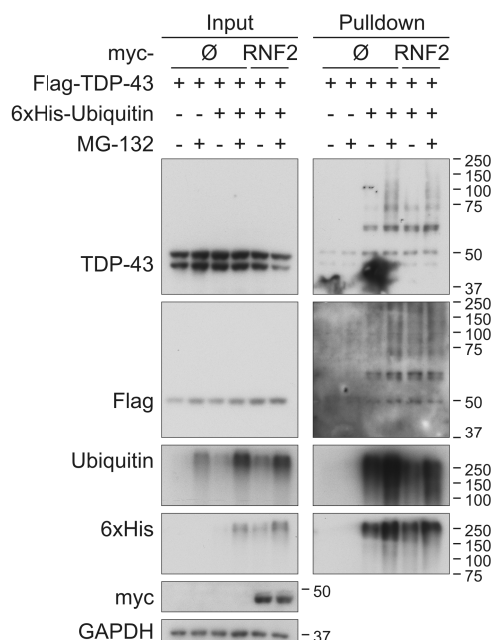
Figure 3.28 RNF2 does not increase TDP-43 ubiquitinylation. HEK293E cells were triple-transfected with Flag-TDP-43, 6xHis-ubiquitin and myc-RNF2 or vector controls (Ø) for 48h, followed by proteasomal inhibition with MG-132 (10μM) for 2h. The cells were lysed with urea buffer and 6xHis-ubiquitin-conjugated proteins were isolated with Ni-NTA agarose. The total protein lysates (Input) and the pulled down proteins (6xHis Pulldown) were subjected to western blot analysis with antibodies detecting TDP-43, Flag, ubiquitin, 6xHis, myc and GAPDH, as indicated. Depicted is one representative experiment out of two.

3.6 Regulation of the ubiquitinylation of pathogenic TDP-43 mutants by UBE2E3 and UBPY

Up to date 48 pathogenic mutations in the *TARDBP* gene were identified, most of them in patients with familial or sporadic ALS, but some are linked to FTLD (Lattante et al., 2013). Here, 15 pathogenic TDP-43 mutants were analyzed regarding their ubiquitinylation status affected by proteasomal inhibition, UBE2E3 and UBPY. These studies were performed together with the master student Jennifer C. Strong (JCS) under guidance of F. Hans (FH). First, the localization and distribution of the overexpressed TDP-43 mutants was investigated by immunofluorescence staining in HEK293E cells (Figure 3.29). All mutants were detected mainly nuclear and displayed a weak granular distribution in this compartment. No obvious differences in the local-
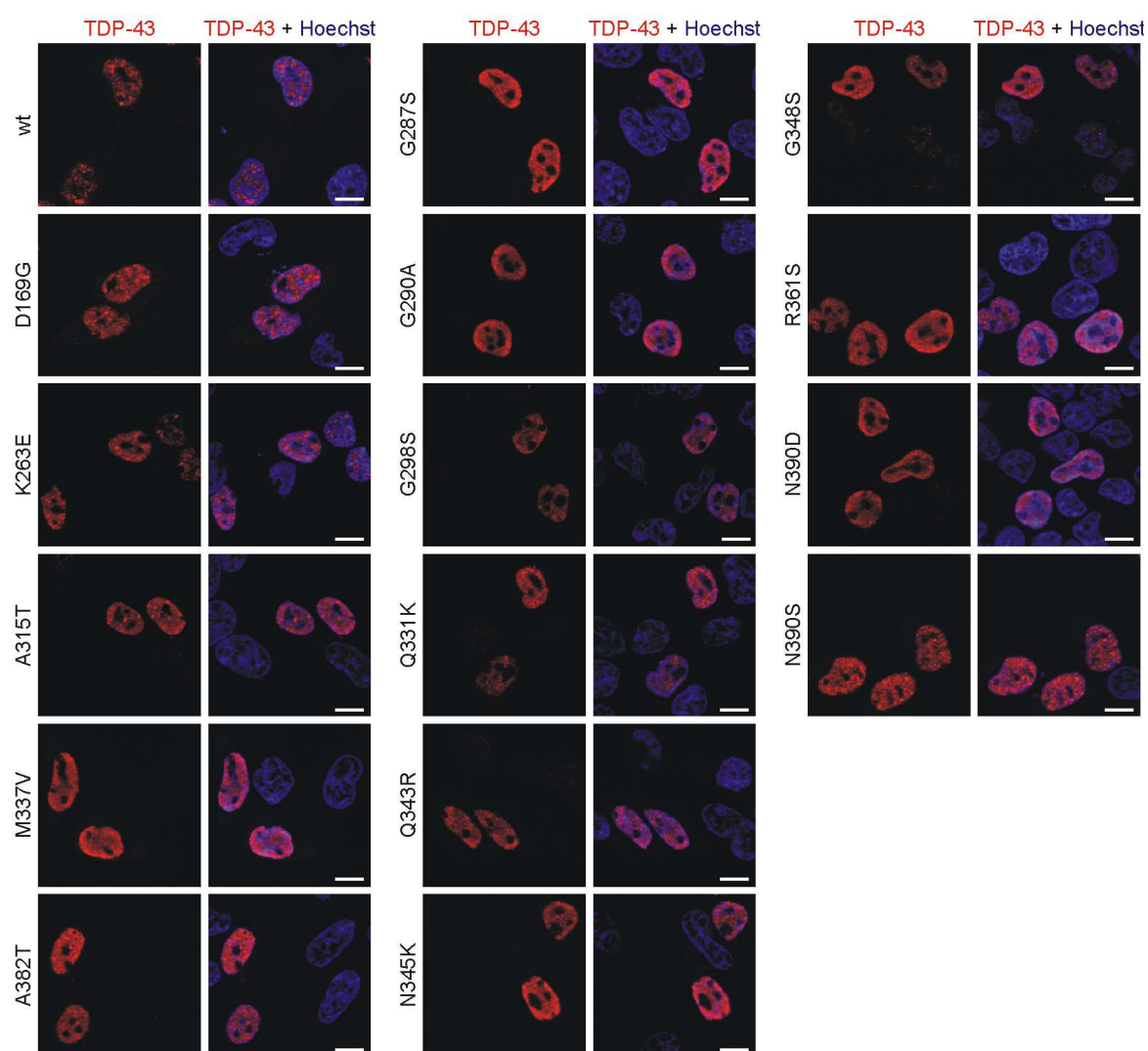
Figure 3.29 Localization of pathogenic TDP-43 mutants. HEK293E cells overexpressing Flag-tagged TDP-43 wt or mutants, as indicated, were immunolabeled with mouse-anti-Flag antibody (red). Merged images show nuclear counterstaining with Hoechst 33342 (blue). Scale bars correspond to 10µm. The experiments were performed by JCS and were analyzed by FH and JCS.

ization and the distribution of the mutants were detected when they were compared with Flag-TDP-43 wt (Figure 3.29).

Second, it was investigated if proteasomal inhibition altered the ubiquitinylation of the TDP-43 mutants (Figure 3.30). Flag-tagged mutants or TDP-43 wt were co-expressed with 6xHis-ubiquitin for 48h in HEK293E cells, followed by the inhibition of the proteasome with MG-132 for 2h. Then, 6xHis-ubiquitin-conjugated proteins were isolated and analyzed with western blot. The steady-state levels of all mutants were not altered (Figure 3.30, input). The ubiquitinylation of almost all mutants was increased upon MG-132 treatment equivalent to TDP-43 wt. Interestingly, the increase of the ubiquitinylation of the two lysine mutants Q331K and N345K was comparable to TDP-43 wt. On the other hand, D169G ubiquitinylation was hardly detectable upon proteasomal inhibition, maybe due to decreased expression levels of D169G compared to TDP-43 wt or the other mutants (Figure 3.30A). Most interestingly, K263E mutant was stronger ubiquitinylated than TDP-43 wt and the other mutants under basal conditions, and proteasomal inhibition strongly increased the level
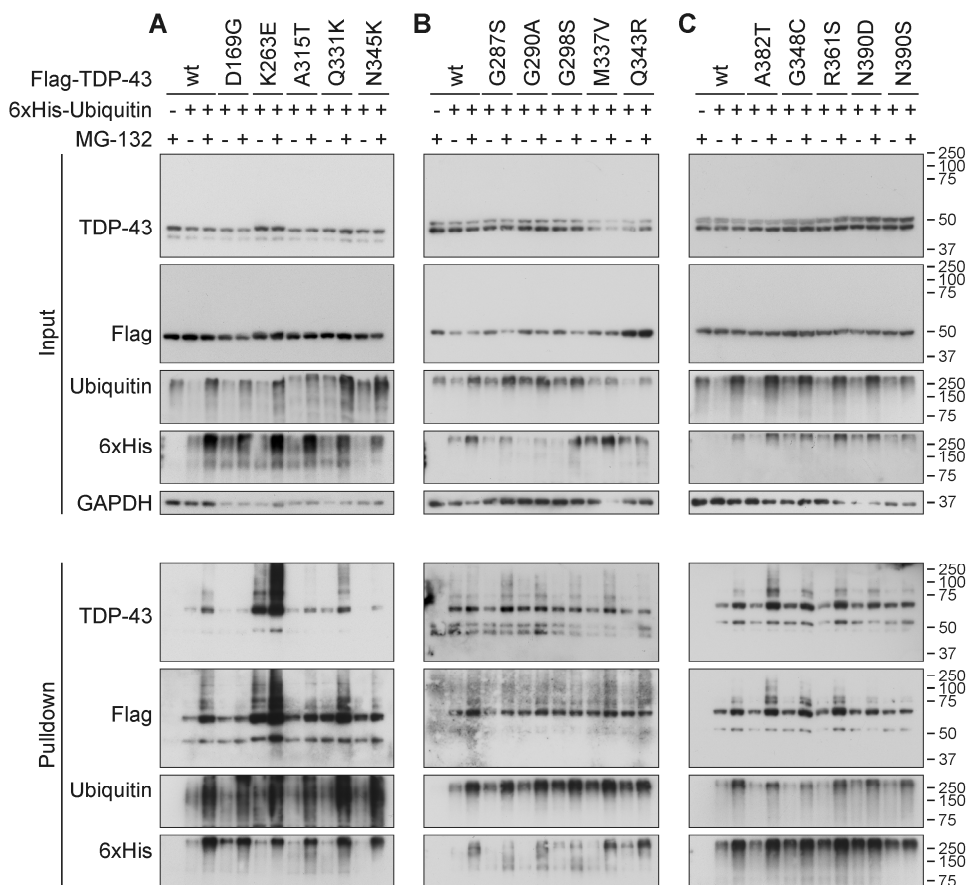
Figure 3.30 Effect of proteasomal inhibition on pathogenic TDP-43 mutant ubiquitinylation. A-C HEK293E cells overexpressing 6xHis-ubiquitin (+) or vector-control (-) and Flag-TDP-43 wt or mutants, as indicated, for 48h were treated with MG-132 for 2h. The urea soluble cell lysates were prepared and 6xHis-ubiquitin-conjugated proteins were isolated with Ni-NTA-agarose. The total cell lysates (Input) and pulldown eluates (6xHis Pulldown) were analyzes with western blot and stained for TDP-43, Flag, 6xHis and GAPDH. The experiments were performed by JCS.

of ubiquitinylated K263E (Figure 3.30A). It is also noteworthy that there is a slight higher molecular weight shift of the unconjugated mutant protein, probably due to altered charge of K263E, in which a positively charged lysine residue is substituted with a negatively charged glutamic acid. This mutation is also very interesting, as it was the first reported *TARDBP* mutation not associated with ALS, but with a neurodegenerative syndrome (Kovacs et al., 2009). K263E was described in a single Hungarian patient, who developed FTLD at a young age with additional supranuclear palsy and chorea.

Third, it was analyzed whether UBE2E3 can regulate the ubiquitinylation of the TDP-43 mutants to the same degree as TDP-43 wt (Figure 3.31). Most of the mutants were ubiquitinylated upon UBE2E3 overexpression to the same degree as TDP-43 wt. As seen before (Figure 3.30), the ubiquitinylation of K263E was stronger under basal conditions and UBE2E3 co-expression dramatically increased the amounts of ubiquitinylated TDP-43 K263E mutant (Figure 3.31A). The very strong K263E ubiquitinylation was even detected in total cell lysates (input). Consistent with the results from
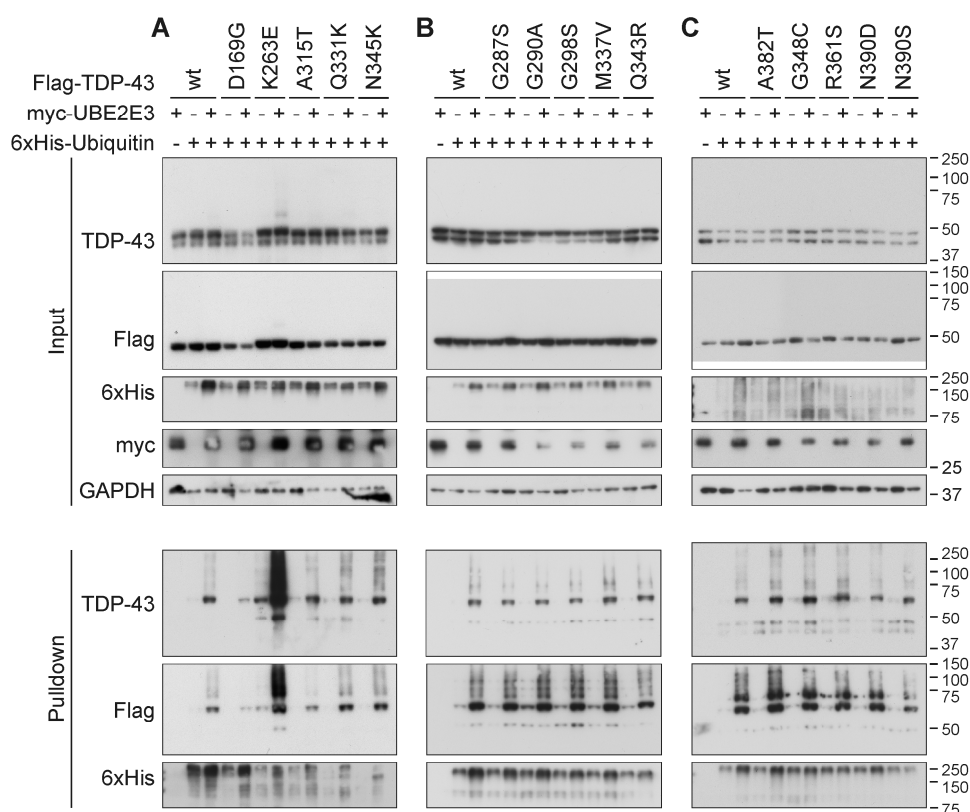
Figure 3.31 Effect of UBE2E3 overexpression on ubiquitinylation status of pathogenic TDP-43 mutants. A-C HEK293E cells were triple-transfected with 6xHis-ubiquitin (+) or vector-control (-), myc-UBE2E3 (+) or vector-control (-) and Flag-TDP-43 wt or mutants, as indicated. The urea soluble cell lysates were prepared and 6xHis-ubiquitin-conjugated proteins were purified with Ni-NTA-agarose. The total cell lysates (Input) and pulldown eluates (6xHis Pulldown) were subjected to western blotting analysis and were stained for TDP-43, Flag, 6xHis, myc and GAPDH. The experiments were performed by FH (B) and JCS (A-C).

the proteasomal inhibition experiment (Figure 3.30A), an ubiquitinylation of D169G was hardly detected, even upon UBE2E3 overexpression. The total amount of this mutant was much lower than TDP-43 wt and the other mutants, suggesting a faster turnover and instability.

Since the K263E mutant is heavily ubiquitinylated, its regulation of the ubiquitinyla-tion by UBE2E3 and UBPY was investigated in detail (Figure 3.32). First, it was con-firmed that both proteasomal inhibition and UBE2E3 overexpression enhance K263E and TDP-43 wt ubiquitinylation (Figure 3.32A). Consistent, the catalytically inactive UBE2E3 variant C145S did not increase the amount of ubiquitinylated K263E or TDP-43 wt. The already strong ubiquitinylation of K263E in the presence of UBE2E3 was not further enhanced upon proteasomal inhibition. Furthermore, the silencing of UBE2E3 with si1 decreased the K263E and TDP-43 wt ubiquitinylation (Figure 3.32B). Consistent with the above observation, the UBPY wt co-expression decreased the Flag-K263E ubiquitinylation, while the UBPY variants C786S and ΔC did not the alter ubiquitinylation of the mutant.

Next, it was asked if K263E was able to bind stronger to UBPY and UBE2E3 compared to TDP-43 wt. Therefore, coimmunoprecipitation of Flag-TDP-43 wt or K263E with HA-tagged UBE2E3 or UBPY was performed (Figure 3.32D). Both TDP-43 wt and K263E were coimmunoprecipitated with E2 and DUB. We found a stronger binding of Flag-TDP-43 K263E to UBPY and UBE2E3. However, the K263E mutant seemed to be more abundant in the total protein lysates. Thus, it cannot be estimated if UBE2E3 and UBPY bound more efficiently to the mutant or TDP-43 wt. Nonetheless, these re-sults demonstrate that the heavily ubiquitinylated K263E is regulated by UBE2E3 and UBPY in a comparable manner to TDP-43 wt and that the mutant can bind the E2 and DUB. The question why K263E showed an elevated ubiquitinylation pattern remains to be solved.
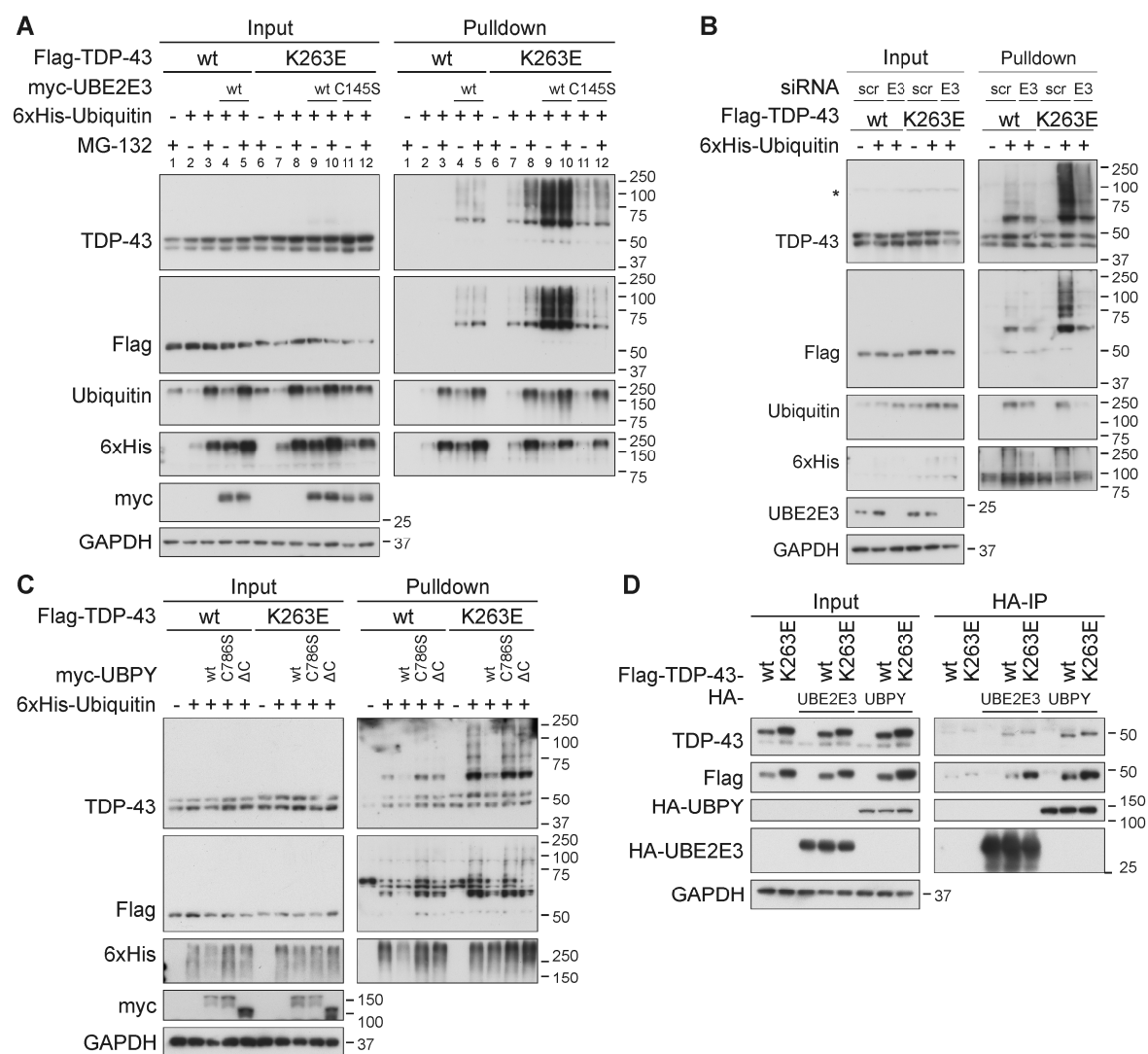
Figure 3.32 Regulation of TDP-43 K263E ubiquitinylation by proteasomal inhibition and UBE2E3 and UBPY. A Proteasomal inhibition and UBE2E3 overexpression increase the amount of ubiquitinylated K263E. HEK293E cells were triple-transfected with Flag-TDP-43 wt or K263E, 6xHis-vector control (-) or 6xHis-ubiquitin (+) and myc-vector control or myc-UBE2E3 or the catalytically inactive UBE2E3 C145S. The cells were treated with MG-132 (10µM) or DMSO for 2h, lysed with urea buffer and 6xHis-ubiquitin-conjugated proteins were pulled down from cell lysates. The total protein lysates and the Ni-NTA agarose eluates were subjected to western blot analysis with antibodies detecting TDP-43, Flag, ubiquitin, 6xHis, myc and GAPDH. **B** Knockdown of UBE2E3 decreases level of ubiquitinylated K263E. HEK293E cells were silenced three times with scrambled (scr) or siUBE2E3 (E3). 4h after the third silencing, the cells were double-transfected with Flag-TDP-43 wt or K263E and 6xHis-vector control (-) or -ubiquitin. 24h after the transfection urea lysates were prepared and a pulldown of 6xHis-ubiquitin-conjugated proteins was performed. The total cell lysates (Input) and the eluates (6xHis Pulldown) were western blotted and stained with antibodies against TDP-43, Flag, ubiquitin, 6xHis, UBE2E3 and GAPDH, as indicated. **C** UBPY can deubiquitinylate K263E. Flag-tagged TDP-43 wt or K263E was overexpressed with 6xHis-ubiquitin and myc-UBPY wt, C786S or ΔC or vector controls in HEK293E cells. The urea lysates were prepared and Ni-NTA purification of 6xHis-tagged proteins was performed. The total cell lysates and the pulldown eluates were subjected to western blot analysis and stained with antibodies against TDP-43, Flag, and ubiquitin, 6xHis, myc and GAPDH. **D** Co-immunoprecipitation of K263E with UBE2E3 and UBPY. HEK293E cells were co-transfected with Flag-TDP-43 wt or K263E along with HA-tagged UBE2E3 or UBPY, and HA-immunoprecipitation was performed. The total protein lysates (Input) and the immunoprecipitates (HA-IP) were subjected to western blotting and TDP-43, Flag, HA and GAPDH were detected with their respective antibodies. The experiments were performed by FH (A,B+D) and JCS (B+C).

3.7   Specificity of the UBE2E3 and UBPY regulated TDP-43 ubiquitinylation

In many neurodegenerative diseases aggregating proteins are ubiquitinylated. Here, it was investigated whether TDP-43 is a specific substrate of UBE2E3 and UBPY or if other aggregating proteins can be modified by these two enzymes. Ataxin-3 with a short and a long expanded polyglutamine stretch (ataxin-3-Q15 and -Q148) was used as a model for an aggregating protein. The C-terminally EGFP-tagged ataxin-3-Q15 or -Q148 constructs were overexpressed with 6xHis-ubiquitin and either myc-tagged UBE2E3 or UBPY in HEK293E cells (Figure 3.33). The pulldown of 6xHis-ubiquitinylated proteins showed that EGFP alone is not ubiquitinylated, even upon UBE2E3 co-expression. However, ataxin-3-EGFP-positive higher molecular smears were detected among 6xHis-ubiquitinylated proteins, demonstrating that both ataxin-3-Q15-EGFP and -Q148-EGFP were ubiquitinylated under basal conditions. This ubiquitinylation pattern was not altered upon UBE2E3 overexpression. Interestingly, UBPY decreased not only the ubiquitinylation of the aggregating ataxin-3-Q148 (lane 14, pulldown), but also of the non-aggregating ataxin-3-Q15 (lane 12, input and pull-down). Thus, it is tempting to speculate that UBPY is a rather general DUB or a specific DUB for aggregating or accumulating proteins. On the other hand, UBE2E3 did not increase the ubiquitinylation of ataxin-3-Q148, and thus its effect on TDP-43 ubiquitinylation seems to be more specific.
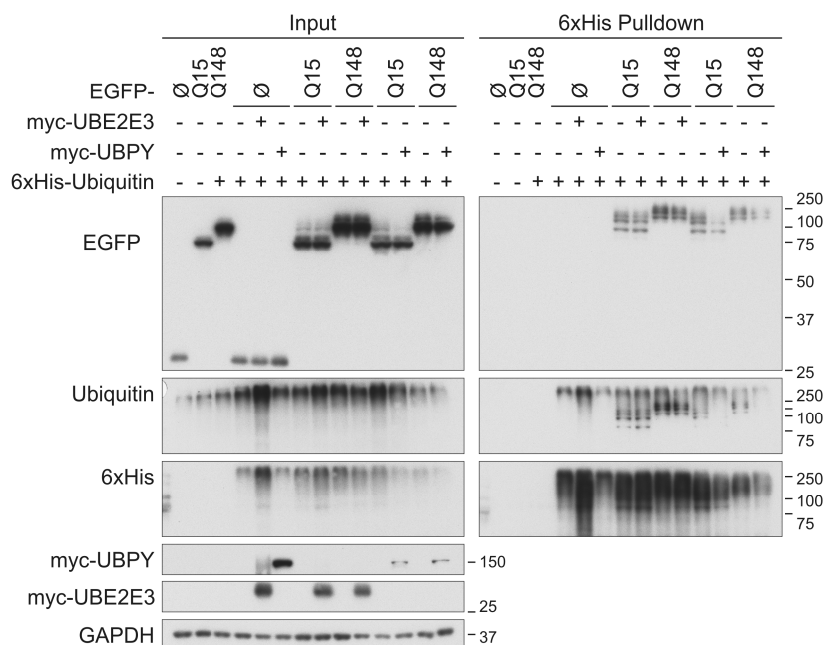
Figure 3.33 Effect of UBE2E3 and UBPY overexpression on ubiquitinylation of ataxin-3-Q148-EGFP. HEK293E cells were triple-transfected with 6xHis-ubiquitin (+) or vector-control (-), myc-UBE2E3 (+) or vector-control (-) and EGFP-N1-ataxin-3-Q148 or -Q15 or vector control (Ø), as indicated and the urea soluble cell lysates were prepared. The 6xHis-ubiquitin-conjugated proteins were purified with Ni-NTA-agarose. Western blot analysis was performed with the total cell lysates (Input) and the pulldown eluates (6xHis Pulldown) and the blots were stained for GFP, ubiquitin, 6xHis, myc and GAPDH. The experiment was repeated twice.

3.8   UBPY knockout enhances TDP-43 neurotoxicity in flies

Based on the results obtained for TDP-43 ubiquitinylation in cell culture studies the effect of the downregulation of the fly ortholog of UBPY was investigated in an established *Drosophila* model of TDP-43 neurotoxicity from our collaborator A. Voigt, RWTH Aachen (Voigt et al., 2010). In *Drosophila* the UAS/Gal4 system from *S. cerevisiae* enables the expression of any transgenic protein or RNAi in a time-dependent manner in any tissue, cell type or even distinct groups of cells of the fly. We used a model where TDP-43-GFP was specifically expressed in the fly eye, induced by the eye specific GMR-Gal4 driver. Two different fly lines were used: a TDP-43-GFP high and a low expression line, #14 and #10, respectively. The high expresser line #14 exhibited a progressive rough eye phenotype (REP) with depigmentation and merged ommatidia (Figure 3.34A, TDP-43 #14). The REP was already observed in one day old flies, which worsened over time, whereas the control GMR-Gal4 driver line displayed at any time point only some ommatidial disorganisation. The low expression line #10 did not develop a REP within 20 days, our latest monitoring time (Figure 3.34A, TDP-43 #10). Normal ommatidial organization is depicted in Figure 3.34C for comparison.

The UBPY fly ortholog dUBPY (CG5798) exhibits an overall amino acid sequence identity of 28% to hUBPY. It also contains the catalytic core with cysteine- and histidine-boxes, the MIT and Rhodanese-like domains as well the SH3-binding motifs (Komada, 2008; Mukai et al., 2010). We had difficulties to knockdown UBPY in mammalian cell cultures (see chapter 3.4.3). However, in flies the actin-driven ubiquitous expression of dUBPY RNAi resulted in a 55% downregulation in *Drosophila* larvae (Figure 3.34B). The ubiquitous knockdown of dUBPY was lethal in adult flies, which is in agreement with previously published reports of UBPY knockout in mice and flies (Mukai et al., 2010; Niendorf et al., 2007).

The effect of dUBPY downregulation by RNAi on the TDP-43 REP was studied. Our collaborator A. Voigt has already identified dUBPY in a modifier screen as a weak genetic interactor of the TDP-43 neurotoxicity phenotype in the *Drosophila* model. Here, the expression of dUPBY RNAi alone resulted in a very mild REP, but without depigmentation (Figure 3.34A, -dUBPY). Interestingly, silencing of dUBPY in flies worsened the REP in the TDP-43-GFP high expresser line (Figure 3.34A, TDP-43 #14 -dUPBY). The depigmentation was increased, black lesions were observed and almost all flies died within ten days. This strong phenotype was never observed in the TDP-43-GFP high expresser line or when GMR-dUBPY RNAi was expressed alone. In contrast, dUBPY RNAi had no visible effect on the structure and pigmentation of the eyes of the low expresser line, even after 20 days of expression (Figure 3.34A, TDP-43 #10 -dUBPY).
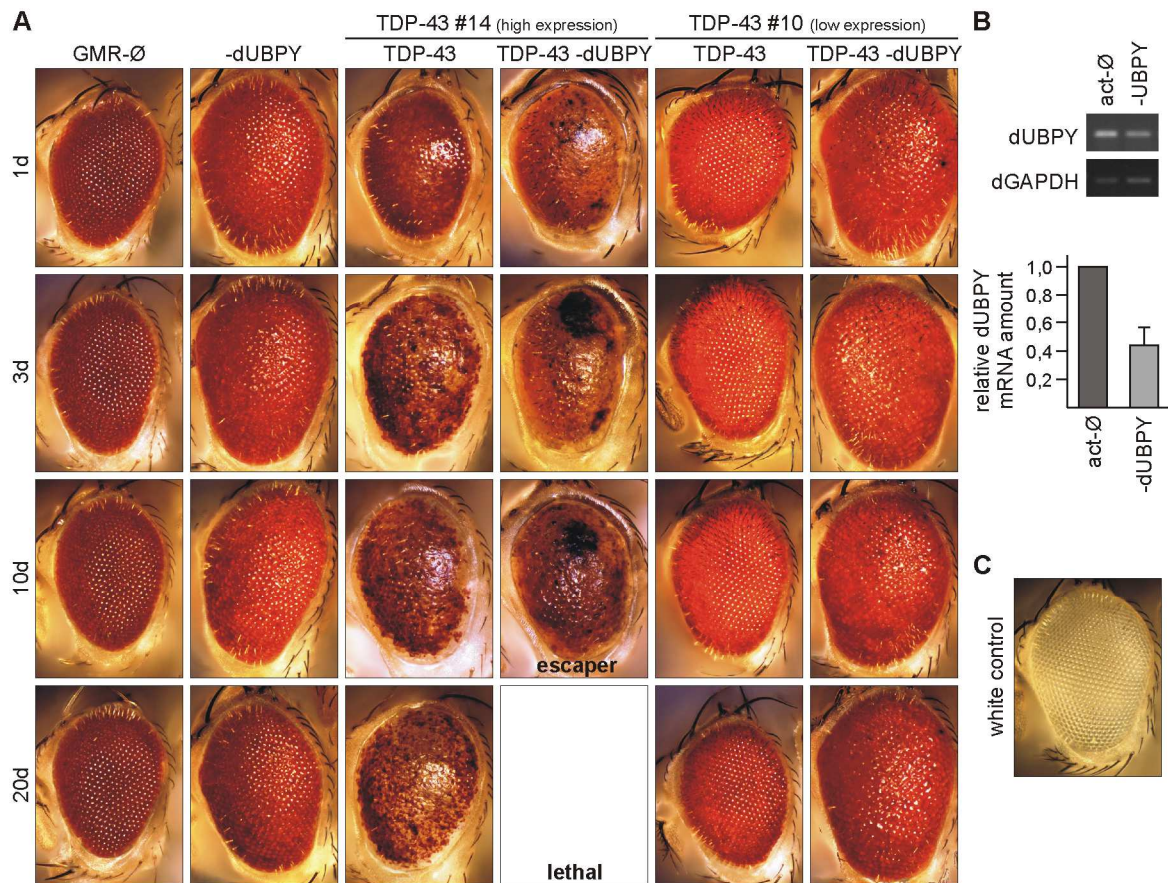
Figure 3.34 UBPY deficiency enhances TDP-43 neurotoxicity in *D. melanogaster*. A Light micro-scope eye images of 1, 3, 10 and 20d old male flies expressing TDP-43-GFP (line #14 high expression, line #10 low expression), dUBPY RNAi (-dUBPY) or both under control of the eye-specific driver GMR-Gal4. The driver line is shown for comparison (GMR-Ø). **B** dUBPY silencing under control of the act-Gal4 driver was lethal. The silencing efficiency was confirmed in third instar larvae expressing dUBPY RNAi. **C** White (*w[1118]* or w;+;+) eyed flies were used as control for ommatidial organization.

Next, the modifier effect of dUBPY RNAi on TDP-43 was investigated biochemically. We asked whether a dUBPY downregulation in the fly eye influences the TDP-43 solubility or ubiquitinylation. Therefore, fly head proteins were sequentially ex-tracted into a soluble RIPA fraction and an insoluble urea fraction (Figure 3.35). The dUBPY knockdown in the TDP-43 high expresser line #14 led to a shift of TDP-43-GFP into the insoluble fraction in one and three days old flies (Figure 3.35A). The higher molecular TDP-43-GFP smear, likely ubiquitinylated TDP-43, was stronger in dUBPY silenced fly heads, especially in the insoluble fraction. A strong decrease of TDP-43 steady state levels within ten days was also detected, probably reflecting the progres-sive degeneration of the fly eye (Figure 3.34A). Furthermore, total ubiquitin levels were increased in dUBPY deficient control and TDP-43 transgenic flies, particularly in the insoluble fraction. This indicates that dUBPY might be a more general DUB in fly.

In addition, the effects of dUBPY knockdown on TDP-43-GFP were analyzed in the low expresser line #10 (Figure 3.35B), although no REP was observed upon dUBPY silencing in this line (Figure 3.34A). TDP-43-GFP and a higher molecular weight TDP-43-GFP were increased in the insoluble fraction of one till ten days old UBPY silenced

flies and an overall decrease of steady-state TDP-43 level within 20 days was observed. While a REP was not detectable in dUBPY knockdown and TDP-43-GFP transgenic flies of the low expresser line #10, these results demonstrate that the silencing of dUBPY affected solubility and - probably - ubiquitinylation of TDP-43 nonetheless. In summary, the TDP-43 REP is enhanced in dUBPY silenced fly eyes, which is also reflected in increased TDP-43 insolubility, more higher molecular TDP-43 and an overall decrease of TDP-43 level over time. Thus we provide *in vivo* support, that UBPY is involved in the regulation of TDP-43 ubiquitinylation.

Next, a possible modifier effect of knockdown of the UBE2E3 *Drosophila* ortholog UbcD2 was investigated in the TDP-43 neurotoxicity model. Unfortunately, UbcD2 knockdown flies already exhibited an eye phenotype with depigmentation. Nonetheless, sequential extractions were prepared of heads from TDP-43-GFP high expresser line #14 flies that expressed UbcD2 RNAi. Upon knockdown of UbcD2, a decrease of higher molecular weight TDP-43 would be expected, but we did not detect altered TDP-43 level in ten days old flies (data not shown). However, in ten days old TDP-43-GFP transgenic flies almost no higher molecular weight smear was observed (Figure 3.35). Thus, the investigation of a modifier effect of UbcD2 knockdown in TDP-43 transgenic flies should be repeated in one or three days old flies. Since UBE2E3 overexpression in a cell culture model resulted in increased ubiquitinylation of TDP-43, the effect of UBE2E3 overexpression in this fly model remains to be shown.
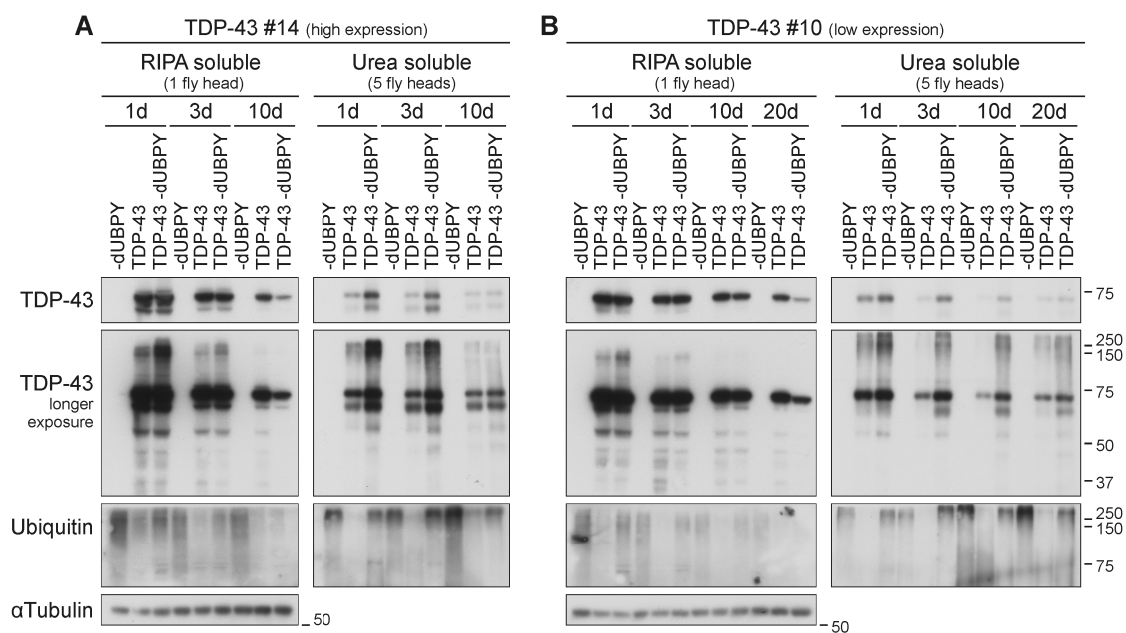
Figure 3.35 dUBPY silencing enhances the ubiquitinylation of TDP-43 and shifts the TDP-43 species into insoluble fractions. A+B Analysis of TDP-43 protein level in flies expressing human TDP-43-GFP (A line #14, high expression, B line #10 low expression), UBPY RNAi or both for 1d, 3d and 10d (A) and 1d, 3d, 10d and 20d (B). Fly heads were collected and subjected to sequential extraction. RIPA and urea lysate volumes equivalent to one and five fly heads, respectively, were western probed as indicated with antibodies against TDP-43, ubiquitin, and α-tubulin as loading control.

3.9   Functional implications of altered TDP-43 ubiquitinylation

Finally, the question arose if the altered ubiquitinylation status of TDP-43 may have implications on the function of this protein. We assumed that ubiquitinylated and/or insoluble TDP-43 might be non-functional, because the ubiquitinylation might interfere with an incorporation of TDP-43 into functional complexes.. TDP-43 regulates splicing and stability of many mRNAs (see chapter 2.3.3). Two TDP-43 mRNA targets were described and functionally validated in our group before: HDAC6 and SKAR. The HDAC6 mRNA is stabilized by TDP-43 (Fiesel et al., 2010) and SKAR is alternatively spliced upon TDP-43 knockdown, resulting in decreased SKARα and increased SKARβ isoform (Fiesel et al., 2012).

The HDAC6 and SKAR mRNA and protein levels were investigated after the increase of ubiquitinylated TDP-43, which was mediated by the overexpression of UBE2E enzymes and an additional proteasomal inhibition for 6h. Two independent repetitions of the same experiment (n=3 in total) are depicted due to the mRNA level variations among them (Figure 3.36A+B). Alternative splicing of SKAR was not observed on mRNA and protein level. The TDP-43 steady-state levels were also unchanged, as was observed above. The protein levels of HDAC6 were not altered. However, some variations of the HDAC6 mRNA amount were detected, but these were not consistent among the three repetitions of this experiment.

The portion of ubiquitinylated, insoluble and potentially not active TDP-43 is very small compared to total protein level of TDP-43, because TDP-43 higher molecular weight smear was usually not detected in western blot analysis of total protein. For the detection of effects on mRNA stability of HDAC6 or alternative splicing of SKAR, the amount of TDP-43 has to be downregulated quite strongly. Thus, the decrease of the possibly non-functional TDP-43 from the active pool by ubiquitinylation was probably too small for the detection of altered HDAC6 or SKAR within 48h of UBE2E E2 enzyme overexpression. However, it could be possible that over a longer period of time enough functional TDP-43 is withdrawn from the active pool by ubiquitinylation.

In summary, this study demonstrated that the ubiquitinylation of TDP-43 wt and of pathogenic mutants can be regulated by the class III E2 enzymes UBE2E1, UBE2E2 and UBE2E3 as well as by the ubiquitin isopeptidase UBPY. Furthermore, the ubiquitinylation of the pathogenic and heavily ubiquitinylated TDP-43 mutant K263E was also regulated by UBE2E3 and UBPY. Finally, the silencing of dUBPY enhanced a neurotoxic eye phenotype in a TDP-43 *Drosophila* model and the accumulation of insoluble TDP-43 species. However, the consequences of the ubiquitinylation on the function of TDP-43 remain to be shown.
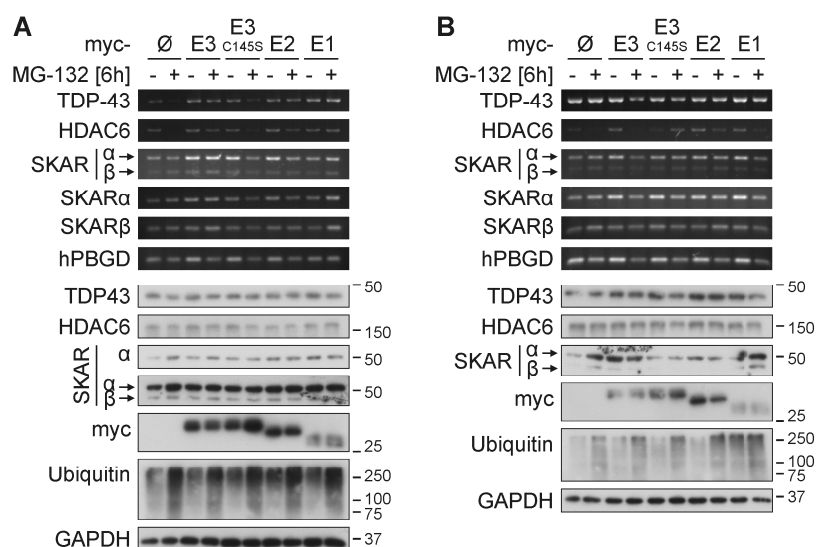
Figure 3.36 Altered ubiquitinylation of TDP-43 has no effect on the stability and alternative splicing of HDAC6 and SKAR mRNA. A+B Depicted are two representatives of this experiment, illustrating the variations - especially on mRNA level - of analyzed targets among this experimental group. UBE2E3 wt, C145S, UBE2E2 and UBE2E1 were overexpressed in HEK293E cells for 48h, followed by 6h inhibition of proteasome with MG-132 (10μM). RNA and RIPA soluble protein were isolated. The change of TDP-43, HDAC6, SKARα, SKARβ and hPBGD mRNA level was analyzed with sqRT-PCR. The protein lysates were subjected to western blot analysis and stained with antibodies against TDP-43, HDAC6, SKARα/β, myc, ubiquitin, and GAPDH as loading control.

4 Discussion

Inclusions positive for ubiquitinylated, fragmented and phosphorylated TDP-43 are a common feature of most cases of ALS and of all FTLD-TDP cases. Under physiological conditions, TDP-43 is thought to function as a part of several multi-protein complexes that are involved in transcription and multiple steps in the RNA metabolism. How TDP-43 is implicated in disease pathogenesis is still unclear. To gain a better insight into the normal and pathological functions, we screened for novel protein interactors of TDP-43. In the three Y2H screens performed in this study, a total of twelve interactors were identified. Seven interactors of the third screen with TDP-43 CTF were confirmed as true TDP-43 binding proteins in HEK293E cells. As TDP-43 is found ubiquitinylated in pathological inclusions in TDP-43 proteinopathies, we focused on the functional validation of two hits which take part in ubiquitinylation reactions: the E2 ubiquitin-conjugating enzyme UBE2E3 and the ubiquitin isopeptidase UBPY.

4.1 Yeast two-hybrid screening for TDP-43 interactors

At the beginning of this work, only a few protein interactors of TDP-43 were known that were identified with several screening approaches. Three protein-protein association studies that used high-throughput techniques identified interactors of TDP-43, among them two proteomic studies utilizing Y2H systems (Lehner and Sanderson, 2004; Stelzl et al., 2005). The third study used an affinity-capture mass spectrometry approach with a HEK293 derived cell line (Jeronimo et al., 2007). The only so far published Y2H screen with TDP-43 as bait used a human fetal brain cDNA library, discovering an interaction of TDP-43 with ubiquilin-1 (Kim et al., 2009). In the beginning of this study a global approach was published, identifying several hundred TDP-43 co-immunoprecipitated proteins from HEK293 cell lysates (Freibaum et al., 2010). In addition, two studies identified potential TDP-43 interactors in HeLa cells, among them hnRNPs, FUS and components of the Drosha microprocessor complex (Buratti et al., 2005; Ling et al., 2010)

In all these studies TDP-43 binding proteins were identified from either non-neuronal cell lines, in Y2H screens with specific baits and preys, or using a fetal brain cDNA library. Here, we identified several novel, and also confirm known protein interactors of TDP-43 in an Y2H screen, using for the first time a cDNA library generated from adult brain mRNAs. Importantly, this library represents the gene expression profile of the brain of people at an age when they might be affected from a neurodegenerative disease. Thus, the novel interactions are likely to take place in the aging brain, and misregulation of some of them might be involved in the development of ALS or FTLD.

The screening for novel protein binding partners with a Y2H system has several advantages, but also some disadvantages. One advantage over classical biochemical or genetic methods is that Y2H is an *in vivo* approach and provides an important first hint for the identification of interaction partners. These interactions take place in a cellular context and not in optimized buffer conditions. In addition, Y2H screens are rather cheap, require no specialized equipment and results are obtained fast. Moreover, also weak and transient interactions can be detected, which is often not possible with other techniques like coimmunoprecipitation or pulldown. Finally, the use of different screening stringencies also allows first conclusions about the strength of interaction.

However, the Y2H system has several disadvantages that are discussed in this section in the context of the screens performed in this study. First, the bait protein might autoactivate the reporter genes, which response to transcriptional activation, especially when the bait protein is a DNA/RNA binding protein like TDP-43. However, we showed that TDP-43 FL and CTF do not exhibit autoactivation activity in the used Y2H system (see Figure 3.2A). Second, some protein interactions may not happen in yeast, because of missing posttranscriptional modifications such as phosphorylation, disulfide bridge formation, or proper folding with the help of certain chaperones that are not present in yeast. In this study, wrong folding or masking of interaction sites with the Gal4-AD- or BD might account for the weak interactions of TDP-43 FL, CTF$_{172-414}$ and CTF with the known interactors SMN1 and hnRNPA2 (see Figure 3.3). Moreover, this might explain at least partially why the two screens with TDP-43 FL yielded only one true positive interactor each.

Third, only nuclear interactions can activate the reporter genes. Therefore, the bait- and prey-fusion proteins are targeted to the nucleus. Thereby interactions of proteins might be detected which are naturally not located in the same compartment or expressed in the same tissue. TDP-43 is a mainly nuclear protein, where also most of the confirmed interactors are localized. Still, TDP-43 is also shuttled to the cytoplasm, where it is associated with several RNA granules (Alami et al., 2014; Dewey et al., 2011; Dewey et al., 2012; Fallini et al., 2012; Moisse et al., 2009; Volkening et al., 2009; Wang et al., 2008). The cytoplasmic Y2H hits UBPY and RACK1 and the partially cytoplasmic LSM6 were shown to bind cytoplasmic TDP-43 (see Figure 3.11). Therefore these interactions could still be functionally meaningful, as confirmed for the role of UBPY in TDP-43 deubiquitinylation. It should also be noted that there is the rather unlikely, but still possible event that a third protein mediates the interaction of bait and prey. This might be an endogenous yeast protein homologous to a mammalian protein, or an exogenous protein from another co-expressed library vector. However, the later was ruled out in this study with the retransformation of the isolated library

plasmids and TDP-43 into yeast, which confirmed the interactions (see Figure 3.6). If an interaction is mediated by a third protein in yeast it can be difficult to confirm this interaction in mammalian cells with current methods.

Furthermore, overexpression of both bait- and prey-proteins and targeting them to the nucleus could be toxic for yeast, especially when unnatural protein concentrations are reached. We did not observe toxicity of TDP-43 FL or CTF when they were expressed as AD- or BD-fusion proteins (see Figure 3.2). In literature, toxicity of TDP-43 in yeast was reported in several studies from the same group (Armakola et al., 2012; Elden et al., 2010; Johnson et al., 2008; Johnson et al., 2009). However, they used other yeast strains than we did, and expressed TDP-43 variants under the control of a galactose-inducible promoter that usually yields high overexpression levels and might explain their observation of TDP-43 toxicity. Also, yeast strains used for Y2H are usually optimized for the identification of protein-protein interactions and not for functional validations. Thus, various yeast strains could be differentially affected by the same protein.

Finally, Y2H screens usually yield a high number of false positive hits, which were estimated as high as 70% (Deane et al., 2002). The prey protein itself could activate the reporter genes, the fusion of the bait or prey proteins with BD- or AD of the Gal4 transcription factor might induce improper folding that reveals interaction sites which are not exposed in mammalian cells, or two proteins could interact, which are usually not expressed in the same tissue, compartment, or at the same time in development. We identified many false positive hits in the three TDP-43 interactor screens. To reduce false positive hits, the screens were performed with several reporter genes and with relatively high stringency. Our cDNA library contained many 3'UTRs and genomic sequences that showed no or only low similarity to mRNAs. The translation of these sequences into actually non-existing proteins was confirmed with western blot (see Figure 5.1). Also, many proteins translated from ORFs exhibited autoactivation activity when they were expressed together with the bait-control vector upon retransformation in yeast. Therefore it is important to confirm the identified interactions and separate them from false positive hits with further validations. We have done this successfully with additional Y2H experiments with retransfected cDNA library plasmids and full-length target cDNAs, and especially with coimmunoprecipitation experiments in HEK293E cells.

There are many aspects why data obtained from Y2H screens should be handled with care. However, our screens yielded true positive interactors of TDP-43. RACK1 and RBM45, as well as EXOSC10 and KPNA4 were already described before to interact or colocalize with TDP-43 (Collins et al., 2012; Lehner and Sanderson, 2004; Nishimura

et al., 2010). This proves that our Y2H screening system was able to identify true novel interactors of TDP-43.

4.2   Interactions of the targets are stronger with CTF than TDP-43 FL

We were able to clone the full-length cDNA of LSM6, MED6, RACK1, RBM45, RNF2, UBE2E3 and UBPY, and confirmed their binding to TDP-43 by coimmunoprecipitation (see Figure 3.8). Interestingly, most interactions were stronger with mCherry-CTF than with TDP-43 FL. This was also observed in the two control experiments with Y2H (see Figure 3.6 and Figure 3.7). All ten primary positive hits interacted moderately or strongly with BD-CTF but for most targets no interaction with BD-TDP-43 FL was observed upon retransformation of the isolated library plasmids with partial cDNAs (see Figure 3.6). Moreover, most full-length targets interacted only weakly with CTF, and interactions with TDP-43 FL were hardly detected in yeast (see Figure 3.7). The only exception was RBM45, showing moderate interaction with TDP-43 FL but weak binding to CTF.

The most successful Y2H screen was performed with CTF, and not TDP-43 FL. Therefore the stronger interactions of the targets with CTF are easily conceivable. The conformation of CTF alone might allow a better access to the binding sites by the interactors. Of course, this could also be true *vice versa* for the targets that were mostly partially expressed in the screen. It is also possible that the fusion to the 22kDa binding and activation domains altered the conformation more strongly of TDP-43 FL, but also of the full-length targets, and covered their binding sites. The same might be true for the mCherry-tagged TDP-43 FL that was used for coimmunoprecipitation experiments. Coimmunoprecipitation of mCherry-tagged CTF with UBE2E3 was only slightly above background and was not observed with mCherry-TDP-43 FL, but myc-UBE2E3 bound clearly to Flag-TDP-43 (see Figure 3.8). This also indicates that the 25kDa N-terminal mCherry-tag interferes with binding of UBE2E3 to TDP-43. In support of this theory, a C-terminal part of EXOSC10 of about 15kDa was identified from the first Y2H screen with TDP-43 FL. However, full-length EXOSC10 of about 100kDa only bound to two CTFs but not TDP-43 FL in Y2H (see Figure 3.5).

The weak interaction of UBE2E3 with mCherry-CTF and undetectable interaction with mCherry-TDP-43 FL in coimmunoprecipitation can be explained at least partially with decreased solubility of TDP-43 upon co-expression with UBE2E3 (see Figure 3.18B). This solubility shift makes interaction studies more difficult. It is not possible to perform coimmunoprecipitation reactions from urea lysates, which also contain the insolubility-shifted TDP-43, because the buffer would denature the antibodies immediately. Moreover, the binding of TDP-43 to some of the targets might be

increased by the interaction with additional proteins, as it takes place in protein complexes with several subunits. The interactors MED6 and LSM6 are components of the Mediator and Lsm complexes, respectively (see below). The discrete interactions of TDP-43 FL with these proteins were rather weak, but might be increased by additionally binding to other proteins or subunits of these complexes.

Finally, it is conceivable that at least some hits rather interact with C-terminal fragments of TDP-43 than with the whole protein *in vivo*. This is possible for UBPY and UBE2E3 as both TDP-43 FL and CTFs are ubiquitinylated in neurodegenerative diseases. In fact, UBPY coimmunoprecipitated an endogenous 35kDa fragment of TDP-43, and very weak binding of this fragment with UBE2E3 was also observed (see Figure). Thus, these interactions could be pathological relevant. However, it is not known whether CTFs are cleaved from TDP-43 FL before or after ubiquitinylation.

4.3 Several disease modifications of TDP-43 were observed upon proteasomal inhibition and after UBE2E3 transfection in cell culture

TDP-43 is ubiquitinylated, fragmented and phosphorylated in pathological inclusions in brain and spinal cord of FTLD and ALS patients (Arai et al., 2006; Neumann et al., 2006). Furthermore, accumulations of TDP-43 and of ALS-linked mutants within degradation pathways implicate a failure of clearance of TDP-43 as a primary disease mechanism (Bendotti et al., 2012; Blokhuis et al., 2013; Ling et al., 2013). Moreover, ubiquitinylated protein depositions are a common feature of many neurodegenerative diseases, indicating a possible failure of clearance contributes to neurodegeneration. The role of the UPS and autophagy in the clearance of physiological but also pathological TDP-43 in patients, animal models and cell lines is widely discussed in literature (see chapter 2.3.4). Here we found that insoluble and ubiquitinylated TDP-43 as well as a 25kDa and especially a 35kDa fragment accumulate upon proteasomal inhibition with MG-132, but not with the autophagy inhibitor bafilomycin A1 (see Figure 3.12). A shift into the insoluble fraction and increased higher molecular weight species of TDP-43 were observed upon UBE2E3 overexpression in HEK293E cells or UBPY silencing in TDP-43 transgenic flies (see Figure 3.18 and Figure 3.35). Thus, the insolubility, ubiquitinylation and fragmentation of TDP-43 recapitulate key features of TDP-43 modification in ALS and FTLD (Arai et al., 2006; Neumann et al., 2006).

Proteasomal inhibition but not blocking autophagy strongly enhanced level of insoluble, ubiquitinylated TDP-43, We also detected no further increased level of ubiquitinylated TDP-43 upon MG-132 and bafilomycin A1 treatment, which is consistent with a recent study from Huang and colleagues (Huang et al., 2014). This indicates that the proteasome is participating in TDP-43 degradation in HEK293E cells, which is also

supported by many reports that demonstrated a role of the UPS in TDP-43 turnover (Brady et al., 2011; Kabashi et al., 2008; Rutherford et al., 2008; Scotter et al., 2014; Tashiro et al., 2012; Urushitani et al., 2010; van Eersel et al., 2011; Wang et al., 2010; Winton et al., 2008a; Zhang et al., 2010). However, we did not observe an increase of steady-state level of endogenous or exogenous TDP-43, even after 24h treatment with MG-132. This would be expected if TDP-43 is degraded by the proteasome. TDP-43 was shown to be a stable protein with a half-life ranging between 34-40h of endogenous TDP-43, 4-40h of overexpressed or induced TDP-43 FL, but only 1.7-11h of CTFs or nuclear import impaired TDP-43 (Austin et al., 2014; Ling et al., 2010; Pesiridis et al., 2011; Scotter et al., 2014; Watanabe et al., 2013). CTFs were readily stabilized upon longer inhibition of the UPS, confirming that these TDP-43 species are cleared by the proteasome. Conversely, it was suggested that elevated level of TDP-43 fragments upon proteasomal inhibition arise from increased caspase activity (Rutherford et al., 2008). Interestingly, TDP-43 regulates its own expression level via a negative-feedback loop (Avendano-Vazquez et al., 2012; Ayala et al., 2011b). Thus, inhibiting the degradation of TDP-43 probably also induces a decrease in *de novo* protein synthesis of endogenous TDP-43. It should also be noted, that levels of ubiquitinylated TDP-43 compared to total TDP-43 levels were low upon proteasomal inhibition for up to 24h. This may indicate that only a small portion of TDP-43 is removed by ubiquitinylation from the pool of free and functional TDP-43.

Interestingly, TDP-43 is monoubiquitinylated without the inhibition of the UPS. This was not reported before. This posttranslational modification can regulate protein trafficking, alter protein function, and serve as docking sites for ubiquitin-binding proteins (Hicke, 2001). It remains to be shown which of the 20 lysine residues of TDP-43 are monoubiquitinylated and what is the functional implication.

Upon proteasomal inhibition for 6-24h, we detected the stabilization of a 25kDa, but more prominent of a 35kDa fragment of TDP-43 (see Figure 3.12A), which are most likely C-terminal fragments (Neumann et al., 2006; Zhang et al., 2007b). Studies in cell lines and transgenic mice reflect our findings, where usually insoluble 35kDa species are detected (Araki et al., 2014; Kabashi et al., 2008; Rutherford et al., 2008; Urushitani et al., 2010; van Eersel et al., 2011; Wang et al., 2012; Winton et al., 2008a), while 25kDa fragments are rarely seen (Caccamo et al., 2009; Rutherford et al., 2008; Wang et al., 2012). More specifically, the inhibition of the UPS with epoxomicin for 20h, but not inhibition of autophagy, also prevented degradation of an insoluble 35kDa CTF (Araki et al., 2014). Furthermore, 35kDa fragments are even present in urea soluble and cytoskeleton fractions without the application of inhibitors (Urushitani et al., 2010). However, TDP-43 fragments of about 35kDa are only occasionally observed, whereas the 25kDa species are predominant in ALS and FTLD

brain tissue (Hasegawa et al., 2008; Igaz et al., 2008; Inukai et al., 2008; Neumann et al., 2006). This could mean that the generation of CTFs underlies different mechanisms in cell culture or animal models than in patients. In cell culture, these fragments can be cleaved by caspase 3 (Dormann et al., 2009; Rutherford et al., 2008; Zhang et al., 2007b), but which enzymes participate in the generation of TDP-43 fragments in diseased brain remains to be shown. Another aspect that might contribute to the different TDP-43 fragment pattern in cell culture models versus patient brain tissue is the period of time in which the fragments are generated. In cell culture models, the formation of TDP-43 fragments usually occurs within hours upon treatment with various inhibitors of the proteasome or autophagy, while CTFs rather accumulate over months and years in disease.

In our cell culture model we could not distinguish if TDP-43 FL, CTFs or even N-terminal fragments were ubiquitinylated and pulled down. The utilized polyclonal anti-TDP-43 antibody recognizes TDP-43$_{1-260}$, thus also including the 25kDa and 35kDa CTFs. A C-terminal specific antibody would also detect TDP-43 FL. In addition, overexpressed TDP-43 FL contains an N-terminal Flag-tag, implying that at least a part of the ubiquitinylated TDP-43 recognized with an anti-Flag was TDP-43 FL. It is possible that CTFs were generated from Flag-TDP-43, but these cannot be detected with anti-Flag antibody. To distinguish between TDP-43 FL and CTFs, a differential N- and C-terminal double-tagged TDP-43 has to be used. It is noteworthy, that the composition of TDP-43 positive inclusions in ALS and FTLD differs. TDP-43 FL is predominantly detected in ALS spinal cord, whereas inclusions in ALS and FTLD brain tissue are composed of TDP-43 FL and CTFs (Igaz et al., 2008; Neumann et al., 2009).

We did not observe any aggregate formation, mislocalization and only very weak phosphorylation of endogenous or Flag-tagged TDP-43 FL under physiological conditions and upon proteasomal inhibition with MG-132. Only mCherry-CTF accumulated after MG-132 treatment for 14h, which was not altered by UBPY (see Figure 3.27). Aggregation of exogenous TDP-43 in cell culture systems is usually observed upon disruption of nuclear trafficking, or with pathogenic mutants or aggregation-prone CTFs (Arai et al., 2010; Brady et al., 2011; Igaz et al., 2009; Nonaka et al., 2009a; Nonaka et al., 2009b; Scotter et al., 2014; Wang et al., 2010; Winton et al., 2008a). In addition, mislocalization and aggregate formation of overexpressed TDP-43 FL were usually seen after a second hit like inhibition of protein clearance pathways (Scotter et al., 2014; Urushitani et al., 2010; van Eersel et al., 2011; Wang et al., 2010). In fact, enhanced ubiquitinylation and insolubility of TDP-43 upon proteasomal inhibition are not necessarily linked to the formation of aggregates (Urushitani et al., 2010). The proteasomal inhibition alone did not induce aggregate formation in that study, but upon additional blocking of autophagy aggregates were observe. Furthermore, we

observed CTF aggregates after 14h of proteasomal inhibition, whereas for most pull-down experiments of ubiquitinylated TDP-43 the cells were treated for 2-3h. Thus, CTFs can be ubiquitinylated after a short period of MG-132 treatment, but might not form visible aggregates in this time frame.

HEK293E cells are immortalized and undergo cell division, which distinguishes them from primary neuronal cell cultures. Thus, cell divisions could prevent the formation of aggregates or compensate for cell damage. In fact, proteasomal inhibition was shown to have much greater effects on the localization and solubility of TDP-43 in primary neurons compared to immortalized motor neurons (van Eersel et al., 2011). Thus, aggregates may not be visible in the dividing HEK293E cells, or the cells which contain aggregates just die due to a possible toxicity of the aggregates. Moreover, we only observed a very weak S409/410 phosphorylation of ubiquitinylated TDP-43 when UBE2E3 strongly increased level of ubiquitinylated TDP-43 (see Figure 3.18C), though aggregate formation of CTFs was shown to be phosphorylation dependent before (Brady et al., 2011). It should also be kept in mind that inhibition of the proteasome, but also other treatments that lead to TDP-43 pathology in cell culture models, induce cell death after some time. Thus, there are two possibilities: either pathological alterations of TDP-43 contribute to cell toxicity or TDP-43 pathology arises from the induced cell death in the cellular HEK293E model. Moreover, aggregate formation might take weeks or months in *in vivo* models, whereas in cell lines this process occurs within days. Therefore, the mechanisms underlying the accumulation of TDP-43 in immortalized cells, but also the composition of the aggregates themselves, could be different compared to aggregates detected in TDP-43 transgenic animals.

In summary, the used HEK293E ubiquitinylation cell model is sufficient to study the regulation of TDP-43 ubiquitinylation, but cannot recapitulate all disease specific TDP-43 modifications.

4.4   Ubiquitinylation of TDP-43 by class III UBE2E ubiquitin-conjugating enzymes

We identified for the first time that the class III UBE2E ubiquitin-conjugating enzymes participate in ubiquitinylation of TDP-43. Endogenous UBE2E1, UBE2E3 and TDP-43 are localized in the nucleus, though upon overexpression about 50% of cells show additional cytoplasmic staining. We provide evidence for a functional interaction, since the UBE2Es enhanced TDP-43 ubiquitinylation. In support of their specificity, a catalytically inactive UBE2E3 failed to ubiquitinylate TDP-43, whereas the more distant UBE2C and UBE2N only slightly increased ubiquitinylated TDP-43. This was rather due to the proteasomal inhibition. It is not surprising that all UBE2Es promote

TDP-43 ubiquitinylation. They share high homology, especially in their UBC domain, which was identified as a TDP-43 CTF interactor in the Y2H screen. Thus it is also possible that UBE2E1 or UBE2E2 or all three E2s might contribute *in vivo* to the ubiquitinylation of TDP-43. However, the expression levels of UBE2E3 are predicted to be higher than the other two UBE2Es in many tissues and in various cell lines (www.proteinatlas.org).

Further support for a role of UBE2E3 comes from the decrease of ubiquitinylated TDP-43 upon silencing of the E2 enzyme with a specific siRNA. This was rescued by overexpression of UBE2E3 wt and a siRNA resistant UBE2E3, but not by C145S (sees Figure 3.22). That rules out off-target effects. However, three other siRNAs failed to alter the amount of TDP-43 ubiquitinylation, which is mentioned in the results part (see chapter 4.3.4). In *Drosophila*, we could not study the effects of downregulation of the ortholog UbcD2, because GMR-driven expression in the eye of UbcD2 RNAi exhibited an eye specific phenotype on its own. We conclude that UBE2E3 seems to be a specific E2 for TDP-43, as the ubiquitinylation of two aggregation prone polyglutamine-expanded ataxin-3 variants were not further enhanced by the overexpression of UBE2E3 in cell culture (see Figure 3.33). Nonetheless, there are open questions regarding the interaction of UBE2E3 with TDP-43 and their functional impact.

Can the E2 enzyme UBE2E3 directly interact with its substrate TDP-43? It is unusual that an E2 interacts with a putative substrate. Instead, it is widely believed that an E3 ligase mediates the ubiquitinylation and therefore is binding the substrate. Hence, what might be the cognate E3 ubiquitin ligase? In the ubiquitin conjugating cascade a RING finger type E3 ubiquitin ligase can bind simultaneously the substrate and the E2, which transfers the activated ubiquitin moiety directly onto the substrate (Metzger et al., 2012). In this E2-E3 complex the E2 might influence the substrate specificity and type of linkage. In addition, E3 independent *in vitro* ubiquitinylation by E2 enzymes has already been reported (Hoeller et al., 2007). Thus there might be a direct interaction of E2s and substrates. The interaction may be transient. However, in Y2H also transient and weak interactions can be detected. In this system the contact area of UBE2E3 for TDP-43 might have been exposed, allowing a direct interaction with TDP-43 without an additional E3, and subsequently activated the reporter genes. However, it is possible that a homolog of the connecting E3 ligase that mediated the interaction is expressed in yeast. On the other hand, the co-immunoprecipitation of overexpressed TDP-43 and UBE2E3 from HEK293E cell lysates were barely detectable or non-existing, depending on the tag and TDP-43 variant, and which of the two proteins was pulled down from the lysates. Since co-immunorecipitations are performed under optimized conditions it might be that an E3 ligase is required for the stabilization of the interaction.

The E3 ligase(s) for TDP-43 were suggested to reside in the cytoplasm (Urushitani et al., 2010), though TDP-43 is mainly nuclear. A possible candidate ubiquitin ligase is parkin, which belongs to the new class of RING HECT hybrid E3s (Riley et al., 2013; Wenzel et al., 2011a). Parkin was suggested to ubiquitinylate TDP-43 *in vitro* (Hebron et al., 2013). Conversely, the parkin mRNA levels are also regulated by TDP-43 (Lagier-Tourenne et al., 2012), and parkin interacts with UBE2E2 (Imai et al., 2000; Zhang et al., 2000). As UBE2E2 and UBE2E3 share 85% homology it is possible that parkin may also bind to UBE2E3. However, preliminary results from our group indicate that exogenous parkin is not enhancing ubiquitinylation of TDP-43 in 6xHis-ubiquitin pulldowns from HeLa cells, which do not express endogenous parkin (data not shown). Therefore, further investigations are needed to show whether parkin mediates UBE2E3 dependent TDP-43 ubiquitinylation.

We identified the E3 ligase RNF2 as a TDP-43 interactor in the Y2H screen. RNF2 is located in the nucleus like TDP-43, but the overexpression did not show effects on ubiquitinylation of TDP-43 (see Figure 3.28). This might reflect technical problems with the transfection of functional and catalytically active RNF2, or RNF2 is no functional positive interactor. Silencing of the RNF2 ortholog in fly eyes with GMR-driven RNAi had already an eye specific phenotype, constricting further investigations in the TDP-43 neurotoxicity animal model (not shown observation from Dr. S. Jäckel, our group). However, a functional interaction of UBE2E1 with RNF2, which promotes the autoubiquitinylation of RNF2, was reported (Buchwald et al., 2006).

However, there might be other, especially nuclear, E3 ubiquitin ligases that participate in the ubiquitinylation of TDP-43 by UBE2E3. A comprehensive framework of E2–RING E3 interactions revealed interactions of UBE2Es with many E3s, among them RNF2 but not parkin (van Wijk and Timmers, 2010). Therefore it was suggested that UBE2E ubiquitin-conjugating enzymes are hub E2s, which interact with a large number of E3s.

It is also possible that the ubiquitinylation of TDP-43 by UBE2E3 is a novel example of a direct interaction of an E2 with a substrate. In support of this, UBC9 can SUMOylate substrate proteins without an E3 ligase, although with lower reaction efficiency (Tozluoglu et al., 2010). Moreover, *in vitro* ubiquitinylation studies showed E3 independent ubiquitinylation via E2 enzymes (David et al., 2010; Hoeller et al., 2007). Therefore, *in vitro* ubiquitinylation assays without or with distinct E3s, including parkin and RNF2, could give insight to whether UBE2Es need a linking E3 or if they can ubiquitinylate TDP-43 in the absence of an E3. Thus, the ubiquitin ligase(s) for the UBE2E enzyme/TDP-43 complex still remain to be shown and if UBE2E3 can ubiquitinylate TDP-43 in an E3 independent manner.

Next, we have to ask why the ubiquitinylation of TDP-43 by UBE2Es does not lead to degradation of TDP-43. Instead, the ubiquitinylated TDP-43 species accumulate and shift into the insoluble fractions, but do not from aggregates within the observed timeframe. We observed that proteasomal inhibition does not further stabilize TDP-43 ubiquitinylation by UBE2Es. This suggests that ubiquitinylation of TDP-43 by UBE2Es is not a straightforward proteasome-targeting signal or leads to a saturation of TDP-43 ubiquitinylation that cannot be further enhanced by proteasomal inhibition. The co-expression of UBE2E3 shifted TDP-43 into more insoluble fractions, and UBE2E3 C145S increased the amount of insoluble TDP-43 even stronger. Thus, the ubiquitinylation by UBE2E enzymes may change the conformation of TDP-43 slightly and direct TDP-43 into protein complexes in distinct subcellular localizations. The increased amount of ubiquitinylated TDP-43 might also induce a pathological proteasomal overload, preventing an effective degradation of ubiquitinylated TDP-43, which then becomes too insoluble to be degraded. However, this was not observed for UBE2E1, since this enzyme binds and ubiquitinylates ataxin-1 and promotes the degradation of ataxin-1 (Hong et al., 2008).

The UBE2E3 overexpression did not induce the formation of TDP-43 positive aggregates under physiological conditions. In addition, the aggregate formation of EGFP-tagged TDP-43 FL and CTF induced by proteasomal inhibition was not further enhanced by UBE2E3 overexpression (unpublished data). It is possible that UBE2E3 induces the formation of microaggregates that are not detectable with immunofluorescence. A longer observation time could allow the formation and, hence, detection of these aggregates as they are growing. It was supposed that visible macroaggregates might be sinks for the real toxic species of accumulating neurodegenerative disease associated proteins (Caughey and Lansbury, 2003; Haass and Selkoe, 2007). These are predominantly lower-order oligomers with greater mobility and surface area. Hence, they possess an enhanced potential for aberrant interactions. This could mean that ubiquitinylated TDP-43 species might be toxic. This interesting assumption needs to be further investigated.

TDP-43 is monoubiquitinylated in the presence of UBE2E3 (see Figure 3.19). However, high background of polyubiquitinylated proteins was detected in this experiment. When 6xHis-ubiquitin was used in pulldowns, a 6xHis-ubiquitin higher molecular weight smear was only observed when TDP-43 was co-expressed with UBE2E3 or upon proteasomal inhibition. This demonstrates the specificity of the pulldown assay for 6xHis-ubiquitin-conjugated proteins.

The type of ubiquitin linkage can give a hint on the function of the ubiquitinylation of TDP-43. A K48-linked polyubiquitinylation was detected on TDP-43, indicating a signal for proteasomal degradation (Urushitani et al., 2010). The three UBE2E enzymes

were shown to mediate K11- and K48-linked polyubiquitinylations indicating proteasomal degradation, as well as K63-linked polyubiquitinylation, which reflects the autophagic degradation pathway (David et al., 2010). It is not known which of the 20 lysine residues of TDP-43 can be ubiquitinylated. Four potential ubiquitinylation sites were identified in RRM1 (K102, K114, K145 and K161) of a 33.5kDa N-terminal splicing variant of TDP-43, comprised of amino acids 1-277 (Dammer et al., 2012). Thus, these lysine residues cannot be the ubiquitinylation sites of the highly ubiquitinylated CTF$_{193\text{-}414}$ used in this study, which contains four lysine residues. Mutagenesis of these four lysine residues would further provide evidence of CTF ubiquitinylation.

We observed low amounts of insoluble, ubiquitinylated TDP-43 compared to the total levels. In addition, the insoluble TDP-43 species are considered to be non-functional and are only slightly increased upon overexpression of UBE2E enzymes and proteasomal inhibition for 6h. Thus, the ubiquitinylation of TDP-43 and therefore depletion of minimal amounts of active TDP-43 species did not alter levels of HDAC6 and SKAR splicing (see Figure 3.36). Splicing alterations are usually just observed when TDP-43 is strongly downregulated. Nonetheless, the accumulation of ubiquitinylated TDP-43 in aging human patients could deplete enough active TDP-43 with the resulting effects becoming noticeable after a long period of time.

4.5   Deubiquitinylation of TDP-43 by UBPY

In this work we show that the ubiquitin isopeptidase UBPY binds TDP-43 and deubiquitinylates overexpressed TDP-43 wt, nuclear import impaired TDP-43 NLSmut, and a CTF which was stabilized with a mCherry tag. The two catalytically inactive UBPY variants C786S and ΔC did not decrease ubiquitinylation of TDP-43 (see Figure 3.25), instead these variants occasionally showed a dominant-negative effect resulting in increased TDP-43 ubiquitinylation (see Figure 3.25C). This is in agreement with a previous report (Alwan and van Leeuwen, 2007). Moreover, our *in vivo* data obtained from a neurotoxicity fly model overexpressing human TDP-43 in the eye strengthen the role of UBPY as a DUB for TDP-43. UBPY silencing increased the TDP-43 induced neurodegenerative phenotype, and enhanced insolubility and a higher molecular weight smear of TDP-43 (see Figure 3.34 and Figure 3.35).

The knockdown of UBPY in HEK293E cells was not sufficient for appropriate investigations of TDP-43 ubiquitinylation without affecting the cell viability, neither by transient transfection with siRNA nor in a lentiviral approach (sees Figure 3.26). UBPY is a growth regulated protein, which accumulates upon growth stimulation in human fibroblasts, but is decreased when the cells undergo growth arrest by contact inhibition (Naviglio et al., 1998). Additionally, silencing of UBPY enhances the degradation

of the EGFR, inducing a proliferation stop (Berlin et al., 2010b; Cai et al., 2010; Mizuno et al., 2005; Niendorf et al., 2007). Moreover, the knockout of UBPY in mice is embryonic lethal due to the growth arrest (Niendorf et al., 2007). This gives a possible explanation for the toxicity of the silencing of UBPY that we attempted. We generated stably silenced HEK293E cells, in which UBPY was strongly downregulated. However, after a few passages UBPY knockdown efficiency was almost not detectable. The strongly silenced cells probably grew much slower than weakly silenced cells, resulting in low silencing efficiency after passaging the cells a few times. Therefore, the generation of stably silenced cells from single clones could yield a cell line with robust downregulation of UBPY, but probably slow growth. Another possibility to decrease DUB activity of UBPY is the application of a specific inhibitor or increasing phosphorylation of S680, which was shown to reduce UBPY DUB activity through enhanced 14-3-3 binding (Ballif et al., 2006; Mizuno et al., 2007). However, specific kinases for S680 phosphorylation or inhibitors of UBPY DUB activity were not reported so far.

At the moment it is still not clear whether ubiquitinylated TDP-43 aggregates are pathogenic or neuroprotective. Neuroprotective aggregates might serve as a sink for probably more toxic TDP-43 lower order oligomeric species. Inhibition of UBPY DUB activity might facilitate the formation of the protective aggregates. In the case of pathogenic TDP-43 aggregation the deubiquitinylation of TDP-43 could either protect from the formation of insoluble pathogenic aggregates or even dissolve them, also resulting in increased level of active TDP-43. One hint supporting this view comes from a report which showed that inclusions of ubiquitinylated CTF are reversible and can be cleared by the proteasome (Zhang et al., 2010). It would be interesting to know if UBPY may facilitate this deubiquitinylation and clearance.

UBPY is highly expressed in neurons of the brain (Bruzzone et al., 2008; Gnesutta et al., 2001), and increased level and aggregates of UBPY are also associated with an artificial neurodegenerative mouse model, the Wobbler mouse (Paiardi et al., 2014). Thus, UBPY level or localization might also be altered in *post mortem* brain or spinal cord tissue with TDP-43 pathology. A decrease of UBPY might contribute to an enhanced formation of ubiquitin-positive inclusions. Therefore it would be interesting to study the expression and localization of UBPY in ALS and FTLD affected *post mortem* brain and spinal cord tissue. We have initially performed histopathological stainings for UBPY of brain tissue in collaboration with M. Neumann at the Neuropathology, University Clinics Tübingen. Unfortunately, the available antibodies did not work properly in immunohistochemistry. Thus further antibodies need to be tested.

TDP-43 accumulates in the cytoplasm of cells depleted of ESCRT-I and ESCRT-III (Filimonenko et al., 2007). Thus, there might be a faint link between the ESCRT-

associated UBPY and TDP-43 in FTLD. Interestingly, UBPY interacts with several CHMP proteins of the ESCRT-III complex, among them also CHMP2B (Row et al., 2007). Mutations in CHMP2B are associated with autosomal dominant FTLD-UPS, connecting aberrant endosomal sorting with this disease (Skibinski et al., 2005). However, inclusions in FTLD-UPS were TDP-43 negative, but ubiquitin positive (Holm et al., 2007; Liscic et al., 2008).

Ubiquitinylated TDP-43 is an interesting new substrate of UBPY. However, it remains unclear where the interaction takes place. We showed by a stronger coimmunopre-cipitation of UBPY with TDP-43 NLSmut or cytoplasmic CTF than with TDP-43 wt that a cytoplasmic interaction is most likely (see Figure 3.11). Immunofluorescence stain-ing suggests an interaction in cytoplasmic vesicles or granules, but not stress gran-ules, because UBPY did not colocalize with the stress granule marker eIF3 (see Figure 3.24E). Since UBPY is found to interact with the ESCRT machinery the interaction with TDP-43 may take place at endosomes. However, an association of TDP-43 with endosomes was not described so far and UBPY did not colocalize with early en-dosomes. The interaction site has to be further narrowed. Staining of UPBY and other RNA granule markers could reveal the place of interaction. Noteworthy, we observed a previously unknown localization of endogenous UBPY in HEK293E cells at the Golgi network. Both proteins also interact with the 14-3-3 protein that might serve as a scaffold for the interaction (Ballif et al., 2006; Volkening et al., 2009)

UBPY was suggested to be a rather general DUB, as depletion of UBPY results in increased overall ubiquitinylation (Naviglio et al., 1998). A similar effect was observed in our fly model upon UBPY silencing (see Figure 3.35), whereas overespression of UBPY in 6xHis-ubiquitin pulldown experiments decreased the amount of polyubiquitinylated proteins (see Figure 3.25). However, a large amount of ubiquitinylated proteins in mCherry-CTF overexpressing cells seems to consist of ubiquitinylated CTF (see Figure 3.25A). Thus, the deubiquitinylation of mCherry-CTF should also be visible in an overall decrease of polyubiquitinylated proteins. Moreover, UBPY overexpression slightly decreased the ubiquitinylation of ataxin-3 with a short or long polyglutamine tract (see Figure 3.33). Interestingly, the *C. elegans* ortholog of UBPY was detected in a screen for suppressors of polyglutamine-protein aggregation (Nollen et al., 2004). This might indicate that this DUB can deubiquitinylate aggregation-prone proteins in general, making UBPY a promising target for many diseases with ubiquitinylated and aggregating proteins.

UBPY is a possible and interesting new therapeutic target for the treatment of ALS and FTLD patients. It could be a potential neuroprotective DUB, which might decrease level of accumulated and ubiquitinylated TDP-43 and increase level of free, functional TDP-43. It is noteworthy here, that USP10 is another DUB that might interact with

TDP-43 (Freibaum et al., 2010). Furthermore, USP21 was previously identified as an enhancer of TDP-43 toxicity in a yeast screen (Kim et al., 2014). However, a possible neuroprotective role of UBPY in TDP-43 proteinopathies remains to be shown.

4.6   Ubiquitinylation of pathogenic TDP-43 mutants

Several missense mutations in TDP-43 are linked to TDP-43 proteinopathies, most of them to ALS. A cytoplasmic mislocalization and an elevated half-life are characteristic for most of the mutants. The pathogenic mutants exhibit increased aggregation and toxicity, and accumulate upon proteasomal inhibition (Kabashi et al., 2008; Rutherford et al., 2008). The exact mechanisms how the mutations contribute to disease development are poorly understood. Therefore, we asked if the ubiquitinylation of pathogenic TDP-43 mutants is altered by UBE2E3, UBPY or by the inhibition of the UPS. We found that most of the 15 investigated mutants were ubiquitinylated like TDP-43 wt after UBE2E3 overexpression or MG-132 treatment (see Figure 3.30 and Figure 3.31) within our investigated time frame in transiently transfected HEK293E cells. Additionally, all of them predominantly localized diffusely to the nucleus like TDP-43 wt (see Figure 3.29). This is in agreement with two reports (Voigt et al., 2010; Zhou et al., 2010), while others demonstrated aggregate formation upon overexpression of pathogenic mutants (Arai et al., 2010; Guo et al., 2011; Johnson et al., 2009; Kabashi et al., 2010; Nonaka et al., 2009b; Sreedharan et al., 2008).

Remarkably, in our system the highly conserved K263E mutant was heavily ubiquitinylated, even in the absence of proteasomal inhibition or UBE2E3 overexpression. The ubiquitinylation of this mutant was altered similar to TDP-43 wt by MG-132 treatment, UBE2E3 overexpression and silencing, and UBPY overexpression, though the effects were much more prominent (see Figure 3.32). Ubiquitinylation is often a signal for degradation, but the increased protein level of K263E points to an enhanced stability, which is in agreement with an elevated half-life (Austin et al., 2014). Despite this strong ubiquitinylation, K263E did not form aggregates in HEK293E cells under normal conditions within 96h of transient overexpression. It would be of interest whether the strong increase of K263E ubiquitinylation upon proteasomal inhibition induces aggregate formation. However, it was demonstrated that K263E is resistant to aggregation *in vitro* (Austin et al., 2014).

The K263E mutation is not located in the GRD domain like most pathogenic mutations, but in the linker region of RRM2 and GRD. The lysine 263 of TDP-43 is part of a nucleic acid binding site and intercalates with bound RNA (Lukavsky et al., 2013). Therefore, an exchange of this amino acid might alter RNA binding properties and even RNA related functions of TDP-43. Since the GRD domain mediates protein-

protein interactions, the nearby K263E mutation may alter or even disrupt TDP-43 binding to different physiological complexes, consequently affecting proper TDP-43 function. We showed in coimmunoprecipitation that it is difficult to compare the binding strength of UBE2E3 and UBPY with TDP-43 wt against K263E, because the mutant is more stable (see Figure 3.32D). However, this mutation might exhibit a different, yet to be identified pathogenic function.

What might be the reason for the heavy ubiquitin modification of K263E? It is possible that the conformation of TDP-43 K263E is altered, so that other lysine residues are exposed. It may be that the cell recognizes K263E as misfolded protein, which is subsequently ubiquitinylated with the intent of clearance. However, the K263E mutation in a partial mouse TDP-43 variant comprised of amino acids 101-265 does not cause conformational changes (Austin et al., 2014). Anyway, this might not be true for the full-length human K263E TDP-43.

The other noticeable mutant regarding ubiquitinylation is D169G, which is like K263E not located in the C-terminus, but in RRM1. D169G seemed to be less stable than TDP-43 wt and the other mutants in some experiments, which is in contrast to a reported elevated half-life (Austin et al., 2014). Moreover, D169G was much less ubiquitinylated upon proteasomal inhibition or UBE2E3 overexpression, consistent with a previous report (Kim et al., 2009). This report also shows that D169G does not bind the ubiquilin-1 UBA domain as strong as TDP-43 wt, possibly due to the reduced ubiquitinylation.

4.7   A model of UBE2E3 and UBPY dependent TDP-43 ubiquitinylation

The data of this study can be summarized in a model of TDP-43 ubiquitinylation (Figure 4.1). We find that TDP-43 is ubiquitinylated upon inhibition of proteasomal degradation. Moreover, UBE2E ubiquitin-conjugating enzymes ubiquitinylate TDP-43 in an unknown E3 ligase dependent or independent manner, that leads to an accumulation and solubility shift instead of degradation of TDP-43. Finally, TDP-43 can be deubiquitinylated by UBPY.

The alterations of localization, ubiquitinylation, solubility, fragmentation, aggregation and proteolytic breakdown might all account for the neurotoxicity of TDP-43. The proteasome seems to be important for the degradation of accumulating proteins in ALS and FTLD in general (Ling et al., 2013). Moreover, proteasomal dysfunction has been implicated in several other neurodegenerative diseases like Alzheimer's or Huntington's disease (Schipper-Krom et al., 2012; Tai and Schuman, 2008; Tanaka and Matsuda, 2014). The underlying mechanisms for neurodegeneration in general and specifically for TDP-43 are still not very well understood and require further in-
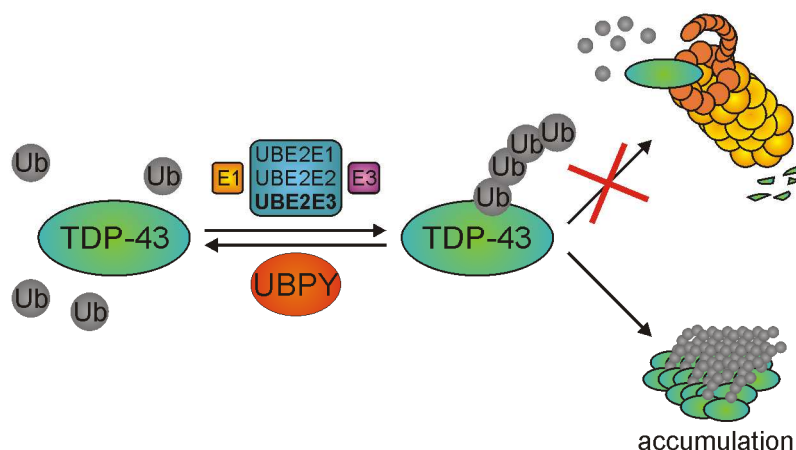
Figure 4.1 A model of the regulation of TDP-43 ubiquitinylation by UBE2E ubiquitin-conjugating enzymes and the ubiquitin isopeptidase UBPY.

vestigations. One possibility is that insoluble, ubiquitinylated TDP-43 might form neurotoxic aggregates over a longer period of time, and maybe UBPY is a potential suppressor of TDP-43 neurotoxicity.

4.8 Potential functional implications of the novel TDP-43 interactors

Several RNA-associated proteins were also found in the Y2H screens for TDP-43 interactors. Interestingly, TDP-43, RBM45, LSM6, EXOSC10 and RACK1, as well as FUS, were found in mRNA interactomes from HeLa or HEK293 cells (Baltz et al., 2012; Castello et al., 2012). Thus, the interactions of TDP-43 with EXOSC10, LSM6, MED6 and RBM45 further strengthen the role of TDP-43 in the RNA metabolism. What might be the functional consequence of TDP-43 interactions with these proteins?

EXOSC10 is a protein component of the nuclear exosome complex that degrades various types of RNA (Allmang et al., 1999). The already known interaction with EXOSC10 from a study on human mRNA degradation implicates a role of TDP-43 in the degradation of various types of RNA (Lehner and Sanderson, 2004). Indeed, the autoregulation of TDP-43 seems to involve an exosome mediated pathway of mRNA degradation, as blocking of this complex partially recovers TDP-43 levels (Ayala et al., 2011b). The binding of TDP-43 to LSM6 suggest an association of TDP-43 with Lsm complexes that are involved in the degradation of mRNA in the cytoplasm or pre-mRNA splicing and decay in the nucleus (Tharun, 2009). Thus, the function of TDP-43 in splicing of various pre-mRNAs might be dependent on the nuclear Lsm complex.

MED6 is part of the head molecule of the nuclear Mediator complex, which regulates the transcription of RNA polymerase II dependent genes at nearly all stages of transcription (Carlsten et al., 2013). TDP-43 was also shown to interact with further subunits of the Mediator complex, more precisely MED10, MED19 and MED29 (Sato et al.,

2004). The interaction with MED6 as well as with the other subunits points to an association of TDP-43 with the Mediator complex for its transcription regulation functions. It would be interesting to investigate whether TDP-43 can alter the transcription of distinct genes via its interaction with MED6 or other Mediator complex subunits or if this affects the general transcription of genes.

RBM45 colocalized with ubiquitin and TDP-43 in pathological inclusions in most ALS and all FTLD-TDP human patients tested, with the most abundant pathology in patients with C9ORF72 expansions (Collins et al., 2012). However, we are the first demonstrating a direct interaction of the two proteins. Moreover, silencing of the RBM45 ortholog in *Drosophila* increased the TDP-43 phenotype in the neurotoxicity fly model (data not shown, observation by Dr. S. Jäckel). It is of interest whether this interaction is RNA dependent as both are RNA binding proteins. The role of this interactions is speculative, because the particular functions of RBM45 remain unknown. This RRM-type RNA-binding protein is developmentally regulated in the nervous system and contains structural similarities to TDP-43 and FUS (Collins et al., 2012; Tamada et al., 2002).

The lysosomal integral membrane protein GPR137B is highly expressed in brain, heart, liver and kidney (Gao et al., 2012), and its mRNA is differentially regulated upon TDP-43 silencing in HEK293E and HeLa cells (Ayala et al., 2008a; Fiesel et al., 2010).

An interaction of TDP-43 with the multifunctional protein RACK1 was identified in a global proteomic approach (Freibaum et al., 2010), and the two proteins associated in a global protein interaction map of *Drosophila* (Giot et al., 2003). Furthermore, RACK1 was found in a coaggregation proteome of TDP-43, together with several other RNA binding proteins that are part of stress granules and participate in translational control (Dammer et al., 2012). RACK1 interacts with a wide variety of proteins and plays a significant role in shuttling proteins around the cell, anchoring proteins at particular locations and in stabilising protein activity (reviewed in Adams et al., 2011; Gandin et al., 2013). More particularly, RACK1 is a component of the 40S ribosome near the mRNA exit and recruits activated protein kinase C (PKC) to the ribosome, leading to a stimulation of translation (Sengupta et al., 2004). In response to stress, RACK1 - like TDP-43 - is sequestered into stress granules and inhibits apoptosis by suppressing a stress-responsive MAPK pathway (Anderson and Kedersha, 2006; Arimoto et al., 2008). Furthermore, RACK1 is involved in neurite outgrowth (Dwane et al., 2014). Recently, RACK1 was associated with miRNA-dependent repression of translation in *C. elegans* and humans through the interaction with the miRISC complex (Jannot et al., 2011). RACK1 also promotes the docking of ribosomes via the association with membrane-bound receptors at sites where local protein synthesis is

required (Nilsson et al., 2004). Though a role of TDP-43 in the regulation of local translation is less well established, RACK1 could act as an adaptor for TDP-43 or TDP-43 associated RNA granules to distinct subcellular foci. Thus, like TDP-43, RACK1 is also associated with stress granule formation, neurite outgrowth, regulation of translation, and miRNA biosynthesis. Therefore, at certain points of these processes the interaction of TDP-43 and RACK1 might play a functional role. It is quite challenging to identify the function of this interaction due to the various possibilities where these could take place.

RACK1 was also shown to promote the ubiquitinylation and proteasome mediated degradation of the C-type lectin domain family 1 member B and hypoxia-inducible factor 1-α (Liu et al., 2007; Ruan et al., 2009). Moreover, RACK1 was suggested to form a bridge between Bim proteins and the ElonginB/C-Cullin2-CIS E3 ligase complex, thus promoting the polyubiquitinylation and proteasomal degradation of Bim (Zhang et al., 2008). Therefore, a possible RACK1 dependent function in the context of TDP-43 ubiquitinylation needs to be further investigated.

The functional validation of the interaction of TDP-43 with many of the novel interactors can yield important information about the function and regulation of TDP-43. Thus, further investigations are required (see below). These might help us to understand the important role of TDP-43 in neurodegenerative diseases.

4.9   Outlook

Emerging evidence suggests that the alterations in protein homeostasis and RNA metabolism are two major contributions to the development of ALS, FTLD and FLTD-MND. We have identified several interactors of TDP-43 that could contribute to TDP-43 pathogenesis related to one or both of these areas. UBPY and UBE2E ubiquitin-conjugating enzymes were validated in this study to regulate the ubiquitinylation of TDP-43. However, there are open questions regarding the ubiquitinylation of TDP-43.

The possibly linking E3 ubiquitin ligase for the UBE2E3 mediated TDP-43 ubiquitinylation has to be identified. In a preliminary experiment in HeLa cells we could not confirm that parkin is an E3 ligase for TDP-43. Nevertheless, this experiment has to be optimized and repeated. Unexpectedly, we did not observe a robust TDP-43 ubiquitinylation in HeLa cells after MG-132 treatment. Additionally, the UBE2E dependent ubiquitinylation of TDP-43 in parkin silenced HEK293E cells could be investigated. Further TDP-43 and UBE2E3 binding E3 ligases could be identified with mass spectrometry from a TDP-43 and/or UBE2E3 coimmunoprecipitated proteome. Thus, further TDP-43 interacting E2 and E3 proteins may be identified. However, it should also be investigated whether UBE2Es can ubiquitinylate TDP-43 in an E3 independent

manner with *in vitro* ubiquitinylation assays. In this setup a role for parkin in TDP-43 ubiquitinylation together with recombinant UBE2Es can also be tested. UBE2N and UBE2C could serve as negative control, because they do not promote ubiquitinylation of TDP-43 in the HEK293E cell model. Subsequently, *in vitro* ubiquitinylated TDP-43 could be used as a substrate for recombinant UBPY to further confirm its deubiquitinylation activity on TDP-43. Additionally, the already strongly ubiquitinylated TDP-43 mutant K263E, can be overexpressed and immunoprecipitated from HEK293E cells, followed by *in vitro* deubiquitinylation with recombinant UBPY. A possible role of RACK1 in TDP-43 ubiquitinylation events could be investigated with RACK1 overexpression and silencing approaches, respectively. Here, RACK1 might be a bridging protein for the substrate TDP-43 with a cullin E3 ligase complex.

The quality of TDP-43 ubiquitinylation is of interest. We showed that TDP-43 is monoubiquitinylated, and higher molecular smears were observed among 6xHis-ubiquitin-conjugated proteins. To identify whether this higher molecular weight smear is polyubiquitinylated or multi-monoubiquitinylated TDP-43, specific antibodies which recognize mono- and polyubiquitin chains may be utilized. Furthermore, the type of ubiquitin chain linkage on TDP-43 can be identified in cell culture with linkage-specific antibodies for K48- and K63-linked polyubiquitin. The overexpression of various linkage-restricted 6xHis-ubiquitin constructs in the TDP-43 ubiquitinylation pulldown assay, such as K11, K11R, K48, K48R, K63 or K63R may identify ubiquitin linkages on TDP-43 *in vitro* ubiquitinylated TDP-43 wt, but also K263E could be subjected to mass spectrometry analysis for the identification of the type(s) of ubiquitin-linkage as well as the lysine residues that are conjugated with ubiquitin. The location of these lysine residues could give a hint on functions that might be altered upon ubiquitinylation of TDP-43, such as nuclear-cytoplasmic shuttling, RNA binding, as well as dimerization, conformational changes and aggregation (see also Figure 2.3).

The regulation and the effects of TDP-43 ubiquitinylation can be studied more thoroughly in the TDP-43 neurotoxicity fly model. A positive aspect of the fly model is that aggregate formation might be observed due to the longer expression of TDP-43-GFP in various tissues or cells. Thus, effects of UBPY silencing or overexpression in neurons, or more specifically in motor-neurons on TDP-43 aggregation may be determined. Moreover, this would also allow the investigation of movement, behaviour and longevity upon UBPY silencing in TDP-43-GFP expressing larvae and adult flies. The establishment of a TDP-43 K263E mutant fly disease model would provide *in vivo* insights whether this pathogenic mutant impairs TDP-43 functions in the fly. It was shown that pathogenic mutants impair axonal trafficking of TDP-43 granules in motor neurons derived from ALS patients with TDP-43 mutations and in *Drosophila* motor

neurons (Alami et al., 2014). Additionally, the effect of parkin knockdown or overexpression on the TDP-43 UBPY knockdown phenotype could be investigated. Our collaborator A. Voigt, RWTH Aachen identified more modifiers of the TDP-43 phenotype in fly. These could be further validated in fly and cell culture.

Protein homeostasis is likely disrupted in ALS and FTLD. Therefore, it may be promising to identify targets that prevent, slow down or even reverse the accumulation and aggregation of TDP-43 in TDP-43 proteinopathies. Thus, the analysis of the expression and localization of UBPY, UBE2Es and ubiquitin in *post mortem* brain and spinal cord samples from ALS and FTLD-TDP patients may provide new insights in TDP-43 pathology. However, first the nature of the TDP-43 toxic functions has to be determined: What is the toxic function of TDP-43 in neurons and glia cells? Are the inclusions the toxic species or rather a neuroprotective sink for the potential toxic oligomers? Are the observed inclusions only a mere by-product and the loss-of functional nuclear TDP-43 is the cause for neurodegeneration? If TDP-43 inclusions protect from harmful oligomers, then inhibition of UBPY deubiquitinylation activity would be in favour. On the other hand, if ubiquitinylated and aggregated TDP-43 is toxic an increase in UBPY function and inhibition of UBE2Es would be beneficial and increase the amount of soluble, functional TDP-43. In the end, these investigations on the ubiquitinylation and aggregation of TDP-43 may help to understand the regulation of the TDP-43 ubiquitinylation and its possible contribution to neurodegeneration.

The disruption of RNA homeostasis is also likely contributing to ALS and FTLD pathology. ALS- and FTLD-linked mutations were detected in the RNA-binding proteins TDP-43, FUS, EWSR1, TAF15, ataxin-2, hnRNPA1, and hnRNPA2/B1 and some of these proteins are also found in pathological inclusions (see Table 2.1). Thus, the role of TDP-43 in RNA metabolism and gene expression needs further investigation. We know thousands of RNAs that are bound and a part of them spliced by TDP-43, but for most of them we do not know the functional aspect of the interaction. We identified several RNA binding proteins in the Y2H screens, some of them linking TDP-43 to certain RNA processing complexes. Thus, the analysis of these interactions and especially of pathogenic mutants may shed some light on TDP-43 RNA functions and pathogenesis. As for UBPY and UBE2E enzymes, the staining of RBM45, RACK1, LSM6, MED6 and EXOSC10 in *post mortem* neuronal tissue is an option to determine whether levels of these proteins are altered and thus might contribute to ALS and FTLD pathogenesis.

The interaction with LSM6 associates TDP-43 either with nuclear pre-mRNA splicing and decay or with cytoplasmic mRNA degradation via the distinct Lsm complexes. Thus, the localization of the LSM6-TDP-43 interaction should be detected. If TDP-43

associates with the nuclear Lsm complex, a possible role of this complex in TDP-43 mediated alternative splicing of known targets such as CTFR or SKAR could be investigated. A cytoplasmic interaction may point towards an involvement of TDP-43 in mRNA decay or cytoplasmic splicing. Here, the stabilization of HDAC6 mRNA by TDP-43 might be dependent on the interaction of TDP-43 with LSM6.

TDP-43 and FUS are components of stress granules. The main function of stress granules is the temporal repression of translation and storage of mRNAs during stress. When the stress is removed stress granules are dissolved (Anderson and Kedersha, 2009). It was suggested that upon chronic stress, TDP-43 or FUS positive stress granules serve as the core of irreversible pathological inclusions (Dewey et al., 2012; Dormann et al., 2010; Li et al., 2013; Wolozin, 2012). If stress granules are indeed the origin of insoluble protein inclusions, pharmacological treatment which dissolves stress granules before they become insoluble aggregates may be beneficial for TDP-43 proteinopathies. Therefore, the composition and dynamics of TDP-43 or FUS positive stress granules have to be better investigated.

RBM45 was found in TDP-43 positive inclusions (Collins et al., 2012). However, the functions of RBM45 are unknown. Thus it would be interesting to know if RBM45 or RACK1, that was also associated with stress granules, integrate with TDP-43 into stress granules upon cellular stress, like arsenide, heat shock or H_2O_2 treatment. Moreover, it could be investigated whether TDP-43 incorporation into stress granules might be dependent on RACK1 or RBM45 by knockdown or silencing of these proteins. Eventually, the so far unknown function(s) of RBM45 have to be characterized to shed light on the interaction of TDP-43 with RBM45.

The ultimate goal in studying TDP-43 functions, regulations and toxicity is to identify therapeutic targets for the treatment of ALS and FTLD-TDP. However, therefore it is important to know when pathological alterations occur. This has not been studied for TDP-43 proteinopathies so far. In case of Alzheimer's or Parkinson's disease, neurodegeneration starts long before the first symptoms appear. Thus, presymptomatic diagnoses likely have to be established for ALS and FTLD, so that a possible causative treatment can begin before the onset of symptoms. Screens may identify markers of ALS and FTLD-TDP that could be used for diagnosis. However, a challenge is to distinguish whether alterations in TDP-43 will cause FTLD-TDP or ALS, as these two diseases might need distinct treatments.

5   Material and Methods

5.1   Material

All chemicals (analytical grade) were purchased from Applichem, Calbiochem, Fluka, Merck, Roth or Sigma, unless otherwise indicated in Table 5.1.

Table 5.1 Chemicals and reagents

Chemical	Supplier
40% Acrylamide/ Bis-Acrylamid solution 19:1	Bio-Rad
Adenine hemisulfate	Sigma
Adenosine-triphosphate (ATP)	Sigma
Agar (for bacterial LB plates)	Fluka Analytical
Agarose	Biozyme Scientific
Ammonium persulfate (APS)	Sigma
Ampicilin (sodium salt)	Sigma
Arsenite	Sigma
Aureobasidin A (AbA)	Clontech
β-mercaptoethanol	Roth
Bacto agar (for yeast medium plates)	Becton Dickinson
Bacto peptone	Becton Dickinson
Bafilomycin A1 (Baf)	Sigma
BigDye Terminator v3.1	Applied Biosystems
Bovine Serum Albumin (BSA)	Roth
Brompenol blue (sodium salt)	Merck
Collagen	Cohesion
Complete protease inhibitor (also EDTA-free)	Roche
Dimethyl sulfoxide (DMSO)	Sigma
1,4-Dithiothreitol (DTT)	Roth
Drop-out mix (Complete supplement mixture)	Formedium
Dulbecco's modified Eagle Medium (DMEM) high glucose	Biochrom
DMEM/HAM's F12	Fermentas
DNA ladder (1kb)	Fermentas
dNTPs	Fermentas
Ethidium bromide solution (1% in water)	Merck
EZview™ Red anti-Flag/-HA/-myc affinity Gel	Sigma
Fetal calf serum (FCS)	PAA Laboratories
FCS (tetracycline free)	PAA Laboratories
Fluorescent mounting medium	Dako
FuGene6	Roche
Herrings sperm carrier DNA	Clontech
Hexadimethrine bromide	Sigma
HiPerFect	Qiagen
Hoechst 33342	Invitrogen
Imidazol	Merck
Immobiolon Western HRP substrate	Millipore
Kanamycinsulfate	Sigma
Lithium acetate dehydrate (LiOAc)	Sigma
Mate & Plate™ Library (human adult brain cDNA library)	Clontech
3-methyladenine (3-MA)	Sigma
MG-132	Sigma
N,N,N',N'-Tetramethylethylendiamine (TEMED)	Merck
nickel-nitrilotriacetic acid (Ni-NTA) agarose	Qiagen
Non-fat dried milk powder	Sucofin

Chemical	Supplier
Nonident P-40 (NP-40)	United States Biological
Normal goat serum	Sigma
Normal horse serum	Invitrogen
NuPAGE MOPS SDS Running Buffer 20x	Invitrogen
OptiMEM	Invitrogen
PenicillinG/Streptomycin sulphate 100x (Pen/Strep)	Biochrom
Poly-D-lysine (PDL)	Sigma
Precision Plus Protein Standard, prestained	Bio-Rad
Polyethylene glycol (PEG)	Sigma
Puromycin	InvivoGen
Roti®-phenol/chloroform/isoamyle alcohol (25:24:1)	Roth
Sodium azide (NaN_3)	Sigma
Sodium dodecyl sulphate (SDS)	Sigma
Sodium pyrophosphate (NaPPi)	Sigma
Triton-X-100	AppliChem
Trypsin-EDTA (10x)	Invitrogen
Tryptone/peptone	Roth
Tween-20	Merck
Western Blocking Reagent	Roche
X-tremeGENE 9	Roche
Yeast extract	AppliChem
Yeast nitrogen base	Formedium

Table 5.2 Devices

Device	Manufacturer
Agarose gel chamber	Peqlab
AxioImager microscope with ApoTome Imaging System	Zeiss
Blotting chambers, wet (Mini Trans-Blot® Cell, Trans-Blot® Cell)	Bio-Rad
Blotting chambers, semi-dry (PerfectBlue Semi-Dry electroblotter)	Peqlab
Burker chamber	Hecht-Assistent
Developer	Fujifilm
Electroporation cuvettes & device (MicroPulser)	Bio-Rad
Gel documentation system	Vilber Lourmat
Microtiter plate reader	Bio-Rad
Nanodrop (ND1000)	Peqlab
Scanner (Epson Perfection V700 Photo)	Epson
SDS-PAGE gel chamber (PerfectBlue Twin S)	Peqlab
Sequencer (ABI 3100 Genetic Analyzer)	Applied Biosystems
Spectrophotometer (Ultrospec 2100 Pro)	Leica
Thermocycler	Applied Biosystems

Table 5.3 Kits and enzymes

Material	Supplier
Bicinchoninic acid (BCA) Protein Assay kit	Pierce Protein
Bradford Protein Assay kit	Bio-Rad
Ex Taq DNA Polymerase kit	Takara
GoTaq DNA Polymerase kit	Promega
QIAGEN Plasmid Midi/Maxi kit	Qiagen
QIAprep Spin MiniPrep kit	Qiagen
QIAquick Gel Extraction kit	Qiagen
Restriction enzymes and 10x buffers	Fermentas
RNase A	Sigma
RNeasy Mini kit	Qiagen
Shrimp alkaline phosphatise (SAP)	Fermentas
T4 DNA ligase kit	Fermentas
Transcriptor High fidelity cDNA Synthesis kit	Roche

Table 5.4 Consumables

Consumables	Supplier
Amersham Hyperfilm™ ECL High Performance	GE Healthcare
4-12% Bis-Tris NuPAGE Mini/Midi gradient gels	Invitrogen
Coverslips	Roth
Glass beads, acid washed	Sigma
Hybond-P polyvinylidene diflouride (PVDF) membrane	Millipore
Microscope slides	Langenbrinck
Nitrocellulose membrane	GE Healthcare
Whatman paper	Schleicher und Scheull

Table 5.5 Buffer and solutions Chemicals were dissolved in double distilled H_2O (ddH_2O) and autoclaved when necessary.

Buffer/ solution	Chemical composition
Antibody solution, primary	5% (v/v) Western Blocking Reagent, 0.02% NaN_3 in TBST
Antibody solution, secondary and HRP-coupled	5% (w/v) non-fat milk powder in TBST
Blocking solution for western blot	5% (w/v) non-fat milk powder in TBST
CoIP buffer	50mM HEPES pH 7.6; 10mM KCl; 50mM NaCl; 1mM EDTA; 0.5mM EGTA; 1.5mM $MgCl_2$; 10mM NaPPi, 10% glycerol; 0,2% NP-40
HU buffer	200mM Tris pH 6.8; 8M urea; 1mM EDTA; 5% SDS; bromphenole blue; 15mM DTT added fresh
LB medium	1% (w/v) tryptone; 0.5% (w/v) yeast extract; 0.5% (w/v) NaCl
LB medium plates	LB medium with 1.2% (w/v) agar
LB medium plates with antibiotics	LB medium with 1.2% (w/v) agar and 100µg/ml ampicilin or 25µg/ml kanamycin
LiOAc/TE	100mM LiOAc; 10mM Tris pH 7.4 in H_2O
LiOAc/PEG	40% (w/v) PEG; 100mM LiOAc; 10mM Tris pH 7.4 in H_2O
NP-40 buffer	50mM NaH_2PO_4 pH 8.0; 300mM NaCl; 1% NP-40
NuPAGE transfer buffer	25mM Bicine; 25mM BisTris; 1mM EDTA
Phosphate buffered saline (PBS)	2.2mM KH_2PO_4 pH 7.4; 7.8mM Na_2HPO_4; 150mM NaCl
RIPA buffer	50mM Tris/HCl pH 8.0; 150mM NaCl; 1% NP-40; 0.5% deoxycholate; 0.1% SDS; 10mM NaPPi
SDS-PAGE running buffer	25mM Tris, 192mM glycine
SDS-PAGE separating gel buffer	1.5M Tris pH 8.8; 0.4% (w/v) SDS
SDS-PAGE stacking gel buffer	0.5M Tris pH 6.8; 0.4% (w/v) SDS
6x SDS-PAGE sample buffer (Laemmli buffer)	325 mM Tris pH 6.8; 9% (w/v) SDS; 50% glycerol; 9% ß-mercaptoethanol; 0.03% (w/v) bromophenol blue
Stripping solution for western blot	62.5mM Tris pH 7.6; 2% (w/v) SDS; 100mM β-mercaptoethanol
Tris borate buffer (TBE)	45mM Tris pH, 45mM boric acid, 1mM EDTA
Transfer buffer	25mM Tris, 192mM glycine
Tris buffered saline (TBS)	50mM Tris pH 7.4; 150mM NaCl
TBST	50mM Tris pH 7.4; 150mM NaCl, 0.1% (v/v) Tween-20
8M urea buffer	10mM Tris pH 8.0; 100mM NaH_2PO_4; 8M urea
8M urea wash buffer	10mM Tris pH 6.3; 100mM NaH_2PO_4; 8M urea
Yeast lysis buffer	10mM Tris pH 8.0; 100mM NaCl, 1mM EDTA, 1% (w/v) SDS, 2% (v/v) Triton-X-100
Yeast selective medium	0.67% (w/v) yeast nitrogen base; 0.083% (w/v) drop-out mix; 20% (w/v) glucose; pH 5.6
Yeast selective medium plates	Yeast selective medium with 2% (w/v) bacto-agar
Yeast selective medium plates with Aureobasidin A	Yeast selective medium with 2% (w/v) bacto-agar and 80ng/ml Aureobasidin A
YPAD	1% (w/v) yeast extract; 2% (w/v) bacto-peptone; 0.001% (w/v) adenine hemisulfate; 20% (w/v) glucose; pH 6.5
YPAD plates	YPAD medium with 2% (w/v) bacto-agar

5.2   Molecular biology

5.2.1   Production of electro-competent *E. coli*

LB medium was inoculated with one colony of the *E. coli* strain DH5α and grown overnight at 37°C. Next day, 500ml of LB medium was inoculated with 10ml of overnight culture and grown at 37°C until an optical density (OD_{600}) of 0.7 at 600nm was reached. Bacteria were cooled down to 4°C and pelleted at 4000x*g* for 20min at 4°C. Bacteria pellet was washed thrice with 500ml and once with 250ml, 125ml and 50ml ice-cold ddH_2O. The remaining pellet was resuspended in 3ml 10% (v/v) glycerol, 50µl aliquots were snap frozen in liquid nitrogen and stored at -80°C. Transformation efficiency of the electro-competent bacteria was tested by transformation with 10pg pUC19 plasmid DNA (Invitrogen).

5.2.2   Constructs and molecular cloning

The vectors and the constructs used in this study are listed in Table 5.6 and Table 5.7, respectively. Flag-, mCherry and EGFP-tagged TDP-43 wt, $CTF_{172-414}$, $CTF_{193-414}$ and NLS mutated TDP-43 constructs as well as pGADT7- and pGBKT7-TDP-43 wt and $CTF_{172-414}$, $CTF_{193-414}$ and most of pathogenic TDP-43 mutants were described before in Fiesel et al. (2010) and Fiesel (2010).

Human cDNA of SMN1, hnRNPA2, LSM6, MED6, RACK1, RBM45, RNF2, UBPY, UBPY ΔC, UBE2 enzymes UBE2E1, UBE2E2, UBE2E3, UBE2N and UBE2C were amplified from HEK293E or SH-SY5Y cell cDNA by polymerase chain reaction (PCR) with proofreading DNA polymerase ExTaq (Takara) and specific primers (Table 5.8), which also added terminal enzymatic restriction sites to the PCR products. PCR products were separated on 1% agarose (w/v)/TBE gels stained with ethidium bromide

Table 5.6 Vectors used in this study. Restriction sites of additionally inserted tags are indicated.

Vector	Tag (insertion site)	Host system	Reference
pGADT7	5'-HA	yeast	Clontech
pGBKT7	5'-myc	yeast	Clontech
pcDNA3.1(-)-Flag	5'-Flag (NotI/EcoRI)	mammalian cell culture	Invitrogen, (Fiesel et al., 2010)
pcDNA3.1(+)		mammalian cell culture	Invitrogen
pcDNA3.1(-)-mCherry	5'-mCherry (NotI/EcoRI)	mammalian cell culture	Invitrogen, F. Fiesel
pCMV-3xFlag	5'-3xFlag (SfiI/EcoRI)	mammalian cell culture	Clontech, 3xFlag tag cloned by C. Thömmes
pCMV-myc	5'-myc	mammalian cell culture	Clontech
pCMV-HA	5'-HA	mammalian cell culture	Clontech
pCMV-6xHis	5'-6xHis	mammalian cell culture	Clontech
pEGFP-C1	5'-EGFP	mammalian cell culture	Clontech
pEGFP-N1	3'-EGFP	mammalian cell culture	Clontech

and purified with QIAquick Gel Extraction kit (Qiagen). Purified PCR products as well as the target vectors were digested with specific restriction enzymes (Fermentas), followed by ligation into the SAP (Fermentas) dephosphorylated target vectors pcDNA3.1(+) or pCMV-myc. Ligation preparation was transformed into *E. coli* DH5α with electroporation. Bacteria expressing plasmids with inserts were identified by colony PCR using GoTaq DNA polymerase (Promega). Most of the inserts were shuttled into pGADT7, pGBKT7, pCMV-3xFlag, pCMV-myc and pCMV-HA target vectors.

EXOSC10 was subcloned into pGADT7 and pGBKT7 from pCL-neo-VSV-EXOSC10, a kind gift from Ger Pruijn, Nijmegen, Netherlands. For cloning of TDP-43 wt into pCMV-6xHis, TDP-43 wt was amplified from pcDNA3.1(-)-Flag with specific primers and subcloned into the target vector. Point mutations in UBPY (C786S), UBE2E3 (C145S) and TDP-43 (K263E, Q331K and N345K) were introduced by two-step-site-directed mutagenesis of the wt cDNA. The mutation was generated in the first PCR step. This step consisted of two parallel PCR reactions, with a primer complimentary to the 5' or 3' end of the cDNA including restriction sites and specific internal primers containing the point mutation (Table 5.9). PCR products of the first step were used as template in the second PCR step to obtain the full-length cDNA with the mutation.

Table 5.7 Constructs generated and/ or used during this work. Constructs were generated during this work by Friederike Hans (FH) or by Fabienne Fiesel (FS) and described in Fiesel et al. (2010). 6xHis-ubiquitin construct was described in Geisler et al. (2010). Ataxin-3 constructs were provided by T. Schmidt (TS, Department of Medical Genetics, University Clinics Tuebingen). Y2H control vectors pGADT7-T-Ag and pGBKT7-p53 were from Clontech.

construct	pcDNA3.1(+)	pGADT7	pGBKT7	pcDNA3.1(-)-Flag	pcDNA3.1(-)-mCherry	pCMV-3xFlag	pCMV-myc	pCMV-HA	pCMV-6xHis	pEGFP-C1	pEGFP-N1	Reference
TDP-43 wt		●	●	●	●				●	●		FF
TDP-43 CTF$_{172-414}$		●	●									FF
TDP-43 CTF$_{193-414}$ (CTF)		●	●	●	●					●		FF
TDP-43 ΔGRD		●	●									FF
TDP-43 NLSmut				●								FF
TDP-43 mutants (D169G, K263E, G287S, G290A, G298S, A315T, Q331K, M337V, Q343R, N345K, G348C, R361S; A382T, N390D, N390S)				●								FF, FH
SMN1	●	●	●									FH
hnRNPA2		●	●									FH
EXOSC10		●	●									FH
T-Ag		●										
p53			●									
LSM6	●	●				●	●					FH

construct	pcDNA3.1(+)	pGADT7	pGBKT7	pcDNA3.1(-)-Flag	pcDNA3.1(-)-mCherry	pCMV-3xFlag	pCMV-myc	pCMV-HA	pCMV-6xHis	pEGFP-C1	pEGFP-N1	Reference
MED6	●	●				●	●					FH
RACK1		●					●	●				FH
RBM45	●	●				●	●					FH
RNF2	●					●	●					FH
UBPY wt	●	●				●	●	●				FH
UBPY C786S, ΔC							●					FH
UBE2E3 wt		●				●	●	●				FH
UBE2E3 C145S, si1mut							●					FH
UBE2E2							●					FH
UBE2E1							●					FH
UBE2C							●					FH
UBE2N	●						●					FH
Ubiquitin									●			
Ataxin-3-Q15											●	TS
Ataxin-3-Q148											●	TS

Table 5.8 Primers used for molecular cloning (for - forward, rev - reverse)

Primer	Restriction site	Sequence (5'→3')
EXOSC10 for	NdeI	ggggcatATGGCGCCACCCAGTACC
EXOSC10 rev	EcoRI	cccgaattcCTATCTCTGTGGCCAGTTGTAC
hnRNPA2 for	EcoRI	gggggaattcATGGAGAGAGAAAAGGAACAGTTCC
hnRNPA2 rev	XhoI	ccccctcgagTCAGTATCGGCTCCTCCCAC
LSM6 for	KpnI/BamHI	gggggtaccgggatccggATGAGTCTTCGGAAGCAAACCCCTAG
LSM6 rev	NotI	ccccgcggccgcTCACATCCGTCTCTTCTGTGTACTG
MED6 for	KpnI/BglII	gggggtaccgagatctggATGGCGGCGGTGGATATCCGAG
MED6 rev	NotI	ccccgcggccgcTCACTGAAGTCTCATCCGTTTTTCAGGG
RACK1 for	SfiI	ggggccatggaggccATGACTGAGCAGATGACCCTTCGTG
RACK1 rev	SalI	ccccgtcgacCTAGCGTGTGCCAATGGTCACC
RBM45 for	KpnI/BamHI	gggggtaccgggatccggATGGACGAAGCTGGCAGCTCTG
RBM45 rev	NotI	ccccgcggccgcTCAGTAAGTTCTTTGCCGTTTGTTAGATTC
RNF2 for	KpnI/BamHI	gggggtaccgggatccggATGTCTCAGGCTGTGCAGACAAACG
RNF2 rev	NotI	ccccgcggccgcTCATTTGTGCTCCTTTGTAGGTGCG
SMN1 for	EcoRI	gggggaattcATGGCGATGAGCAGCGGC
SMN1 rev	XhoI	ccccctcgagTTAATTTAAGGAATGTGAGCACCTTCC
TDP-43 for	SalI	ggggtcgacgATGTCTGAATATATTCGGGTAACCG
TDP-43 rev	NotI	ccccgcggccgcCTACATTCCCCAGCCAGAAG
UBE2E3 for	KpnI/BglII	gggggtaccgagatctggATGTCCAGTGATAGGCAAAGGTCCG
UBE2E3 rev	NotI	ccccgcggccgcTTATGTTGCGTATCTCTTGGTCCACTG
UBE2E2 for	KpnI/BglII	gggggtaccgagatctggATGTCCACTGAGGCACAAAGAGTTGATG
UBE2E2 rev	NotI	ccccgcggccgcCTATGTGGCGTACCGCTTGGTCC
UBE2E1 for	BglII	gggggagatctggATGTCGGATGACGATTCGAGGGC
UBE2E1 rev	NotI	ccccgcggccgcTTATGTAGCGTATCTCTTGGTCCACTGTC
UBE2C for	BglII	gggggagatctggATGGCTTCCCAAAACCGCGACC
UBE2C rev	NotI	ccccgcggccgcTCAGGGCTCCTGGCTGGTGAC
UBE2N for	KpnI/BglII	gggggtaccgagatctggATGGCCGGGCTGCCCCG
UBE2N rev	NotI	ccccgcggccgcTTAAATATTATTCATGGCATATAGCCTAGTCCATGC
UBPY for	KpnI/BamHI	gggggtaccgggatccggATGCCTGCTGTGGCTTCAGTTCC
UBPY rev	NotI	ccccgcggccgcTTATGTGGCTACATCAGTTACTCGTGG
UBPY ΔC rev	NotI	ccccgcggccgcttATGGCTTCCTCTTCTCTTCCTCTTGAATAG

Table 5.9 Mutagenesis primers (for - forward, rev - reverse)

Primer	Sequence (5'→3')
TDP-43 K263E for	CCAATGCCGAACCTGAGCACAATAGCAATAG
TDP-43 K263E rev	CTATTGCTATTGTGCTCAGGTTCGGCATTGG
TDP-43 Q331K for	CCAGGCAGCACTAAAGAGCAGTTGGGGTATG
TDP-43 Q331K rev	CATACCCCAACTGCTCTTTAGTGCTGCCTGG
TDP-43 N345K for	GCCAGCCAGCAGAAGCAGTCAGGCCC
TDP-43 N345K rev	GGGCCTGACTGCTTCTGCTGGCTGGC
UBE2E3 C145S for	GTCAGGGAGTCATCTCTCTGGACATCC
UBE2E3 C145S rev	GGATGTCCAGAGAGATGACTCCCTGAC
UBE2E3 si1mut for	CCTCTGGTTGGAAGTATCGCAACGCAATACCTGACCAACAGAGC
UBE2E3 si1mut rev	GCTCTGTTGGTCAGGTATTGCGTTGCGATACTTCCAACCAGAGG
UBPY C786S for	CGTAACTTAGGAAATACTTCTTATATGAACTCAATATTGC
UBPY C786S rev	GCAATATTGAGTTCATATAAGAAGTATTTCCTAAGTTACG

All constructs were verified by sequencing using BigDye Terminator v.3.1 kit and an ABI 3100 Genetic Analyzer (Applied Biosystems). Sequence analysis was performed with Staden Package Software Version 1.6 (Staden et al., 2000). DNA concentrations were determined by measuring absorbance at 260nm with a NanoDrop ND-1000 device (Peqlab). For amplification, plasmids were electroporated into *E. coli* DH5α, grown in overnight cultures and purified with Plasmid Mini/Midi/Maxi kit from Qiagen.

5.2.3 Transformation of yeast with LiOAc/PEG

Transformation of the *S. cereviseae* strain Y2HGold with plasmid DNA was performed with the lithium acetate polyethylene glycol (LiOAc/PEG) method. Therefore, YPAD yeast medium was inoculated with one Y2HGold colony and grown overnight at 30°C. Next day, overnight culture was diluted to an OD_{600} of 0.2 and grown at 30°C until OD_{600} reached 0.7. For five transformations, 50ml of yeast culture was pelleted at 1100x*g* for 3min and resuspended in 500μl LiOAc/TE. In 1.5ml tubes 100μl resuspended yeast, 1μg plasmid DNA, 500μg LiOAc/PEG and 10μl herrings sperm carrier DNA were mixed for 15min on a rotator. 50μl DMSO (100%) was added and the yeast were heat shocked at 42°C for 15min. Transformed yeast was pelleted, resuspended in ddH$_2$O, plated onto appropriate selective medium plates and incubated at 30°C for 3d.

5.2.4 DNA isolation from yeast

Isolation of chromosomal and plasmid DNA from the *S. cereviseae* strain Y2HGold was performed according to Hoffman and Winston (1987). A 5ml overnight culture of Y2HGold in medium lacking leucine (-L) selecting for the to-be-isolated plasmid was pelleted at 1100x*g* for 3min and snap frozen shortly in liquid nitrogen. Then, 0.3g glass beads (Sigma), 500μl yeast lysis buffer (10mM Tris pH 8.0; 100mM NaCl, 1mM EDTA, 1% (w/v) SDS, 2% (v/v) Triton-X-100) and 500μl Roti®-

phenol/chloroform/isoamyle alcohol (25:24:1; Roth) were added, mixed by vortexing for 2min and centrifuged at for 5min. DNA was precipitated from aqueous phase with 1ml 100% ethonol/ 10mM NaOAc and dissolved in 50μl ddH$_2$O. To isolate and purify the cDNA library plasmid (pGADT7-RecAB), *E. coli* DH5α was transformed with yeast DNA and grown on ampicillin LB-medium plates, as the pGADT7 vector also codes for an ampicillin resistance.

5.2.5 Yeast Two-hybrid screen

Yeast Two-hybrid is a technique to investigate protein-protein interactions. In this system, a bait protein is fused to the binding domain (BD) and a prey protein is fused to the activation domain (AD) of the Gal4 transcription factor. The bait protein is usually a known protein, whereas the prey protein can either be also known or expressed from a cDNA library. Both fusion proteins are co-expressed in a genetically engineered yeast strain that cannot biosynthesise certain nutrients. These are usually amino acids or nucleic acids. The plasmids coding for BD-bait and AD-prey also encode each for one enzyme which enables the yeast to grow on certain selective medium plates. If bait and prey interact, Gal4 transcription factor is indirectly connected and therefore functional and can activate the transcription of several reporter genes in the yeast genome, allowing the yeast to grow on selective medium plates lacking further nutrients. As there are several reporter genes, stringency of the selective medium is variable. Thus, not only an interaction of two proteins can be found, but also the strength of interaction can be analyzed.

Here, a human adult brain cDNA library (Mate & Plate™ Library) containing partial cDNAs was used for screening for TDP-43 FL and CTF interactors with the Matchmaker Gold Yeast Two-Hybrid System (both Clontech). The cDNA library plasmids (pGADT7) were purchased already transformed into *S. cereviseae* strain Y187. These yeast cells were mated in 2xYPAD medium within 24-28h with *S. cereviseae* strain Y2HGold expressing TDP-43 FL or CTF as bait. The screens were performed on diverse selective medium plates, as indicated in the results part. Yeast colonies grown after 7-11d (size > 1mm) at 30°C were seen as primary positive clones. These were selected for growth on selective medium plates lacking leucine and tryptophane (-LT), leucine, tryptophane, histidine and adenine (-LTHA) with 2.5mM 3-Amino-1,2,4-triazole (3-AT), and -LTHA + X-α -Gal + 80ng/ml Aureobasidin A (-LTHA + X + AbA) for a first confirmation of interaction. Additionally, yeast extracts of individual clones were prepared for western blotting analysis (see 5.5.1) to test for the expression of HA-tagged prey proteins (Figure 5.1B). Clones growing on all three selective media and expressing a prey protein larger than 25kDa (the size of the HA-tagged activation

domain is approx. 22kDa) were chosen for further study. An example of the analysis of ten primary positive clones is depicted in Figure 5.1.

Individual clones were grown in liquid medium lacking leucine to select for cDNA library plasmids, which were isolated as described in 5.2.4. DNA samples were analyzed by PCR with oligonucleotides for cDNA library inserts to assure that each primary positive clone contained only one library plasmid (Figure 5.1A). Plasmids were retransformed into *E. coli* and re-isolated to obtain pure cDNA library plasmids. This was also confirmed by PCR analysis of the isolated plamids (Figure 5.1C). Purified library plasmids were co-transformed (0) into yeast strain Y2HGold with the bait vector pGBKT7-Ø, -TDP-43 FL or CTF (retransformation). 6×10^4 yeast cells were spotted in duplicates on selective medium plates with increasing stringency (Figure 5.1D). Yeast were seen as true positive clones when they expressed a prey protein together with TDP-43 FL or CTF, but not the bait control vector, and grew at least on -LTHA + 2.5mM 3-AT. These cDNA library plasmids were sequenced for identification.
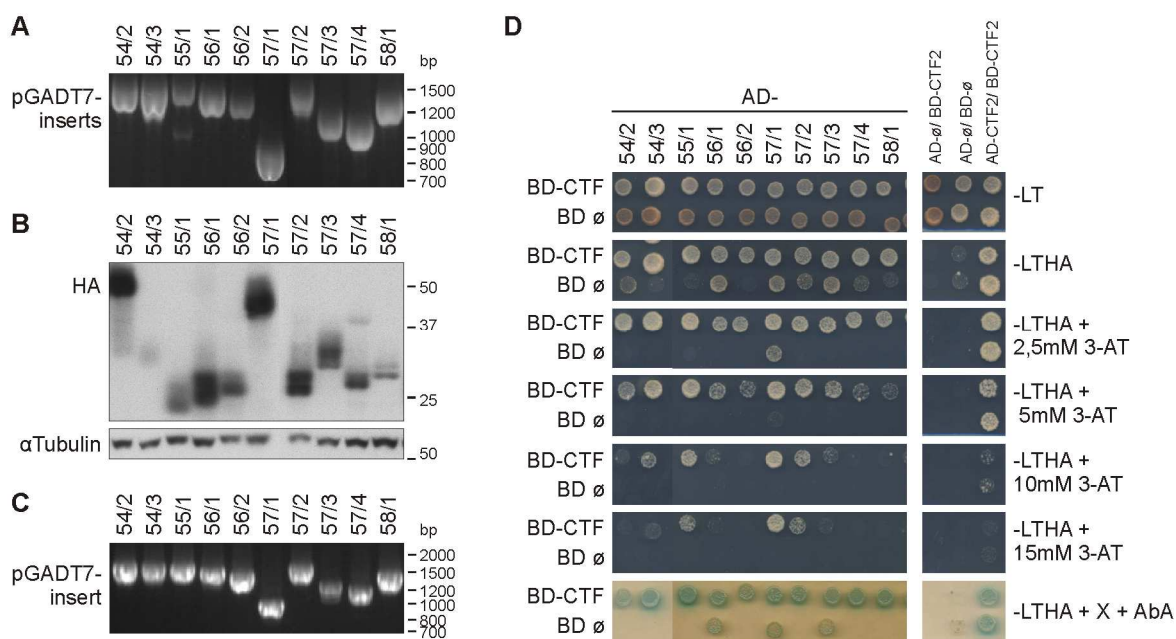
Figure 5.1 Example of analysis of ten primary positive hits from the Y2H screen. A PCR analysis of ten library plasmids (pGADT7) from yeast-DNA extraction. **B** Protein expression of the ten primary positive hits in Y2HGold. Yeast extract of indicated hits were subjected to western blot. Hits were detected with HA antibody, α-tubulin served as loading control. **C** PCR analysis of the purified library plasmids. The sizes of vector inserts do not correlated with the molecular weight of the expressed proteins, because stop codons could be located all over the cDNAs. **D** Spotting of the retransformed primary positive hits. Isolated library plasmids from (C) were retransformed with pGBKT7-CTF or control vector (Ø) into Y2HGold. 6×10^4 yeast cells were spotted onto selective medium plates with increasing stringency and grown for 7d at 30°C: -LT (selecting for co-transformed yeast), -LTHA, -LTHA + 3-AT in increasing concentrations, as indicated, and -LTHA + X-α-Gal + 80ng/ml Aureobasidin A (-LTHA + X + AbA). **A-D** 54/2 - 58/1 are the internal numbers of the primary positive hits.

5.2.6 Extraction of total RNA and semi-quantitative PCR

For investigations of mRNA level in human cell lines HEK293E and MCF-7, RNA was isolated using the RNeasy Mini kit (Qiagen). For RNA isolation from *Drosophila melanogaster* about 10-20 third instar larvae were homogenized in 600µl RNeasy Lysis (RLT) buffer and RNA isolation was performed with the RNeasy Mini kit according to manufactures instructions for animal tissue. 600ng of total RNA was reverse transcribed with anchored oligo-dT primer using the Transcriptor High Fidelity cDNA Synthesis kit (Roche). As a template for transcript amplification in a semi-quantitative reverse transcription PCR (sqRT-PCR) in a 25µl reaction, 17.9µl cDNA (diluted 1:10 with DEPC-H_2O) was used with 5µl 5x GoTaq buffer, 0.1µl GoTaq DNA polymerase (Promega) and 2mM of a primer pair specific for the transcripts. Primer sequences are listed in Table 5.10. PCR products were separated by electrophoresis using a 2% (w/v) agarose/TBE gel stained with ethidium bromide and photoimaged with a gel documentation system (Vilber Lourmat). Quantifications were performed with ImageJ software (version 1.47, National Institute of Health).

Table 5.10 Human and *Drosophila melanogaster* specific primers for sqRT-PCR (for - forward, rev - reverse)

Primer	Start (bp)	Sequence (5'→3')
UBE2E3 for	86	CTCCAGAGCCTGAAGAACAAGAGG
UBE2E3 rev	230	GGATCAAGGGTTATTTCAGCTAGCTCC
UBE2E2 for	10	GAGGCACAAAGAGTTGATGACAGTCC
UBE2E2 rev	114	GGGCTGAACTTGTTCTCTTTCTGGTTC
UBE2E1 for	6	GGATGACGATTCGAGGGCCAGC
UBE2E1 rev	146	GCGCTGGTGGAGAGGAGTTTGG
hUBPY for	2616	GCTTCTGTTCCTAATGGATGGTCTCC
hUBPY rev	2901	GCAATCCTGTAATGTACATTTACTTGTGGATG
endog. TDP-43 for	693	TGTTACATTTGCAGATGATCAGATTGCG
endog. TDP-43 rev	cDNA + 29	CCCACCATTCTATACCAACCAACCAC
HDAC6 for	1085	GGTTCGCCCAGCTAACCCACCT
HDAC6 rev	1692	GGAACTCTCACGGTGCAGCTCC
SKAR Ex2 for	389	CCTTCATAAACCCACCCATTGGGACAG
SKAR Ex 2/3 for	437	CCAAAACCATCCAGGTTCCACAGCAG
SKAR Ex 4 rev	630	GTGGTGGAGAAAGCCGCCTGAG
hPBDG for	410	TGCCAGAGAAGAGTGTGGTG
hPBDG rev	514	TGTTGAGGTTTCCCCGAATA
dUBPY for	2474	CGGTAACACCTAAGACCTACCAGC
dUBPY rev	2607	CGAGACGACCTGATCGTCGAAC
dGAPDH for	786	GATCACGACGTGTTACGGTG
dGAPDH rev	966	CAGGGGGAATTTGTCCTCC

5.3   Cell culture

5.3.1   Maintenance of cells

All cell lines were maintained under humidified conditions at 37°C and 5% CO_2. Human embryonic kidney cells (HEK293E, Invitrogen) were cultured in Dulbecco's modified Eagle medium (DMEM) with 10% fetal calf serum (FCS). Human mamma carcinoma MCF-7 cells were maintained in DMEM with 10% FCS and 1% Pen/Strep. Human neuroblastoma SH-SY5Y cells (ATCC) were grown in DMEM/HAM's F12 with 10% FCS.

5.3.2   Transient transfection of cells with DNA and small interference RNA (siRNA)

HEK293E cells were transfected at approximately 80% confluence. For transient transfection with DNA, FuGENE6 or X-tremeGENE9 (Roche) was used following manufacturer's instructions. For immunofluorescence studies, the ratio of DNA:transfection reagent was 1:4.5 diluted in OptiMEM, for all other studies the ratio was 1:3. Further analysis of the cells was performed 24 - 72h after transfection.

Transient silencing of UBE2E enzymes was performed with siGENOME siRNAs (Thermo Scientific), and UBPY was silenced with GeneSolution siRNA (Qiagen) or Silencer® Validated siRNAs from Ambion (see Table 5.11). A scrambled siRNA was used as control (Qiagen). HEK293E cells were transfected thrice in 72h with 5nM siRNA, unless otherwise indicated, using HiPerFect (Qiagen), following manufacturer's instructions. Briefly, for silencing in a 6-well, 100μl OptiMEM, 12μl HiPerFect

Table 5.11 siRNAs used for transient silencing in HEK293E cells

siRNA	target sequence (5'→3')	Catalogue number	Supplier
UBE2E1_1	GCGAUAACAUCUAUGAAUG	D-007740-01	
UBE2E1_2	GGUGUAUUCUUUCUCGAUA	D-007740-02	
UBE2E1_4	GAGAGUAAAGUCAGCAUGA	D-007740-04	
UBE2E1_5	GUAUGAGGGUGGUGUAUUC	D-007740-05	
UBE2E2_1	UCACCAGACUAUCCGUUUA	D-031782-01	
UBE2E2_2	ACAAAGAGUUGAUGACAGU	D-031782-02	Thermo Scientific
UBE2E2_3	GCUAAAUUGUCAACUAGUG	D-031782-03	
UBE2E2_4	GAGGUCAACUAUAUUGGGA	D-031782-04	
UBE2E3_1	GCAUAGCCACUCAGUAUUU	D-008845-01	
UBE2E3_2	GCUAAGUUAUCCACUAGUG	D-008845-02	
UBE2E3_3	AUAUGAAGGUGGUGUGUUU	D-008845-03	
UBE2E3_4	GGAGCUAGCUGAAAUAACC	D-008845-04	
Hs_USP8_1	CAGGGTCAATTCAAATCTACA	SI00073017	
Hs_USP8_2	AAGGCTCGTATTCATGCAGAA	SI00073024	Qiagen
Hs_USP8_3	CAGGTTCAGGCAAGCCATTTA	SI00073031	
Hs_USP8_5	GAGGATACAGACGATACCGAA	SI03103604	
UBPY	UUCUGCAUGAAUACGAGCC	105117	Ambion
control	AllStarts negative control	1027280	Qiagen

and siRNA in various concentrations were incubated for 10min at room temperature. The transfection mixture was added dropwise to the cells, and 4h after the transfection the medium was changed.

5.3.3   Lentiviral transduction of HEK293E

For stable silencing of UBPY in HEK293E cells, specific MISSION shRNA lentiviral transduction particles from Sigma were used (Table 5.12). MISSION® pLKO.1-puro non-mammalian shRNA control transduction particles were used as negative control. The shRNAs were provided in pLOK.1 vector, coding also for a puromycin resistance. For viral transduction, HEK293E cells were grown for 24h in 96-well plates before the virus was added (multiplicity of infection MOI of 0.5-2). Hexadimethrine bromide (8μg/ml) was used to increase the efficiency of the viral transduction. After 24h the virus was removed by changing the medium and additional 24h later, puromycin (300ng/ml) was added to the medium to select for transduced cells. The antibiotic was changed every third day. The cells were amplified over 1.5 weeks and tested for UBPY knockdown by western blot and sqRT-PCR.

5.3.4   Proteasomal and autophagosomal inhibition

HEK293E cells were treated for the indicated time points with 10μM MG-132 to inhibit proteasomal activity and/or with 20nM bafilomycin A1 (baf) or 5mM 3-methyladenine (3-MA) to inhibit basal autophagy (all Sigma-Aldrich).

5.4   Maintenance of Flies

All *Drosophila* stocks were maintained on standard cornmeal-yeast agar based fly food. The experiments were performed at 25°C. The following lines were obtained from the Bloomington *Drosophila* stock center: w[*]; P{w[+mC]=GAL4-ninaE.GMR}12

Table 5.12 shRNAs for stable silencing of UBPY

TRC number	Sequence	Target region
TRCN0000272433	CCGGTCAAGCAACAGCAGGATTATTCTCGAGAATAATCCTGCTG-TTGCTTGATTTTTG	CDS
TRCN0000272486	CCGGCACTGGAACCTTTCGTTATTACTCGAGTAATAACGAAAGGT-TCCAGTGTTTTTG	CDS
TRCN0000272465	CCGGCTCGAAGAATGCAGGATTATCCTCGAGGATAATCCTG-CATTCTTCGAGTTTTTG	CDS
TRCN0000272467	CCGGCCACAGATTGATCGTACTAAACTCGAGTTTAGTACGAT-CAATCTGTGGTTTTTG	CDS
TRCN0000272469	CCGGGCTGTGTTACTAGCACTATATCTCGAGATATAGTGCTAG-TAACACAGCTTTTTG	3'UTR

(BL1104, GMR-Gal4 in text), y[1] w[*]; P{w[+mC]=Act5C-GAL4}25FO1/CyO, y[+] (BL4414, actin-Gal4 in text), and w[1118] (BL3605, white in text). The RNAi lines dUBPY (v107623, KK library), and UbcD2 (v31158), RNF2 (v27465), and RBM45 (v23851, all GD library) were obtained from the Vienna Drosophila Resource Center (VDRC, Austria). The GD library lines are generated by random insertion of the RNAi's, whereas the KK library line contains a site specific RNAi. The random inserted UAS:TDP-43-GFP GMR-Gal4 driven transgenic lines #14 (high expression) and #10 (low expression) were a kind gift from Aaron Voigt, RWTH Aachen. UAS:TDP-43-GFP insertions were generated by germline transmission (BestGene) and were described before (Voigt et al., 2010). Stable TDP-43 expression in the retina was achieved by recombination of the GMR-Gal4 driver with the UAS:TDP-43-GFP#14/#10 insertions.

5.5 Protein biochemistry

5.5.1 Preparation of yeast extracts for western blot

Cultures of Y2HGold expressing either AD-, BD-fused proteins or both were grown overnight at 30°C. A culture volume according to an OD_{600} of 2 were pelleted and re-suspended in 1ml ice-cold ddH_2O. Then 150μl 1.85M NaOH/7,5% β-mercaptoethanol was added and incubated on ice for 15min. 150μl 55% (v/v) trichloroacetic acid was added to this suspension, incubated on ice for 10min and pelleted at 14000xg for 10min. Pellet was resuspended in 100μl HU buffer + 15mM DTT and boiled at 95°C for 10min. Yeast extracts were analyzed by western blot.

5.5.2 Preparation of cell lysates for western blot

HEK293E or MCF-7 cells were lysed in RIPA buffer containing 1x Complete protease inhibitors for 30min on ice and pelleted at 14,000xg for 15min at 4°C. The concentration of total protein was determined with bicinchoninic acid (BCA) protein assay kit (Pierce) and 10μg were analyzed by western blot.

5.5.3 Immunoprecipitation

HEK293E cells were lysed in CoIP buffer containing 1x Complete protease inhibitors (Roche) for 30min on ice. Cell debris was pelleted at 14,000xg and 4°C for 15min and 750μg of total protein lysate, determined with BCA protein assay kit (Pierce), was incubated with EZview™ Red anti-Flag, anti-HA or anti-myc affinity Gel (Sigma) for 3h or over night at 4°C. The beads were washed three times with CoIP buffer and proteins were eluted in 2x Laemmli buffer at 95°C. 10μg of total protein lysates or one-fifth of eluated protein was subjected to western blot analysis.

5.5.4 Sequential extraction of HEK293E proteins

HEK293E cells were lysed in RIPA buffer with 1x Complete protease inhibitors for 30min on ice and pelleted at 14,000xg for 15min at 4°C. The RIPA-insoluble pellets were washed with RIPA buffer and lysed in 8M urea buffer. The total protein concentration of RIPA lysates was determined with BCA protein assay kit (Pierce). The total protein concentration of urea lysates was determined with Bradford Protein assay kit (Bio-Rad). 10µg of RIPA soluble or 5µg of urea soluble lysate was boiled in 1x Laemmli buffer at 95°C for 10min and subjected to western blot analysis.

5.5.5 Pulldown of total ubiquitinylated proteins

HEK293E cells were co-transfected with the indicated constructs and 6xHis-ubiquitin for 24h or 48h. The cells were harvested by scraping, washed twice with PBS and lysed with 8M urea buffer containing 10mM imidazole. The DNA was sheared by passing the lysate 20 times through a 23-gauge needle. The cell debris was pelleted at 14,000xg for 15min at 4°C and the protein concentration was determined with Bradford Protein assay kit (Bio-Rad protein assay). 500 - 1000µg of total protein lysates were incubated with Ni-NTA agarose beads (Qiagen) for 4h at room temperature. The beads were washed thrice with 8M urea wash buffer containing 20mM imidazole and the proteins were eluted in 3x Laemmli buffer with 500mM imidazole at 95°C for 10min. The total protein and one-fifth of eluates were analyzed by western blotting.

5.5.6 Pulldown of sequentially extracted ubiquitinylated proteins

HEK293E cells co-transfected with the indicated cDNAs and 6xHis-ubiquitin were lysed under native conditions in NP-40 buffer containing 1x Complete protease inhibitors (EDTA-free, Roche) and 10mM imidiazole for 30min on ice and pelleted at 14,000xg for 15min at 4°C. The total protein concentration of the NP-40 soluble fraction was determined with the BCA protein assay kit (Pierce). The NP-40 insoluble pellets were washed twice with NP-40 buffer and lysed in 8M urea buffer. The Bradford protein assay kit (Bio-Rad) was used to determine the protein concentration of the urea soluble fraction. The pulldown with Ni-NTA agarose beads (Qiagen) was performed with 300µg of the NP-40 and 150µg of the urea lysates for 4h at 4°C (NP-40 lysates) or room temperature (urea lysates). The beads were washed thrice with either NP-40 buffer or 8M urea wash buffer containing 20mM imidazole. The proteins were eluted in 3x Laemmli buffer with 500mM imidazole at 95°C for 10min. The total protein or one fifth of eluates was subjected to western blot analysis.

5.5.7   Sequential extraction of fly head proteins

Flies were decapitated and the heads were homogenized in RIPA buffer containing 1x Complete protease inhibitors (Roche). The cell debris was pelleted at 14,000xg for 15min at 4°C to obtain the RIPA soluble lysate. The RIPA-insoluble cell pellets were washed twice with RIPA buffer and lysed with 8M urea buffer. An equivalent of one fly head (RIPA soluble) and of five fly heads (urea soluble) was loaded per lane in western blot analysis.

5.5.8   Western blot analysis

Denatured proteins were separated on either 7.5%, 10%, 12.5% or 15% SDS-polyacrylamide gels (SDS-PAGE) or 4-12% Bis-Tris NuPAGE Mini or Midi gradient gels (Invitrogen) and were transfered onto Hybond‑P polyvinylidene difluoride membrane (Millipore) or nitrocellulose membrane (GE Healthcare), either by wet or semi-dry transfer method. The membranes were blocked in 5% non-fat milk/TBST or 5% BSA/TBST, incubated with primary antibody in 5% (v/v) Western Blocking Reagent (Roche)/0.02% NaN$_3$ in TBST at 4°C overnight. This was followed by incubation with the horseradish peroxidise (HRP)-conjugated secondary antibodies for 1h at room temperature. The incubation of membranes with the primary HRP-coupled antibodies was performed in 5% non-fat milk/TBST for 1h at room temperature or overnight at 4°C. The detection of proteins was performed with the Immobilon Western chemiluminescent HRP substrate (Millipore) on Amersham Hyperfilm™ ECL (GE Healthcare).

5.5.9   Immunofluorescence

HEK293E or MCF-7 cells were seeded on poly-D-lysine (Sigma) and collagen (Cohesion) coated coverslips and fixed with 4% (w/v) PFA/PBS for 20min, permeabilized with 1% Triton-X-100/PBS for 5min and blocked 1h with 10% normal goat serum or horse serum. The primary antibody incubation was performed in 1% BSA/PBS for 2h at RT or overnight at 4°C. The cells were incubated with secondary Alexa Fluor conjugated antibodies in the dark for 2h at room temperature. The nuclei were counterstained with Hoechst 33342 (2μg/ml/PBS) for 10min at room temperature and coverslips were mounted in fluorescent mounting medium (Dako) onto microscope slides. The cells were analyzed with an ApoTome Imaging system using a 63x objective and the images were processed with AxioVision 4.8.1 software (Zeiss).

Table 5.13 Primary antibodies used for western blot (WB) or immunofluorescence (IF).

Antibody	Clone	Species	Dilution WB	IF	Catalogue number	Supplier
αTubulin	B512	mouse	1:10000		T-5168	Sigma
EEA1	14/EEA1	mouse		1:100	610457	Transduction Laboratories
eIF3		goat		1:500	sc-16377	Santa Cruz
Flag	M2, affinity purified	mouse		1:500	F1804	Sigma
Flag-HRP	M2	mouse	1:1000 - 1:30000		A8592	Sigma
Flag		rabbit		1:250	#2368	Cell Signaling
GAPDH	6C5	mouse	1:50000		H86504M	Biodesign International
GM130	35/GM130	mouse		1:500	610822	BD Transduction Laboratories
HA	3F10	rat	1:10000		11867423001	Roche
HA-HRP	3F10	rat	1:10000		12013819001	Roche
HDAC6	H-300	rabbit	1:2000		sc-11420	Santa Cruz
6xHis		mouse	1:3000		27-4710-01	Amersham
LAMP1	H4A3	mouse	1:1000		H4A3	Hybridoma Bank of University of Iowa
LC3B		rabbit	1:1000		#2775	Cell Signaling
Living Colours		rabbit	1:5000		63260	Takara/Clontech
Living Colours dsRed		rabbit	1:2000		632496	Takara/Clontech
myc	9E10	mouse		1:500	11667149001	Sigma
myc-HRP	9E10	mouse	1:10000		11814150001	Sigma
SKAR α		rabbit	1:1000		3235	Cell Signaling
SKAR α/β		rabbit	1:1000		3794S	Cell Signaling
TDP-43		rabbit	1:2000	1:1000	BC001487	ProteinTechGroup
TDP-43	2E2-D3	mouse	1:2000	1:1000	H00023435	Abnova
phospho-TDP-43 (S409/410)	1D3	rat	1:10			M. Neumann
UBE2E1		rabbit	1:2000	1:500	ab36980	Abcam
UBE2E2		rabbit	1:4000	1:500	ARP43437	Aviva Systems Biology
UBE2E3		mouse	1:2000		MABS17	Millipore
UBE2E3	7E8	mouse		1:150 - 500	TA800082	OriGene
Ubiquitin (mono- & poly-)	Ubi-1	mouse	1:4000		MAB1510	Millipore
Ubiquitin (mono- & poly)	6C1	mouse	1:500		U0508	Sigma
polyubiquitin	FK1	mouse	1:500	1:500	PW8805	BIOMOL
UBPY		rabbit	1:1000	1:500	A302-929A	Bethyl Laboratories

Table 5.14 Secondary antibodies used for western blot (WB) or immunofluorescence (IF).

Antibody	Species	Dilution WB	IF	Supplier
anti-mouse-HRP	donkey	1:15000		Jackson ImmunoResearch
anti-rabbit-HRP	donkey	1:7500 - 15000		Laboratories
anti-rat-HRP	donkey	1:5000		
anti-goat-Alexa Fluor 568	donkey		1:2000	Invitrogen
anti-mouse-Alexa Fluor 488/ 568	goat		1:2000	
anti-rabbit-Alexa-Fluor 488/ 568	goat		1:2000	
anti-rabbit-Alexa Fluor 488	donkey		1:2000	

5.6   Statistical analysis

The yeast experiments were performed once or twice, as stated in the figure legends. Spotting of the transformed yeast onto selective medium plates was done in dublicates, of which one representative spot is shown. Each experiment analysed by western blot or PCR was performed at least three times with similar results unless otherwise stated in the figure legends, and images of one representative experiment are shown. The quantification of mRNA or protein levels was performed with ImageJ software (version 1.47, National Institute of Health). The depicted immunofluorescence images show representative cells of at least two independent experiments. For the quantification of TDP-43 aggregation upon UBPY co-expression, at least 100 cells per condition per experiment were counted. The error bars represent the standard deviation of the mean. Images of at least five fly eyes per experiment per genotype were taken, though additional fly eyes were monitored. These experiments were repeated at least three times.

6 References

Abel, O., Powell, J.F., Andersen, P.M., and Al-Chalabi, A. (2012). ALSoD: A user-friendly online bioinformatics tool for amyotrophic lateral sclerosis genetics. Human mutation *33*, 1345-1351.

Abhyankar, M.M., Urekar, C., and Reddi, P.P. (2007). A novel CpG-free vertebrate insulator silences the testis-specific SP-10 gene in somatic tissues: role for TDP-43 in insulator function. The Journal of biological chemistry *282*, 36143-36154.

Adams, D.R., Ron, D., and Kiely, P.A. (2011). RACK1, A multifaceted scaffolding protein: Structure and function. Cell communication and signaling : CCS *9*, 22.

Alami, N.H., Smith, R.B., Carrasco, M.A., Williams, L.A., Winborn, C.S., Han, S.S., Kiskinis, E., Winborn, B., Freibaum, B.D., Kanagaraj, A.*, et al.* (2014). Axonal Transport of TDP-43 mRNA Granules Is Impaired by ALS-Causing Mutations. Neuron *81*, 536-543.

Allmang, C., Petfalski, E., Podtelejnikov, A., Mann, M., Tollervey, D., and Mitchell, P. (1999). The yeast exosome and human PM-Scl are related complexes of 3' --> 5' exonucleases. Genes & development *13*, 2148-2158.

Alwan, H.A., and van Leeuwen, J.E. (2007). UBPY-mediated epidermal growth factor receptor (EGFR) de-ubiquitination promotes EGFR degradation. The Journal of biological chemistry *282*, 1658-1669.

Anderson, P., and Kedersha, N. (2006). RNA granules. The Journal of cell biology *172*, 803-808.

Anderson, P., and Kedersha, N. (2009). RNA granules: post-transcriptional and epigenetic modulators of gene expression. Nature reviews Molecular cell biology *10*, 430-436.

Arai, T., Hasegawa, M., Akiyama, H., Ikeda, K., Nonaka, T., Mori, H., Mann, D., Tsuchiya, K., Yoshida, M., Hashizume, Y.*, et al.* (2006). TDP-43 is a component of ubiquitin-positive tau-negative inclusions in frontotemporal lobar degeneration and amyotrophic lateral sclerosis. Biochemical and biophysical research communications *351*, 602-611.

Arai, T., Hasegawa, M., Nonoka, T., Kametani, F., Yamashita, M., Hosokawa, M., Niizato, K., Tsuchiya, K., Kobayashi, Z., Ikeda, K.*, et al.* (2010). Phosphorylated and cleaved TDP-43 in ALS, FTLD and other neurodegenerative disorders and in cellular models of TDP-43 proteinopathy. Neuropathology : official journal of the Japanese Society of Neuropathology *30*, 170-181.

Arai, T., Nonaka, T., Hasegawa, M., Akiyama, H., Yoshida, M., Hashizume, Y., Tsuchiya, K., Oda, T., and Ikeda, K. (2003). Neuronal and glial inclusions in frontotemporal dementia with or without motor neuron disease are immunopositive for p62. Neuroscience letters *342*, 41-44.

Araki, W., Minegishi, S., Motoki, K., Kume, H., Hohjoh, H., Araki, Y.M., and Tamaoka, A. (2014). Disease-Associated Mutations of TDP-43 Promote Turnover of the Protein Through the Proteasomal Pathway. Molecular neurobiology.

Arimoto, K., Fukuda, H., Imajoh-Ohmi, S., Saito, H., and Takekawa, M. (2008). Formation of stress granules inhibits apoptosis by suppressing stress-responsive MAPK pathways. Nature cell biology *10*, 1324-1332.

Armakola, M., Higgins, M.J., Figley, M.D., Barmada, S.J., Scarborough, E.A., Diaz, Z., Fang, X., Shorter, J., Krogan, N.J., Finkbeiner, S.*, et al.* (2012). Inhibition of RNA lariat debranching enzyme suppresses TDP-43 toxicity in ALS disease models. Nature genetics *44*, 1302-1309.

Arnold, E.S., Ling, S.C., Huelga, S.C., Lagier-Tourenne, C., Polymenidou, M., Ditsworth, D., Kordasiewicz, H.B., McAlonis-Downes, M., Platoshyn, O., Parone, P.A.*, et al.* (2013). ALS-linked TDP-43 mutations produce aberrant RNA splicing and adult-onset motor neuron disease without aggregation or loss of nuclear TDP-43. Proceedings of the National Academy of Sciences of the United States of America *110*, E736-745.

Ash, P.E., Bieniek, K.F., Gendron, T.F., Caulfield, T., Lin, W.L., Dejesus-Hernandez, M., van Blitterswijk, M.M., Jansen-West, K., Paul, J.W., 3rd, Rademakers, R.*, et al.* (2013). Unconventional translation of C9ORF72 GGGGCC expansion generates insoluble polypeptides specific to c9FTD/ALS. Neuron *77*, 639-646.

Austin, J.A., Wright, G.S., Watanabe, S., Grossmann, J.G., Antonyuk, S.V., Yamanaka, K., and Hasnain, S.S. (2014). Disease causing mutants of TDP-43 nucleic acid binding domains are resistant to aggregation and have increased stability and half-life. Proceedings of the National Academy of Sciences of the United States of America.

Avendano-Vazquez, S.E., Dhir, A., Bembich, S., Buratti, E., Proudfoot, N., and Baralle, F.E. (2012). Autoregulation of TDP-43 mRNA levels involves interplay between transcription, splicing, and alternative polyA site selection. Genes & development *26*, 1679-1684.

Ayala, V., Granado-Serrano, A.B., Cacabelos, D., Naudi, A., Ilieva, E.V., Boada, J., Caraballo-Miralles, V., Llado, J., Ferrer, I., Pamplona, R.*, et al.* (2011a). Cell stress induces TDP-43 pathological changes associated with ERK1/2 dysfunction: implications in ALS. Acta neuropathologica *122*, 259-270.

Ayala, Y.M., De Conti, L., Avendano-Vazquez, S.E., Dhir, A., Romano, M., D'Ambrogio, A., Tollervey, J., Ule, J., Baralle, M., Buratti, E.*, et al.* (2011b). TDP-43 regulates its mRNA levels through a negative feedback loop. The EMBO journal *30*, 277-288.

Ayala, Y.M., Misteli, T., and Baralle, F.E. (2008a). TDP-43 regulates retinoblastoma protein phosphorylation through the repression of cyclin-dependent kinase 6 expression. Proceedings of the National Academy of Sciences of the United States of America *105*, 3785-3789.

Ayala, Y.M., Pagani, F., and Baralle, F.E. (2006). TDP43 depletion rescues aberrant CFTR exon 9 skipping. FEBS letters *580*, 1339-1344.

Ayala, Y.M., Pantano, S., D'Ambrogio, A., Buratti, E., Brindisi, A., Marchetti, C., Romano, M., and Baralle, F.E. (2005). Human, Drosophila, and C.elegans TDP43: nucleic acid binding properties and splicing regulatory function. Journal of molecular biology *348*, 575-588.

Ayala, Y.M., Zago, P., D'Ambrogio, A., Xu, Y.F., Petrucelli, L., Buratti, E., and Baralle, F.E. (2008b). Structural determinants of the cellular localization and shuttling of TDP-43. Journal of cell science *121*, 3778-3785.

Badadani, M., Nalbandian, A., Watts, G.D., Vesa, J., Kitazawa, M., Su, H., Tanaja, J., Dec, E., Wallace, D.C., Mukherjee, J.*, et al.* (2010). VCP associated inclusion body myopathy and paget disease of bone knock-in mouse model exhibits tissue pathology typical of human disease. PloS one *5*.

Bak, T.H., and Hodges, J.R. (2001). Motor neurone disease, dementia and aphasia: coincidence, co-occurrence or continuum? Journal of neurology *248*, 260-270.

Baker, M., Mackenzie, I.R., Pickering-Brown, S.M., Gass, J., Rademakers, R., Lindholm, C., Snowden, J., Adamson, J., Sadovnick, A.D., Rollinson, S.*, et al.* (2006). Mutations in progranulin cause tau-negative frontotemporal dementia linked to chromosome 17. Nature *442*, 916-919.

Ballif, B.A., Cao, Z., Schwartz, D., Carraway, K.L., 3rd, and Gygi, S.P. (2006). Identification of 14-3-3epsilon substrates from embryonic murine brain. Journal of proteome research *5*, 2372-2379.

Baloh, R.H. (2011). TDP-43: the relationship between protein aggregation and neurodegeneration in amyotrophic lateral sclerosis and frontotemporal lobar degeneration. The FEBS journal *278*, 3539-3549.

Baltz, A.G., Munschauer, M., Schwanhausser, B., Vasile, A., Murakawa, Y., Schueler, M., Youngs, N., Penfold-Brown, D., Drew, K., Milek, M.*, et al.* (2012). The mRNA-bound proteome and its global occupancy profile on protein-coding transcripts. Molecular cell *46*, 674-690.

Barmada, S.J., Skibinski, G., Korb, E., Rao, E.J., Wu, J.Y., and Finkbeiner, S. (2010). Cytoplasmic mislocalization of TDP-43 is toxic to neurons and enhanced by a mutation associated with familial amyotrophic lateral sclerosis. The Journal of neuroscience : the official journal of the Society for Neuroscience *30*, 639-649.

Bartolome, F., Wu, H.C., Burchell, V.S., Preza, E., Wray, S., Mahoney, C.J., Fox, N.C., Calvo, A., Canosa, A., Moglia, C.*, et al.* (2013). Pathogenic VCP mutations induce mitochondrial uncoupling and reduced ATP levels. Neuron *78*, 57-64.

Bateman, A., and Bennett, H.P. (2009). The granulin gene family: from cancer to dementia. BioEssays : news and reviews in molecular, cellular and developmental biology *31*, 1245-1254.

Belzil, V.V., Bauer, P.O., Prudencio, M., Gendron, T.F., Stetler, C.T., Yan, I.K., Pregent, L., Daughrity, L., Baker, M.C., Rademakers, R.*, et al.* (2013). Reduced C9orf72 gene expression in c9FTD/ALS is caused by histone trimethylation, an epigenetic event detectable in blood. Acta neuropathologica *126*, 895-905.

Bendotti, C., Marino, M., Cheroni, C., Fontana, E., Crippa, V., Poletti, A., and De Biasi, S. (2012). Dysfunction of constitutive and inducible ubiquitin-proteasome system in amyotrophic lateral sclerosis: implication for protein aggregation and immune response. Progress in neurobiology *97*, 101-126.

Bensimon, G., Lacomblez, L., and Meininger, V. (1994). A controlled trial of riluzole in amyotrophic lateral sclerosis. ALS/Riluzole Study Group. The New England journal of medicine *330*, 585-591.

Bentmann, E., Neumann, M., Tahirovic, S., Rodde, R., Dormann, D., and Haass, C. (2012). Requirements for stress granule recruitment of fused in sarcoma (FUS) and TAR DNA-binding protein of 43 kDa (TDP-43). The Journal of biological chemistry *287*, 23079-23094.

Berlin, I., Higginbotham, K.M., Dise, R.S., Sierra, M.I., and Nash, P.D. (2010a). The deubiquitinating enzyme USP8 promotes trafficking and degradation of the chemokine receptor 4 at the sorting endosome. The Journal of biological chemistry *285*, 37895-37908.

Berlin, I., Schwartz, H., and Nash, P.D. (2010b). Regulation of epidermal growth factor receptor ubiquitination and trafficking by the USP8.STAM complex. The Journal of biological chemistry *285*, 34909-34921.

Bernardi, R., and Pandolfi, P.P. (2007). Structure, dynamics and functions of promyelocytic leukaemia nuclear bodies. Nature reviews Molecular cell biology *8*, 1006-1016.

Bilican, B., Serio, A., Barmada, S.J., Nishimura, A.L., Sullivan, G.J., Carrasco, M., Phatnani, H.P., Puddifoot, C.A., Story, D., Fletcher, J*., et al.* (2012). Mutant induced pluripotent stem cell lines recapitulate aspects of TDP-43 proteinopathies and reveal cell-specific vulnerability. Proceedings of the National Academy of Sciences of the United States of America *109*, 5803-5808.

Blokhuis, A.M., Groen, E.J., Koppers, M., van den Berg, L.H., and Pasterkamp, R.J. (2013). Protein aggregation in amyotrophic lateral sclerosis. Acta neuropathologica *125*, 777-794.

Bose, J.K., Huang, C.C., and Shen, C.K. (2011). Regulation of autophagy by neuropathological protein TDP-43. The Journal of biological chemistry *286*, 44441-44448.

Bose, J.K., Wang, I.F., Hung, L., Tarn, W.Y., and Shen, C.K. (2008). TDP-43 overexpression enhances exon 7 inclusion during the survival of motor neuron pre-mRNA splicing. The Journal of biological chemistry *283*, 28852-28859.

Bowers, K., Piper, S.C., Edeling, M.A., Gray, S.R., Owen, D.J., Lehner, P.J., and Luzio, J.P. (2006). Degradation of endocytosed epidermal growth factor and virally ubiquitinated major histocompatibility complex class I is independent of mammalian ESCRTII. The Journal of biological chemistry *281*, 5094-5105.

Braak, H., Ludolph, A., Thal, D.R., and Del Tredici, K. (2010). Amyotrophic lateral sclerosis: dash-like accumulation of phosphorylated TDP-43 in somatodendritic and axonal compartments of somatomotor neurons of the lower brainstem and spinal cord. Acta neuropathologica *120*, 67-74.

Brady, O.A., Meng, P., Zheng, Y., Mao, Y., and Hu, F. (2011). Regulation of TDP-43 aggregation by phosphorylation and p62/SQSTM1. Journal of neurochemistry *116*, 248-259.

Brandmeir, N.J., Geser, F., Kwong, L.K., Zimmerman, E., Qian, J., Lee, V.M., and Trojanowski, J.Q. (2008). Severe subcortical TDP-43 pathology in sporadic frontotemporal lobar degeneration with motor neuron disease. Acta neuropathologica *115*, 123-131.

Brettschneider, J., Van Deerlin, V.M., Robinson, J.L., Kwong, L., Lee, E.B., Ali, Y.O., Safren, N., Monteiro, M.J., Toledo, J.B., Elman, L*., et al.* (2012). Pattern of ubiquilin pathology in ALS and FTLD indicates presence of C9ORF72 hexanucleotide expansion. Acta neuropathologica *123*, 825-839.

Bruzzone, F., Vallarino, M., Berruti, G., and Angelini, C. (2008). Expression of the deubiquitinating enzyme mUBPy in the mouse brain. Brain research *1195*, 56-66.

Buchan, J.R., and Parker, R. (2009). Eukaryotic stress granules: the ins and outs of translation. Molecular cell *36*, 932-941.

Buchwald, G., van der Stoop, P., Weichenrieder, O., Perrakis, A., van Lohuizen, M., and Sixma, T.K. (2006). Structure and E3-ligase activity of the Ring-Ring complex of polycomb proteins Bmi1 and Ring1b. The EMBO journal *25*, 2465-2474.

Budini, M., Baralle, F.E., and Buratti, E. (2014). Targeting TDP-43 in neurodegenerative diseases. Expert opinion on therapeutic targets *18*, 617-632.

Budini, M., and Buratti, E. (2011). TDP-43 autoregulation: implications for disease. Journal of molecular neuroscience : MN *45*, 473-479.

Buratti, E., and Baralle, F.E. (2001). Characterization and functional implications of the RNA binding properties of nuclear factor TDP-43, a novel splicing regulator of CFTR exon 9. The Journal of biological chemistry *276*, 36337-36343.

Buratti, E., and Baralle, F.E. (2008). Multiple roles of TDP-43 in gene expression, splicing regulation, and human disease. Frontiers in bioscience : a journal and virtual library *13*, 867-878.

Buratti, E., and Baralle, F.E. (2010). The multiple roles of TDP-43 in pre-mRNA processing and gene expression regulation. RNA biology *7*, 420-429.

Buratti, E., and Baralle, F.E. (2012). TDP-43: gumming up neurons through protein-protein and protein-RNA interactions. Trends in biochemical sciences *37*, 237-247.

Buratti, E., Brindisi, A., Giombi, M., Tisminetzky, S., Ayala, Y.M., and Baralle, F.E. (2005). TDP-43 binds heterogeneous nuclear ribonucleoprotein A/B through its C-terminal tail: an important region for the inhibition of cystic fibrosis transmembrane conductance regulator exon 9 splicing. The Journal of biological chemistry *280*, 37572-37584.

Buratti, E., De Conti, L., Stuani, C., Romano, M., Baralle, M., and Baralle, F. (2010). Nuclear factor TDP-43 can affect selected microRNA levels. The FEBS journal *277*, 2268-2281.

Buratti, E., Dork, T., Zuccato, E., Pagani, F., Romano, M., and Baralle, F.E. (2001). Nuclear factor TDP-43 and SR proteins promote in vitro and in vivo CFTR exon 9 skipping. The EMBO journal *20*, 1774-1784.

Caccamo, A., Majumder, S., Deng, J.J., Bai, Y., Thornton, F.B., and Oddo, S. (2009). Rapamycin rescues TDP-43 mislocalization and the associated low molecular mass neurofilament instability. The Journal of biological chemistry *284*, 27416-27424.

Cadwell, K., and Coscoy, L. (2005). Ubiquitination on nonlysine residues by a viral E3 ubiquitin ligase. Science *309*, 127-130.

Cai, J., Crotty, T.M., Reichert, E., Carraway, K.L., 3rd, Stafforini, D.M., and Topham, M.K. (2010). Diacylglycerol kinase delta and protein kinase C(alpha) modulate epidermal growth factor receptor abundance and degradation through ubiquitin-specific protease 8. The Journal of biological chemistry *285*, 6952-6959.

Cairns, N.J., Bigio, E.H., Mackenzie, I.R., Neumann, M., Lee, V.M., Hatanpaa, K.J., White, C.L., 3rd, Schneider, J.A., Grinberg, L.T., Halliday, G., *et al.* (2007). Neuropathologic diagnostic and nosologic criteria for frontotemporal lobar degeneration: consensus of the Consortium for Frontotemporal Lobar Degeneration. Acta neuropathologica *114*, 5-22.

Cao, Z., Wu, X., Yen, L., Sweeney, C., and Carraway, K.L., 3rd (2007). Neuregulin-induced ErbB3 downregulation is mediated by a protein stability cascade involving the E3 ubiquitin ligase Nrdp1. Molecular and cellular biology *27*, 2180-2188.

Carlsten, J.O., Zhu, X., and Gustafsson, C.M. (2013). The multitalented Mediator complex. Trends in biochemical sciences *38*, 531-537.

Casafont, I., Bengoechea, R., Tapia, O., Berciano, M.T., and Lafarga, M. (2009). TDP-43 localizes in mRNA transcription and processing sites in mammalian neurons. Journal of structural biology *167*, 235-241.

Cassel, J.A., and Reitz, A.B. (2013). Ubiquilin-2 (UBQLN2) binds with high affinity to the C-terminal region of TDP-43 and modulates TDP-43 levels in H4 cells: characterization of inhibition by nucleic acids and 4-aminoquinolines. Biochimica et biophysica acta *1834*, 964-971.

Castello, A., Fischer, B., Eichelbaum, K., Horos, R., Beckmann, B.M., Strein, C., Davey, N.E., Humphreys, D.T., Preiss, T., Steinmetz, L.M., *et al.* (2012). Insights into RNA biology from an atlas of mammalian mRNA-binding proteins. Cell *149*, 1393-1406.

Caughey, B., and Lansbury, P.T. (2003). Protofibrils, pores, fibrils, and neurodegeneration: separating the responsible protein aggregates from the innocent bystanders. Annual review of neuroscience *26*, 267-298.

Chen, H.J., Anagnostou, G., Chai, A., Withers, J., Morris, A., Adhikaree, J., Pennetta, G., and de Belleroche, J.S. (2010). Characterization of the properties of a novel mutation in VAPB in familial amyotrophic lateral sclerosis. The Journal of biological chemistry *285*, 40266-40281.

Chen, Y.Z., Bennett, C.L., Huynh, H.M., Blair, I.P., Puls, I., Irobi, J., Dierick, I., Abel, A., Kennerson, M.L., Rabin, B.A.*, et al.* (2004). DNA/RNA helicase gene mutations in a form of juvenile amyotrophic lateral sclerosis (ALS4). American journal of human genetics *74*, 1128-1135.

Choksi, D.K., Roy, B., Chatterjee, S., Yusuff, T., Bakhoum, M.F., Sengupta, U., Ambegaokar, S., Kayed, R., and Jackson, G.R. (2014). TDP-43 Phosphorylation by casein kinase Iepsilon promotes oligomerization and enhances toxicity in vivo. Human molecular genetics *23*, 1025-1035.

Chow, C.Y., Landers, J.E., Bergren, S.K., Sapp, P.C., Grant, A.E., Jones, J.M., Everett, L., Lenk, G.M., McKenna-Yasek, D.M., Weisman, L.S.*, et al.* (2009). Deleterious variants of FIG4, a phosphoinositide phosphatase, in patients with ALS. American journal of human genetics *84*, 85-88.

Chow, C.Y., Zhang, Y., Dowling, J.J., Jin, N., Adamska, M., Shiga, K., Szigeti, K., Shy, M.E., Li, J., Zhang, X.*, et al.* (2007). Mutation of FIG4 causes neurodegeneration in the pale tremor mouse and patients with CMT4J. Nature *448*, 68-72.

Christensen, D.E., Brzovic, P.S., and Klevit, R.E. (2007). E2-BRCA1 RING interactions dictate synthesis of mono- or specific polyubiquitin chain linkages. Nature structural & molecular biology *14*, 941-948.

Ciechanover, A., and Ben-Saadon, R. (2004). N-terminal ubiquitination: more protein substrates join in. Trends in cell biology *14*, 103-106.

Cioce, M., and Lamond, A.I. (2005). Cajal bodies: a long history of discovery. Annual review of cell and developmental biology *21*, 105-131.

Ciura, S., Lattante, S., Le Ber, I., Latouche, M., Tostivint, H., Brice, A., and Kabashi, E. (2013). Loss of function of C9orf72 causes motor deficits in a zebrafish model of amyotrophic lateral sclerosis. Annals of neurology *74*, 180-187.

Clague, M.J., Coulson, J.M., and Urbe, S. (2012). Cellular functions of the DUBs. Journal of cell science *125*, 277-286.

Clague, M.J., and Urbe, S. (2010). Ubiquitin: same molecule, different degradation pathways. Cell *143*, 682-685.

Cohen, T.J., Hwang, A.W., Unger, T., Trojanowski, J.Q., and Lee, V.M. (2012). Redox signalling directly regulates TDP-43 via cysteine oxidation and disulphide cross-linking. The EMBO journal *31*, 1241-1252.

Cohen, T.J., Lee, V.M., and Trojanowski, J.Q. (2011). TDP-43 functions and pathogenic mechanisms implicated in TDP-43 proteinopathies. Trends in molecular medicine *17*, 659-667.

Collins, M., Riascos, D., Kovalik, T., An, J., Krupa, K., Krupa, K., Hood, B.L., Conrads, T.P., Renton, A.E., Traynor, B.J.*, et al.* (2012). The RNA-binding motif 45 (RBM45) protein accumulates in inclusion bodies in amyotrophic lateral sclerosis (ALS) and frontotemporal lobar degeneration with TDP-43 inclusions (FTLD-TDP) patients. Acta neuropathologica *124*, 717-732.

Colombrita, C., Onesto, E., Megiorni, F., Pizzuti, A., Baralle, F.E., Buratti, E., Silani, V., and Ratti, A. (2012). TDP-43 and FUS RNA-binding proteins bind distinct sets of cytoplasmic messenger RNAs and differently regulate their post-transcriptional fate in motoneuron-like cells. The Journal of biological chemistry *287*, 15635-15647.

Colombrita, C., Zennaro, E., Fallini, C., Weber, M., Sommacal, A., Buratti, E., Silani, V., and Ratti, A. (2009). TDP-43 is recruited to stress granules in conditions of oxidative insult. Journal of neurochemistry *111*, 1051-1061.

Couthouis, J., Hart, M.P., Erion, R., King, O.D., Diaz, Z., Nakaya, T., Ibrahim, F., Kim, H.J., Mojsilovic-Petrovic, J., Panossian, S.*, et al.* (2012). Evaluating the role of the FUS/TLS-related gene EWSR1 in amyotrophic lateral sclerosis. Human molecular genetics *21*, 2899-2911.

Couthouis, J., Hart, M.P., Shorter, J., DeJesus-Hernandez, M., Erion, R., Oristano, R., Liu, A.X., Ramos, D., Jethava, N., Hosangadi, D.*, et al.* (2011). A yeast functional screen predicts new candidate ALS disease genes. Proceedings of the National Academy of Sciences of the United States of America *108*, 20881-20890.

Cox, L.E., Ferraiuolo, L., Goodall, E.F., Heath, P.R., Higginbottom, A., Mortiboys, H., Hollinger, H.C., Hartley, J.A., Brockington, A., Burness, C.E., *et al.* (2010). Mutations in CHMP2B in lower motor neuron predominant amyotrophic lateral sclerosis (ALS). PloS one *5*, e9872.

Crippa, V., Sau, D., Rusmini, P., Boncoraglio, A., Onesto, E., Bolzoni, E., Galbiati, M., Fontana, E., Marino, M., Carra, S., *et al.* (2010). The small heat shock protein B8 (HspB8) promotes autophagic removal of misfolded proteins involved in amyotrophic lateral sclerosis (ALS). Human molecular genetics *19*, 3440-3456.

Cruts, M., Gijselinck, I., van der Zee, J., Engelborghs, S., Wils, H., Pirici, D., Rademakers, R., Vandenberghe, R., Dermaut, B., Martin, J.J., *et al.* (2006). Null mutations in progranulin cause ubiquitin-positive frontotemporal dementia linked to chromosome 17q21. Nature *442*, 920-924.

Cushman, M., Johnson, B.S., King, O.D., Gitler, A.D., and Shorter, J. (2010). Prion-like disorders: blurring the divide between transmissibility and infectivity. Journal of cell science *123*, 1191-1201.

D'Ambrogio, A., Buratti, E., Stuani, C., Guarnaccia, C., Romano, M., Ayala, Y.M., and Baralle, F.E. (2009). Functional mapping of the interaction between TDP-43 and hnRNP A2 in vivo. Nucleic acids research *37*, 4116-4126.

Dammer, E.B., Fallini, C., Gozal, Y.M., Duong, D.M., Rossoll, W., Xu, P., Lah, J.J., Levey, A.I., Peng, J., Bassell, G.J., *et al.* (2012). Coaggregation of RNA-binding proteins in a model of TDP-43 proteinopathy with selective RGG motif methylation and a role for RRM1 ubiquitination. PloS one *7*, e38658.

Daoud, H., Zhou, S., Noreau, A., Sabbagh, M., Belzil, V., Dionne-Laporte, A., Tranchant, C., Dion, P., and Rouleau, G.A. (2012). Exome sequencing reveals SPG11 mutations causing juvenile ALS. Neurobiology of aging *33*, 839 e835-839.

David, Y., Ziv, T., Admon, A., and Navon, A. (2010). The E2 ubiquitin-conjugating enzymes direct polyubiquitination to preferred lysines. The Journal of biological chemistry *285*, 8595-8604.

Davidson, Y., Kelley, T., Mackenzie, I.R., Pickering-Brown, S., Du Plessis, D., Neary, D., Snowden, J.S., and Mann, D.M. (2007). Ubiquitinated pathological lesions in frontotemporal lobar degeneration contain the TAR DNA-binding protein, TDP-43. Acta neuropathologica *113*, 521-533.

De Ceuninck, L., Wauman, J., Masschaele, D., Peelman, F., and Tavernier, J. (2013). Reciprocal cross-regulation between RNF41 and USP8 controls cytokine receptor sorting and processing. Journal of cell science *126*, 3770-3781.

De Vos, K.J., Morotz, G.M., Stoica, R., Tudor, E.L., Lau, K.F., Ackerley, S., Warley, A., Shaw, C.E., and Miller, C.C. (2012). VAPB interacts with the mitochondrial protein PTPIP51 to regulate calcium homeostasis. Human molecular genetics *21*, 1299-1311.

Deane, C.M., Salwinski, L., Xenarios, I., and Eisenberg, D. (2002). Protein interactions: two methods for assessment of the reliability of high throughput observations. Molecular & cellular proteomics : MCP *1*, 349-356.

Debonneville, C., and Staub, O. (2004). Participation of the ubiquitin-conjugating enzyme UBE2E3 in Nedd4-2-dependent regulation of the epithelial Na+ channel. Molecular and cellular biology *24*, 2397-2409.

DeJesus-Hernandez, M., Mackenzie, I.R., Boeve, B.F., Boxer, A.L., Baker, M., Rutherford, N.J., Nicholson, A.M., Finch, N.A., Flynn, H., Adamson, J., *et al.* (2011). Expanded GGGGCC hexanucleotide repeat in noncoding region of C9ORF72 causes chromosome 9p-linked FTD and ALS. Neuron *72*, 245-256.

Del Bo, R., Tiloca, C., Pensato, V., Corrado, L., Ratti, A., Ticozzi, N., Corti, S., Castellotti, B., Mazzini, L., Soraru, G., *et al.* (2011). Novel optineurin mutations in patients with familial and sporadic amyotrophic lateral sclerosis. Journal of neurology, neurosurgery, and psychiatry *82*, 1239-1243.

Deng, H.X., Bigio, E.H., Zhai, H., Fecto, F., Ajroud, K., Shi, Y., Yan, J., Mishra, M., Ajroud-Driss, S., Heller, S., *et al.* (2011a). Differential involvement of optineurin in amyotrophic lateral sclerosis with or without SOD1 mutations. Archives of neurology *68*, 1057-1061.

Deng, H.X., Chen, W., Hong, S.T., Boycott, K.M., Gorrie, G.H., Siddique, N., Yang, Y., Fecto, F., Shi, Y., Zhai, H., *et al.* (2011b). Mutations in UBQLN2 cause dominant X-linked juvenile and adult-onset ALS and ALS/dementia. Nature *477*, 211-215.

Deshaies, R.J., and Joazeiro, C.A. (2009). RING domain E3 ubiquitin ligases. Annual review of biochemistry *78*, 399-434.

Dewey, C.M., Cenik, B., Sephton, C.F., Dries, D.R., Mayer, P., 3rd, Good, S.K., Johnson, B.A., Herz, J., and Yu, G. (2011). TDP-43 is directed to stress granules by sorbitol, a novel physiological osmotic and oxidative stressor. Molecular and cellular biology *31*, 1098-1108.

Dewey, C.M., Cenik, B., Sephton, C.F., Johnson, B.A., Herz, J., and Yu, G. (2012). TDP-43 aggregation in neurodegeneration: are stress granules the key? Brain research *1462*, 16-25.

Dikic, I., Wakatsuki, S., and Walters, K.J. (2009). Ubiquitin-binding domains - from structures to functions. Nature reviews Molecular cell biology *10*, 659-671.

Donnelly, C.J., Zhang, P.W., Pham, J.T., Heusler, A.R., Mistry, N.A., Vidensky, S., Daley, E.L., Poth, E.M., Hoover, B., Fines, D.M.*, et al.* (2013). RNA toxicity from the ALS/FTD C9ORF72 expansion is mitigated by antisense intervention. Neuron *80*, 415-428.

Dormann, D., Capell, A., Carlson, A.M., Shankaran, S.S., Rodde, R., Neumann, M., Kremmer, E., Matsuwaki, T., Yamanouchi, K., Nishihara, M.*, et al.* (2009). Proteolytic processing of TAR DNA binding protein-43 by caspases produces C-terminal fragments with disease defining properties independent of progranulin. Journal of neurochemistry *110*, 1082-1094.

Dormann, D., Rodde, R., Edbauer, D., Bentmann, E., Fischer, I., Hruscha, A., Than, M.E., Mackenzie, I.R.A., Capell, A., Schmid, B.*, et al.* (2010). ALS-associated fused in sarcoma (FUS) mutations disrupt Transportin-mediated nuclear import. Embo Journal *29*, 2841-2857.

Dreumont, N., Hardy, S., Behm-Ansmant, I., Kister, L., Branlant, C., Stevenin, J., and Bourgeois, C.F. (2010). Antagonistic factors control the unproductive splicing of SC35 terminal intron. Nucleic acids research *38*, 1353-1366.

Dwane, S., Durack, E., O'Connor, R., and Kiely, P.A. (2014). RACK1 promotes neurite outgrowth by scaffolding AGAP2 to FAK. Cellular signalling *26*, 9-18.

Dziuba, N., Ferguson, M.R., O'Brien, W.A., Sanchez, A., Prussia, A.J., McDonald, N.J., Friedrich, B.M., Li, G., Shaw, M.W., Sheng, J.*, et al.* (2012). Identification of cellular proteins required for replication of human immunodeficiency virus type 1. AIDS research and human retroviruses *28*, 1329-1339.

Elden, A.C., Kim, H.J., Hart, M.P., Chen-Plotkin, A.S., Johnson, B.S., Fang, X., Armakola, M., Geser, F., Greene, R., Lu, M.M.*, et al.* (2010). Ataxin-2 intermediate-length polyglutamine expansions are associated with increased risk for ALS. Nature *466*, 1069-1075.

Fallini, C., Bassell, G.J., and Rossoll, W. (2012). The ALS disease protein TDP-43 is actively transported in motor neuron axons and regulates axon outgrowth. Human molecular genetics *21*, 3703-3718.

Farg, M.A., Sundaramoorthy, V., Sultana, J.M., Yang, S., Atkinson, R.A., Levina, V., Halloran, M.A., Gleeson, P.A., Blair, I.P., Soo, K.Y.*, et al.* (2014). C9ORF72, implicated in amytrophic lateral sclerosis and frontotemporal dementia, regulates endosomal trafficking. Human molecular genetics *23*, 3579-3595.

Fecto, F., Yan, J., Vemula, S.P., Liu, E., Yang, Y., Chen, W., Zheng, J.G., Shi, Y., Siddique, N., Arrat, H.*, et al.* (2011). SQSTM1 mutations in familial and sporadic amyotrophic lateral sclerosis. Archives of neurology *68*, 1440-1446.

Ferguson, C.J., Lenk, G.M., and Meisler, M.H. (2009). Defective autophagy in neurons and astrocytes from mice deficient in PI(3,5)P2. Human molecular genetics *18*, 4868-4878.

Fiesel, F.C. (2010). Physiological function and pathogenic impact of the amyotrophic lateral sclerosis and frontotemporal dementia-associated protein TDP-43. In Fakultät für Biologie (Eberhard Karls Universität Tübingen), pp. 216.

Fiesel, F.C., Schurr, C., Weber, S.S., and Kahle, P.J. (2011). TDP-43 knockdown impairs neurite outgrowth dependent on its target histone deacetylase 6. Molecular neurodegeneration *6*, 64.

Fiesel, F.C., Voigt, A., Weber, S.S., Van den Haute, C., Waldenmaier, A., Gorner, K., Walter, M., Anderson, M.L., Kern, J.V., Rasse, T.M.*, et al.* (2010). Knockdown of transactive response DNA-binding protein (TDP-43) downregulates histone deacetylase 6. The EMBO journal *29*, 209-221.

Fiesel, F.C., Weber, S.S., Supper, J., Zell, A., and Kahle, P.J. (2012). TDP-43 regulates global translational yield by splicing of exon junction complex component SKAR. Nucleic acids research *40*, 2668-2682.

Filimonenko, M., Stuffers, S., Raiborg, C., Yamamoto, A., Malerod, L., Fisher, E.M., Isaacs, A., Brech, A., Stenmark, H., and Simonsen, A. (2007). Functional multivesicular bodies are required for autophagic

clearance of protein aggregates associated with neurodegenerative disease. The Journal of cell biology *179*, 485-500.

Freibaum, B.D., Chitta, R.K., High, A.A., and Taylor, J.P. (2010). Global analysis of TDP-43 interacting proteins reveals strong association with RNA splicing and translation machinery. Journal of proteome research *9*, 1104-1120.

Fuentealba, R.A., Udan, M., Bell, S., Wegorzewska, I., Shao, J., Diamond, M.I., Weihl, C.C., and Baloh, R.H. (2010). Interaction with polyglutamine aggregates reveals a Q/N-rich domain in TDP-43. The Journal of biological chemistry *285*, 26304-26314.

Fukuda, T., Yamagata, K., Fujiyama, S., Matsumoto, T., Koshida, I., Yoshimura, K., Mihara, M., Naitou, M., Endoh, H., Nakamura, T.*, et al.* (2007). DEAD-box RNA helicase subunits of the Drosha complex are required for processing of rRNA and a subset of microRNAs. Nature cell biology *9*, 604-611.

Furukawa, Y., Kaneko, K., Watanabe, S., Yamanaka, K., and Nukina, N. (2011). A seeding reaction recapitulates intracellular formation of Sarkosyl-insoluble transactivation response element (TAR) DNA-binding protein-43 inclusions. The Journal of biological chemistry *286*, 18664-18672.

Gandin, V., Senft, D., Topisirovic, I., and Ronai, Z.A. (2013). RACK1 Function in Cell Motility and Protein Synthesis. Genes & cancer *4*, 369-377.

Gao, J., Xia, L., Lu, M., Zhang, B., Chen, Y., Xu, R., and Wang, L. (2012). TM7SF1 (GPR137B): a novel lysosome integral membrane protein. Molecular biology reports *39*, 8883-8889.

Geisler, S., Holmstrom, K.M., Skujat, D., Fiesel, F.C., Rothfuss, O.C., Kahle, P.J., and Springer, W. (2010). PINK1/Parkin-mediated mitophagy is dependent on VDAC1 and p62/SQSTM1. Nature cell biology *12*, 119-131.

Geser, F., Lee, V.M., and Trojanowski, J.Q. (2010). Amyotrophic lateral sclerosis and frontotemporal lobar degeneration: a spectrum of TDP-43 proteinopathies. Neuropathology : official journal of the Japanese Society of Neuropathology *30*, 103-112.

Geser, F., Winton, M.J., Kwong, L.K., Xu, Y., Xie, S.X., Igaz, L.M., Garruto, R.M., Perl, D.P., Galasko, D., Lee, V.M.*, et al.* (2008). Pathological TDP-43 in parkinsonism-dementia complex and amyotrophic lateral sclerosis of Guam. Acta neuropathologica *115*, 133-145.

Ghazi-Noori, S., Froud, K.E., Mizielinska, S., Powell, C., Smidak, M., Fernandez de Marco, M., O'Malley, C., Farmer, M., Parkinson, N., Fisher, E.M.*, et al.* (2012). Progressive neuronal inclusion formation and axonal degeneration in CHMP2B mutant transgenic mice. Brain : a journal of neurology *135*, 819-832.

Gijselinck, I., Van Broeckhoven, C., and Cruts, M. (2008). Granulin mutations associated with frontotemporal lobar degeneration and related disorders: an update. Human mutation *29*, 1373-1386.

Gijselinck, I., Van Langenhove, T., van der Zee, J., Sleegers, K., Philtjens, S., Kleinberger, G., Janssens, J., Bettens, K., Van Cauwenberghe, C., Pereson, S.*, et al.* (2012). A C9orf72 promoter repeat expansion in a Flanders-Belgian cohort with disorders of the frontotemporal lobar degeneration-amyotrophic lateral sclerosis spectrum: a gene identification study. Lancet neurology *11*, 54-65.

Giordana, M.T., Piccinini, M., Grifoni, S., De Marco, G., Vercellino, M., Magistrello, M., Pellerino, A., Buccinna, B., Lupino, E., and Rinaudo, M.T. (2010). TDP-43 redistribution is an early event in sporadic amyotrophic lateral sclerosis. Brain pathology *20*, 351-360.

Giot, L., Bader, J.S., Brouwer, C., Chaudhuri, A., Kuang, B., Li, Y., Hao, Y.L., Ooi, C.E., Godwin, B., Vitols, E.*, et al.* (2003). A protein interaction map of Drosophila melanogaster. Science *302*, 1727-1736.

Gitcho, M.A., Strider, J., Carter, D., Taylor-Reinwald, L., Forman, M.S., Goate, A.M., and Cairns, N.J. (2009). VCP mutations causing frontotemporal lobar degeneration disrupt localization of TDP-43 and induce cell death. The Journal of biological chemistry *284*, 12384-12398.

Gnesutta, N., Ceriani, M., Innocenti, M., Mauri, I., Zippel, R., Sturani, E., Borgonovo, B., Berruti, G., and Martegani, E. (2001). Cloning and characterization of mouse UBPy, a deubiquitinating enzyme that interacts with the ras guanine nucleotide exchange factor CDC25(Mm)/Ras-GRF1. The Journal of biological chemistry *276*, 39448-39454.

Godena, V.K., Romano, G., Romano, M., Appocher, C., Klima, R., Buratti, E., Baralle, F.E., and Feiguin, F. (2011). TDP-43 regulates Drosophila neuromuscular junctions growth by modulating Futsch/MAP1B levels and synaptic microtubules organization. PloS one *6*, e17808.

Goldberg, A.L. (2003). Protein degradation and protection against misfolded or damaged proteins. Nature *426*, 895-899.

Gordon, P.H. (2013). Amyotrophic Lateral Sclerosis: An update for 2013 Clinical Features, Pathophysiology, Management and Therapeutic Trials. Aging and disease *4*, 295-310.

Greenway, M.J., Andersen, P.M., Russ, C., Ennis, S., Cashman, S., Donaghy, C., Patterson, V., Swingler, R., Kieran, D., Prehn, J.*, et al.* (2006). ANG mutations segregate with familial and 'sporadic' amyotrophic lateral sclerosis. Nature genetics *38*, 411-413.

Gregory, J.M., Barros, T.P., Meehan, S., Dobson, C.M., and Luheshi, L.M. (2012). The aggregation and neurotoxicity of TDP-43 and its ALS-associated 25 kDa fragment are differentially affected by molecular chaperones in Drosophila. PloS one *7*, e31899.

Gregory, R.I., Yan, K.P., Amuthan, G., Chendrimada, T., Doratotaj, B., Cooch, N., and Shiekhattar, R. (2004). The Microprocessor complex mediates the genesis of microRNAs. Nature *432*, 235-240.

Guo, W., Chen, Y., Zhou, X., Kar, A., Ray, P., Chen, X., Rao, E.J., Yang, M., Ye, H., Zhu, L.*, et al.* (2011). An ALS-associated mutation affecting TDP-43 enhances protein aggregation, fibril formation and neurotoxicity. Nature structural & molecular biology *18*, 822-830.

Haass, C., and Selkoe, D.J. (2007). Soluble protein oligomers in neurodegeneration: lessons from the Alzheimer's amyloid beta-peptide. Nature reviews Molecular cell biology *8*, 101-112.

Hadano, S., Hand, C.K., Osuga, H., Yanagisawa, Y., Otomo, A., Devon, R.S., Miyamoto, N., Showguchi-Miyata, J., Okada, Y., Singaraja, R.*, et al.* (2001). A gene encoding a putative GTPase regulator is mutated in familial amyotrophic lateral sclerosis 2. Nature genetics *29*, 166-173.

Halliday, G., Bigio, E.H., Cairns, N.J., Neumann, M., Mackenzie, I.R., and Mann, D.M. (2012). Mechanisms of disease in frontotemporal lobar degeneration: gain of function versus loss of function effects. Acta neuropathologica *124*, 373-382.

Hand, C.K., Khoris, J., Salachas, F., Gros-Louis, F., Lopes, A.A., Mayeux-Portas, V., Brewer, C.G., Brown, R.H., Jr., Meininger, V., Camu, W.*, et al.* (2002). A novel locus for familial amyotrophic lateral sclerosis, on chromosome 18q. American journal of human genetics *70*, 251-256.

Handwerger, K.E., and Gall, J.G. (2006). Subnuclear organelles: new insights into form and function. Trends in cell biology *16*, 19-26.

Harkiolaki, M., Lewitzky, M., Gilbert, R.J., Jones, E.Y., Bourette, R.P., Mouchiroud, G., Sondermann, H., Moarefi, I., and Feller, S.M. (2003). Structural basis for SH3 domain-mediated high-affinity binding between Mona/Gads and SLP-76. The EMBO journal *22*, 2571-2582.

Harms, M., Benitez, B.A., Cairns, N., Cooper, B., Cooper, P., Mayo, K., Carrell, D., Faber, K., Williamson, J., Bird, T.*, et al.* (2013). C9orf72 hexanucleotide repeat expansions in clinical Alzheimer disease. JAMA neurology *70*, 736-741.

Hasdemir, B., Murphy, J.E., Cottrell, G.S., and Bunnett, N.W. (2009). Endosomal deubiquitinating enzymes control ubiquitination and down-regulation of protease-activated receptor 2. The Journal of biological chemistry *284*, 28453-28466.

Hasegawa, M., Arai, T., Nonaka, T., Kametani, F., Yoshida, M., Hashizume, Y., Beach, T.G., Buratti, E., Baralle, F., Morita, M.*, et al.* (2008). Phosphorylated TDP-43 in frontotemporal lobar degeneration and amyotrophic lateral sclerosis. Annals of neurology *64*, 60-70.

Hatanpaa, K.J., Bigio, E.H., Cairns, N.J., Womack, K.B., Weintraub, S., Morris, J.C., Foong, C., Xiao, G., Hladik, C., Mantanona, T.Y.*, et al.* (2008). TAR DNA-binding protein 43 immunohistochemistry reveals extensive neuritic pathology in FTLD-U: a midwest-southwest consortium for FTLD study. Journal of neuropathology and experimental neurology *67*, 271-279.

He, Z., and Bateman, A. (2003). Progranulin (granulin-epithelin precursor, PC-cell-derived growth factor, acrogranin) mediates tissue repair and tumorigenesis. Journal of molecular medicine *81*, 600-612.

He, Z., Ismail, A., Kriazhev, L., Sadvakassova, G., and Bateman, A. (2002). Progranulin (PC-cell-derived growth factor/acrogranin) regulates invasion and cell survival. Cancer research *62*, 5590-5596.

Hebron, M.L., Lonskaya, I., Sharpe, K., Weerasinghe, P.P., Algarzae, N.K., Shekoyan, A.R., and Moussa, C.E. (2013). Parkin ubiquitinates Tar-DNA binding protein-43 (TDP-43) and promotes its cytosolic

accumulation via interaction with histone deacetylase 6 (HDAC6). The Journal of biological chemistry *288*, 4103-4115.

Heutink, P., Jansen, I.E., and Lynes, E.M. (2014). C9orf72; abnormal RNA expression is the key. Experimental neurology.

Hicke, L. (2001). Protein regulation by monoubiquitin. Nature reviews Molecular cell biology *2*, 195-201.

Hislop, J.N., Henry, A.G., Marchese, A., and von Zastrow, M. (2009). Ubiquitination regulates proteolytic processing of G protein-coupled receptors after their sorting to lysosomes. The Journal of biological chemistry *284*, 19361-19370.

Hodges, J.R., Davies, R., Xuereb, J., Kril, J., and Halliday, G. (2003). Survival in frontotemporal dementia. Neurology *61*, 349-354.

Hoeller, D., Hecker, C.M., Wagner, S., Rogov, V., Dotsch, V., and Dikic, I. (2007). E3-independent monoubiquitination of ubiquitin-binding proteins. Molecular cell *26*, 891-898.

Hoffman, C.S., and Winston, F. (1987). A ten-minute DNA preparation from yeast efficiently releases autonomous plasmids for transformation of Escherichia coli. Gene *57*, 267-272.

Holm, I.E., Englund, E., Mackenzie, I.R., Johannsen, P., and Isaacs, A.M. (2007). A reassessment of the neuropathology of frontotemporal dementia linked to chromosome 3. Journal of neuropathology and experimental neurology *66*, 884-891.

Hong, S., Lee, S., Cho, S.G., and Kang, S. (2008). UbcH6 interacts with and ubiquitinates the SCA1 gene product ataxin-1. Biochemical and biophysical research communications *371*, 256-260.

Huang, C.C., Bose, J.K., Majumder, P., Lee, K.H., Huang, J.T., Huang, J.K., and Shen, C.K. (2014). Metabolism and mis-metabolism of the neuropathological signature protein TDP-43. Journal of cell science *127*, 3024-3038.

Huey, E.D., Putnam, K.T., and Grafman, J. (2006). A systematic review of neurotransmitter deficits and treatments in frontotemporal dementia. Neurology *66*, 17-22.

Hutton, M., Lendon, C.L., Rizzu, P., Baker, M., Froelich, S., Houlden, H., Pickering-Brown, S., Chakraverty, S., Isaacs, A., Grover, A*., et al.* (1998). Association of missense and 5'-splice-site mutations in tau with the inherited dementia FTDP-17. Nature *393*, 702-705.

Igaz, L.M., Kwong, L.K., Chen-Plotkin, A., Winton, M.J., Unger, T.L., Xu, Y., Neumann, M., Trojanowski, J.Q., and Lee, V.M. (2009). Expression of TDP-43 C-terminal Fragments in Vitro Recapitulates Pathological Features of TDP-43 Proteinopathies. The Journal of biological chemistry *284*, 8516-8524.

Igaz, L.M., Kwong, L.K., Lee, E.B., Chen-Plotkin, A., Swanson, E., Unger, T., Malunda, J., Xu, Y., Winton, M.J., Trojanowski, J.Q*., et al.* (2011). Dysregulation of the ALS-associated gene TDP-43 leads to neuronal death and degeneration in mice. The Journal of clinical investigation *121*, 726-738.

Igaz, L.M., Kwong, L.K., Xu, Y., Truax, A.C., Uryu, K., Neumann, M., Clark, C.M., Elman, L.B., Miller, B.L., Grossman, M*., et al.* (2008). Enrichment of C-terminal fragments in TAR DNA-binding protein-43 cytoplasmic inclusions in brain but not in spinal cord of frontotemporal lobar degeneration and amyotrophic lateral sclerosis. The American journal of pathology *173*, 182-194.

Iguchi, Y., Katsuno, M., Niwa, J., Yamada, S., Sone, J., Waza, M., Adachi, H., Tanaka, F., Nagata, K., Arimura, N*., et al.* (2009). TDP-43 depletion induces neuronal cell damage through dysregulation of Rho family GTPases. The Journal of biological chemistry *284*, 22059-22066.

Ihara, R., Matsukawa, K., Nagata, Y., Kunugi, H., Tsuji, S., Chihara, T., Kuranaga, E., Miura, M., Wakabayashi, T., Hashimoto, T*., et al.* (2013). RNA binding mediates neurotoxicity in the transgenic Drosophila model of TDP-43 proteinopathy. Human molecular genetics *22*, 4474-4484.

Imai, Y., Soda, M., and Takahashi, R. (2000). Parkin suppresses unfolded protein stress-induced cell death through its E3 ubiquitin-protein ligase activity. The Journal of biological chemistry *275*, 35661-35664.

Ingre, C., Pinto, S., Birve, A., Press, R., Danielsson, O., de Carvalho, M., Gudmundsson, G., and Andersen, P.M. (2013). No association between VAPB mutations and familial or sporadic ALS in Sweden, Portugal and Iceland. Amyotrophic lateral sclerosis & frontotemporal degeneration *14*, 620-627.

Inukai, Y., Nonaka, T., Arai, T., Yoshida, M., Hashizume, Y., Beach, T.G., Buratti, E., Baralle, F.E., Akiyama, H., Hisanaga, S*., et al.* (2008). Abnormal phosphorylation of Ser409/410 of TDP-43 in FTLD-U and ALS. FEBS letters *582*, 2899-2904.

Ishikura, S., Weissman, A.M., and Bonifacino, J.S. (2010). Serine residues in the cytosolic tail of the T-cell antigen receptor alpha-chain mediate ubiquitination and endoplasmic reticulum-associated degradation of the unassembled protein. The Journal of biological chemistry *285*, 23916-23924.

Ito, H., Nakamura, M., Komure, O., Ayaki, T., Wate, R., Maruyama, H., Nakamura, Y., Fujita, K., Kaneko, S., Okamoto, Y*., et al.* (2011). Clinicopathologic study on an ALS family with a heterozygous E478G optineurin mutation. Acta neuropathologica *122*, 223-229.

Ito, K., Adachi, S., Iwakami, R., Yasuda, H., Muto, Y., Seki, N., and Okano, Y. (2001). N-Terminally extended human ubiquitin-conjugating enzymes (E2s) mediate the ubiquitination of RING-finger proteins, ARA54 and RNF8. European journal of biochemistry / FEBS *268*, 2725-2732.

Ito, K., Kato, S., Matsuda, Y., Kimura, M., and Okano, Y. (1999). cDNA cloning, characterization, and chromosome mapping of UBE2E3 (alias UbcH9), encoding an N-terminally extended human ubiquitin-conjugating enzyme. Cytogenetics and cell genetics *84*, 99-104.

Jannot, G., Bajan, S., Giguere, N.J., Bouasker, S., Banville, I.H., Piquet, S., Hutvagner, G., and Simard, M.J. (2011). The ribosomal protein RACK1 is required for microRNA function in both C. elegans and humans. EMBO reports *12*, 581-586.

Janssens, J., and Van Broeckhoven, C. (2013). Pathological mechanisms underlying TDP-43 driven neurodegeneration in FTLD-ALS spectrum disorders. Human molecular genetics *22*, R77-87.

Jeronimo, C., Forget, D., Bouchard, A., Li, Q., Chua, G., Poitras, C., Therien, C., Bergeron, D., Bourassa, S., Greenblatt, J*., et al.* (2007). Systematic analysis of the protein interaction network for the human transcription machinery reveals the identity of the 7SK capping enzyme. Molecular cell *27*, 262-274.

Johnson, B.S., McCaffery, J.M., Lindquist, S., and Gitler, A.D. (2008). A yeast TDP-43 proteinopathy model: Exploring the molecular determinants of TDP-43 aggregation and cellular toxicity. Proceedings of the National Academy of Sciences of the United States of America *105*, 6439-6444.

Johnson, B.S., Snead, D., Lee, J.J., McCaffery, J.M., Shorter, J., and Gitler, A.D. (2009). TDP-43 is intrinsically aggregation-prone, and amyotrophic lateral sclerosis-linked mutations accelerate aggregation and increase toxicity. The Journal of biological chemistry *284*, 20329-20339.

Johnson, J.O., Mandrioli, J., Benatar, M., Abramzon, Y., Van Deerlin, V.M., Trojanowski, J.Q., Gibbs, J.R., Brunetti, M., Gronka, S., Wuu, J*., et al.* (2010). Exome sequencing reveals VCP mutations as a cause of familial ALS. Neuron *68*, 857-864.

Kabashi, E., Lin, L., Tradewell, M.L., Dion, P.A., Bercier, V., Bourgouin, P., Rochefort, D., Bel Hadj, S., Durham, H.D., Vande Velde, C*., et al.* (2010). Gain and loss of function of ALS-related mutations of TARDBP (TDP-43) cause motor deficits in vivo. Human molecular genetics *19*, 671-683.

Kabashi, E., Valdmanis, P.N., Dion, P., Spiegelman, D., McConkey, B.J., Vande Velde, C., Bouchard, J.P., Lacomblez, L., Pochigaeva, K., Salachas, F*., et al.* (2008). TARDBP mutations in individuals with sporadic and familial amyotrophic lateral sclerosis. Nature genetics *40*, 572-574.

Kaneko, T., Kumasaka, T., Ganbe, T., Sato, T., Miyazawa, K., Kitamura, N., and Tanaka, N. (2003). Structural insight into modest binding of a non-PXXP ligand to the signal transducing adaptor molecule-2 Src homology 3 domain. The Journal of biological chemistry *278*, 48162-48168.

Kanekura, K., Nishimoto, I., Aiso, S., and Matsuoka, M. (2006). Characterization of amyotrophic lateral sclerosis-linked P56S mutation of vesicle-associated membrane protein-associated protein B (VAPB/ALS8). The Journal of biological chemistry *281*, 30223-30233.

Kato, M., Han, T.W., Xie, S., Shi, K., Du, X., Wu, L.C., Mirzaei, H., Goldsmith, E.J., Longgood, J., Pei, J*., et al.* (2012). Cell-free formation of RNA granules: low complexity sequence domains form dynamic fibers within hydrogels. Cell *149*, 753-767.

Kato, M., Miyazawa, K., and Kitamura, N. (2000). A deubiquitinating enzyme UBPY interacts with the Src homology 3 domain of Hrs-binding protein via a novel binding motif PX(V/I)(D/N)RXXKP. The Journal of biological chemistry *275*, 37481-37487.

Kawahara, Y., and Mieda-Sato, A. (2012). TDP-43 promotes microRNA biogenesis as a component of the Drosha and Dicer complexes. Proceedings of the National Academy of Sciences of the United States of America *109*, 3347-3352.

Kessenbrock, K., Frohlich, L., Sixt, M., Lammermann, T., Pfister, H., Bateman, A., Belaaouaj, A., Ring, J., Ollert, M., Fassler, R.*, et al.* (2008). Proteinase 3 and neutrophil elastase enhance inflammation in mice by inactivating antiinflammatory progranulin. The Journal of clinical investigation *118*, 2438-2447.

Kim, H.J., Kim, N.C., Wang, Y.D., Scarborough, E.A., Moore, J., Diaz, Z., MacLea, K.S., Freibaum, B., Li, S., Molliex, A.*, et al.* (2013). Mutations in prion-like domains in hnRNPA2B1 and hnRNPA1 cause multisystem proteinopathy and ALS. Nature *495*, 467-473.

Kim, H.J., Raphael, A.R., LaDow, E.S., McGurk, L., Weber, R.A., Trojanowski, J.Q., Lee, V.M., Finkbeiner, S., Gitler, A.D., and Bonini, N.M. (2014). Therapeutic modulation of eIF2alpha phosphorylation rescues TDP-43 toxicity in amyotrophic lateral sclerosis disease models. Nature genetics *46*, 152-160.

Kim, S.H., Shanware, N.P., Bowler, M.J., and Tibbetts, R.S. (2010). Amyotrophic lateral sclerosis-associated proteins TDP-43 and FUS/TLS function in a common biochemical complex to co-regulate HDAC6 mRNA. The Journal of biological chemistry *285*, 34097-34105.

Kim, S.H., Shi, Y., Hanson, K.A., Williams, L.M., Sakasai, R., Bowler, M.J., and Tibbetts, R.S. (2009). Potentiation of amyotrophic lateral sclerosis (ALS)-associated TDP-43 aggregation by the proteasome-targeting factor, ubiquilin 1. The Journal of biological chemistry *284*, 8083-8092.

King, O.D., Gitler, A.D., and Shorter, J. (2012). The tip of the iceberg: RNA-binding proteins with prion-like domains in neurodegenerative disease. Brain research *1462*, 61-80.

Ko, H.S., Uehara, T., Tsuruma, K., and Nomura, Y. (2004). Ubiquilin interacts with ubiquitylated proteins and proteasome through its ubiquitin-associated and ubiquitin-like domains. FEBS letters *566*, 110-114.

Kohli, M.A., John-Williams, K., Rajbhandary, R., Naj, A., Whitehead, P., Hamilton, K., Carney, R.M., Wright, C., Crocco, E., Gwirtzman, H.E.*, et al.* (2013). Repeat expansions in the C9ORF72 gene contribute to Alzheimer's disease in Caucasians. Neurobiology of aging *34*, 1519 e1515-1512.

Komada, M. (2008). Controlling receptor downregulation by ubiquitination and deubiquitination. Current drug discovery technologies *5*, 78-84.

Komander, D., Clague, M.J., and Urbe, S. (2009). Breaking the chains: structure and function of the deubiquitinases. Nature reviews Molecular cell biology *10*, 550-563.

Komander, D., and Rape, M. (2012). The ubiquitin code. Annual review of biochemistry *81*, 203-229.

Koppers, M., van Blitterswijk, M.M., Vlam, L., Rowicka, P.A., van Vught, P.W., Groen, E.J., Spliet, W.G., Engelen-Lee, J., Schelhaas, H.J., de Visser, M.*, et al.* (2012). VCP mutations in familial and sporadic amyotrophic lateral sclerosis. Neurobiology of aging *33*, 837 e837-813.

Korac, J., Schaeffer, V., Kovacevic, I., Clement, A.M., Jungblut, B., Behl, C., Terzic, J., and Dikic, I. (2013). Ubiquitin-independent function of optineurin in autophagic clearance of protein aggregates. Journal of cell science *126*, 580-592.

Kovacs, G.G., Murrell, J.R., Horvath, S., Haraszti, L., Majtenyi, K., Molnar, M.J., Budka, H., Ghetti, B., and Spina, S. (2009). TARDBP variation associated with frontotemporal dementia, supranuclear gaze palsy, and chorea. Movement disorders : official journal of the Movement Disorder Society *24*, 1843-1847.

Kuo, P.H., Chiang, C.H., Wang, Y.T., Doudeva, L.G., and Yuan, H.S. (2014). The crystal structure of TDP-43 RRM1-DNA complex reveals the specific recognition for UG- and TG-rich nucleic acids. Nucleic acids research.

Kuo, P.H., Doudeva, L.G., Wang, Y.T., Shen, C.K., and Yuan, H.S. (2009). Structural insights into TDP-43 in nucleic-acid binding and domain interactions. Nucleic acids research *37*, 1799-1808.

Kwiatkowski, T.J., Jr., Bosco, D.A., Leclerc, A.L., Tamrazian, E., Vanderburg, C.R., Russ, C., Davis, A., Gilchrist, J., Kasarskis, E.J., Munsat, T.*, et al.* (2009). Mutations in the FUS/TLS gene on chromosome 16 cause familial amyotrophic lateral sclerosis. Science *323*, 1205-1208.

Kwok, C.T., Morris, A., and de Belleroche, J.S. (2014). Sequestosome-1 (SQSTM1) sequence variants in ALS cases in the UK: prevalence and coexistence of SQSTM1 mutations in ALS kindred with PDB. European journal of human genetics : EJHG *22*, 492-496.

Kwong, L.K., Uryu, K., Trojanowski, J.Q., and Lee, V.M. (2008). TDP-43 proteinopathies: neurodegenerative protein misfolding diseases without amyloidosis. Neuro-Signals *16*, 41-51.

Lagier-Tourenne, C., Baughn, M., Rigo, F., Sun, S., Liu, P., Li, H.R., Jiang, J., Watt, A.T., Chun, S., Katz, M.*, et al.* (2013). Targeted degradation of sense and antisense C9orf72 RNA foci as therapy for ALS and frontotemporal degeneration. Proceedings of the National Academy of Sciences of the United States of America *110*, E4530-4539.

Lagier-Tourenne, C., Polymenidou, M., and Cleveland, D.W. (2010). TDP-43 and FUS/TLS: emerging roles in RNA processing and neurodegeneration. Human molecular genetics *19*, R46-64.

Lagier-Tourenne, C., Polymenidou, M., Hutt, K.R., Vu, A.Q., Baughn, M., Huelga, S.C., Clutario, K.M., Ling, S.C., Liang, T.Y., Mazur, C.*, et al.* (2012). Divergent roles of ALS-linked proteins FUS/TLS and TDP-43 intersect in processing long pre-mRNAs. Nature neuroscience *15*, 1488-1497.

Lamond, A.I., and Spector, D.L. (2003). Nuclear speckles: a model for nuclear organelles. Nature reviews Molecular cell biology *4*, 605-612.

Landers, J.E., Leclerc, A.L., Shi, L., Virkud, A., Cho, T., Maxwell, M.M., Henry, A.F., Polak, M., Glass, J.D., Kwiatkowski, T.J.*, et al.* (2008). New VAPB deletion variant and exclusion of VAPB mutations in familial ALS. Neurology *70*, 1179-1185.

Larkin, M.A., Blackshields, G., Brown, N.P., Chenna, R., McGettigan, P.A., McWilliam, H., Valentin, F., Wallace, I.M., Wilm, A., Lopez, R.*, et al.* (2007). Clustal W and Clustal X version 2.0. Bioinformatics *23*, 2947-2948.

Lattante, S., Rouleau, G.A., and Kabashi, E. (2013). TARDBP and FUS mutations associated with amyotrophic lateral sclerosis: summary and update. Human mutation *34*, 812-826.

Le Ber, I., Camuzat, A., Guerreiro, R., Bouya-Ahmed, K., Bras, J., Nicolas, G., Gabelle, A., Didic, M., De Septenville, A., Millecamps, S.*, et al.* (2013). SQSTM1 mutations in French patients with frontotemporal dementia or frontotemporal dementia with amyotrophic lateral sclerosis. JAMA neurology *70*, 1403-1410.

Leblond, C.S., Kaneb, H.M., Dion, P.A., and Rouleau, G.A. (2014). Dissection of genetic factors associated with amyotrophic lateral sclerosis. Experimental neurology.

Lee, B.H., Lee, M.J., Park, S., Oh, D.C., Elsasser, S., Chen, P.C., Gartner, C., Dimova, N., Hanna, J., Gygi, S.P.*, et al.* (2010). Enhancement of proteasome activity by a small-molecule inhibitor of USP14. Nature *467*, 179-184.

Lee, E.B., Lee, V.M., and Trojanowski, J.Q. (2012). Gains or losses: molecular mechanisms of TDP43-mediated neurodegeneration. Nature reviews Neuroscience *13*, 38-50.

Lee, S., Hong, S., and Kang, S. (2008). The ubiquitin-conjugating enzyme UbcH6 regulates the transcriptional repression activity of the SCA1 gene product ataxin-1. Biochemical and biophysical research communications *372*, 735-740.

Lehner, B., and Sanderson, C.M. (2004). A protein interaction framework for human mRNA degradation. Genome research *14*, 1315-1323.

Levine, T.P., Daniels, R.D., Gatta, A.T., Wong, L.H., and Hayes, M.J. (2013). The product of C9orf72, a gene strongly implicated in neurodegeneration, is structurally related to DENN Rab-GEFs. Bioinformatics *29*, 499-503.

Li, H.Y., Yeh, P.A., Chiu, H.C., Tang, C.Y., and Tu, B.P. (2011). Hyperphosphorylation as a defense mechanism to reduce TDP-43 aggregation. PloS one *6*, e23075.

Li, S., Chen, Y., Shi, Q., Yue, T., Wang, B., and Jiang, J. (2012). Hedgehog-regulated ubiquitination controls smoothened trafficking and cell surface expression in Drosophila. PLoS biology *10*, e1001239.

Li, Y., Ray, P., Rao, E.J., Shi, C., Guo, W., Chen, X., Woodruff, E.A., 3rd, Fushimi, K., and Wu, J.Y. (2010). A Drosophila model for TDP-43 proteinopathy. Proceedings of the National Academy of Sciences of the United States of America *107*, 3169-3174.

Li, Y.R., King, O.D., Shorter, J., and Gitler, A.D. (2013). Stress granules as crucibles of ALS pathogenesis. The Journal of cell biology *201*, 361-372.

Liachko, N.F., Guthrie, C.R., and Kraemer, B.C. (2010). Phosphorylation promotes neurotoxicity in a Caenorhabditis elegans model of TDP-43 proteinopathy. The Journal of neuroscience : the official journal of the Society for Neuroscience *30*, 16208-16219.

Liachko, N.F., McMillan, P.J., Guthrie, C.R., Bird, T.D., Leverenz, J.B., and Kraemer, B.C. (2013). CDC7 inhibition blocks pathological TDP-43 phosphorylation and neurodegeneration. Annals of neurology *74*, 39-52.

Lindquist, S.G., Duno, M., Batbayli, M., Puschmann, A., Braendgaard, H., Mardosiene, S., Svenstrup, K., Pinborg, L.H., Vestergaard, K., Hjermind, L.E.*, et al.* (2013). Corticobasal and ataxia syndromes widen the spectrum of C9ORF72 hexanucleotide expansion disease. Clinical genetics *83*, 279-283.

Ling, S.C., Albuquerque, C.P., Han, J.S., Lagier-Tourenne, C., Tokunaga, S., Zhou, H., and Cleveland, D.W. (2010). ALS-associated mutations in TDP-43 increase its stability and promote TDP-43 complexes with FUS/TLS. Proceedings of the National Academy of Sciences of the United States of America *107*, 13318-13323.

Ling, S.C., Polymenidou, M., and Cleveland, D.W. (2013). Converging mechanisms in ALS and FTD: disrupted RNA and protein homeostasis. Neuron *79*, 416-438.

Liscic, R.M., Grinberg, L.T., Zidar, J., Gitcho, M.A., and Cairns, N.J. (2008). ALS and FTLD: two faces of TDP-43 proteinopathy. European journal of neurology : the official journal of the European Federation of Neurological Societies *15*, 772-780.

Liu-Yesucevitz, L., Bilgutay, A., Zhang, Y.J., Vanderweyde, T., Citro, A., Mehta, T., Zaarur, N., McKee, A., Bowser, R., Sherman, M.*, et al.* (2010). Tar DNA binding protein-43 (TDP-43) associates with stress granules: analysis of cultured cells and pathological brain tissue. PloS one *5*, e13250.

Liu, Y.C., Chiang, P.M., and Tsai, K.J. (2013). Disease animal models of TDP-43 proteinopathy and their pre-clinical applications. International journal of molecular sciences *14*, 20079-20111.

Liu, Y.V., Baek, J.H., Zhang, H., Diez, R., Cole, R.N., and Semenza, G.L. (2007). RACK1 competes with HSP90 for binding to HIF-1alpha and is required for O(2)-independent and HSP90 inhibitor-induced degradation of HIF-1alpha. Molecular cell *25*, 207-217.

Lukavsky, P.J., Daujotyte, D., Tollervey, J.R., Ule, J., Stuani, C., Buratti, E., Baralle, F.E., Damberger, F.F., and Allain, F.H. (2013). Molecular basis of UG-rich RNA recognition by the human splicing factor TDP-43. Nature structural & molecular biology *20*, 1443-1449.

Luty, A.A., Kwok, J.B., Dobson-Stone, C., Loy, C.T., Coupland, K.G., Karlstrom, H., Sobow, T., Tchorzewska, J., Maruszak, A., Barcikowska, M.*, et al.* (2010). Sigma nonopioid intracellular receptor 1 mutations cause frontotemporal lobar degeneration-motor neuron disease. Annals of neurology *68*, 639-649.

Mackenzie, I.R., Bigio, E.H., Ince, P.G., Geser, F., Neumann, M., Cairns, N.J., Kwong, L.K., Forman, M.S., Ravits, J., Stewart, H.*, et al.* (2007). Pathological TDP-43 distinguishes sporadic amyotrophic lateral sclerosis from amyotrophic lateral sclerosis with SOD1 mutations. Annals of neurology *61*, 427-434.

Mackenzie, I.R., Frick, P., and Neumann, M. (2014). The neuropathology associated with repeat expansions in the C9ORF72 gene. Acta neuropathologica *127*, 347-357.

Mackenzie, I.R., and Neumann, M. (2012). FET proteins in frontotemporal dementia and amyotrophic lateral sclerosis. Brain research *1462*, 40-43.

Mackenzie, I.R., Neumann, M., Baborie, A., Sampathu, D.M., Du Plessis, D., Jaros, E., Perry, R.H., Trojanowski, J.Q., Mann, D.M., and Lee, V.M. (2011). A harmonized classification system for FTLD-TDP pathology. Acta neuropathologica *122*, 111-113.

Mackenzie, I.R., Neumann, M., Bigio, E.H., Cairns, N.J., Alafuzoff, I., Kril, J., Kovacs, G.G., Ghetti, B., Halliday, G., Holm, I.E.*, et al.* (2010a). Nomenclature and nosology for neuropathologic subtypes of frontotemporal lobar degeneration: an update. Acta neuropathologica *119*, 1-4.

Mackenzie, I.R., Rademakers, R., and Neumann, M. (2010b). TDP-43 and FUS in amyotrophic lateral sclerosis and frontotemporal dementia. Lancet neurology *9*, 995-1007.

Mackness, B.C., Tran, M.T., McClain, S.P., Matthews, C.R., and Zitzewitz, J.A. (2014). Folding of the RNA Recognition Motif (RRM) Domains of the ALS-Linked Protein TDP-43 Reveals an Intermediate State. The Journal of biological chemistry.

Maruyama, H., Morino, H., Ito, H., Izumi, Y., Kato, H., Watanabe, Y., Kinoshita, Y., Kamada, M., Nodera, H., Suzuki, H., *et al.* (2010). Mutations of optineurin in amyotrophic lateral sclerosis. Nature *465*, 223-226.

Matuschewski, K., Hauser, H.P., Treier, M., and Jentsch, S. (1996). Identification of a novel family of ubiquitin-conjugating enzymes with distinct amino-terminal extensions. The Journal of biological chemistry *271*, 2789-2794.

McDonald, K.K., Aulas, A., Destroismaisons, L., Pickles, S., Beleac, E., Camu, W., Rouleau, G.A., and Vande Velde, C. (2011). TAR DNA-binding protein 43 (TDP-43) regulates stress granule dynamics via differential regulation of G3BP and TIA-1. Human molecular genetics *20*, 1400-1410.

Medicherla, B., and Goldberg, A.L. (2008). Heat shock and oxygen radicals stimulate ubiquitin-dependent degradation mainly of newly synthesized proteins. The Journal of cell biology *182*, 663-673.

Mercado, P.A., Ayala, Y.M., Romano, M., Buratti, E., and Baralle, F.E. (2005). Depletion of TDP 43 overrides the need for exonic and intronic splicing enhancers in the human apoA-II gene. Nucleic acids research *33*, 6000-6010.

Metzger, M.B., Hristova, V.A., and Weissman, A.M. (2012). HECT and RING finger families of E3 ubiquitin ligases at a glance. Journal of cell science *125*, 531-537.

Meyer, H., Bug, M., and Bremer, S. (2012). Emerging functions of the VCP/p97 AAA-ATPase in the ubiquitin system. Nature cell biology *14*, 117-123.

Mirza, S., Plafker, K.S., Aston, C., and Plafker, S.M. (2010). Expression and distribution of the class III ubiquitin-conjugating enzymes in the retina. Molecular vision *16*, 2425-2437.

Mitchell, J., Paul, P., Chen, H.J., Morris, A., Payling, M., Falchi, M., Habgood, J., Panoutsou, S., Winkler, S., Tisato, V., *et al.* (2010). Familial amyotrophic lateral sclerosis is associated with a mutation in D-amino acid oxidase. Proceedings of the National Academy of Sciences of the United States of America *107*, 7556-7561.

Mizielinska, S., Lashley, T., Norona, F.E., Clayton, E.L., Ridler, C.E., Fratta, P., and Isaacs, A.M. (2013). C9orf72 frontotemporal lobar degeneration is characterised by frequent neuronal sense and antisense RNA foci. Acta neuropathologica *126*, 845-857.

Mizuno, E., Iura, T., Mukai, A., Yoshimori, T., Kitamura, N., and Komada, M. (2005). Regulation of epidermal growth factor receptor down-regulation by UBPY-mediated deubiquitination at endosomes. Molecular biology of the cell *16*, 5163-5174.

Mizuno, E., Kitamura, N., and Komada, M. (2007). 14-3-3-dependent inhibition of the deubiquitinating activity of UBPY and its cancellation in the M phase. Experimental cell research *313*, 3624-3634.

Moisse, K., Volkening, K., Leystra-Lantz, C., Welch, I., Hill, T., and Strong, M.J. (2009). Divergent patterns of cytosolic TDP-43 and neuronal progranulin expression following axotomy: implications for TDP-43 in the physiological response to neuronal injury. Brain research *1249*, 202-211.

Mori, K., Weng, S.M., Arzberger, T., May, S., Rentzsch, K., Kremmer, E., Schmid, B., Kretzschmar, H.A., Cruts, M., Van Broeckhoven, C., *et al.* (2013). The C9orf72 GGGGCC repeat is translated into aggregating dipeptide-repeat proteins in FTLD/ALS. Science *339*, 1335-1338.

Mukai, A., Yamamoto-Hino, M., Awano, W., Watanabe, W., Komada, M., and Goto, S. (2010). Balanced ubiquitylation and deubiquitylation of Frizzled regulate cellular responsiveness to Wg/Wnt. The EMBO journal *29*, 2114-2125.

Mukherjee, O., Pastor, P., Cairns, N.J., Chakraverty, S., Kauwe, J.S., Shears, S., Behrens, M.I., Budde, J., Hinrichs, A.L., Norton, J., *et al.* (2006). HDDD2 is a familial frontotemporal lobar degeneration with ubiquitin-positive, tau-negative inclusions caused by a missense mutation in the signal peptide of progranulin. Annals of neurology *60*, 314-322.

Narayanan, R.K., Mangelsdorf, M., Panwar, A., Butler, T.J., Noakes, P.G., and Wallace, R.H. (2013). Identification of RNA bound to the TDP-43 ribonucleoprotein complex in the adult mouse brain. Amyotrophic lateral sclerosis & frontotemporal degeneration *14*, 252-260.

Naviglio, S., Mattecucci, C., Matoskova, B., Nagase, T., Nomura, N., Di Fiore, P.P., and Draetta, G.F. (1998). UBPY: a growth-regulated human ubiquitin isopeptidase. The EMBO journal *17*, 3241-3250.

Neumann, M., Bentmann, E., Dormann, D., Jawaid, A., DeJesus-Hernandez, M., Ansorge, O., Roeber, S., Kretzschmar, H.A., Munoz, D.G., Kusaka, H., *et al.* (2011). FET proteins TAF15 and EWS are selective

markers that distinguish FTLD with FUS pathology from amyotrophic lateral sclerosis with FUS mutations. Brain : a journal of neurology *134*, 2595-2609.

Neumann, M., Kwong, L.K., Lee, E.B., Kremmer, E., Flatley, A., Xu, Y., Forman, M.S., Troost, D., Kretzschmar, H.A., Trojanowski, J.Q.*, et al.* (2009). Phosphorylation of S409/410 of TDP-43 is a consistent feature in all sporadic and familial forms of TDP-43 proteinopathies. Acta neuropathologica *117*, 137-149.

Neumann, M., Kwong, L.K., Truax, A.C., Vanmassenhove, B., Kretzschmar, H.A., Van Deerlin, V.M., Clark, C.M., Grossman, M., Miller, B.L., Trojanowski, J.Q.*, et al.* (2007). TDP-43-positive white matter pathology in frontotemporal lobar degeneration with ubiquitin-positive inclusions. Journal of neuropathology and experimental neurology *66*, 177-183.

Neumann, M., Sampathu, D.M., Kwong, L.K., Truax, A.C., Micsenyi, M.C., Chou, T.T., Bruce, J., Schuck, T., Grossman, M., Clark, C.M.*, et al.* (2006). Ubiquitinated TDP-43 in frontotemporal lobar degeneration and amyotrophic lateral sclerosis. Science *314*, 130-133.

Niendorf, S., Oksche, A., Kisser, A., Lohler, J., Prinz, M., Schorle, H., Feller, S., Lewitzky, M., Horak, I., and Knobeloch, K.P. (2007). Essential role of ubiquitin-specific protease 8 for receptor tyrosine kinase stability and endocytic trafficking in vivo. Molecular and cellular biology *27*, 5029-5039.

Nihei, Y., Ito, D., and Suzuki, N. (2012). Roles of ataxin-2 in pathological cascades mediated by TAR DNA-binding protein 43 (TDP-43) and Fused in Sarcoma (FUS). The Journal of biological chemistry *287*, 41310-41323.

Nilsson, J., Sengupta, J., Frank, J., and Nissen, P. (2004). Regulation of eukaryotic translation by the RACK1 protein: a platform for signalling molecules on the ribosome. EMBO reports *5*, 1137-1141.

Nishimoto, Y., Ito, D., Yagi, T., Nihei, Y., Tsunoda, Y., and Suzuki, N. (2010). Characterization of alternative isoforms and inclusion body of the TAR DNA-binding protein-43. The Journal of biological chemistry *285*, 608-619.

Nishimura, A.L., Mitne-Neto, M., Silva, H.C., Richieri-Costa, A., Middleton, S., Cascio, D., Kok, F., Oliveira, J.R., Gillingwater, T., Webb, J.*, et al.* (2004). A mutation in the vesicle-trafficking protein VAPB causes late-onset spinal muscular atrophy and amyotrophic lateral sclerosis. American journal of human genetics *75*, 822-831.

Nishimura, A.L., Zupunski, V., Troakes, C., Kathe, C., Fratta, P., Howell, M., Gallo, J.M., Hortobagyi, T., Shaw, C.E., and Rogelj, B. (2010). Nuclear import impairment causes cytoplasmic trans-activation response DNA-binding protein accumulation and is associated with frontotemporal lobar degeneration. Brain : a journal of neurology *133*, 1763-1771.

Nollen, E.A., Garcia, S.M., van Haaften, G., Kim, S., Chavez, A., Morimoto, R.I., and Plasterk, R.H. (2004). Genome-wide RNA interference screen identifies previously undescribed regulators of polyglutamine aggregation. Proceedings of the National Academy of Sciences of the United States of America *101*, 6403-6408.

Nonaka, T., Arai, T., Buratti, E., Baralle, F.E., Akiyama, H., and Hasegawa, M. (2009a). Phosphorylated and ubiquitinated TDP-43 pathological inclusions in ALS and FTLD-U are recapitulated in SH-SY5Y cells. FEBS letters *583*, 394-400.

Nonaka, T., Kametani, F., Arai, T., Akiyama, H., and Hasegawa, M. (2009b). Truncation and pathogenic mutations facilitate the formation of intracellular aggregates of TDP-43. Human molecular genetics *18*, 3353-3364.

Okamoto, K., Mizuno, Y., and Fujita, Y. (2008). Bunina bodies in amyotrophic lateral sclerosis. Neuropathology : official journal of the Japanese Society of Neuropathology *28*, 109-115.

Osawa, T., Mizuno, Y., Fujita, Y., Takatama, M., Nakazato, Y., and Okamoto, K. (2011). Optineurin in neurodegenerative diseases. Neuropathology : official journal of the Japanese Society of Neuropathology *31*, 569-574.

Ou, S.H., Wu, F., Harrich, D., Garcia-Martinez, L.F., and Gaynor, R.B. (1995). Cloning and characterization of a novel cellular protein, TDP-43, that binds to human immunodeficiency virus type 1 TAR DNA sequence motifs. Journal of virology *69*, 3584-3596.

Paiardi, C., Pasini, M.E., Amadeo, A., Gioria, M., and Berruti, G. (2014). The ESCRT-deubiquitinating enzyme USP8 in the cervical spinal cord of wild-type and Vps54-recessive (wobbler) mutant mice. Histochemistry and cell biology *141*, 57-73.

Pamphlett, R., Luquin, N., McLean, C., Jew, S.K., and Adams, L. (2009). TDP-43 neuropathology is similar in sporadic amyotrophic lateral sclerosis with or without TDP-43 mutations. Neuropathology and applied neurobiology *35*, 222-225.

Parker, S.J., Meyerowitz, J., James, J.L., Liddell, J.R., Crouch, P.J., Kanninen, K.M., and White, A.R. (2012). Endogenous TDP-43 localized to stress granules can subsequently form protein aggregates. Neurochemistry international *60*, 415-424.

Parkinson, N., Ince, P.G., Smith, M.O., Highley, R., Skibinski, G., Andersen, P.M., Morrison, K.E., Pall, H.S., Hardiman, O., Collinge, J.*, et al.* (2006). ALS phenotypes with mutations in CHMP2B (charged multivesicular body protein 2B). Neurology *67*, 1074-1077.

Passoni, M., De Conti, L., Baralle, M., and Buratti, E. (2012). UG repeats/TDP-43 interactions near 5' splice sites exert unpredictable effects on splicing modulation. Journal of molecular biology *415*, 46-60.

Pesiridis, G.S., Tripathy, K., Tanik, S., Trojanowski, J.Q., and Lee, V.M. (2011). A "two-hit" hypothesis for inclusion formation by carboxyl-terminal fragments of TDP-43 protein linked to RNA depletion and impaired microtubule-dependent transport. The Journal of biological chemistry *286*, 18845-18855.

Pickart, C.M. (1997). Targeting of substrates to the 26S proteasome. FASEB journal : official publication of the Federation of American Societies for Experimental Biology *11*, 1055-1066.

Plafker, K.S., Farjo, K.M., Wiechmann, A.F., and Plafker, S.M. (2008). The human ubiquitin conjugating enzyme, UBE2E3, is required for proliferation of retinal pigment epithelial cells. Investigative ophthalmology & visual science *49*, 5611-5618.

Plafker, K.S., Nguyen, L., Barneche, M., Mirza, S., Crawford, D., and Plafker, S.M. (2010). The ubiquitin-conjugating enzyme UbcM2 can regulate the stability and activity of the antioxidant transcription factor Nrf2. The Journal of biological chemistry *285*, 23064-23074.

Plafker, K.S., Singer, J.D., and Plafker, S.M. (2009). The ubiquitin conjugating enzyme, UbcM2, engages in novel interactions with components of cullin-3 based E3 ligases. Biochemistry *48*, 3527-3537.

Plafker, S.M., Plafker, K.S., Weissman, A.M., and Macara, I.G. (2004). Ubiquitin charging of human class III ubiquitin-conjugating enzymes triggers their nuclear import. The Journal of cell biology *167*, 649-659.

Polymenidou, M., Lagier-Tourenne, C., Hutt, K.R., Huelga, S.C., Moran, J., Liang, T.Y., Ling, S.C., Sun, E., Wancewicz, E., Mazur, C.*, et al.* (2011). Long pre-mRNA depletion and RNA missplicing contribute to neuronal vulnerability from loss of TDP-43. Nature neuroscience *14*, 459-468.

Qiu, L., Qiao, T., Beers, M., Tan, W., Wang, H., Yang, B., and Xu, Z. (2013). Widespread aggregation of mutant VAPB associated with ALS does not cause motor neuron degeneration or modulate mutant SOD1 aggregation and toxicity in mice. Molecular neurodegeneration *8*, 1.

Rabinovici, G.D., and Miller, B.L. (2010). Frontotemporal lobar degeneration: epidemiology, pathophysiology, diagnosis and management. CNS drugs *24*, 375-398.

Renton, A.E., Majounie, E., Waite, A., Simon-Sanchez, J., Rollinson, S., Gibbs, J.R., Schymick, J.C., Laaksovirta, H., van Swieten, J.C., Myllykangas, L.*, et al.* (2011). A hexanucleotide repeat expansion in C9ORF72 is the cause of chromosome 9p21-linked ALS-FTD. Neuron *72*, 257-268.

Riley, B.E., Lougheed, J.C., Callaway, K., Velasquez, M., Brecht, E., Nguyen, L., Shaler, T., Walker, D., Yang, Y., Regnstrom, K.*, et al.* (2013). Structure and function of Parkin E3 ubiquitin ligase reveals aspects of RING and HECT ligases. Nature communications *4*, 1982.

Ringholz, G.M., Appel, S.H., Bradshaw, M., Cooke, N.A., Mosnik, D.M., and Schulz, P.E. (2005). Prevalence and patterns of cognitive impairment in sporadic ALS. Neurology *65*, 586-590.

Ritson, G.P., Custer, S.K., Freibaum, B.D., Guinto, J.B., Geffel, D., Moore, J., Tang, W., Winton, M.J., Neumann, M., Trojanowski, J.Q.*, et al.* (2010). TDP-43 mediates degeneration in a novel Drosophila model of disease caused by mutations in VCP/p97. The Journal of neuroscience : the official journal of the Society for Neuroscience *30*, 7729-7739.

Romano, M., Feiguin, F., and Buratti, E. (2012). Drosophila Answers to TDP-43 Proteinopathies. Journal of amino acids *2012*, 356081.

Rosen, D.R., Siddique, T., Patterson, D., Figlewicz, D.A., Sapp, P., Hentati, A., Donaldson, D., Goto, J., O'Regan, J.P., Deng, H.X.*, et al.* (1993). Mutations in Cu/Zn superoxide dismutase gene are associated with familial amyotrophic lateral sclerosis. Nature *362*, 59-62.

Rossor, M.N., Fox, N.C., Mummery, C.J., Schott, J.M., and Warren, J.D. (2010). The diagnosis of young-onset dementia. Lancet neurology *9*, 793-806.

Rothenberg, C., Srinivasan, D., Mah, L., Kaushik, S., Peterhoff, C.M., Ugolino, J., Fang, S., Cuervo, A.M., Nixon, R.A., and Monteiro, M.J. (2010). Ubiquilin functions in autophagy and is degraded by chaperone-mediated autophagy. Human molecular genetics *19*, 3219-3232.

Rotunno, M.S., and Bosco, D.A. (2013). An emerging role for misfolded wild-type SOD1 in sporadic ALS pathogenesis. Frontiers in cellular neuroscience *7*, 253.

Row, P.E., Liu, H., Hayes, S., Welchman, R., Charalabous, P., Hofmann, K., Clague, M.J., Sanderson, C.M., and Urbe, S. (2007). The MIT domain of UBPY constitutes a CHMP binding and endosomal localization signal required for efficient epidermal growth factor receptor degradation. The Journal of biological chemistry *282*, 30929-30937.

Row, P.E., Prior, I.A., McCullough, J., Clague, M.J., and Urbe, S. (2006). The ubiquitin isopeptidase UBPY regulates endosomal ubiquitin dynamics and is essential for receptor down-regulation. The Journal of biological chemistry *281*, 12618-12624.

Ruan, Y., Guo, L., Qiao, Y., Hong, Y., Zhou, L., Sun, L., Wang, L., Zhu, H., Wang, L., Yun, X.*, et al.* (2009). RACK1 associates with CLEC-2 and promotes its ubiquitin-proteasome degradation. Biochemical and biophysical research communications *390*, 217-222.

Rubino, E., Rainero, I., Chio, A., Rogaeva, E., Galimberti, D., Fenoglio, P., Grinberg, Y., Isaia, G., Calvo, A., Gentile, S.*, et al.* (2012). SQSTM1 mutations in frontotemporal lobar degeneration and amyotrophic lateral sclerosis. Neurology *79*, 1556-1562.

Rutherford, A.C., Traer, C., Wassmer, T., Pattni, K., Bujny, M.V., Carlton, J.G., Stenmark, H., and Cullen, P.J. (2006). The mammalian phosphatidylinositol 3-phosphate 5-kinase (PIKfyve) regulates endosome-to-TGN retrograde transport. Journal of cell science *119*, 3944-3957.

Rutherford, N.J., Zhang, Y.J., Baker, M., Gass, J.M., Finch, N.A., Xu, Y.F., Stewart, H., Kelley, B.J., Kuntz, K., Crook, R.J.*, et al.* (2008). Novel mutations in TARDBP (TDP-43) in patients with familial amyotrophic lateral sclerosis. PLoS genetics *4*, e1000193.

Sapp, P.C., Hosler, B.A., McKenna-Yasek, D., Chin, W., Gann, A., Genise, H., Gorenstein, J., Huang, M., Sailer, W., Scheffler, M.*, et al.* (2003). Identification of two novel loci for dominantly inherited familial amyotrophic lateral sclerosis. American journal of human genetics *73*, 397-403.

Sareen, D., O'Rourke, J.G., Meera, P., Muhammad, A.K., Grant, S., Simpkinson, M., Bell, S., Carmona, S., Ornelas, L., Sahabian, A.*, et al.* (2013). Targeting RNA foci in iPSC-derived motor neurons from ALS patients with a C9ORF72 repeat expansion. Science translational medicine *5*, 208ra149.

Sato, S., Tomomori-Sato, C., Parmely, T.J., Florens, L., Zybailov, B., Swanson, S.K., Banks, C.A., Jin, J., Cai, Y., Washburn, M.P.*, et al.* (2004). A set of consensus mammalian mediator subunits identified by multidimensional protein identification technology. Molecular cell *14*, 685-691.

Sato, T., Takeuchi, S., Saito, A., Ding, W., Bamba, H., Matsuura, H., Hisa, Y., Tooyama, I., and Urushitani, M. (2009). Axonal ligation induces transient redistribution of TDP-43 in brainstem motor neurons. Neuroscience *164*, 1565-1578.

Schipper-Krom, S., Juenemann, K., and Reits, E.A. (2012). The Ubiquitin-Proteasome System in Huntington's Disease: Are Proteasomes Impaired, Initiators of Disease, or Coming to the Rescue? Biochemistry research international *2012*, 837015.

Schumacher, F.R., Wilson, G., and Day, C.L. (2013). The N-terminal extension of UBE2E ubiquitin-conjugating enzymes limits chain assembly. Journal of molecular biology *425*, 4099-4111.

Scotter, E.L., Vance, C., Nishimura, A.L., Lee, Y.B., Chen, H.J., Urwin, H., Sardone, V., Mitchell, J.C., Rogelj, B., Rubinsztein, D.C.*, et al.* (2014). Differential roles of the ubiquitin proteasome system (UPS) and autophagy in the clearance of soluble and aggregated TDP-43 species. Journal of cell science.

Sengupta, J., Nilsson, J., Gursky, R., Spahn, C.M., Nissen, P., and Frank, J. (2004). Identification of the versatile scaffold protein RACK1 on the eukaryotic ribosome by cryo-EM. Nature structural & molecular biology *11*, 957-962.

Sephton, C.F., Cenik, C., Kucukural, A., Dammer, E.B., Cenik, B., Han, Y., Dewey, C.M., Roth, F.P., Herz, J., Peng, J.*, et al.* (2011). Identification of neuronal RNA targets of TDP-43-containing ribonucleoprotein complexes. The Journal of biological chemistry *286*, 1204-1215.

Seufert, W., and Jentsch, S. (1990). Ubiquitin-conjugating enzymes UBC4 and UBC5 mediate selective degradation of short-lived and abnormal proteins. The EMBO journal *9*, 543-550.

Sheng, Y., Hong, J.H., Doherty, R., Srikumar, T., Shloush, J., Avvakumov, G.V., Walker, J.R., Xue, S., Neculai, D., Wan, J.W.*, et al.* (2012). A human ubiquitin conjugating enzyme (E2)-HECT E3 ligase structure-function screen. Molecular & cellular proteomics : MCP *11*, 329-341.

Shiga, A., Ishihara, T., Miyashita, A., Kuwabara, M., Kato, T., Watanabe, N., Yamahira, A., Kondo, C., Yokoseki, A., Takahashi, M.*, et al.* (2012). Alteration of POLDIP3 splicing associated with loss of function of TDP-43 in tissues affected with ALS. PloS one *7*, e43120.

Shiina, Y., Arima, K., Tabunoki, H., and Satoh, J. (2010). TDP-43 dimerizes in human cells in culture. Cellular and molecular neurobiology *30*, 641-652.

Shimizu, Y., Okuda-Shimizu, Y., and Hendershot, L.M. (2010). Ubiquitylation of an ERAD substrate occurs on multiple types of amino acids. Molecular cell *40*, 917-926.

Skibinski, G., Parkinson, N.J., Brown, J.M., Chakrabarti, L., Lloyd, S.L., Hummerich, H., Nielsen, J.E., Hodges, J.R., Spillantini, M.G., Thusgaard, T.*, et al.* (2005). Mutations in the endosomal ESCRTIII-complex subunit CHMP2B in frontotemporal dementia. Nature genetics *37*, 806-808.

Sparmann, A., and van Lohuizen, M. (2006). Polycomb silencers control cell fate, development and cancer. Nature reviews Cancer *6*, 846-856.

Sreedharan, J., Blair, I.P., Tripathi, V.B., Hu, X., Vance, C., Rogelj, B., Ackerley, S., Durnall, J.C., Williams, K.L., Buratti, E.*, et al.* (2008). TDP-43 mutations in familial and sporadic amyotrophic lateral sclerosis. Science *319*, 1668-1672.

Stallings, N.R., Puttaparthi, K., Luther, C.M., Burns, D.K., and Elliott, J.L. (2010). Progressive motor weakness in transgenic mice expressing human TDP-43. Neurobiology of disease *40*, 404-414.

Stelzl, U., Worm, U., Lalowski, M., Haenig, C., Brembeck, F.H., Goehler, H., Stroedicke, M., Zenkner, M., Schoenherr, A., Koeppen, S.*, et al.* (2005). A human protein-protein interaction network: a resource for annotating the proteome. Cell *122*, 957-968.

Stoica, R., De Vos, K.J., Paillusson, S., Mueller, S., Sancho, R.M., Lau, K.F., Vizcay-Barrena, G., Lin, W.L., Xu, Y.F., Lewis, J.*, et al.* (2014). ER-mitochondria associations are regulated by the VAPB-PTPIP51 interaction and are disrupted by ALS/FTD-associated TDP-43. Nature communications *5*, 3996.

Strong, M.J., Volkening, K., Hammond, R., Yang, W., Strong, W., Leystra-Lantz, C., and Shoesmith, C. (2007). TDP43 is a human low molecular weight neurofilament (hNFL) mRNA-binding protein. Molecular and cellular neurosciences *35*, 320-327.

Suh, H.S., Choi, N., Tarassishin, L., and Lee, S.C. (2012). Regulation of progranulin expression in human microglia and proteolysis of progranulin by matrix metalloproteinase-12 (MMP-12). PloS one *7*, e35115.

Suzuki, K., and Ohsumi, Y. (2007). Molecular machinery of autophagosome formation in yeast, Saccharomyces cerevisiae. FEBS letters *581*, 2156-2161.

Swarup, V., Phaneuf, D., Bareil, C., Robertson, J., Rouleau, G.A., Kriz, J., and Julien, J.P. (2011). Pathological hallmarks of amyotrophic lateral sclerosis/frontotemporal lobar degeneration in transgenic mice produced with TDP-43 genomic fragments. Brain : a journal of neurology *134*, 2610-2626.

Tai, H.C., and Schuman, E.M. (2008). Ubiquitin, the proteasome and protein degradation in neuronal function and dysfunction. Nature reviews Neuroscience *9*, 826-838.

Tait, S.W., de Vries, E., Maas, C., Keller, A.M., D'Santos, C.S., and Borst, J. (2007). Apoptosis induction by Bid requires unconventional ubiquitination and degradation of its N-terminal fragment. The Journal of cell biology *179*, 1453-1466.

Tamada, H., Sakashita, E., Shimazaki, K., Ueno, E., Hamamoto, T., Kagawa, Y., and Endo, H. (2002). cDNA cloning and characterization of Drb1, a new member of RRM-type neural RNA-binding protein. Biochemical and biophysical research communications *297*, 96-104.

Tan, A.Y., and Manley, J.L. (2009). The TET family of proteins: functions and roles in disease. Journal of molecular cell biology *1*, 82-92.

Tan, C.F., Eguchi, H., Tagawa, A., Onodera, O., Iwasaki, T., Tsujino, A., Nishizawa, M., Kakita, A., and Takahashi, H. (2007). TDP-43 immunoreactivity in neuronal inclusions in familial amyotrophic lateral sclerosis with or without SOD1 gene mutation. Acta neuropathologica *113*, 535-542.

Tanaka, K., and Matsuda, N. (2014). Proteostasis and neurodegeneration: the roles of proteasomal degradation and autophagy. Biochimica et biophysica acta *1843*, 197-204.

Tashiro, Y., Urushitani, M., Inoue, H., Koike, M., Uchiyama, Y., Komatsu, M., Tanaka, K., Yamazaki, M., Abe, M., Misawa, H._, et al._ (2012). Motor neuron-specific disruption of proteasomes, but not autophagy, replicates amyotrophic lateral sclerosis. The Journal of biological chemistry *287*, 42984-42994.

Teyssou, E., Takeda, T., Lebon, V., Boillee, S., Doukoure, B., Bataillon, G., Sazdovitch, V., Cazeneuve, C., Meininger, V., LeGuern, E._, et al._ (2013). Mutations in SQSTM1 encoding p62 in amyotrophic lateral sclerosis: genetics and neuropathology. Acta neuropathologica *125*, 511-522.

Tharun, S. (2009). Roles of eukaryotic Lsm proteins in the regulation of mRNA function. International review of cell and molecular biology *272*, 149-189.

Todd, P.K., Oh, S.Y., Krans, A., He, F., Sellier, C., Frazer, M., Renoux, A.J., Chen, K.C., Scaglione, K.M., Basrur, V._, et al._ (2013). CGG repeat-associated translation mediates neurodegeneration in fragile X tremor ataxia syndrome. Neuron *78*, 440-455.

Tollervey, J.R., Curk, T., Rogelj, B., Briese, M., Cereda, M., Kayikci, M., Konig, J., Hortobagyi, T., Nishimura, A.L., Zupunski, V._, et al._ (2011). Characterizing the RNA targets and position-dependent splicing regulation by TDP-43. Nature neuroscience *14*, 452-458.

Tozluoglu, M., Karaca, E., Nussinov, R., and Haliloglu, T. (2010). A mechanistic view of the role of E3 in sumoylation. PLoS computational biology *6*.

Tsai, K.J., Yang, C.H., Fang, Y.H., Cho, K.H., Chien, W.L., Wang, W.T., Wu, T.W., Lin, C.P., Fu, W.M., and Shen, C.K. (2010). Elevated expression of TDP-43 in the forebrain of mice is sufficient to cause neurological and pathological phenotypes mimicking FTLD-U. The Journal of experimental medicine *207*, 1661-1673.

Tse, W.K., Eisenhaber, B., Ho, S.H., Ng, Q., Eisenhaber, F., and Jiang, Y.J. (2009). Genome-wide loss-of-function analysis of deubiquitylating enzymes for zebrafish development. BMC genomics *10*, 637.

Tsuiji, H., Iguchi, Y., Furuya, A., Kataoka, A., Hatsuta, H., Atsuta, N., Tanaka, F., Hashizume, Y., Akatsu, H., Murayama, S._, et al._ (2013). Spliceosome integrity is defective in the motor neuron diseases ALS and SMA. EMBO molecular medicine *5*, 221-234.

Tsuji, H., Arai, T., Kametani, F., Nonaka, T., Yamashita, M., Suzukake, M., Hosokawa, M., Yoshida, M., Hatsuta, H., Takao, M._, et al._ (2012). Molecular analysis and biochemical classification of TDP-43 proteinopathy. Brain : a journal of neurology *135*, 3380-3391.

Tudor, E.L., Galtrey, C.M., Perkinton, M.S., Lau, K.F., De Vos, K.J., Mitchell, J.C., Ackerley, S., Hortobagyi, T., Vamos, E., Leigh, P.N._, et al._ (2010). Amyotrophic lateral sclerosis mutant vesicle-associated membrane protein-associated protein-B transgenic mice develop TAR-DNA-binding protein-43 pathology. Neuroscience *167*, 774-785.

Urushitani, M., Sato, T., Bamba, H., Hisa, Y., and Tooyama, I. (2010). Synergistic effect between proteasome and autophagosome in the clearance of polyubiquitinated TDP-43. Journal of neuroscience research *88*, 784-797.

Van Deerlin, V.M., Leverenz, J.B., Bekris, L.M., Bird, T.D., Yuan, W., Elman, L.B., Clay, D., Wood, E.M., Chen-Plotkin, A.S., Martinez-Lage, M._, et al._ (2008). TARDBP mutations in amyotrophic lateral sclerosis with TDP-43 neuropathology: a genetic and histopathological analysis. Lancet neurology *7*, 409-416.

Van Deerlin, V.M., Sleiman, P.M., Martinez-Lage, M., Chen-Plotkin, A., Wang, L.S., Graff-Radford, N.R., Dickson, D.W., Rademakers, R., Boeve, B.F., Grossman, M._, et al._ (2010). Common variants at 7p21 are associated with frontotemporal lobar degeneration with TDP-43 inclusions. Nature genetics *42*, 234-239.

van Eersel, J., Ke, Y.D., Gladbach, A., Bi, M., Gotz, J., Kril, J.J., and Ittner, L.M. (2011). Cytoplasmic accumulation and aggregation of TDP-43 upon proteasome inhibition in cultured neurons. PloS one *6*, e22850.

van Wijk, S.J., and Timmers, H.T. (2010). The family of ubiquitin-conjugating enzymes (E2s): deciding between life and death of proteins. FASEB journal : official publication of the Federation of American Societies for Experimental Biology *24*, 981-993.

Vance, C., Rogelj, B., Hortobagyi, T., De Vos, K.J., Nishimura, A.L., Sreedharan, J., Hu, X., Smith, B., Ruddy, D., Wright, P.*, et al.* (2009). Mutations in FUS, an RNA processing protein, cause familial amyotrophic lateral sclerosis type 6. Science *323*, 1208-1211.

Voigt, A., Herholz, D., Fiesel, F.C., Kaur, K., Muller, D., Karsten, P., Weber, S.S., Kahle, P.J., Marquardt, T., and Schulz, J.B. (2010). TDP-43-mediated neuron loss in vivo requires RNA-binding activity. PloS one *5*, e12247.

Volkening, K., Leystra-Lantz, C., Yang, W., Jaffee, H., and Strong, M.J. (2009). Tar DNA binding protein of 43 kDa (TDP-43), 14-3-3 proteins and copper/zinc superoxide dismutase (SOD1) interact to modulate NFL mRNA stability. Implications for altered RNA processing in amyotrophic lateral sclerosis (ALS). Brain research *1305*, 168-182.

von Mikecz, A. (2006). The nuclear ubiquitin-proteasome system. Journal of cell science *119*, 1977-1984.

Waite, A.J., Baumer, D., East, S., Neal, J., Morris, H.R., Ansorge, O., and Blake, D.J. (2014). Reduced C9orf72 protein levels in frontal cortex of amyotrophic lateral sclerosis and frontotemporal degeneration brain with the C9ORF72 hexanucleotide repeat expansion. Neurobiology of aging *35*, 1779 e1775-1779 e1713.

Wang, H., Wang, L., Erdjument-Bromage, H., Vidal, M., Tempst, P., Jones, R.S., and Zhang, Y. (2004a). Role of histone H2A ubiquitination in Polycomb silencing. Nature *431*, 873-878.

Wang, H.Y., Wang, I.F., Bose, J., and Shen, C.K. (2004b). Structural diversity and functional implications of the eukaryotic TDP gene family. Genomics *83*, 130-139.

Wang, I.F., Guo, B.S., Liu, Y.C., Wu, C.C., Yang, C.H., Tsai, K.J., and Shen, C.K. (2012). Autophagy activators rescue and alleviate pathogenesis of a mouse model with proteinopathies of the TAR DNA-binding protein 43. Proceedings of the National Academy of Sciences of the United States of America *109*, 15024-15029.

Wang, I.F., Reddy, N.M., and Shen, C.K. (2002). Higher order arrangement of the eukaryotic nuclear bodies. Proceedings of the National Academy of Sciences of the United States of America *99*, 13583-13588.

Wang, I.F., Wu, L.S., Chang, H.Y., and Shen, C.K. (2008). TDP-43, the signature protein of FTLD-U, is a neuronal activity-responsive factor. Journal of neurochemistry *105*, 797-806.

Wang, X., Fan, H., Ying, Z., Li, B., Wang, H., and Wang, G. (2010). Degradation of TDP-43 and its pathogenic form by autophagy and the ubiquitin-proteasome system. Neuroscience letters *469*, 112-116.

Wang, Y.T., Kuo, P.H., Chiang, C.H., Liang, J.R., Chen, Y.R., Wang, S., Shen, J.C., and Yuan, H.S. (2013). The truncated C-terminal RNA recognition motif of TDP-43 protein plays a key role in forming proteinaceous aggregates. The Journal of biological chemistry *288*, 9049-9057.

Watanabe, S., Kaneko, K., and Yamanaka, K. (2013). Accelerated disease onset with stabilized familial amyotrophic lateral sclerosis (ALS)-linked mutant TDP-43 proteins. The Journal of biological chemistry *288*, 3641-3654.

Watts, G.D., Wymer, J., Kovach, M.J., Mehta, S.G., Mumm, S., Darvish, D., Pestronk, A., Whyte, M.P., and Kimonis, V.E. (2004). Inclusion body myopathy associated with Paget disease of bone and frontotemporal dementia is caused by mutant valosin-containing protein. Nature genetics *36*, 377-381.

Wegorzewska, I., and Baloh, R.H. (2011). TDP-43-based animal models of neurodegeneration: new insights into ALS pathology and pathophysiology. Neuro-degenerative diseases *8*, 262-274.

Wegorzewska, I., Bell, S., Cairns, N.J., Miller, T.M., and Baloh, R.H. (2009). TDP-43 mutant transgenic mice develop features of ALS and frontotemporal lobar degeneration. Proceedings of the National Academy of Sciences of the United States of America *106*, 18809-18814.

Wenzel, D.M., Lissounov, A., Brzovic, P.S., and Klevit, R.E. (2011a). UBCH7 reactivity profile reveals parkin and HHARI to be RING/HECT hybrids. Nature *474*, 105-108.

Wenzel, D.M., Stoll, K.E., and Klevit, R.E. (2011b). E2s: structurally economical and functionally replete. The Biochemical journal *433*, 31-42.

Wheaton, M.W., Salamone, A.R., Mosnik, D.M., McDonald, R.O., Appel, S.H., Schmolck, H.I., Ringholz, G.M., and Schulz, P.E. (2007). Cognitive impairment in familial ALS. Neurology *69*, 1411-1417.

Wild, P., Farhan, H., McEwan, D.G., Wagner, S., Rogov, V.V., Brady, N.R., Richter, B., Korac, J., Waidmann, O., Choudhary, C*., et al.* (2011). Phosphorylation of the autophagy receptor optineurin restricts Salmonella growth. Science *333*, 228-233.

Wils, H., Kleinberger, G., Janssens, J., Pereson, S., Joris, G., Cuijt, I., Smits, V., Ceuterick-de Groote, C., Van Broeckhoven, C., and Kumar-Singh, S. (2010). TDP-43 transgenic mice develop spastic paralysis and neuronal inclusions characteristic of ALS and frontotemporal lobar degeneration. Proceedings of the National Academy of Sciences of the United States of America *107*, 3858-3863.

Winton, M.J., Igaz, L.M., Wong, M.M., Kwong, L.K., Trojanowski, J.Q., and Lee, V.M. (2008a). Disturbance of nuclear and cytoplasmic TAR DNA-binding protein (TDP-43) induces disease-like redistribution, sequestration, and aggregate formation. The Journal of biological chemistry *283*, 13302-13309.

Winton, M.J., Van Deerlin, V.M., Kwong, L.K., Yuan, W., Wood, E.M., Yu, C.E., Schellenberg, G.D., Rademakers, R., Caselli, R., Karydas, A*., et al.* (2008b). A90V TDP-43 variant results in the aberrant localization of TDP-43 in vitro. FEBS letters *582*, 2252-2256.

Wolozin, B. (2012). Regulated protein aggregation: stress granules and neurodegeneration. Molecular neurodegeneration *7*, 56.

Wu, C.H., Fallini, C., Ticozzi, N., Keagle, P.J., Sapp, P.C., Piotrowska, K., Lowe, P., Koppers, M., McKenna-Yasek, D., Baron, D.M*., et al.* (2012). Mutations in the profilin 1 gene cause familial amyotrophic lateral sclerosis. Nature *488*, 499-503.

Wu, X., Yen, L., Irwin, L., Sweeney, C., and Carraway, K.L., 3rd (2004). Stabilization of the E3 ubiquitin ligase Nrdp1 by the deubiquitinating enzyme USP8. Molecular and cellular biology *24*, 7748-7757.

Xia, R., Jia, H., Fan, J., Liu, Y., and Jia, J. (2012). USP8 promotes smoothened signaling by preventing its ubiquitination and changing its subcellular localization. PLoS biology *10*, e1001238.

Xiao, S., Sanelli, T., Dib, S., Sheps, D., Findlater, J., Bilbao, J., Keith, J., Zinman, L., Rogaeva, E., and Robertson, J. (2011). RNA targets of TDP-43 identified by UV-CLIP are deregulated in ALS. Molecular and cellular neurosciences *47*, 167-180.

Xu, Y.F., Gendron, T.F., Zhang, Y.J., Lin, W.L., D'Alton, S., Sheng, H., Casey, M.C., Tong, J., Knight, J., Yu, X*., et al.* (2010). Wild-type human TDP-43 expression causes TDP-43 phosphorylation, mitochondrial aggregation, motor deficits, and early mortality in transgenic mice. The Journal of neuroscience : the official journal of the Society for Neuroscience *30*, 10851-10859.

Xu, Y.F., Prudencio, M., Hubbard, J.M., Tong, J., Whitelaw, E.C., Jansen-West, K., Stetler, C., Cao, X., Song, J., and Zhang, Y.J. (2013). The pathological phenotypes of human TDP-43 transgenic mouse models are independent of downregulation of mouse Tdp-43. PloS one *8*, e69864.

Xu, Y.F., Zhang, Y.J., Lin, W.L., Cao, X., Stetler, C., Dickson, D.W., Lewis, J., and Petrucelli, L. (2011). Expression of mutant TDP-43 induces neuronal dysfunction in transgenic mice. Molecular neurodegeneration *6*, 73.

Yamashita, T., Hideyama, T., Hachiga, K., Teramoto, S., Takano, J., Iwata, N., Saido, T.C., and Kwak, S. (2012). A role for calpain-dependent cleavage of TDP-43 in amyotrophic lateral sclerosis pathology. Nature communications *3*, 1307.

Yang, C., Tan, W., Whittle, C., Qiu, L., Cao, L., Akbarian, S., and Xu, Z. (2010). The C-terminal TDP-43 fragments have a high aggregation propensity and harm neurons by a dominant-negative mechanism. PloS one *5*, e15878.

Zhang, D., Iyer, L.M., He, F., and Aravind, L. (2012). Discovery of Novel DENN Proteins: Implications for the Evolution of Eukaryotic Intracellular Membrane Structures and Human Disease. Frontiers in genetics *3*, 283.

Zhang, J., Du, J., Lei, C., Liu, M., and Zhu, A.J. (2014). Ubpy controls the stability of the ESCRT-0 subunit Hrs in development. Development *141*, 1473-1479.

Zhang, W., Cheng, G.Z., Gong, J., Hermanto, U., Zong, C.S., Chan, J., Cheng, J.Q., and Wang, L.H. (2008). RACK1 and CIS mediate the degradation of BimEL in cancer cells. The Journal of biological chemistry *283*, 16416-16426.

Zhang, Y., Gao, J., Chung, K.K., Huang, H., Dawson, V.L., and Dawson, T.M. (2000). Parkin functions as an E2-dependent ubiquitin- protein ligase and promotes the degradation of the synaptic vesicle-associated protein, CDCrel-1. Proceedings of the National Academy of Sciences of the United States of America *97*, 13354-13359.

Zhang, Y., Zolov, S.N., Chow, C.Y., Slutsky, S.G., Richardson, S.C., Piper, R.C., Yang, B., Nau, J.J., Westrick, R.J., Morrison, S.J.*, et al.* (2007a). Loss of Vac14, a regulator of the signaling lipid phosphatidylinositol 3,5-bisphosphate, results in neurodegeneration in mice. Proceedings of the National Academy of Sciences of the United States of America *104*, 17518-17523.

Zhang, Y.J., Caulfield, T., Xu, Y.F., Gendron, T.F., Hubbard, J., Stetler, C., Sasaguri, H., Whitelaw, E.C., Cai, S., Lee, W.C.*, et al.* (2013). The dual functions of the extreme N-terminus of TDP-43 in regulating its biological activity and inclusion formation. Human molecular genetics *22*, 3112-3122.

Zhang, Y.J., Gendron, T.F., Xu, Y.F., Ko, L.W., Yen, S.H., and Petrucelli, L. (2010). Phosphorylation regulates proteasomal-mediated degradation and solubility of TAR DNA binding protein-43 C-terminal fragments. Molecular neurodegeneration *5*, 33.

Zhang, Y.J., Xu, Y.F., Cook, C., Gendron, T.F., Roettges, P., Link, C.D., Lin, W.L., Tong, J., Castanedes-Casey, M., Ash, P.*, et al.* (2009). Aberrant cleavage of TDP-43 enhances aggregation and cellular toxicity. Proceedings of the National Academy of Sciences of the United States of America *106*, 7607-7612.

Zhang, Y.J., Xu, Y.F., Dickey, C.A., Buratti, E., Baralle, F., Bailey, R., Pickering-Brown, S., Dickson, D., and Petrucelli, L. (2007b). Progranulin mediates caspase-dependent cleavage of TAR DNA binding protein-43. The Journal of neuroscience : the official journal of the Society for Neuroscience *27*, 10530-10534.

Zhao, C., Beaudenon, S.L., Kelley, M.L., Waddell, M.B., Yuan, W., Schulman, B.A., Huibregtse, J.M., and Krug, R.M. (2004). The UbcH8 ubiquitin E2 enzyme is also the E2 enzyme for ISG15, an IFN-alpha/beta-induced ubiquitin-like protein. Proceedings of the National Academy of Sciences of the United States of America *101*, 7578-7582.

Zhao, C., Hsiang, T.Y., Kuo, R.L., and Krug, R.M. (2010). ISG15 conjugation system targets the viral NS1 protein in influenza A virus-infected cells. Proceedings of the National Academy of Sciences of the United States of America *107*, 2253-2258.

Zhou, H., Huang, C., Chen, H., Wang, D., Landel, C.P., Xia, P.Y., Bowser, R., Liu, Y.J., and Xia, X.G. (2010). Transgenic rat model of neurodegeneration caused by mutation in the TDP gene. PLoS genetics *6*, e1000887.

Danksagung

Nun, da ich meine Dissertation beendet habe, möchte ich denen danken die dazu beigetragen haben, dass ich meine Forschung durchführen und diese Arbeit verfassen konnte.

An erster Stelle möchte ich meinen Betreuer Prof. Philipp J. Kahle dafür danken, dass er mir die Möglichkeit gegeben hat in seinem Labor dieses interessante Projekt zu bearbeiten und auch nach meinen Vorstellungen zu gestalten, und für seine Anleitung, Ideen und Unterstützung. Außerdem: Dank der häufigen Diskussionen während des Mittagessens kann die Zombie Apokalypse nun kommen – ich weiß nun wie ich diese überleben kann!

Ich danke den Mitgliedern meines Advisory Boards Prof. Ralf-Peter Jansen und Prof. Elisa Izaurralde für ihre Zeit und ihren Rat, und besonders Prof. Ralf-Peter Jansen für die Übernahme des zweiten Gutachtens meiner Arbeit. Dem Deutschen Zentrum für Neurodegenerative Erkrankungen gilt ein besonderer Dank für die Verleihung eines Stipendiums, welches mich über vier Jahre finanziell unterstützte.

Ich danke Fabienne Fiesel für die sehr gute Betreuung, für die vielen Hilfestellungen während der ersten beiden Jahre dieser Arbeit und für die Ermunterung den dritten Y2H Screen nach den ersten beiden Fehlschlägen anzupacken – diesmal erfolgreich!

Bei der Etablierung der Ubiquitinylierungs-Versuche und beim Arbeiten mit dem Mikroskop habe ich viel Unterstützung von Sven Geisler erhalten. Außerdem hat er mir durch viel Zuhören beim Verfassen dieser Arbeit geholfen den Roten Faden des Öfteren wieder zu finden. Dafür, und für das umfassende Korrekturlesen dieser Arbeit bin ich ihm sehr, sehr dankbar.

Vielen Dank an Sandra Jäckel, Aaron Voigt und an die AG Rasse für die Einführung in die Welt der Fliegen. Danke an Aaron Voigt für die TDP-43 Fliegen und ein stetig offenes Ohr für Fragen bezüglich dieser, und an Tobias Rasse für die Mitbenutzung des Fliegenlabors. Einen ganz besonderen Dank möchte ich Sandra Jäckel zusprechen, die mir geduldig die Arbeit mit *Drosophila* gezeigt hat, immer Zeit für Fragen hatte und den Fliegen-Teil dieser Arbeit überprüft hat.

Another special thank you goes to my Master student Jennifer Strong, who helped me a lot with the ubiquitinylation studies of the TDP-43 mutants. I am sure I will never forget the difference between slug, snail and leech.

Ich möchte mich bei allen derzeitigen wie auch ehemaligen Kollegen - den Funkies - für viele Hilfestellungen, Diskussionen und Anregungen, sowie für die schöne Zeit im

Publications

Parts of this work have been published in:

Original article

Hans, F., Fiesel, F.C., Strong, J.C., Jackel, S., Rasse, T.M., Geisler, S., Springer, W., Schulz, J.B., Voigt, A., and Kahle, P.J. (2014). UBE2E Ubiquitin-conjugating Enzymes and Ubiquitin Isopeptidase Y Regulate TDP-43 Protein Ubiquitination. The Journal of Biological Chemistry 289, 19164-19179.

Poster Presentation

43th Annual Meeting of the Society for Neuroscience, San Diego, CA, USA,

09. - 13. November 2013

Hans, F., Fiesel, F.C., Strong, J.C., Jackel, S., Rasse, T.M., Geisler, S., Springer, W., Schulz, J.B., Voigt, A., and Kahle, P.J.; UBE2E ubiquitin-conjugating enzymes and ubiquitin isopeptidase Y regulate TDP-43 ubiquitinylation.